

Middle Rio Grande Montaño Reach Report:

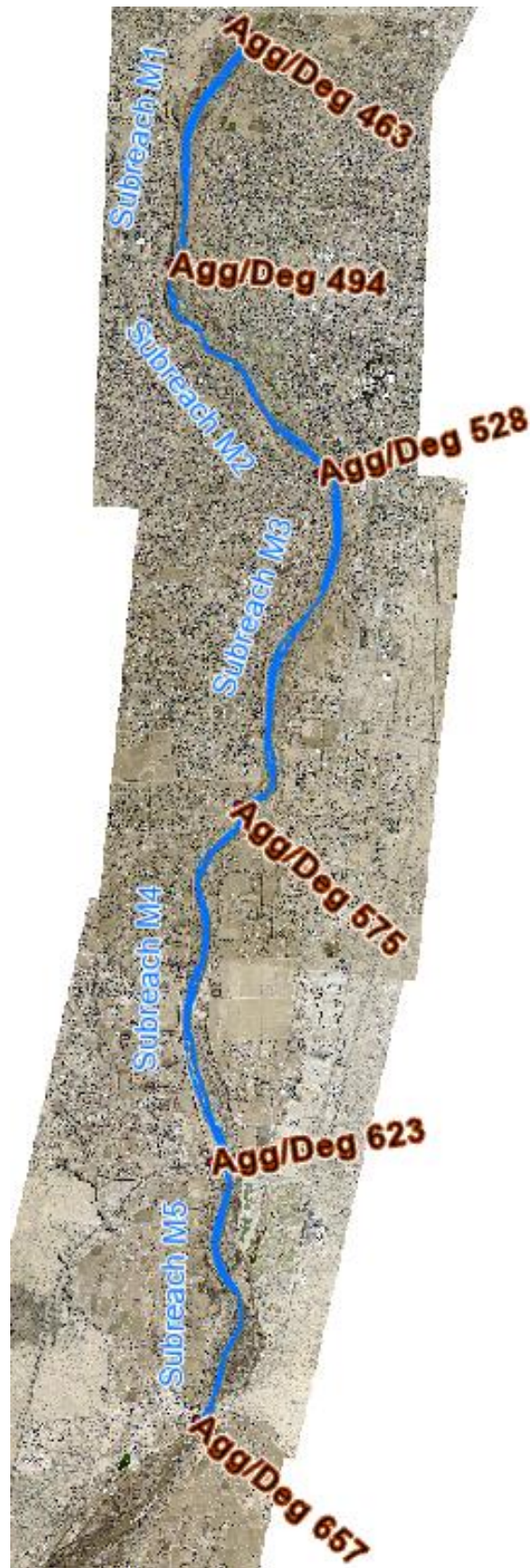
Morphodynamic Processes and
Silvery Minnow Habitat from the
Montaño Road Bridge Crossing to
the Isleta Diversion Dam

February 2023
Master of Science
Plan B Technical Report

Prepared by:
Tristen Anderson

Prepared for:
Dr. Pierre Julien
Dr. Peter Nelson
Dr. Ellen Wohl

Colorado State University
Engineering Research Center
Department of Civil and
Environmental Engineering
Fort Collins, Colorado 80523



Acknowledgement

This report has been prepared in conjunction with a more extensive reach study for the United States Bureau of Reclamation (USBR) under Award Number R17AC00064. Thank you to my graduate research partners on this project, Brianna Corsi and Chelsey Radobenko, for all their contributions and support. I would like to thank the USBR for providing all the data and for also reviewing the draft version of the larger reach study report. Thank you to the biologists with the University of New Mexico (UNM) and the American Southwest Ichthyological Researchers (ASIR) for providing their aquatic habitat expertise on the Rio Grande Silvery Minnow (RSGM). Thank you to Dr. Julien, my advisor, for his support and guidance throughout my time at Colorado State University. Lastly, thank you to my mother, Karen; this would not have been possible without her love and support.

Abstract

The Montaña Reach of the Middle Rio Grande (MRG) spans approximately 19 miles from the Montaña bridge crossing in Albuquerque, New Mexico, to the Isleta Diversion Dam. This reach report was prepared in conjunction with a more extensive Montaña Reach report (Anderson, 2023) for the United States Bureau of Reclamation (USBR). This report presents a summary of results to better understand the morphodynamic processes and habitat availability for the endangered Rio Grande Silvery Minnow (RSGM) along the Montaña Reach. The MRG is a dynamic river still responding to anthropogenic impacts over the last century. The Montaña reach was split into five subreaches (M1, M2, M3, M4, and M5), and the analysis of these five subreaches illustrates the spatial and temporal trends that have been observed.

Discharge and sediment data from the United States Geological Survey (USGS) and precipitation data from the Bosque Ecosystem Monitoring Program from the University of New Mexico (BEMP Data, 2017) were used to identify the timing and magnitude of flow and sediment discharge in the reach. Spring snowmelt typically supplies the largest water and sediment discharge volumes, while monsoonal thunderstorms often transport the largest concentration of suspended sediment.

Georeferenced linen maps from 1918 and aerial photography dating back to 1935 were analyzed with GIS to evaluate the changes in channel width and sinuosity. Anthropogenic impacts (Cochiti dam, channelization efforts, etc.) and climate changes (i.e., droughts) have resulted in significant channel narrowing of the Montaña Reach. Between 1918 and 1962, the average channel width (defined by vegetation) was reduced from 1470 ft to 500 ft. The channel has continued to narrow gradually from 1962 to 2019 to an average of 375 ft. Historically, the Montaña Reach has had a low sinuosity (less than 1.3), and anthropogenic influences have further reduced the sinuosity from 1.1 to 1.05 between 1935 and 2019.

Changes to bed elevation from 1962 to 2012 were analyzed using cross-section geometry files provided by the USBR Technical Service Center. Cycles of degradation and aggradation have occurred, although the magnitude of these cycles is small relative to other reaches along the MRG. Between 1962 and 1972, the Montaña Reach was in the process of aggrading (~1 ft). Following the completion of Cochiti dam, 1972-2002, the channel began to incise (~2.5 ft). From 2002 to 2012, slight aggradation occurred (~1 ft).

The overall trend of channel bed degradation indicates that the Montaña Reach has a sediment transport capacity larger than the supply. Rivers with excess transport capacity tend to degrade and progress towards a single-thread meandering (M) planform within the Massong geomorphic conceptual model. The subreaches follow a similar but not identical progression through this conceptual model. The river was classified as Stage 1 (e.g., wide and braided) in the early- to mid-1900s and transitioned towards Stage M5 (e.g., narrow, straight, and single-threaded) by the early 2000s. Channelization efforts (jetty jacks and levees) have stabilized sections along the riverbank, which prevent the river from meandering. Therefore, the likely end-stage planform for the Montaña reach is Stage M5 – where the river has found a relative equilibrium between slope, grain size, and sediment supply/transport.

One-dimensional hydraulic models, developed with HEC-RAS software, were used to estimate habit availability for the endangered Rio Grande Silvery Minnow (RSGM) throughout the Montaña Reach. A width-slice method was implemented to determine the velocity and depth variations of the flow across each cross-section at 1,500, 3,000, and 5,000 cfs. This data was used to calculate the hydraulically suitable RSGM habitat based on the velocity and depth criteria for the larval, juvenile, and adult life stages. Hydraulically suitable habitat was calculated for five historical river conditions: 1962, 1972, 1992, 2002, and 2012. Subreaches M2, M4, and M5 show the greatest habitat availability for all life stages of the RSGM. Detailed mapping using 2012 LiDAR was used to generate 'habitat maps' that spatially illustrate the RSGM habitat areas and relative quantity.

Table of Contents

Acknowledgement	I
Abstract	II
List of Appendix A Figures and Tables	VII
List of Appendix B Figures and Tables	VII
List of Appendix C Figures and Tables	VII
List of Appendix D Figures and Tables	VIII
List of Appendix E Figures and Tables	VIII
List of Appendix F Figures and Tables.....	VIII
1 Introduction.....	1
1.1 Site Description.....	2
1.2 Aggradation/Degradation Lines and Rangelines	3
1.3 Subreach Delineation	3
2 Precipitation, Flow, and Sediment Discharge Analysis	7
2.1 Precipitation	7
2.2 River Flow	10
2.2.1 USGS Gage Data	10
2.2.2 Raster Hydrographs.....	12
2.2.3 Yearly Peak Flow Events	13
2.2.4 Cumulative Discharge Curves	15
2.2.5 Flow Duration	20
2.2.6 Days of Flow	22
2.3 Suspended Sediment Load.....	23
2.3.1 Single Mass Curve	23
2.3.2 Double Mass Curve.....	26
2.3.3 Monthly Sediment Variation.....	27
3 River Geomorphology.....	32
3.1 Wetted Top Width.....	32
3.2 Width (Defined by Vegetation).....	37
3.3 Bed Elevation.....	38
3.4 Bed Material.....	39
3.5 Sinuosity	40
3.6 Hydraulic Geometry.....	41
3.7 Mid-Channel Bars and Islands.....	45
3.8 Channel Response Models.....	47
3.9 Geomorphic Conceptual Model	48

4	HEC-RAS Modeling for Silvery Minnow Habitat.....	61
4.1	Modeling Data and Background	61
4.1.1	Ineffective Flow Analysis	61
4.2	Width Slices Methodology.....	63
4.3	Width Slices Habitat Results.....	64
4.4	RAS-Mapper Methodology.....	68
4.5	RAS-Mapper Habitat Results in 2012	68
4.6	Disconnected Areas	71
5	Conclusions.....	72
6	Bibliography	73

List of Tables

Table 1-1	Montaño subreach delineation.....	3
Table 2-1	List of Relevant USGS Gages	10
Table 2-2	Probabilities of daily exceedance	20
Table 3-1	Julien-Wargadalam channel width prediction	47
Table 3-2	Channel bed slope by subreach	49
Table 4-1	Rio Grande Silvery Minnow habitat velocity and depth range requirements (from Mortensen et al., 2019)	61

List of Figures

Figure 1-1	Map with the Middle Rio Grande outlined in blue. It begins at Cochiti Dam (Red line) and continues downstream to the narrows just upstream of Elephant Butte Reservoir (Orange line). The green line highlights the Montaño Reach.	1
Figure 1-2	Timeline of Significant events for the Middle Rio Grande River (Makar 2006)	2
Figure 1-3	Montaño Subreach Delineation Overview Map.....	4
Figure 1-4	Subreach delineation with aerial imagery of Subreach M1.....	5
Figure 1-5	Subreach delineation with aerial imagery of Subreach M2.....	5
Figure 1-6	Subreach delineation with aerial imagery of Subreach M3.....	6
Figure 1-7	Subreach delineation with aerial imagery of Subreach M4.....	6
Figure 1-8	Subreach delineation with aerial imagery of Subreach M5.....	7
Figure 2-1	BEMP data collection sites (figure source: http://bemp.org)	8
Figure 2-2	Monthly precipitation near the Bernalillo and Montaño Reach over time (1996 – 2017).	9
Figure 2-3	Cumulative monthly precipitation near the Montaño Reach (1996 – 2017).	9
Figure 2-4	USGS gage data overview map.....	11
Figure 2-5	Raster hydrograph of daily discharge at USGS Station 08329000 (left) and USGS Station 0832950 (right) below the Jemez Dam. (Source: https://waterwatch.usgs.gov).	13
Figure 2-6	Raster hydrograph of daily discharge at USGS Station 08319000 at San Felipe (left) and USGS Station 08330000 at Albuquerque (right). (Source: https://waterwatch.usgs.gov).....	13
Figure 2-7	Yearly peak flow events for the Rio Grande before Cochiti Dam at historical USGS gage 08314500 (1926-1970) and USGS Gage 08317400 (1970-present).....	14

Figure 2-8 Yearly peak flow events for the Rio Grande after Cochiti Dam at USGS Gage 08317400 (1970-present).	14
Figure 2-9 Yearly peak flow events for the Jemez River.....	15
Figure 2-10 Discharge single mass curve at historical USGS gage 8314500 (Cochiti) before dam construction.....	16
Figure 2-11 Discharge single mass curve at USGS gage 08317400 (below Cochiti Dam) after dam construction.....	16
Figure 2-12 Discharge single mass curve at USGS gage 08319000 (San Felipe) before dam construction.	17
Figure 2-13 Discharge single mass curve at USGS gage 08319000 (San Felipe) after dam construction.	17
Figure 2-14 Discharge single mass curve at USGS gage 08330000 (Albuquerque).	18
Figure 2-15 Discharge single mass curve at historical USGS gage 08329000 (Jemez) before dam construction in 1953.	19
Figure 2-16 Discharge single mass curve at historical USGS gage 08329000 and USGS gage 08328950 (Jemez) after dam construction in 1953.....	19
Figure 2-17 Flow duration curves for the Rio Grande gages before and after dam construction in 1970. .	21
Figure 2-18 Flow duration curves for the Jemez River gages before and after dam construction in 1953.	21
Figure 2-19 Number of days greater than an identified discharge at the Cochiti gages before (left) and after (right) dam construction.	22
Figure 2-20 Number of days greater than an identified discharge at the San Felipe gage before (left) and after (right) dam construction.	22
Figure 2-21 Number of days greater than an identified discharge at the Jemez gages before (left) and after (right) dam construction in 1953.	23
Figure 2-22 Suspended sediment discharge single mass curve for USGS gage 08329000 at Jemez River Below Jemez Canyon Dam, NM	24
Figure 2-23 Suspended sediment discharge single mass curve for USGS gage 08317400 at Rio Grande Below Cochiti Dam, NM.....	24
Figure 2-24 Suspended sediment discharge single mass curve for USGS gage 08329500 at Rio Grande Near Bernalillo, NM.....	25
Figure 2-25 Suspended sediment discharge single mass curve for USGS gage 08330000 at Rio Grande at Albuquerque, NM	25
Figure 2-26 Double mass curve for USGS gage 08329500 at Rio Grande Near Bernalillo, NM	26
Figure 2-27 Cumulative suspended sediment (data from the Rio Grande at Albuquerque (USGS 08330000) gage) versus cumulative precipitation at the Alameda gage.....	27
Figure 2-28 Monthly average suspended sediment and water discharge at USGS gage 08329000 at Jemez River Below Jemez Canyon Dam, NM	28
Figure 2-29 Monthly average suspended sediment concentration and water discharge at USGS gage 08329000 at Jemez River Below Jemez Canyon Dam, NM.....	28
Figure 2-30 Monthly average suspended sediment and water discharge at USGS gage 08317400 at Rio Grande Below Cochiti Dam, NM	29
Figure 2-31 Monthly average suspended sediment concentration and water discharge at USGS gage 08317400 at Rio Grande Below Cochiti Dam, NM.....	29
Figure 2-32 Monthly average suspended sediment and water discharge at USGS gage 08329500 at Rio Grande Near Bernalillo, NM	30

Figure 2-33 Monthly average suspended sediment concentration and water discharge at USGS gage 08329500 at Rio Grande Near Bernalillo, NM.....	30
Figure 2-34 Monthly average suspended sediment and water discharge at USGS gage 08330000 at Rio Grande at Albuquerque, NM	31
Figure 2-35 Monthly average suspended sediment concentration and water discharge at USGS gage 08330000 at Rio Grande at Albuquerque, NM.....	31
Figure 3-1 Moving cross-sectional average of the wetted top width at a discharge of 1,000 cfs.	32
Figure 3-2 Cumulative top width at a discharge at 1,000 cfs.....	33
Figure 3-3 Moving cross-sectional average of the wetted top width at a discharge of 3,000 cfs.	34
Figure 3-4 Cumulative top width at a discharge of 3,000 cfs.	34
Figure 3-5 Moving cross-sectional average of the wetted top width at a discharge of 5,000 cfs.	35
Figure 3-6 Cumulative top width at a discharge of 5,000 cfs	35
Figure 3-7 Average top width for each subreach at discharges from 500 cfs to 10,000 cfs; M1 (top left), M2 (top right), M3 (middle left), M4 (middle right), M5 (bottom middle).	36
Figure 3-8 Averaged active channel width by subreach from historical imagery (defined by vegetation).37	
Figure 3-9 Longitudinal bed elevation profile.	38
Figure 3-10 Aggradation and degradation by subreach	39
Figure 3-11 Median grain diameter size of samples taken throughout the Montaña Reach. (Circles represent 2014-2005, triangles represent 2004-1996, and squares represent 1995-1990).....	39
Figure 3-12 Median grain diameter size of samples taken throughout the Montaña reach over time	40
Figure 3-13 Sinuosity by subreach.....	41
Figure 3-14 HEC-RAS wetted top width of Montaña Subreaches at 1,000 cfs (top), 3,000 cfs (middle), and 5,000 cfs (bottom).....	42
Figure 3-15 HEC-RAS Hydraulic depth of Montaña Subreaches at 1,000 cfs (top), 3,000 cfs (middle), and 5,000 cfs (bottom).....	43
Figure 3-16 HEC-RAS main channel wetted perimeter at 1,000 cfs (top), 3,000 cfs (middle), 5,000 cfs (bottom).	44
Figure 3-17 Bed Slope from Bed Elevations (left) and Water Surface at 500 cfs (right).	45
Figure 3-18 Average number of channels at the Agg/Deg lines in each subreach.	45
Figure 3-19 Percentage of Agg/Deg lines with multiple channels, by year, segregated by number of channels between 1 and 4.	46
Figure 3-20 Julien and Wargadalam predicted widths and observed widths of the channel	48
Figure 3-21 Planform evolution model from Massong et al. (2010). The river undergoes stages 1-3 first and then continues to stages A4-A6 or stages M4-M8 depending on the sediment transport capacity.	49
Figure 3-22 Planform evolution model from Massong et al. (2010) applied to channel cross sectional view (modified 2022).	50
Figure 3-23 Subreach M1: Channel evolution of representative cross section Agg/Deg 483. Displaying a trend of incision from 1962 to 2012.	51
Figure 3-24 Subreach M1: Massong (2012) classification (left), historical cross section profiles (center) and corresponding aerial images (right) at Agg/Deg 483.....	52
Figure 3-25 Subreach M2: Channel evolution of representative cross section Agg/Deg 515. Significant channel degradation and narrowing occurred between 1972 and 2012.	53

Figure 3-26 Subreach M2: Massong (2010) classification (left), historical cross section profiles (center) and corresponding aerial images (right) at Agg/Deg 515.....	54
Figure 3-27 Subreach M3: Channel evolution of representative cross section Agg/Deg 554. Significant channel degradation occurring between 1972 and 2012.....	55
Figure 3-28 Subreach M3: Massong (2010) classification (left), historical cross section profiles (center) and corresponding aerial images (right) at Agg/Deg 554.....	56
Figure 3-29 Subreach M4: Channel evolution of representative cross section Agg/Deg 596.	57
Figure 3-30 Subreach M4: Massong (2010) classification (left), historical cross section profiles (center) and corresponding aerial images (right) at Agg/Deg 596.....	58
Figure 3-31 Subreach M5: Channel evolution of representative cross section Agg/Deg 629.	59
Figure 3-32 Subreach M5: Massong (2010) classification (left), historical cross section profiles (center) and corresponding aerial images (right) at Agg/Deg 629.....	60
Figure 4-1 Example cross section with ineffective flow areas at 10,000 cfs, hatched areas are those below the trigger elevation and will not convey water in the model.	62
Figure 4-2 Cross section at a discharge of 5,000 cfs with the flow distribution from HEC-RAS of 20 vertical slices in the floodplain (10 ROB and 10 LOB) and 25 vertical slices in the main channel. The slices are small enough that the discrete color changes look more like a gradient.....	63
Figure 4-3 Larval RSGM habitat availability throughout the Montaña Reach.....	64
Figure 4-4 Juvenile RSGM habitat availability throughout the Montaña Reach.....	65
Figure 4-5 Adult RSGM habitat availability throughout the Montaña Reach.....	65
Figure 4-6 Stacked habitat charts at different scales to display spatial variations of habitat throughout the Montaña Reach in 2012.....	67
Figure 4-7 Suitable habitat in 2012 for each life stage at 1,500 cfs in Subreach M2.	69
Figure 4-8 Suitable habitat in 2012 for each life stage at 3,000 cfs in Subreach M2.	70
Figure 4-9 Suitable habitat for each life stage at 5,000 cfs in Subreach M2.	70
Figure 4-10 Disconnected low-laying areas that are no longer connected to the main channel at 5,000 cfs in Subreach M5.....	71

List of Appendix A Figures and Tables

Montaña Subreach Delineation Report	A-1
---	-----

List of Appendix B Figures and Tables

Table B-1 Years used in JW Calculations for D50.....	B-1
--	-----

List of Appendix C Figures and Tables

Figure C-1 Wetted top width at each Agg/Deg line in the Montaña reach at a discharge of 1,000 cfs.....	C-2
Figure C-2 Wetted top width at each Agg/Deg line in the Montaña reach at a discharge of 3,000 cfs	C-2
Figure C-3 Wetted top width at each Agg/Deg line in the Montaña reach at a discharge of 5,000 cfs	C-3

List of Appendix D Figures and Tables

Figure D-1 RGSM habitat availability in Montaña Subreach M1	D-2
Figure D-2 RGSM habitat availability in Montaña Subreach M2	D-3
Figure D-3 RGSM habitat availability in Montaña Subreach M3	D-4
Figure D-4 RGSM habitat availability in Montaña Subreach M4	D-5
Figure D-5 RGSM habitat availability in Montaña Subreach M5.....	D-6
Figure D-6 Stacked habitat charts to display spatial variations of habitat throughout the Montaña reach in 1962	D-7
Figure D-7 Stacked habitat charts to display spatial variations of habitat throughout the Montaña reach in 1972	D-8
Figure D-8 Stacked habitat charts to display spatial variations of habitat throughout the Montaña reach in 1992	D-9
Figure D-9 Stacked habitat charts to display spatial variations of habitat throughout the Montaña reach in 2002	D-10
Figure D-10 Stacked habitat charts to display spatial variations of habitat throughout the Montaña reach in 2012	D-11
Figure D-11 Life stage habitat curves for subreach M1	D-13
Figure D-12 Life stage habitat curves for subreach M2	D-15
Figure D-13 Life stage habitat curves for subreach M3	D-17
Figure D-14 Life stage habitat curves for subreach M4	D-19
Figure D-15 Life stage habitat curves for subreach M5	D-21

List of Appendix E Figures and Tables

Habitat Map at 1,500 cfs.....	E-2 through E-16
Habitat Map at 3,000 cfs.....	E-17 through E-31
Habitat Map at 5,000 cfs.....	E-32 through E-46

List of Appendix F Figures and Tables

Geomorphic Habitat Linkage Quad: Subreach M1.....	F-2
Geomorphic Habitat Linkage Quad: Subreach M2.....	F-3
Geomorphic Habitat Linkage Quad: Subreach M3.....	F-4
Geomorphic Habitat Linkage Quad: Subreach M4.....	F-5
Geomorphic Habitat Linkage Quad: Subreach M5.....	F-6

1 Introduction

This reach report aims to evaluate the morphodynamic conditions and quantify the Rio Grande Silvery Minnow (RSGM) habitat within the Montañero Reach of the Middle Rio Grande (MRG). The MRG extends from Cochiti Dam to the narrows upstream of the Elephant Butte Reservoir. The Montañero Reach begins at the Montañero Road Bridge crossing in Albuquerque, New Mexico, and ends at the Isleta Diversion Dam (**Figure 1-1**).

This reach report was completed in conjunction with a more extensive Montañero Reach report (Anderson, 2023) prepared for the United States Bureau of Reclamation (USBR) as part of a series of reports supporting the USBR's mission to improve habitat for the endangered species. The specific objectives of this reach report include:

- Summarize trends and conditions for precipitation and flow and sediment discharge using Bosque Ecosystem Monitoring Program data from the University of New Mexico (BEMP Data, 2017) and flow and sediment data from the United States Geological Survey (USGS) Gages.
- Analyze the subreach level geomorphic characteristics over time using USBR-provided HEC-RAS models from 1962, 1972, 1992, 2002, and 2012.
- Classify the Montañero subreaches using the Massong geomorphic conceptual model (Massong et al. 2010) to help quantify historical and future river changes.
- Quantify the hydraulically suitable habitat, based on velocity and depth criteria, for all life stages of the RSGM (larvae, juvenile, and adult) using a one-dimensional HEC-RAS hydraulic model. Spatially locate the areas of available RSGM habitat and generate habitat maps using ArcGIS Pro.



outlined in blue. It begins at Cochiti Dam (Red line) and continues downstream to the narrows just upstream of Elephant Butte Reservoir (Orange line). The green line highlights the Montañero Reach.

1.1 Site Description

The Rio Grande begins in the San Juan Mountain range of Colorado and continues into New Mexico. It travels along the Texas-Mexico border before reaching the Gulf of Mexico. The MRG has historically been affected by periods of drought and large spring flooding events due to snowmelt. Monsoons have caused some of the largest peak flows the river has seen. These floods often caused large scale shifts in the course of the river and rapid aggradation (Massong et al., 2010). Floods helped maintain aquatic ecosystems by enabling connection of water between the main channel and the floodplains (Scurlock, 1998), but consequently threatened human establishments that were built near the Rio Grande.

Beginning in the 1930s, levees were installed to prevent flooding. Beginning in the 1950s, the USBR undertook a significant channelization effort involving jetty jacks, river straightening, and other techniques. Upstream dams built in the 1950s were used to store and regulate flow in the river. While these efforts enabled agriculture and large-scale human developments to thrive along the MRG, they also fundamentally changed the river, which led to reduced peak flows and sediment supply while altering the channel geometry and vegetation (Makar, 2006). In parts of the MRG, narrowing of the river continues, with channel degradation due to limited sediment supply and the formation of vegetated bars that encroach into the channel (Varyu, 2013; Massong et al., 2010). Farther downstream, closer to Elephant Butte Reservoir, aggradation and sediment plugs have been observed. These factors have created an ecologically stressed environment, as seen in the decline of species such as the RGSM (Mortensen et al., 2019). **Figure 1-2** shows a diagram detailing major historical events and alterations to the Rio Grande (provided by Makar, 2006).

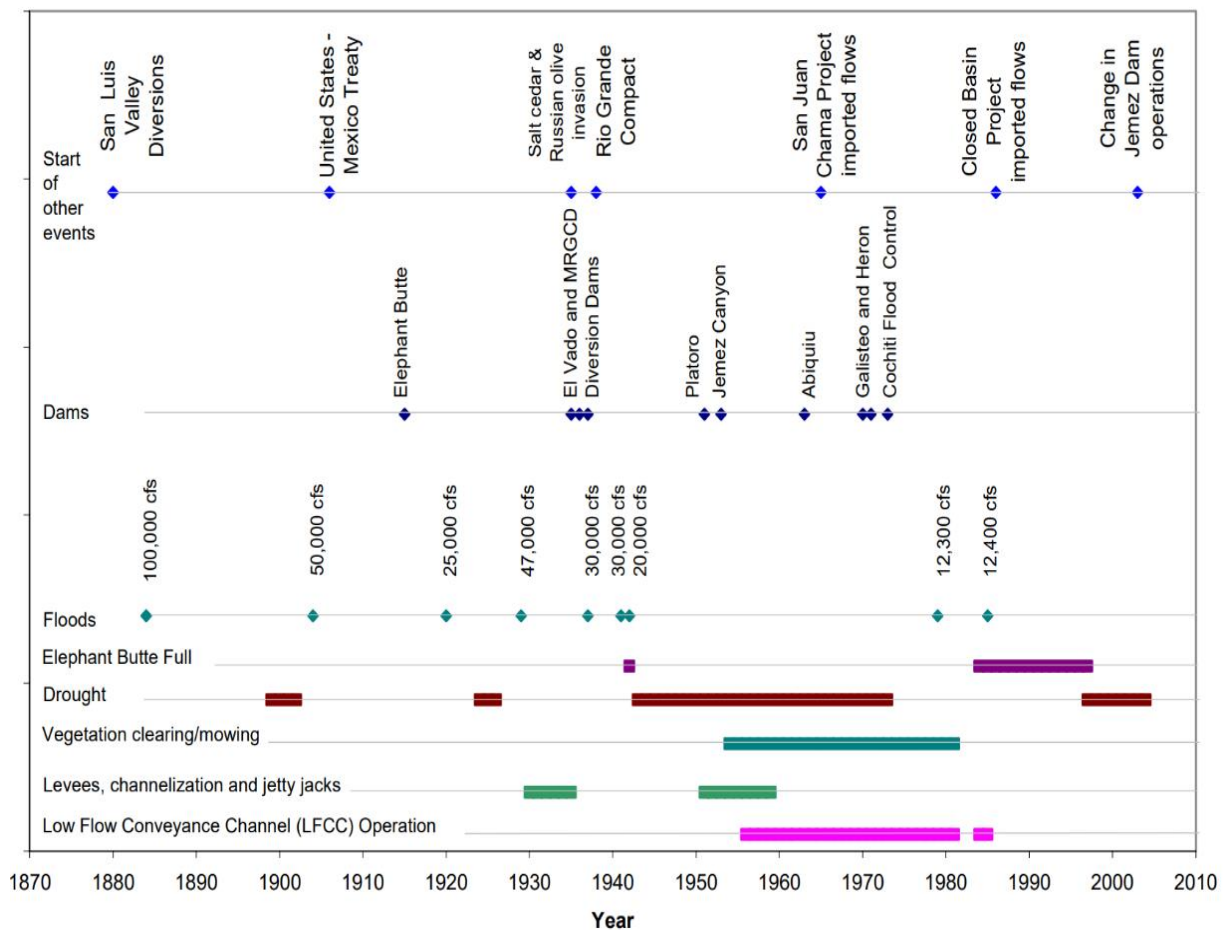


Figure 1-2. Timeline of Significant events for the Middle Rio Grande River (Makar 2006)

1.2 Aggradation/Degradation Lines and Rangelines

Aggradation/degradation lines (Agg/Deg lines), spaced at approximately 500-foot intervals along the entire MRG, were established in 1962 and are used as baselines to estimate changes in sedimentation and morphological characteristics in the river channel and floodplain over time (Posner 2017). Each Agg/Deg line has been surveyed approximately every 10 years, when the USBR performs monitoring, available for 1962, 1972, 1992, 2002 and 2012. The cross-sectional geometry at each Agg/Deg line for all 5 survey years are available within the HEC-RAS models that were developed for the MRG by the Technical Service Center (Varyu, 2013). The most recent 2012 survey was performed using LiDAR data, while surveys prior to 2012 were developed using photogrammetry techniques. All models use the North American Vertical Datum of 1988 (NAVD88). LiDAR and photogrammetric survey techniques do not deliver accurate ground elevation measurements underwater. For modeling purposes, it is necessary to appropriately characterize bathymetry of the channel for an accurate representation of channel conveyance. To accomplish this, an underwater prism was estimated using the measured water surface elevation and the flow on the date of survey and has been incorporated within the HEC-RAS geometry files (Varyu, 2013). In addition to Agg/Deg lines, rangelines are used as location identifiers in this analysis. Rangelines, created prior to the Agg/Deg lines, were determined in association with geomorphic factors, such as migrating bends, incision, or river maintenance issues.

1.3 Subreach Delineation

The Montaña Reach spans approximately 19 miles beginning at Agg/Deg line 463 (Montaña Bridge Crossing) and ending at Agg/Deg line 657 (just downstream of the Isleta Diversion Dam). This reach is located within an urban river corridor. For the purposes of hydraulic and geomorphic analysis, this reach was split into multiple subreaches based on notable urban and geomorphic features.

The Montaña reach was delineated into five subreaches based on notable features such as bridge crossings, arroyo outlets, and geomorphic features (e.g. wetted top width). **Table 1-1** below summarizes each subreach. **Figure 1-3** shows an overview map of the reach delineation. Individual subreach maps with Agg/Deg lines and 2012 aerial imagery are shown in **Figure 1-4**, **Figure 1-5**, **Figure 1-6**, **Figure 1-7**, and **Figure 1-8**. A full subreach delineation report for the Montaña reach is provided in **Appendix A**. This subreach delineation report includes an analysis of the 3,000 cfs flow widths and channel widths identified by the bank stations were considered for the years 2002 and 2012. Along with the longitudinal profile and particle distribution throughout the reach. All analyses performed identified boundaries consistent with the subreach delineation.

Table 1-1 Montaña subreach delineation

Subreach Name	Agg/Deg Lines	Approximate Length	Description
M-1	463 – 494	3.0 miles	Montaña Bridge to Coronado Fwy (I-40)
M-2	494 – 528	3.5 miles	Coronado Fwy (I-40) to Bridge Blvd
M-3	528 – 575	4.5 miles	Bridge Blvd to Tijeras Arroyo
M-4	575 – 623	4.5 miles	Tijeras Arroyo to I-25 Bridge
M-5	623 – 657	3.5 miles	I-25 Bridge to Isleta Diversion Dam

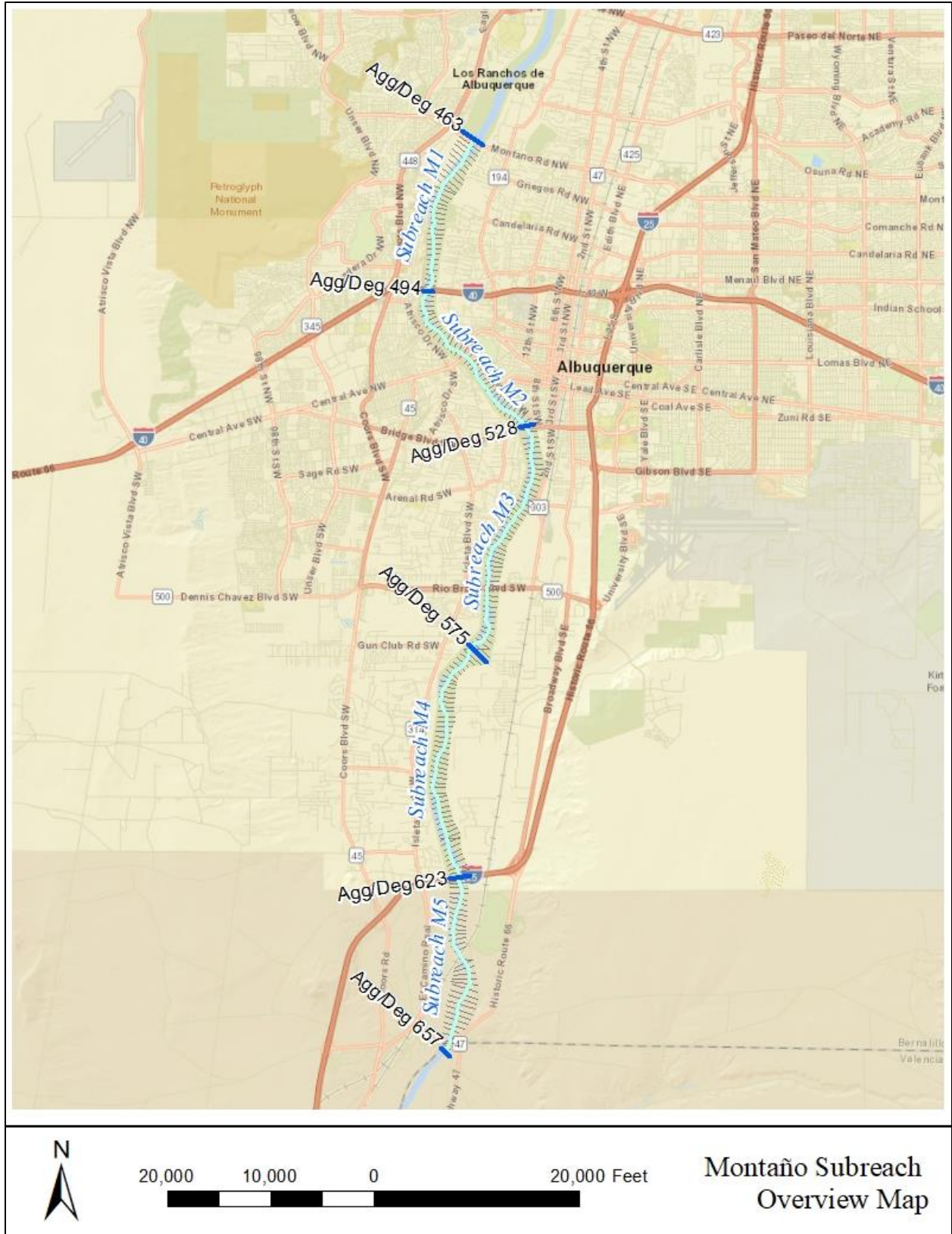


Figure 1-3 Montaño Subreach Delineation Overview Map

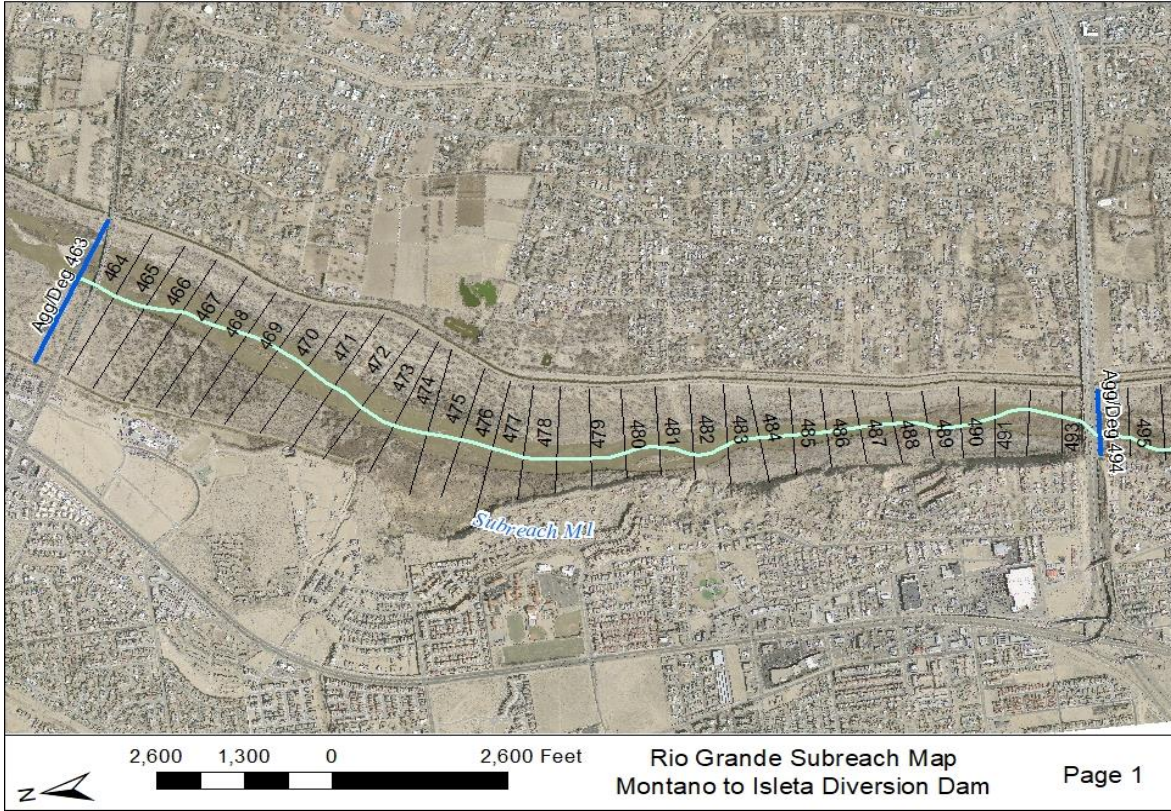


Figure 1-4 Subreach delineation with aerial imagery of Subreach M1

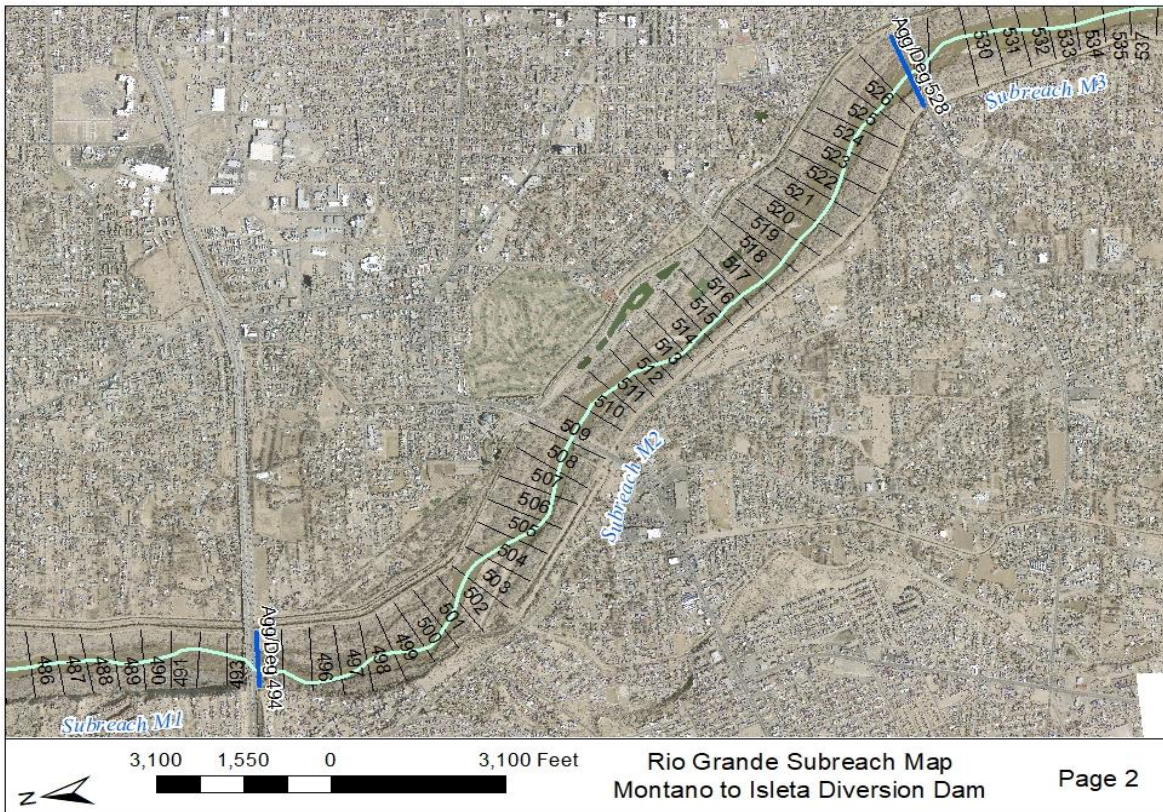


Figure 1-5 Subreach delineation with aerial imagery of Subreach M2

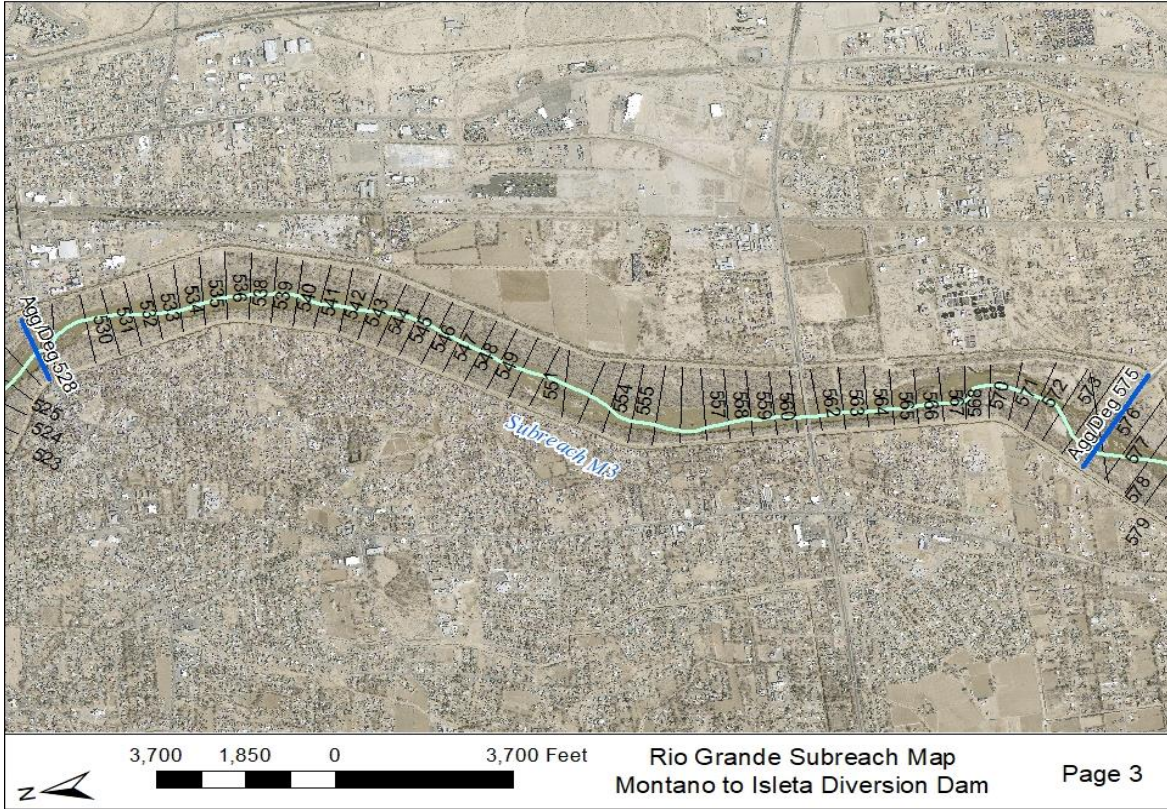


Figure 1-6 Subreach delineation with aerial imagery of Subreach M3

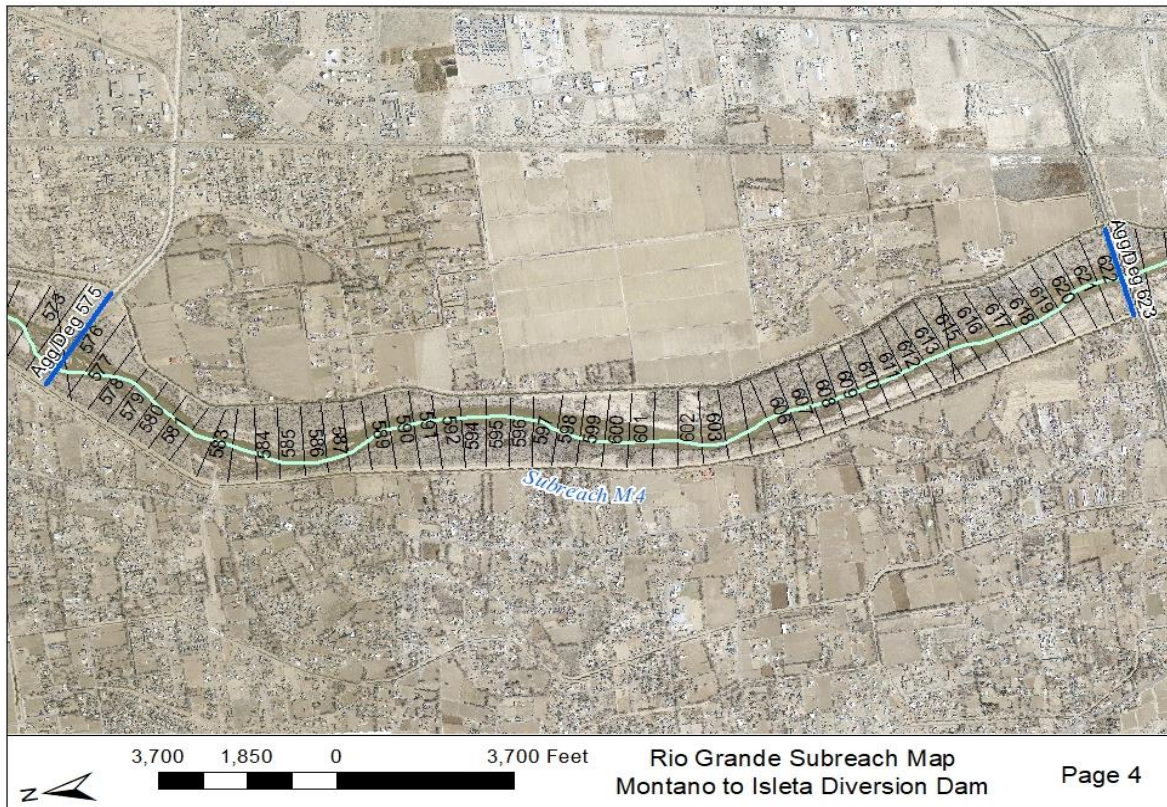


Figure 1-7 Subreach delineation with aerial imagery of Subreach M4

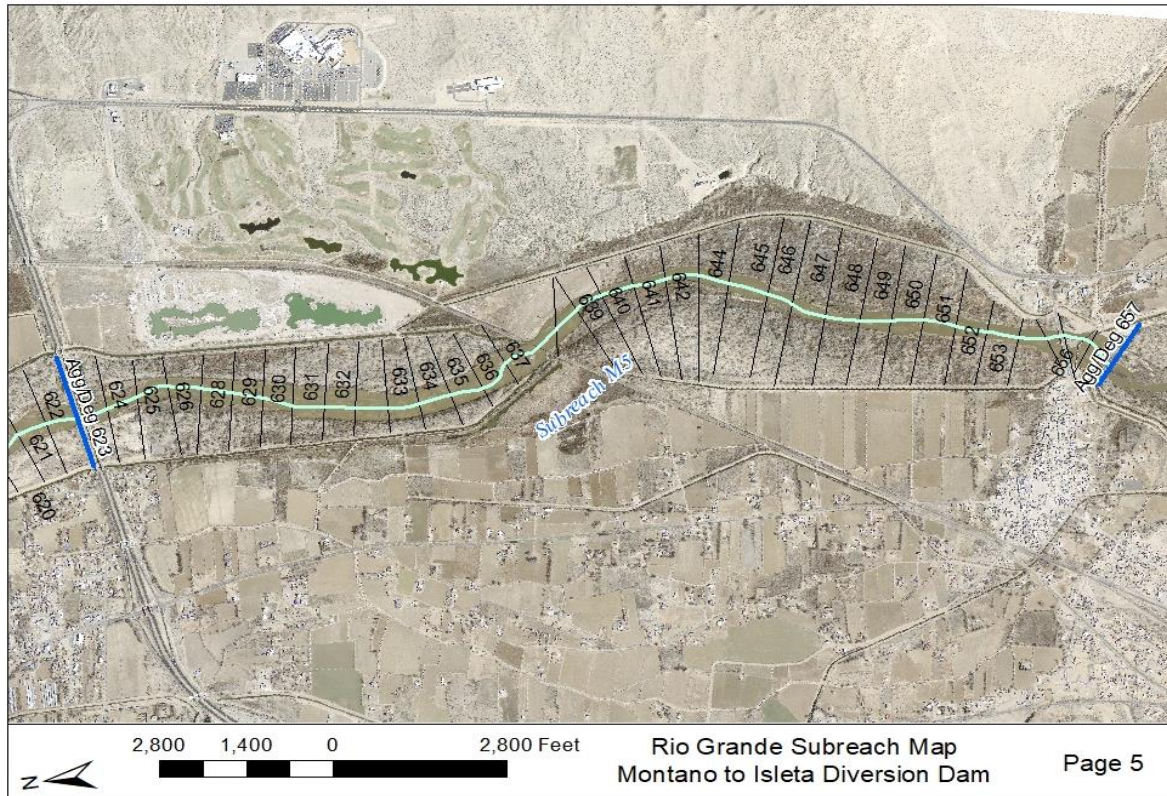


Figure 1-8 Subreach delineation with aerial imagery of Subreach M5

2 Precipitation, Flow, and Sediment Discharge Analysis

For the larger USBR reach report study, the adjacent upstream reach (Bernalillo Reach) and Montañito Reach were analyzed simultaneously. Due to the proximity of the reaches a combined evaluation of precipitation, flow, and sediment characteristics was conducted for the Bernalillo and Montañito Reaches collectively.

2.1 Precipitation

Precipitation data was collected along the MRG by the Bosque Ecosystem Monitoring Program from University of New Mexico (BEMP Data, 2017). The locations of the data collection sites are shown in **Figure 2-1**. The four gage sites used in the precipitation analysis, from north to south, include Santa Ana, Alameda, Rio Grande Nature Center (RGNC), and Harrison. These sites were highlighted in the following analyses based on their proximity to the relevant river reaches and period of record. The Santa Ana gage site is just north of the upstream boundary of the Bernalillo reach and the Harrison site is near the downstream boundary of the Montañito Reach. Meaning the other two precipitation gages are located within the study reaches.

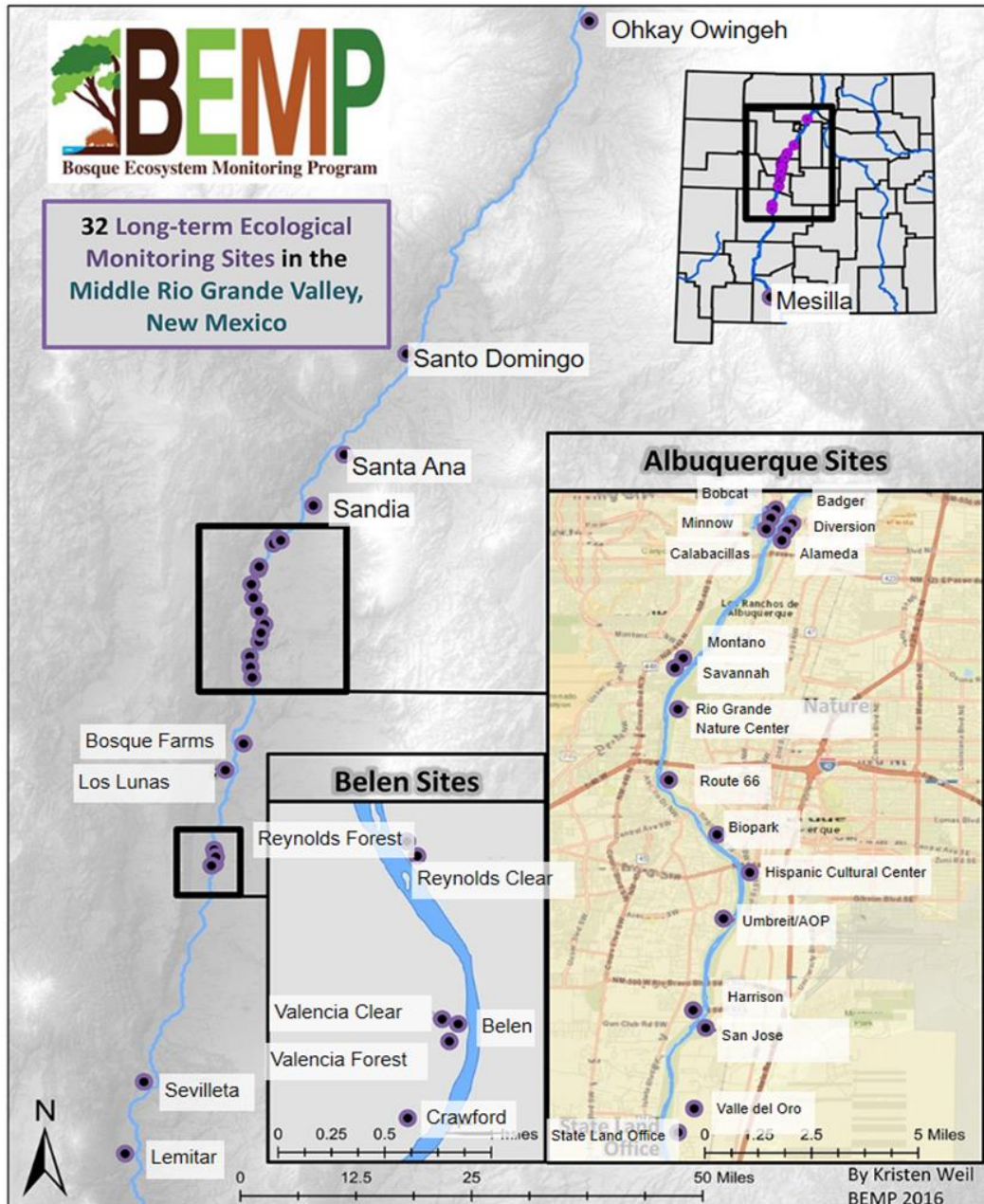


Figure 2-1 BEMP data collection sites (figure source: <http://bemp.org>)

The monthly precipitation data is shown in **Figure 2-2**. The highest precipitation peak, 5.7 inches of rainfall, occurred in August of 2006 at the Alameda gage. A general trend was observed with the highest precipitation values occurring during the monsoon season (June 15th – September 30th). A cumulative rainfall plot of the monthly precipitation data, **Figure 2-3**, shows that individual rain events can greatly affect the overall trend of the data. It further highlights the monsoonal rains, which create a “stepping” pattern with higher rainfall in June through September, and lower precipitation totals throughout the rest of the year. The same pattern is observed across all the gages indicating that the precipitation trends (timing and magnitude) around the Bernalillo and Montañó Reaches are spatially consistent. From the two gages with the longest period of record, Alameda, and RGNC, the cumulative rainfall pattern is nearly identical until 2006. Since then, the Alameda gage has received slightly more precipitation (~10 inches) than the RGNC gage.

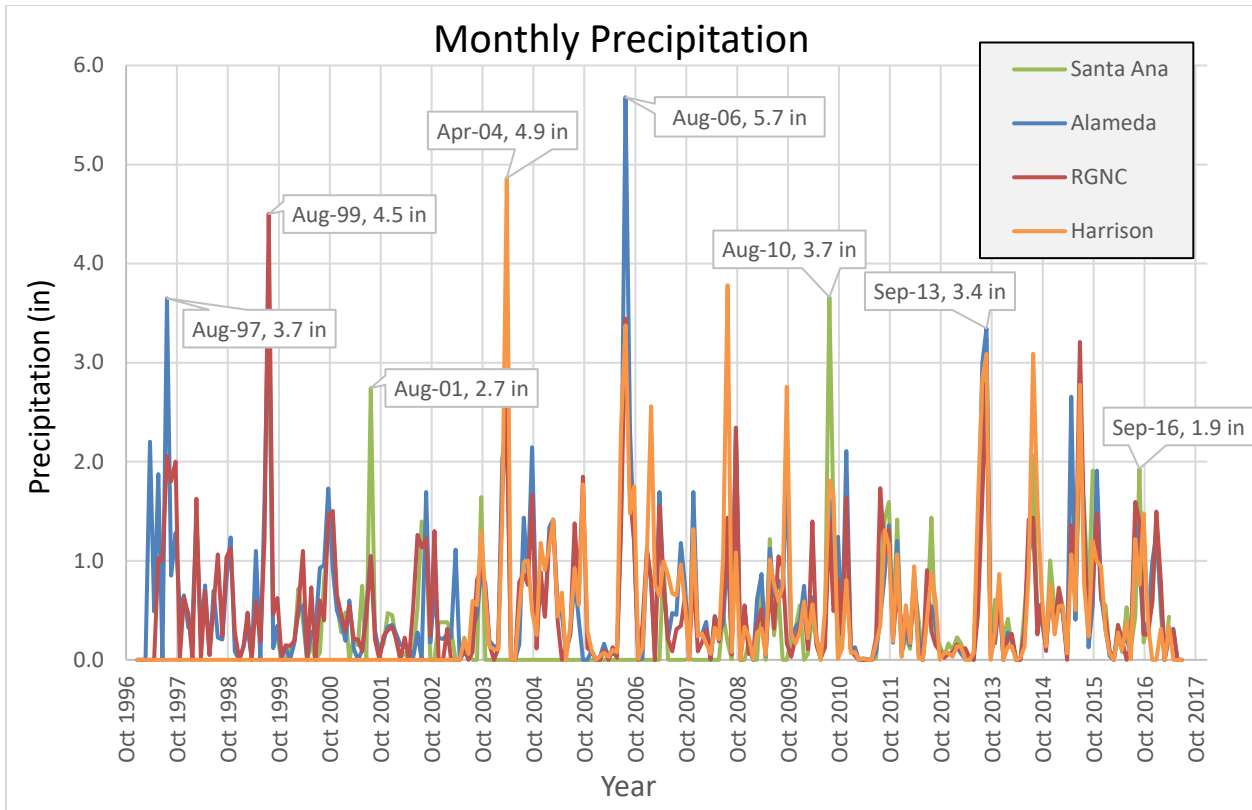


Figure 2-2 Monthly precipitation near the Bernalillo and Montaño Reach over time (1996 – 2017).

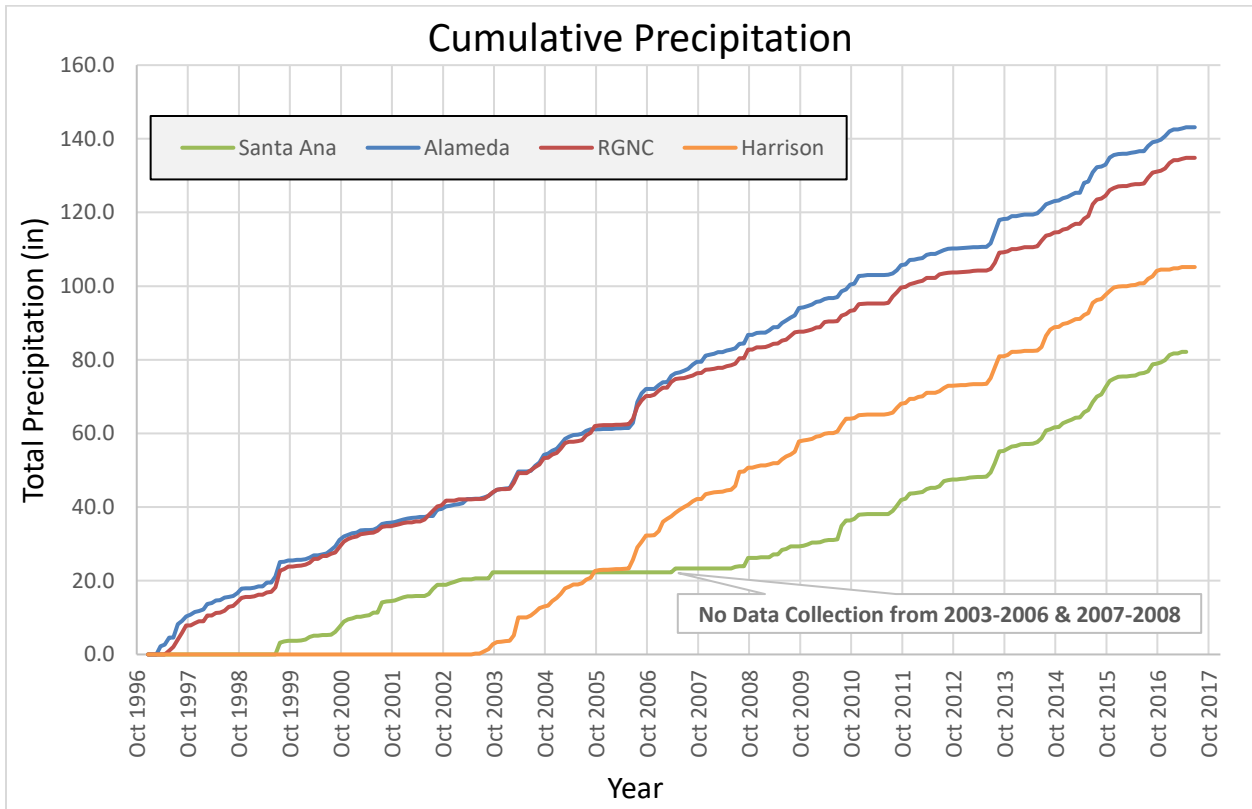


Figure 2-3 Cumulative monthly precipitation near the Montaño Reach (1996 – 2017).

2.2 River Flow

2.2.1 USGS Gage Data

Information regarding river flow was gathered from the United States Geological Survey (USGS) National Water Information System. The gages relevant to the study area are included in **Table 2-1**, and gage locations are shown in **Figure 2-4**. The gages highlighted in purple were chosen for closer analysis due to their location, longer period of record, and/or sediment data record.

Table 2-1 List of Relevant USGS Gages

Reach	Station Name	Station #	Mean Daily Discharge	Suspended Sediment
Upstream	Rio Grande at Otowi Bridge, NM	08313000	February 2, 1895 to September 10, 2022	October 1, 1955 to September 30, 2021
	Rio Grande at Cochiti, NM (Historical)	08314500	June 1, 1926 to October 30, 1970	No Data
	Rio Grande Below Cochiti Dam, NM	08317400	October 1, 1970 to Present	July 1, 1974 to September 29, 1988
	Rio Grande At San Felipe, NM	08319000	January 1, 1927 to Present	No Data
	Jemez River Below Jemez Canyon Dam (Historical)	08329000	April 1, 1936 to September 29, 2009	November 15, 1955 to September 30, 2021
	Jemez River Outlet Below Jemez Dam, NM	08328950	September 30, 2009 to Present	No Data
Bernalillo Reach	Rio Grande Near Bernalillo, NM (Historical)	08329500	October 1, 1941 to September 29, 1969	October 1, 1955 to September 29, 1969
	Rio Grande at Alameda Bridge at Alameda, NM	08329918	July 4, 2003 to October 12-2020	No Data
	Rio Grande Nr. Alameda, NM	08329928	March 1, 1989 to October 12-2021	No Data
Montaño Reach	Rio Grande At Albuquerque, NM	08330000	October 1, 1965 to Present	October 1, 1969 to September 29, 2020
	Rio Grande At Isleta Lakes Nr. Isleta, NM	08330875	October 1, 2002 to September 18, 2021	No Data
Down-Stream	Rio Grande Near Bosque Farms, NM	08331160	March 16, 2006 to Present	No Data

**Note: Gages highlighted in purple were chosen for closer analysis due to their location, longer period of record, and/or sediment data record*

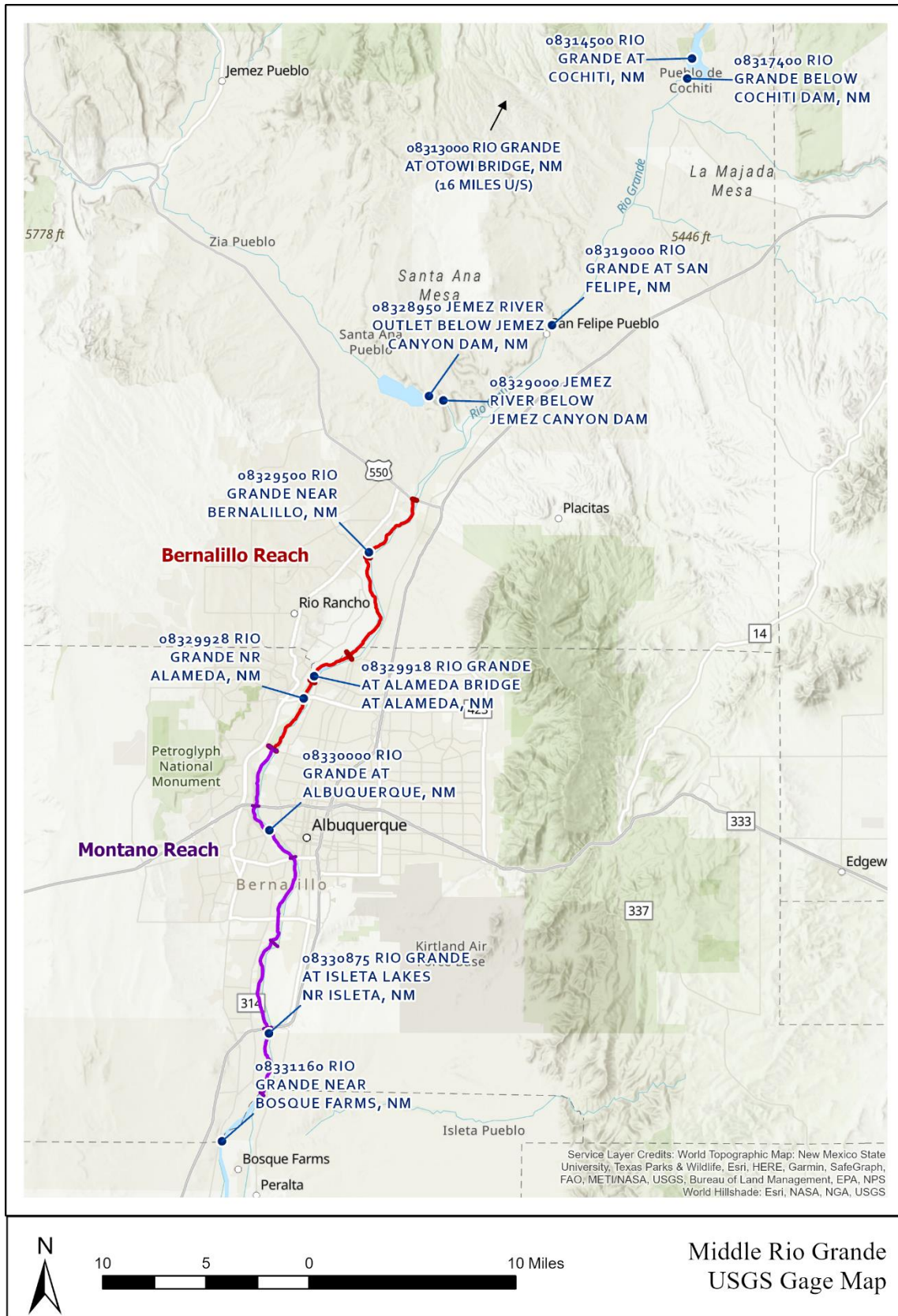


Figure 2-4. USGS gage data overview map

Construction of the Cochiti Dam commenced in 1965 and was completed in 1973. A USGS gage (08317400) was installed in 1970 during construction of the dam. Prior to dam completion, a historical gage (08314500) with a period of record between 1926 and 1970 was located 1 mile upstream of the current operating gage. The current operating gage at Cochiti Dam has sediment data for a 66-year period of record between 1974 and 2021. Given the location of this gage directly downstream of the dam, it serves as a baseline for the sediment loading prior to any sediment input from tributaries or from bank and bed erosion along the Rio Grande.

Construction of the Jemez Dam was completed in 1953. A historical gage (08329000) was installed upstream of the Jemez River and Rio Grande confluence in 1936, 17 years prior to Jemez Dam construction, and has a period of record of 73-years of flow data between 1936 and 2009. This gage also has a 71-year sediment record extending between 1955 and 2021; however, the record shows 0 tons/day of suspended sediment load between 1958 and 2014, indicating that sediment was not sampled during this time. In 2009, a new gage (08328950) that is currently operational was installed 0.7 miles upstream of the historical gage. This gage only records flow data. Due to the proximity of the gages, the flow records for USGS Gage 08329000 and 08328950 were combined for this analysis. In 2014, a pass-through channel was constructed through the Jemez Dam to allow for sediment passage through the dam. At the time of this study, 7 years of sediment data are available to evaluate any effects that the additional sediment loading has had on the Bernalillo and Montaña Reaches. See **Section 2.3** for additional information on the sediment loading through the Bernalillo and Montaña Reaches.

The San Felipe gage (08319000) is located 10 miles upstream of the Bernalillo reach and 7 miles upstream of the Rio Grande confluence with the Jemez River. This gage is still operational today and has a period of record of 95 years, between 1927 and 2022. This gage has a significant period of record both before and after the construction of Cochiti Dam in 1973 and, consequently, was the ideal candidate to evaluate the effects of the dam on flow and characteristics within the Bernalillo and Montaña Reaches. This gage does not include sediment data.

The historical gage near Bernalillo (08329500), located in Subreach B1 near Agg/Deg 337, has 28 years of flow data between 1941 and 1969 as well as 14 years of sediment data between 1955 and 1969. Combined with the Albuquerque gage (below), this gage was useful in evaluating sediment loading within the Bernalillo and Montaña Reaches.

The Albuquerque gage (08330000) has been in operation from 1965 to present and has a sediment record between 1969 and 2020, located in Subreach M2 of the Montaña Reach at Central Ave. in Albuquerque. Sediment data from this gage was helpful in evaluating sediment loading within the Bernalillo and Montaña Reaches of the MRG.

2.2.2 Raster Hydrographs

The raster hydrographs of daily discharge at the gages located directly downstream of the Jemez Dam are shown in **Figure 2-5**. Both gages are operational today, with a period of record of 95 years for the San Felipe gage and 57 years for the Albuquerque gage. These raster hydrographs show seasonal flow patterns, with peak flows often occurring from snowmelt runoff in April through June, low flow throughout the rest of the summer (except for strong summer thunderstorms), and medium flow from November onwards representing the end of the irrigation season. These raster hydrographs also highlight differences in flood magnitude before and after the Cochiti dam construction in 1970. Prior to 1970, the San Felipe gage shows long duration spring flood events that are sometimes on the order of magnitude between 8,000 cfs and 20,000 cfs. Conversely, the Albuquerque gage after 1970 shows these longer duration spring floods on an order of magnitude between 4,000 cfs and 6,000 cfs.

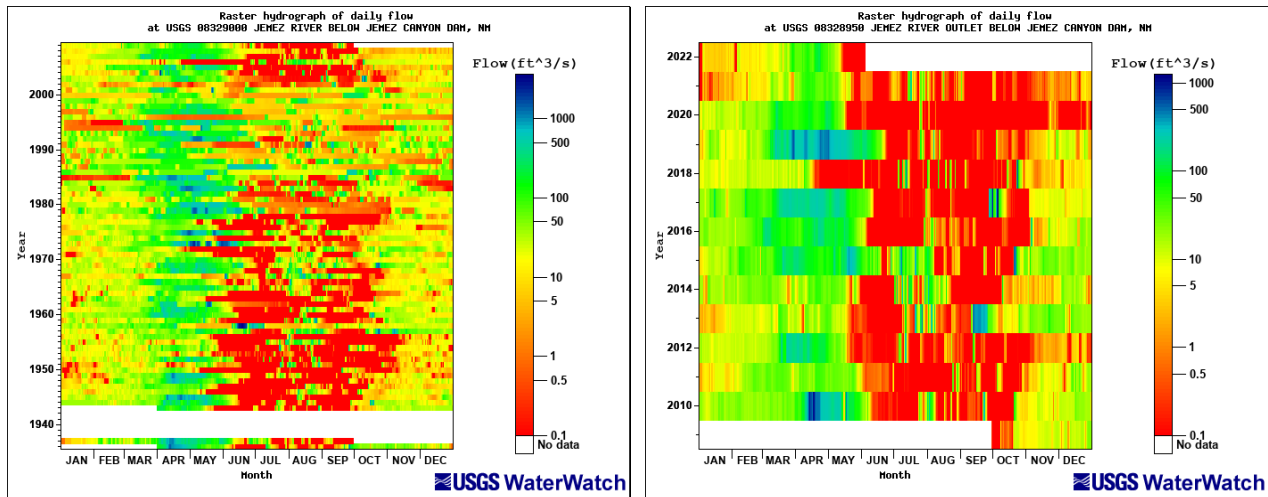


Figure 2-5 Raster hydrograph of daily discharge at USGS Station 08329000 (left) and USGS Station 0832950 (right) below the Jemez Dam. (Source: <https://waterwatch.usgs.gov>).

The raster hydrographs of daily discharge at the gages located directly downstream of the Jemez Dam are shown in **Figure 2-6**. The combined period of record for these gages is 86 years between 1936 and present. The figures show seasonal flow patterns, with peak flows often occurring from snowmelt runoff in April through June, low flow throughout the rest of the summer (except for strong summer thunderstorms), and medium flow from November onwards representing the end of the irrigation season. The Jemez River regularly experiences very low flows (below 1 cfs) or no flow during long periods of the summer season.

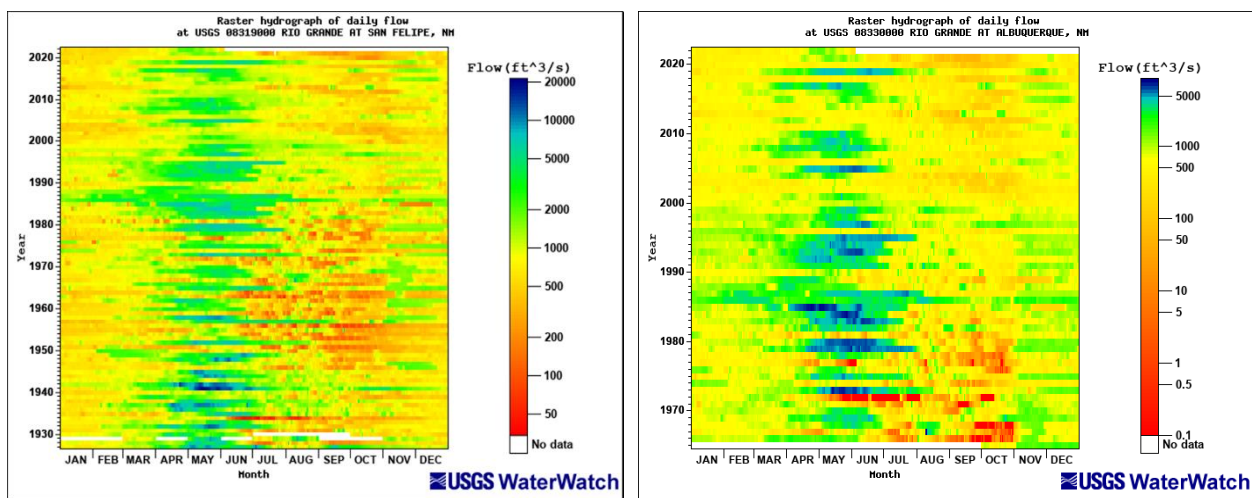


Figure 2-6 Raster hydrograph of daily discharge at USGS Station 08319000 at San Felipe (left) and USGS Station 08330000 at Albuquerque (right). (Source: <https://waterwatch.usgs.gov>)

2.2.3 Yearly Peak Flow Events

Yearly peak flow events for the Cochiti, San Felipe, and Albuquerque gages are shown in **Figure 2-7** and **Figure 2-8**. These peak flow events were determined from average daily flow data. **Figure 2-7** shows the yearly peak flow events prior to the Cochiti Dam completion in 1970, while **Figure 2-8** shows the peak events after dam completion to present day. Like the raster hydrographs shown above, these graphs show a clear distinction between pre- and post-dam conditions. In the 44 years of gage record prior to Cochiti Dam completion there were 11 flood events with peak daily flows larger than 10,000 cfs. In the 52 years of gage record after dam completion, peak flows became less variable and have not peaked above 9,000 cfs.

The flood of record at these gages occurred in May of 1941, with a peak of 21,300 cfs at the San Felipe gage. The following April of 1942 had the second largest recorded flood, with a peak of 17,200 cfs at the San Felipe gage. The 3 years between 1983 and 1985 show larger than normal spring flood events, with a peak flood at 8,100 cfs in May 1985 at the San Felipe gage. The more recent larger flood events occurred in May of 2017 and June of 2019, with daily peak flows of 5,800 cfs and 6,200 cfs, respectively.

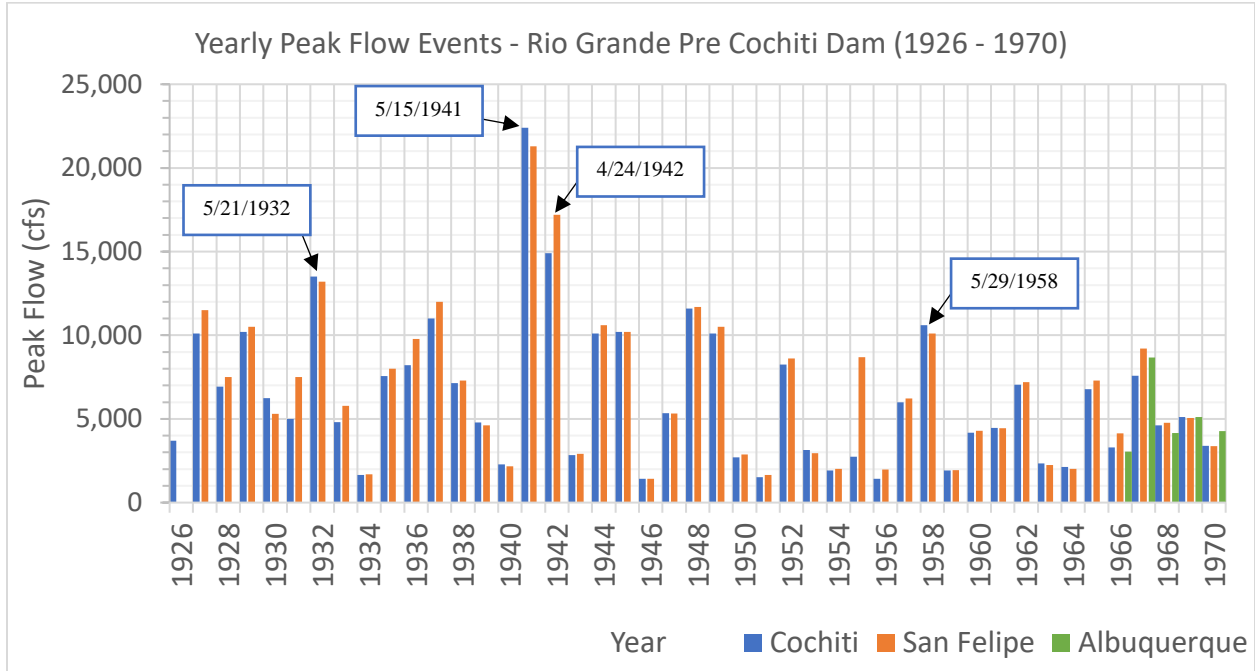


Figure 2-7 Yearly peak flow events for the Rio Grande before Cochiti Dam at historical USGS gage 08314500 (1926-1970) and USGS Gage 08317400 (1970-present).

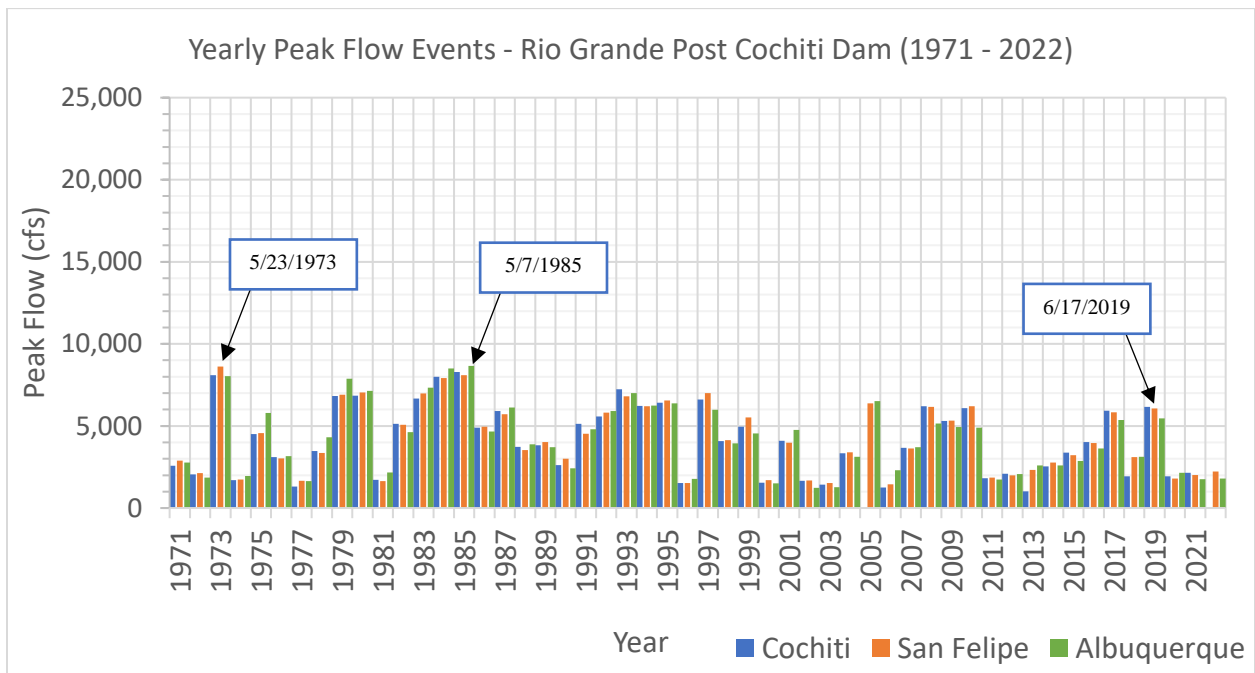


Figure 2-8 Yearly peak flow events for the Rio Grande after Cochiti Dam at USGS Gage 08317400 (1970-present).

Yearly peak flow events for the Jemez River gages are shown in **Figure 2-9**. The flow record does not show a clear influence on peak flow rates for the Jemez River caused by completion of the Jemez Dam in 1953, although this may be due to an insufficient length of gage record prior to 1953. The largest flood event for the period of record occurred in June of 1958, with a daily peak flow rate of 3,640 cfs. This timing corresponds to a large flood event along the Rio Grande that occurred in May of 1958 and had a peak flow rate of 10,100 cfs. A large flood event with a peak flow rate of 2,410 cfs, occurring in May of 1973, also corresponds with flooding along the Rio Grande in May of 1973.

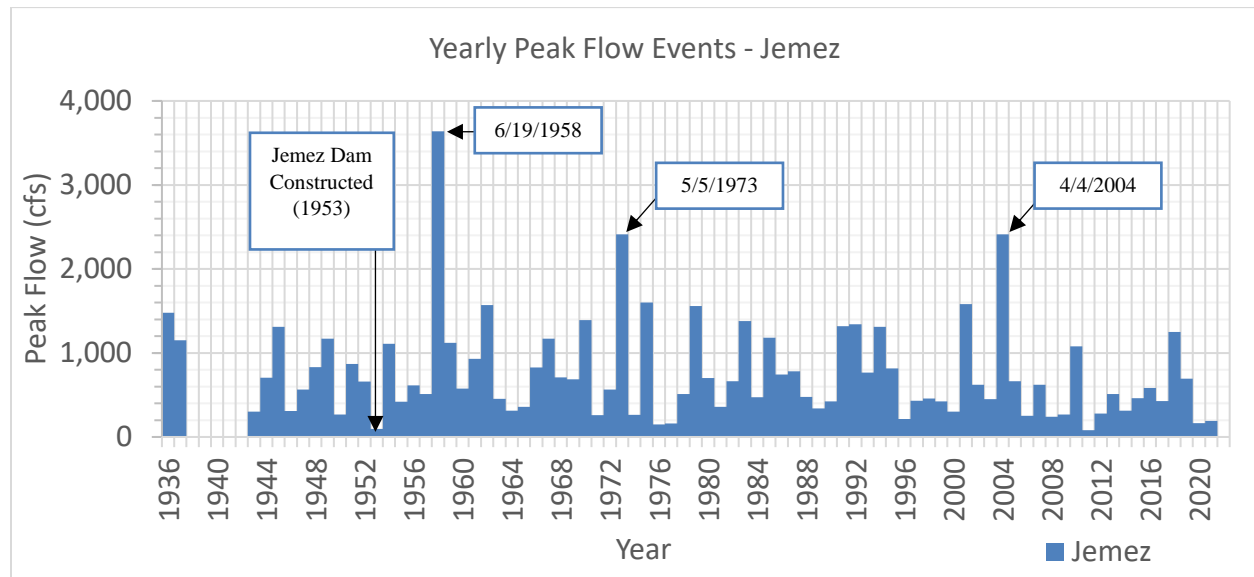


Figure 2-9 Yearly peak flow events for the Jemez River

2.2.4 Cumulative Discharge Curves

Cumulative discharge curves show changes in annual flow volume over a given time period. The slope of the line of the mass curve gives the mean annual discharge, while breaks in the slope show changes in flow volume trends. **Figure 2-10** through **Figure 2-14** show the single mass curves at Cochiti, San Felipe, and Albuquerque. The gage records for Cochiti and San Felipe were split into pre- and post-dam construction, with October of 1970 chosen as the break point, because there was sufficient record before and after dam construction to compare differences in flow trends. The gage record at Albuquerque only begins 8 years before completion of the dam, and so the full gage record was shown in one graph. The single mass curves were divided into time periods of similar slopes to analyze long term patterns in discharge. While cumulative discharge plots are particularly useful for analyzing long-term trends in flows, occasionally, large flow-altering events can be identified from spikes in the curve.

The pre- and post-dam mass curves for Cochiti are shown by **Figure 2-10** and **Figure 2-11**, respectively. Between 1926 and 1941, the mean discharge was 1,375 cfs. The curve becomes steeper for a short time between spring of 1941 and fall of 1942, which corresponds to the two large flood events that occurred, as described above in **Section 2.2.3**. Between 1943 and 1970 the trend flattens out, with an average flow rate of 1,113 cfs.

In the years following dam completion until 1979 the slope of the curve flattens, giving an average flow rate of 966. Between 1979 and 1995 the slope of the curve steepens to an average flow rate of 1,714 cfs, indicating that this is a wetter than normal period. This trend can also be seen in the yearly peak flood events shown by **Figure 2-8** (above). Between 1995 and present day the slope of the curve again flattens, giving an average flow rate for this period of 974 cfs. Similar trends can be seen in the San Felipe and Albuquerque mass curves shown in **Figure 2-12** through **Figure 2-14**.

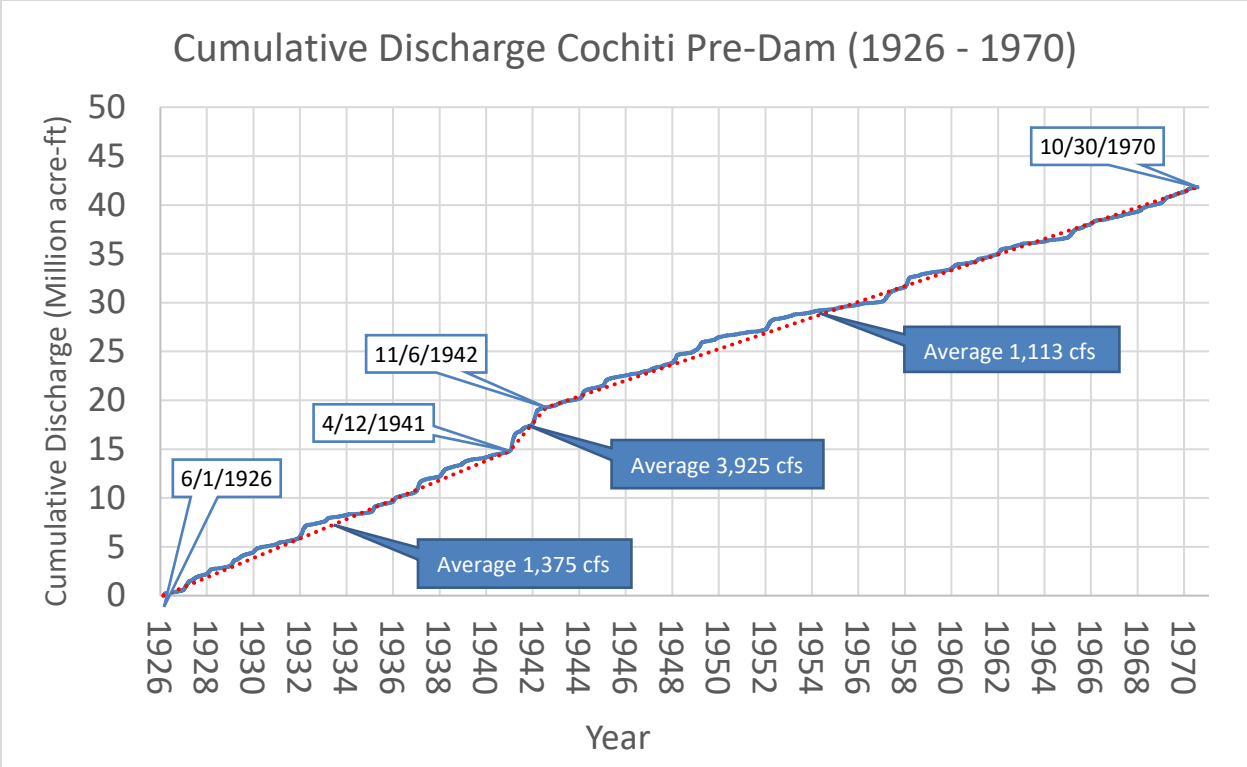


Figure 2-10 Discharge single mass curve at historical USGS gage 8314500 (Cochiti) before dam construction.

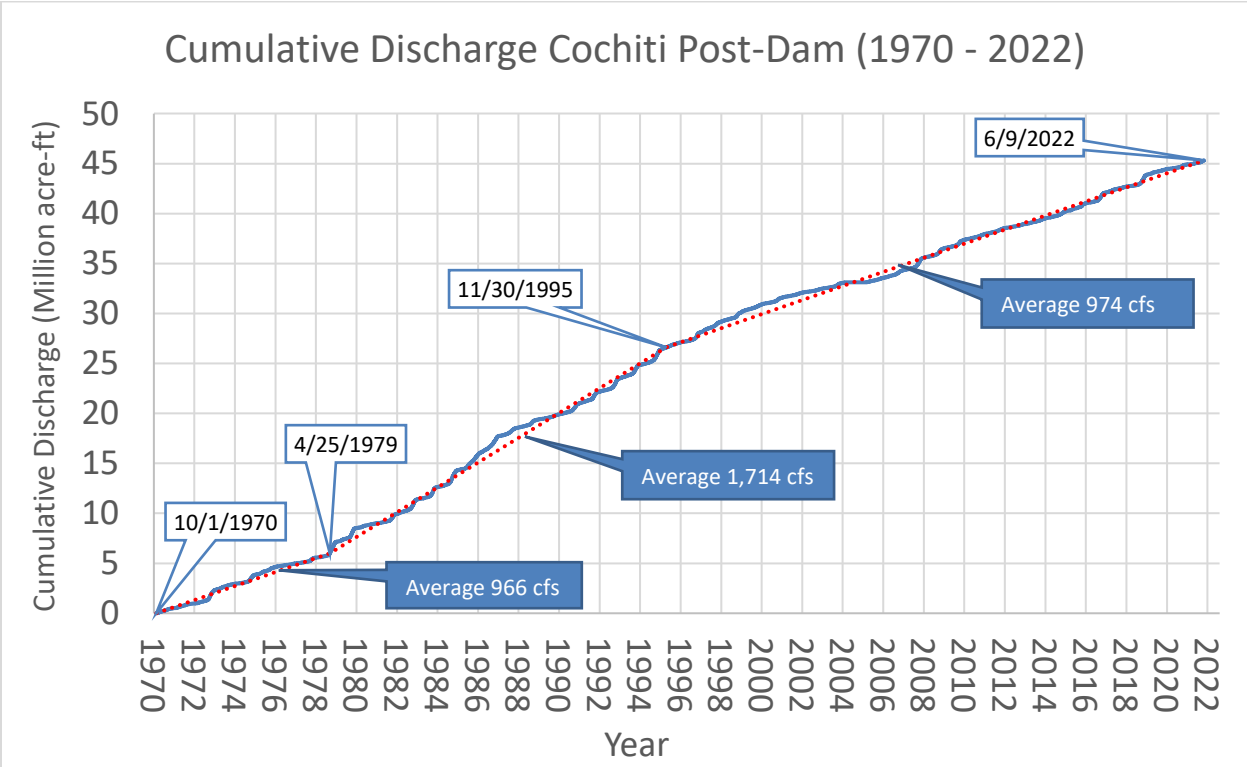


Figure 2-11 Discharge single mass curve at USGS gage 08317400 (below Cochiti Dam) after dam construction.

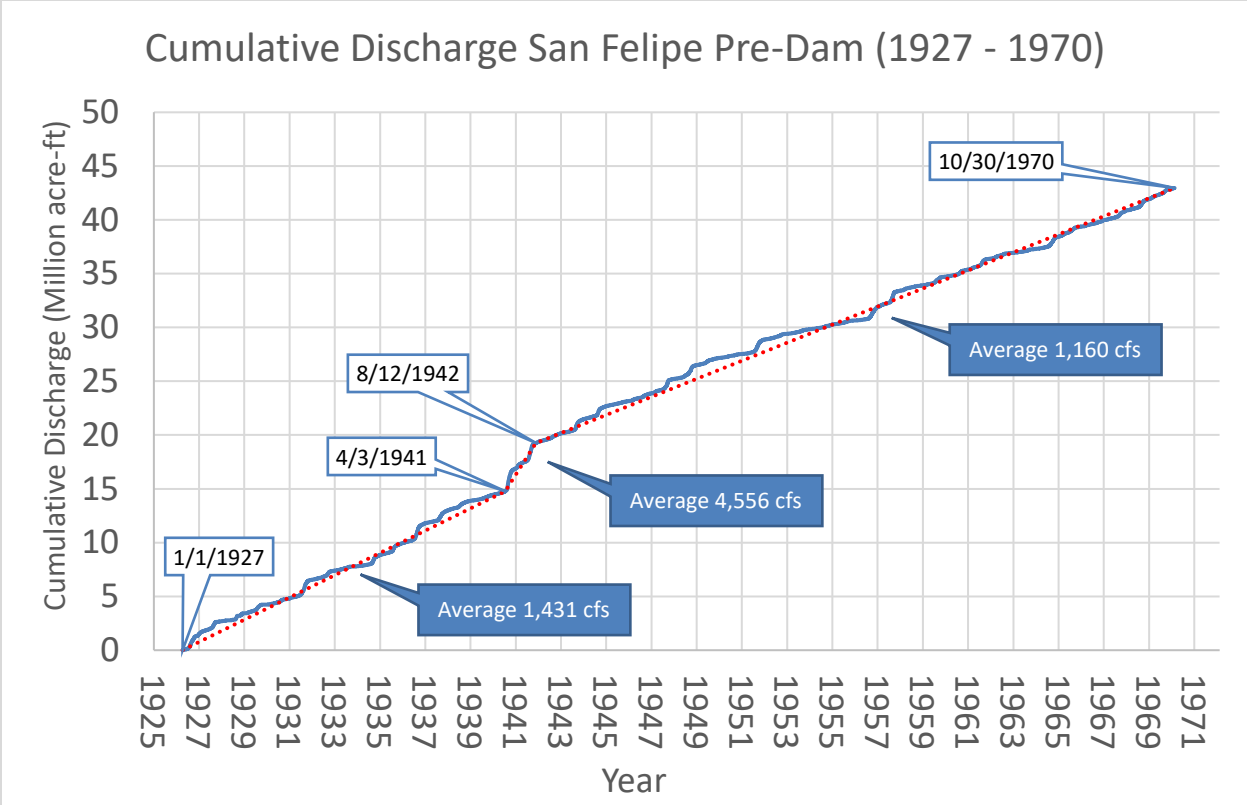


Figure 2-12 Discharge single mass curve at USGS gage 08319000 (San Felipe) before dam construction.

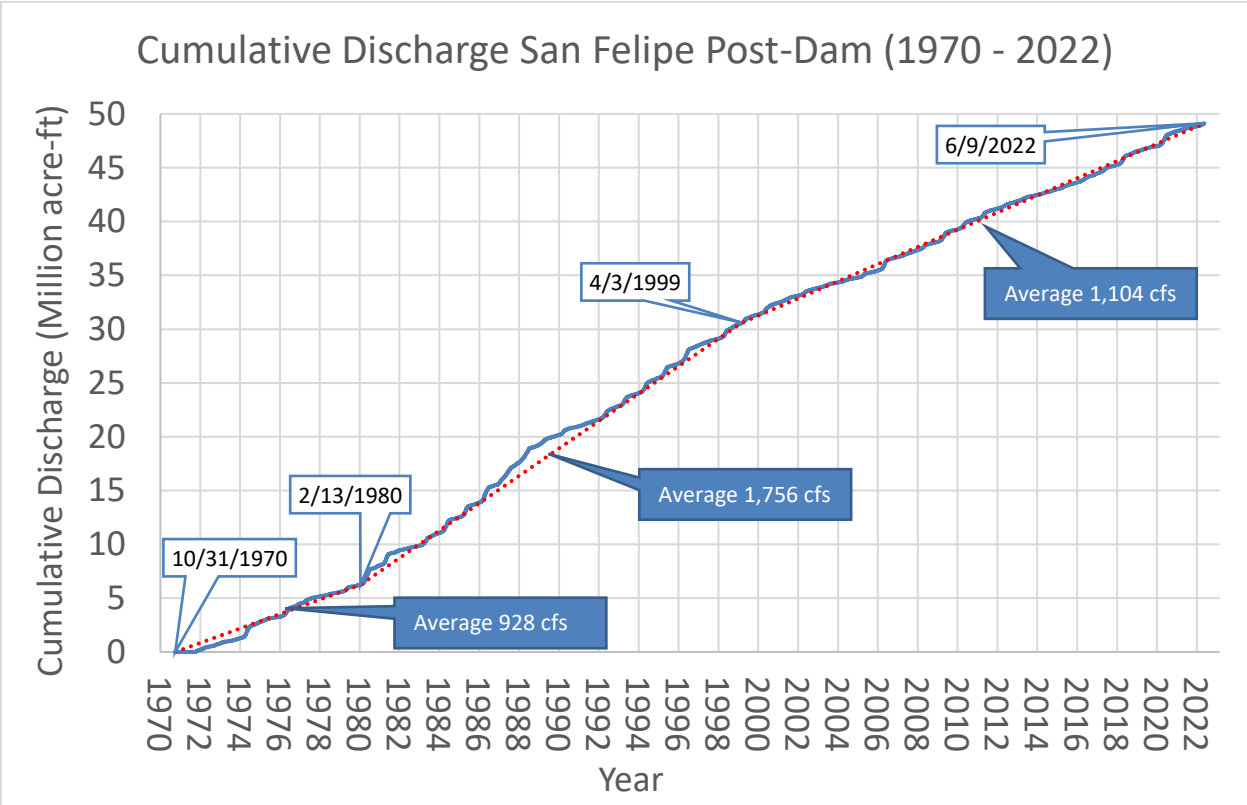


Figure 2-13 Discharge single mass curve at USGS gage 08319000 (San Felipe) after dam construction.

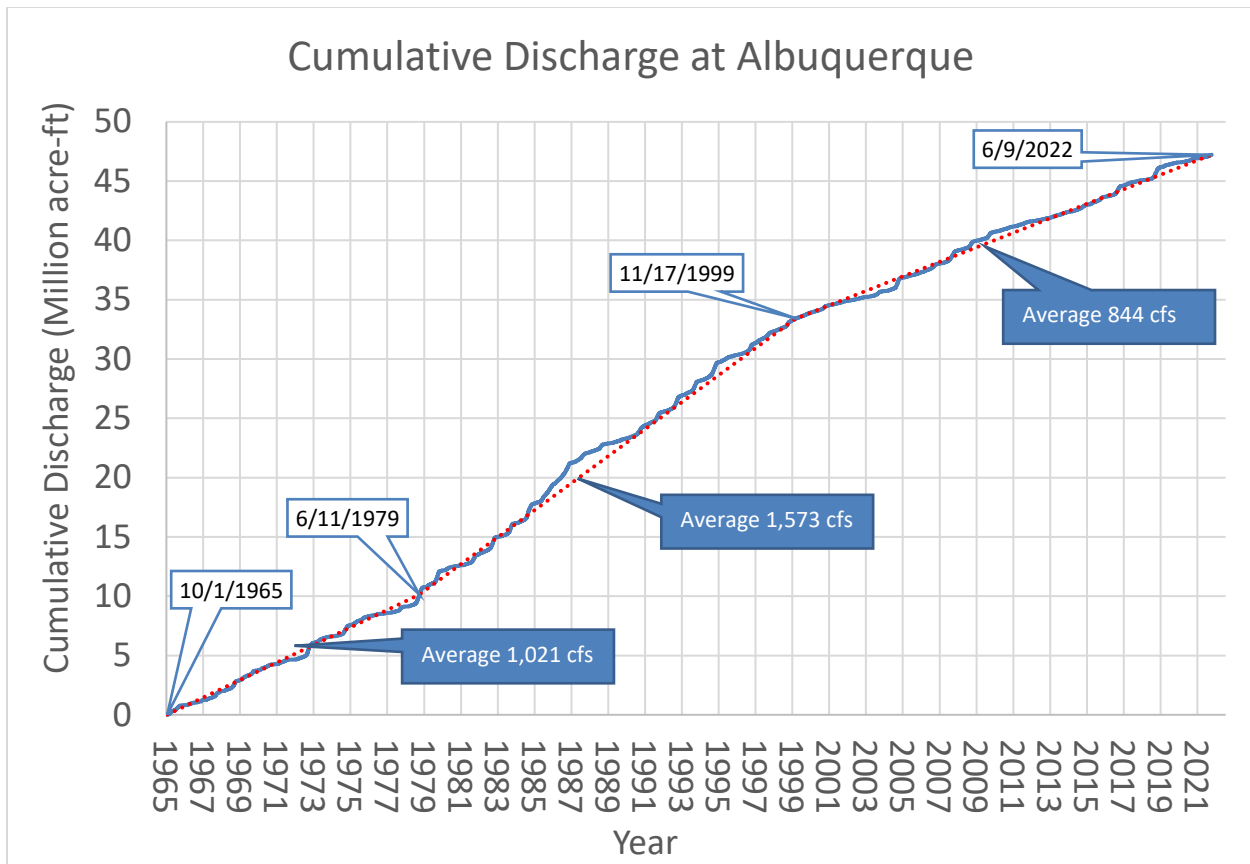


Figure 2-14 Discharge single mass curve at USGS gage 08330000 (Albuquerque).

Figure 2-15 and Figure 2-16 show the single mass curves at the Jemez River gages. These gage records were also split into pre- and post-dam construction to compare differences in flow trends. No flow record is available between September of 1937 and March of 1943. In the two years before this gap, the average flow rate was 123 cfs. In the 10 years between 1943 and dam completion in 1953, the average flow rate was 47 cfs.

In the 26 years following completion of the dam between 1953 and 1979, the average flow rate is 54 cfs. The period between 1979 and 1995 show a similar trend of wetter than normal years as the Rio Grande gages, with an average flow rate increasing to 89 cfs. Between 1995 and present day the slope of the curve flattens, giving an average flow rate of 42 cfs.

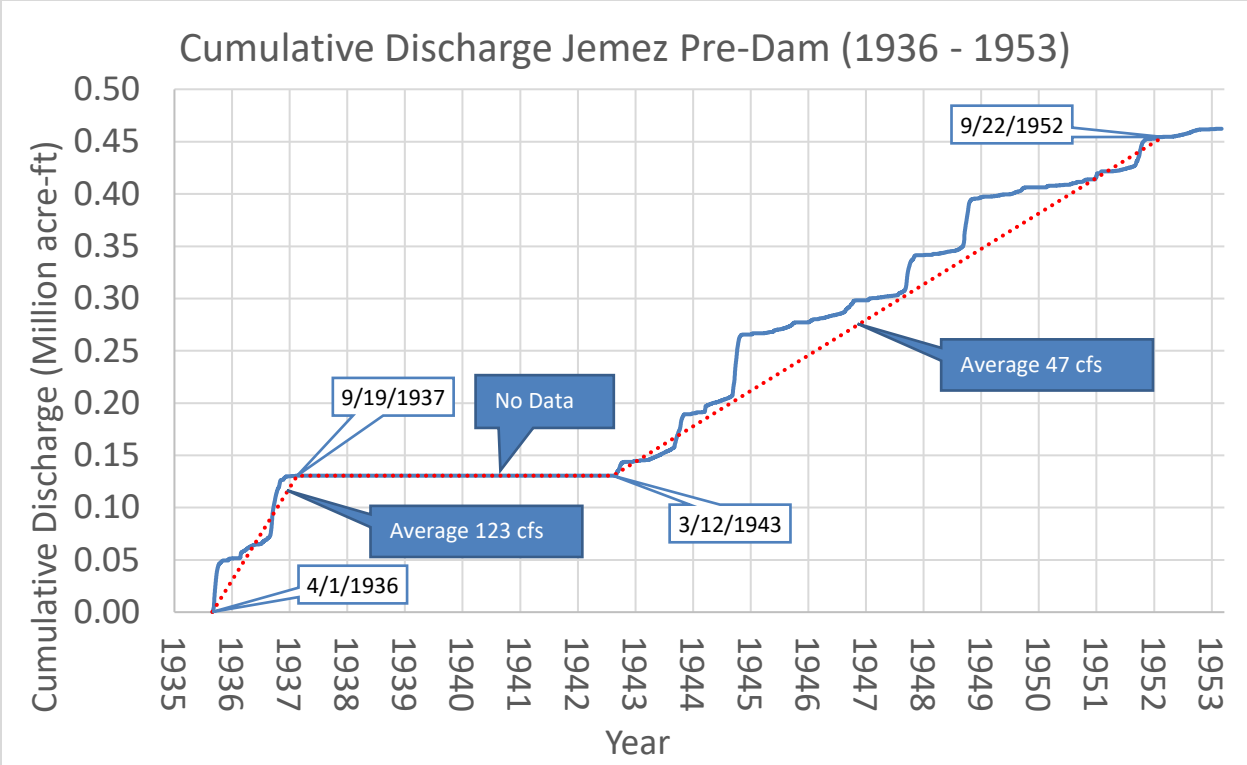


Figure 2-15 Discharge single mass curve at historical USGS gage 08329000 (Jemez) before dam construction in 1953.

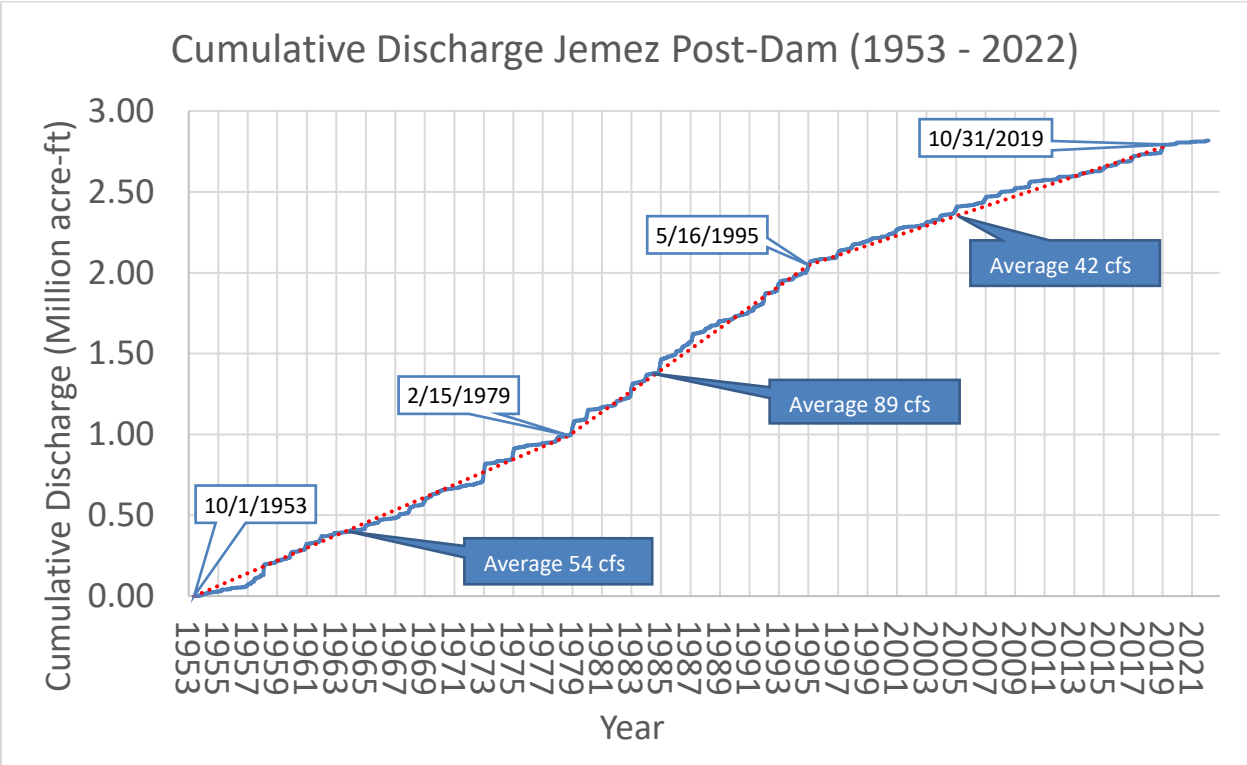


Figure 2-16 Discharge single mass curve at historical USGS gage 08329000 and USGS gage 08328950 (Jemez) after dam construction in 1953.

2.2.5 Flow Duration

Flow duration curves were developed using the mean daily flow discharge values for the Cochiti, San Felipe, Albuquerque, and Jemez River gages. **Table 2-2** shows the probabilities of daily exceedance values calculated from the flow duration curves for a range of exceedance probabilities. The gage records were split between pre- and post- construction of the Cochiti Dam for the Rio Grande gages. Gage records were similarly split for the Jemez River gages to account for any differences in flow conditions before and after the completion of the Jemez Dam. The curves for the Rio Grande gages are shown in **Figure 2-17**, and the curves for the Jemez River gages are shown in **Figure 2-18**.

While more frequent flood events with daily exceedance probabilities less than 10% do not appear to be significantly impacted by the Cochiti Dam, the less frequent flood events greater than 10% exceedance probability show a clear divergence between pre and post Cochiti Dam construction (**Figure 2-17**). The 1% daily exceedance probability shows a 3,000 cfs reduction in flow magnitude after completion of the dam. This does not appear to be the case for the Jemez Dam for the period of record. **Figure 2-18** shows a similar pattern in flows before and after the completion of the Jemez Dam in 1953.

Table 2-2 Probabilities of daily exceedance

Daily Probability of Exceedance	Discharge (cfs)						
	Pre Cochiti Dam (1926 to 1970)		Post Cochiti Dam (1970 - Present)			Pre Jemez Dam (1936 to 1953)	Post Jemez Dam (1953 to Present)
	8314500 Rio Grande at Cochiti, NM	8319000 Rio Grande at San Felipe, NM	8317400 Rio Grande Below Cochiti Dam, NM	8319000 Rio Grande At San Felipe, NM	⁽¹⁾ 8330000 Rio Grande at Albuquerque, NM	⁽²⁾ 8329000 Jemez River Below Jemez Canyon Dam	⁽³⁾ 8329000 & 08328950 Jemez River Below Jemez Dam
	June 1, 1926 to October 30, 1970	January 1, 1927 to September 30, 1970	October 1, 1970 to Present	October 1, 1970 to Present	October 1, 1970 to Present	April 1, 1936 to September 30, 1953	October 1, 1953 to Present
1%	9,280	9,560	6,190	6,320	6,160	750	650
10%	2,860	3,010	2,980	3,100	2,940	110	143
25%	1,320	1,410	1,250	1,330	1,220	36	45
50%	726	780	808	895	704	11	16
75%	487	529	573	651	467	0	2
90%	277	325	383	461	268	0	0

Notes:

⁽¹⁾ The pre-Cochiti Dam gage record between 1965 and 1970 for USGS gage 8330000 at Albuquerque were omitted from this analysis.

⁽²⁾ Six years of missing data between 1938 and 1943 for the USGS 8329000 Jemez River gage.

⁽³⁾ USGS gage 8328950 below Jemez Dam is located approximately 0.7 miles upstream of historical USGS gage 8329000. Gage records were combined for this analysis.

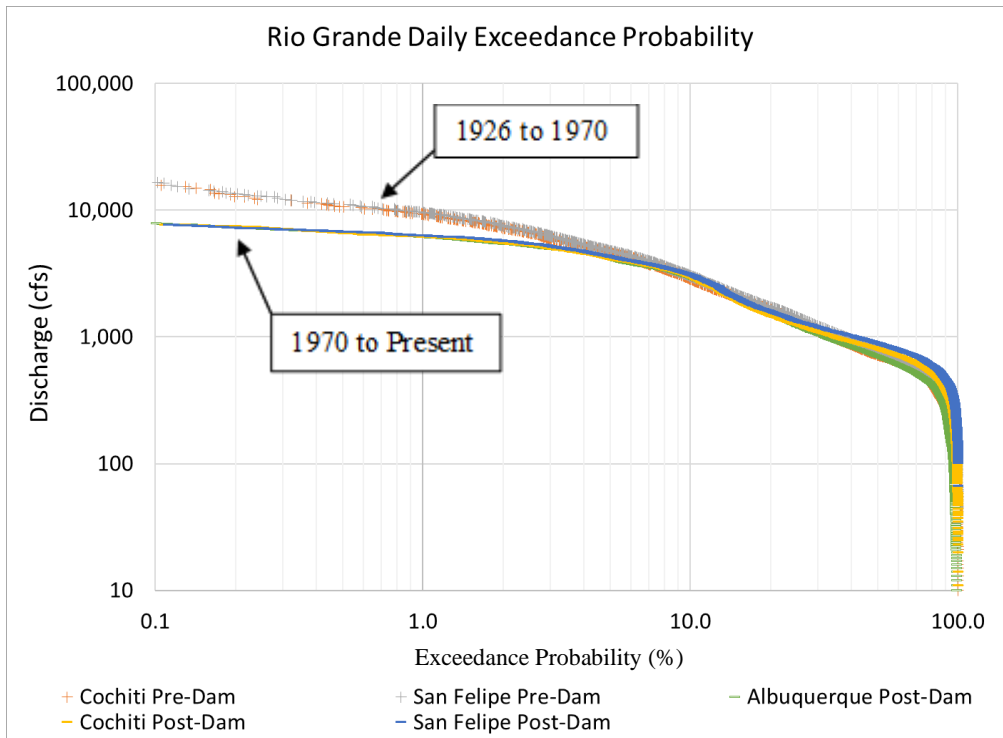


Figure 2-17 Flow duration curves for the Rio Grande gages before and after dam construction in 1970.

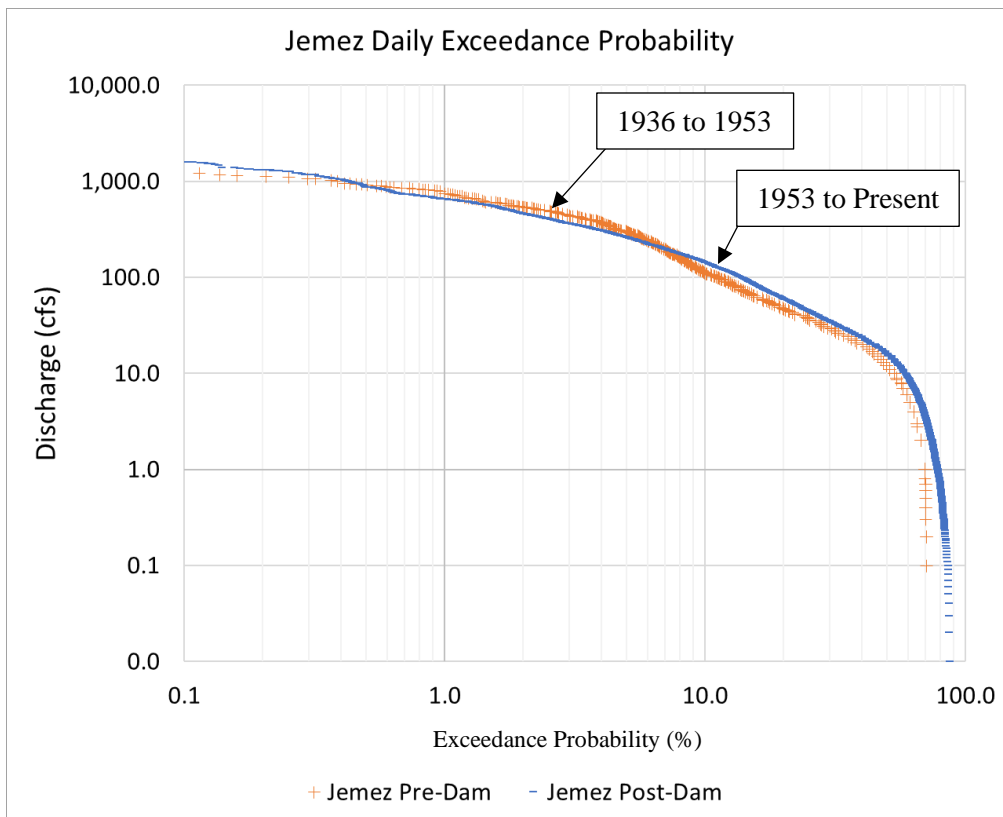


Figure 2-18 Flow duration curves for the Jemez River gages before and after dam construction in 1953.

2.2.6 Days of Flow

In addition to flow duration curves, the number of days in the water year exceeding the identified flow values at each gage were analyzed. This is purely a count of days and does not consider consecutive days. This analysis was performed for the entire record at the Cochiti, San Felipe, and Jemez River gages shown by **Figure 2-19**, **Figure 2-20**, and **Figure 2-21**, respectively. Like previous analyses, the gage records were split between pre and post dam construction for the purposes of comparison.

The Cochiti graphs have a very similar pattern to the San Felipe graphs, which is an indication that these two gages see very similar magnitude of flows. The most notable difference between the Cochiti and San Felipe graphs before and after Cochiti Dam construction is that pre-dam flow conditions saw a greater number of days above 6,000 cfs. The graphs also seem to indicate that the years between 1979 and 1999 show a greater number of days (around half of the year, on average) above 1,000 cfs. These graphs also give a good indication of dry years. For example, between 2003 and 2006, fewer than 50 days of the year saw flows greater than 1000 cfs. In general, the larger flows become less frequent after 2001.

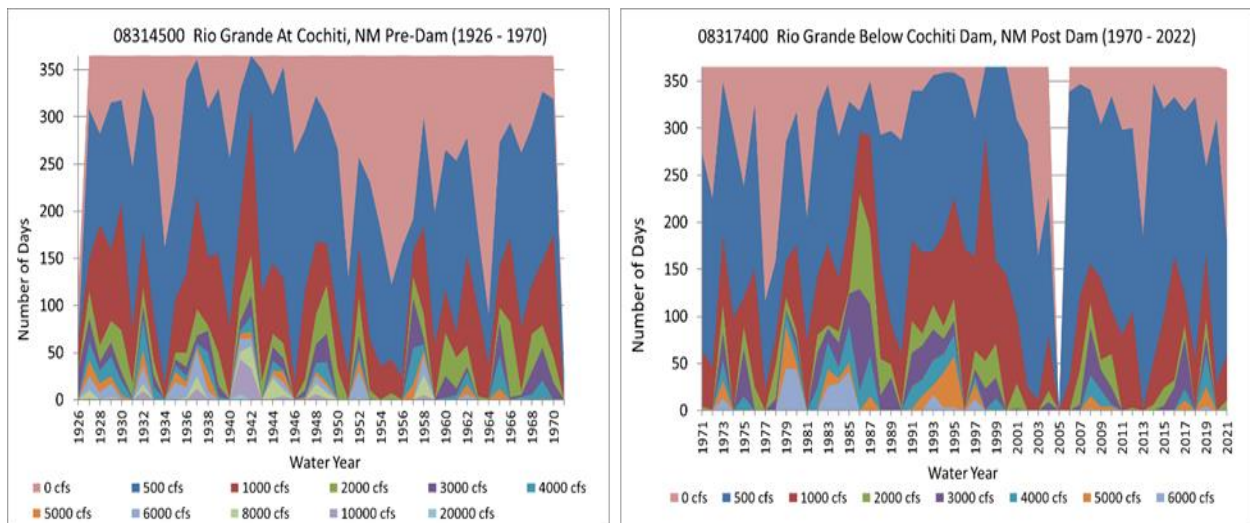


Figure 2-19 Number of days greater than an identified discharge at the Cochiti gages before (left) and after (right) dam construction.

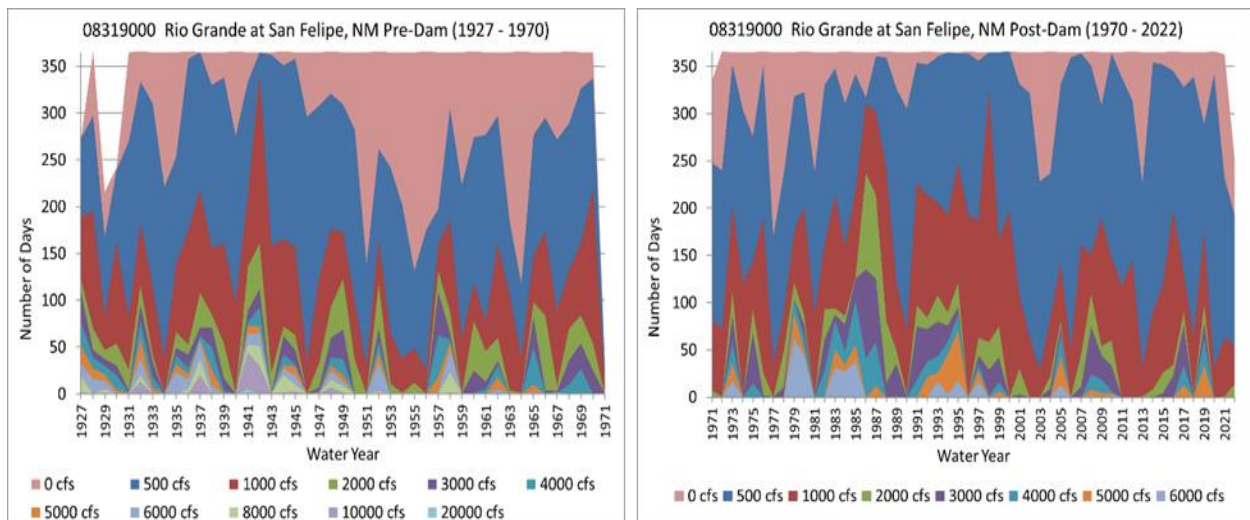


Figure 2-20 Number of days greater than an identified discharge at the San Felipe gage before (left) and after (right) dam construction.

The Jemez River is much more likely to see days with no flow. Before dam construction, the river appears to have had more frequent days with no flow than after dam construction. In the years between 1999 and present day, the Jemez River has generally seen fewer than 100 days of the year with flows greater than 50 cfs.

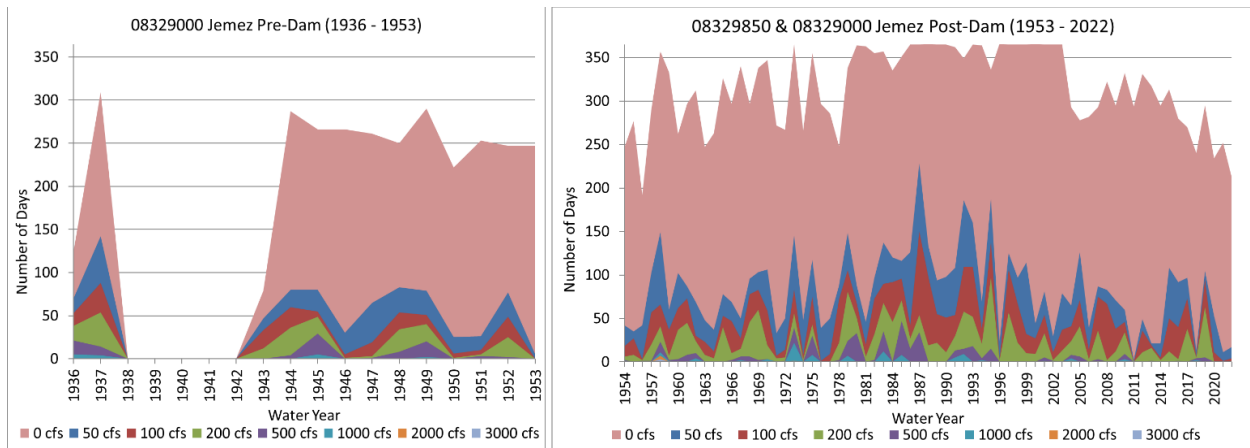


Figure 2-21 Number of days greater than an identified discharge at the Jemez gages before (left) and after (right) dam construction in 1953.

2.3 Suspended Sediment Load

2.3.1 Single Mass Curve

Single mass curves of cumulative suspended sediment (in millions of tons) at the Jemez River (USGS 08329000), Rio Grande Below Cochiti (USGS 08317400), Rio Grande Near Bernalillo (USGS 08329500), and Rio Grande at Albuquerque (USGS 08330000) gages are shown in **Figure 2-22** through **Figure 2-25**, respectively. These curves were created from the average daily sediment data.

The single mass curves show changes in daily sediment volume over a given time period. The slope of the line of the mass curve gives the mean sediment discharge, while breaks in the slope along the single mass curve show the changes in sediment flux. The Cochiti Dam was constructed in 1973. Downstream of Cochiti, at the Albuquerque gage, there is a large decrease in the mean sediment discharge after 1973 and the historical Bernalillo gage data showed large mean sediment discharges before 1973. The correlation shows that the construction of Cochiti Dam had a dramatic impact on the sediment discharge going through the MRG. The mean sediment discharge at the Cochiti gage after construction is relatively low and consistent compared to other inputs to the system, which indicates that a majority of the sediment upstream of Cochiti is getting stopped at the dam. There are no major tributaries that enter the MRG below Cochiti, however there are several small arroyos that enter the river and two flood controlled channels (Towne 2007). As mentioned in **Section 1.1**, the ephemeral tributaries are the primary source of sediment input into to MRG (Fitzner 2018). Other sources of sediment include bed erosion as the channel degrades and bank erosion during channel migration.

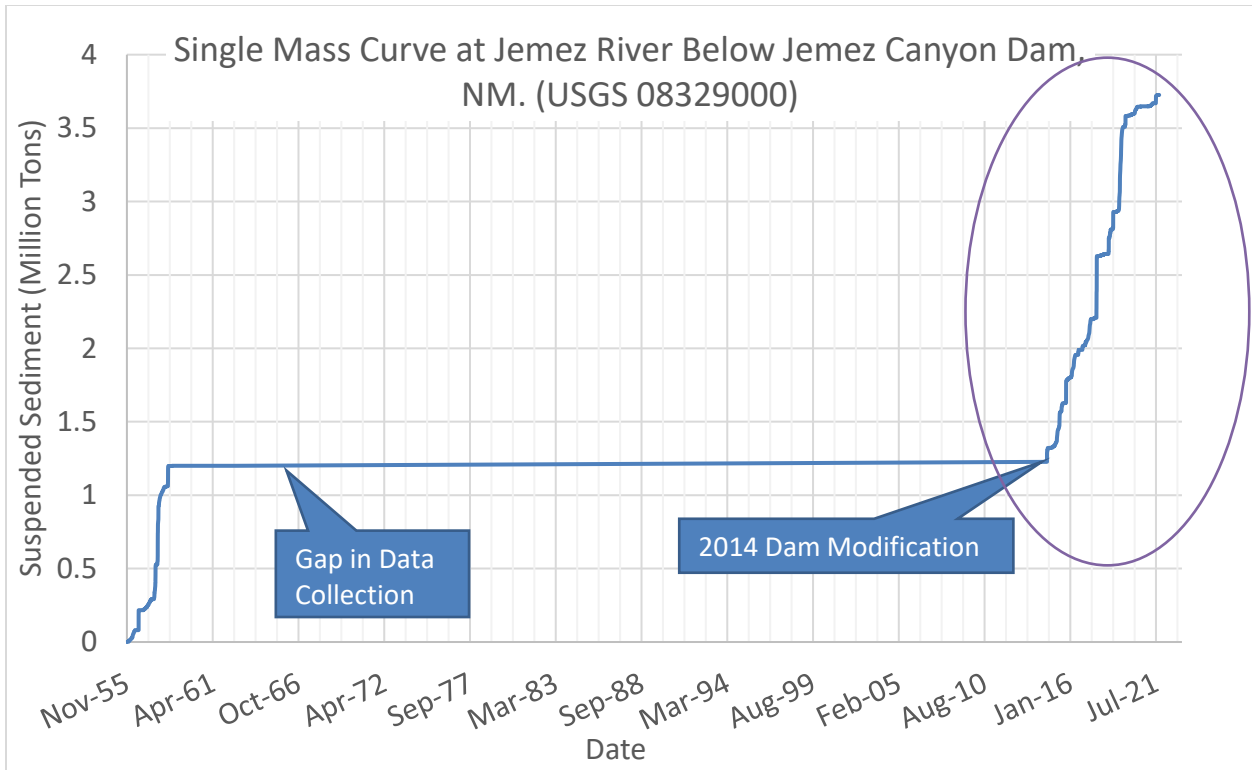


Figure 2-22 Suspended sediment discharge single mass curve for USGS gage 08329000 at Jemez River Below Jemez Canyon Dam, NM

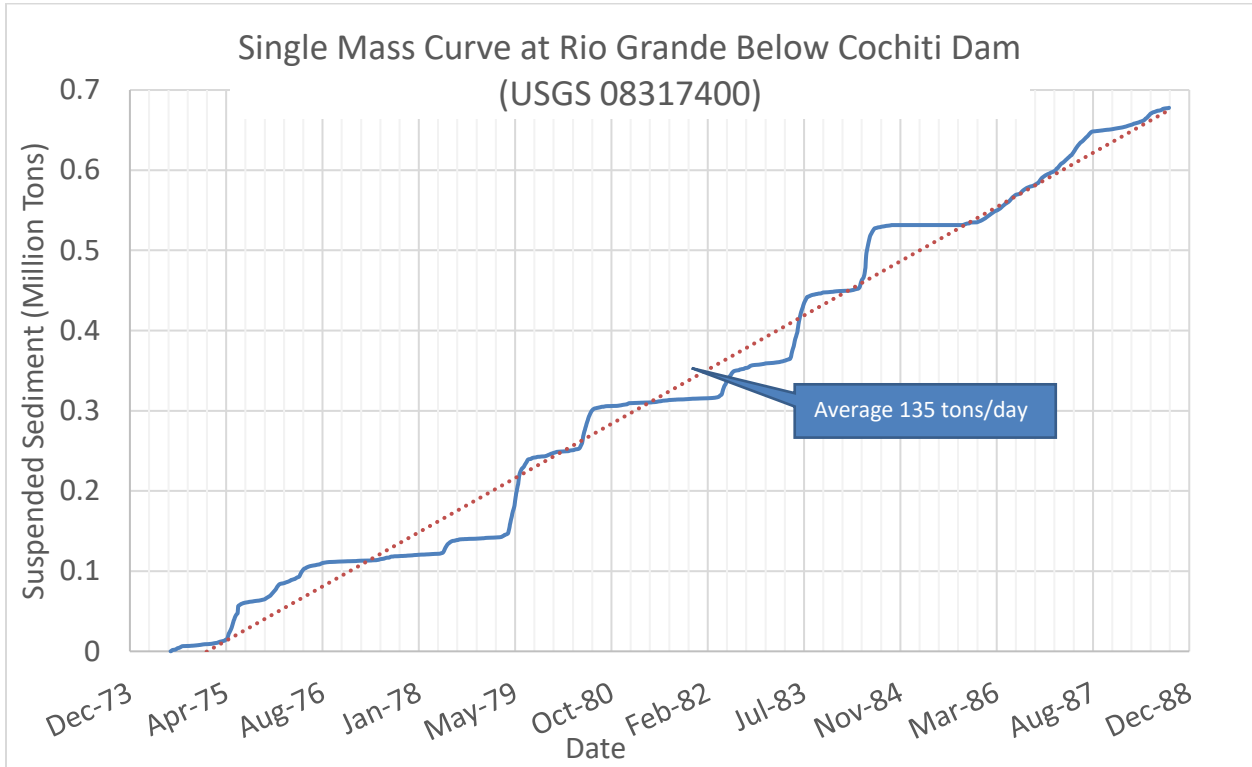


Figure 2-23 Suspended sediment discharge single mass curve for USGS gage 08317400 at Rio Grande Below Cochiti Dam, NM

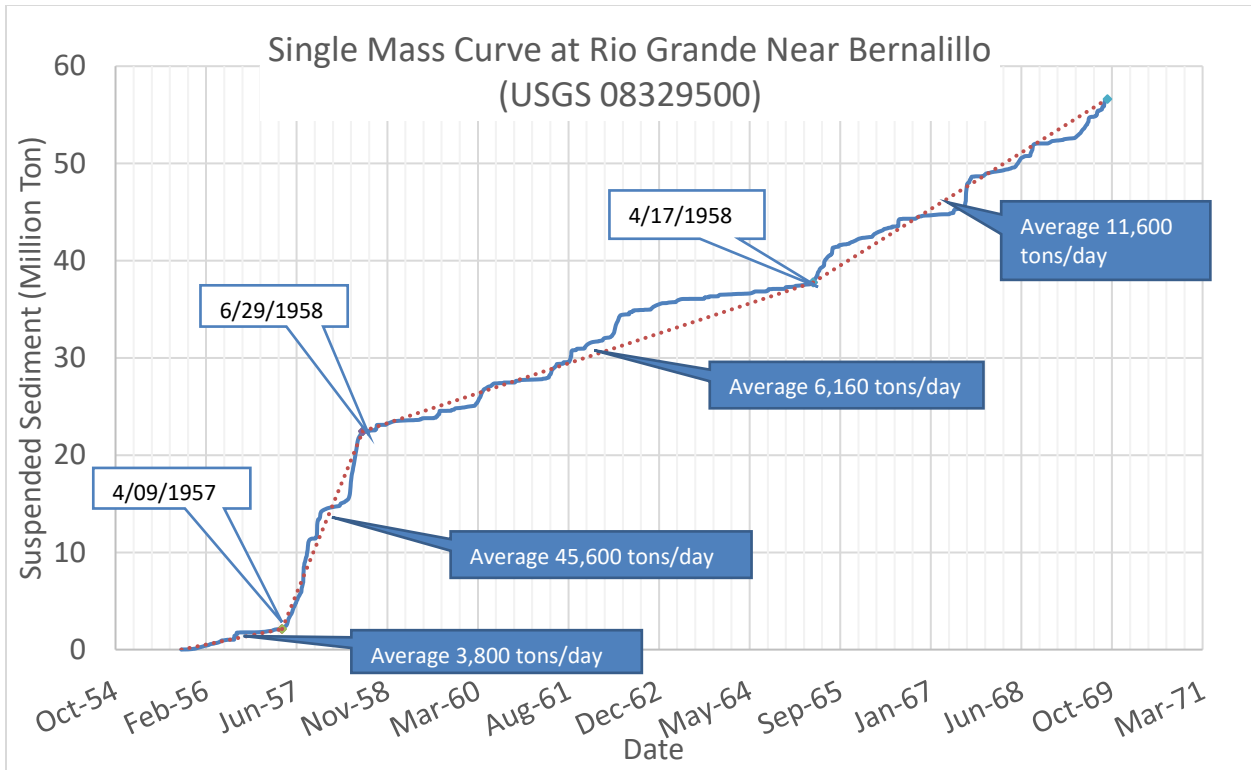


Figure 2-24 Suspended sediment discharge single mass curve for USGS gage 08329500 at Rio Grande Near Bernalillo, NM

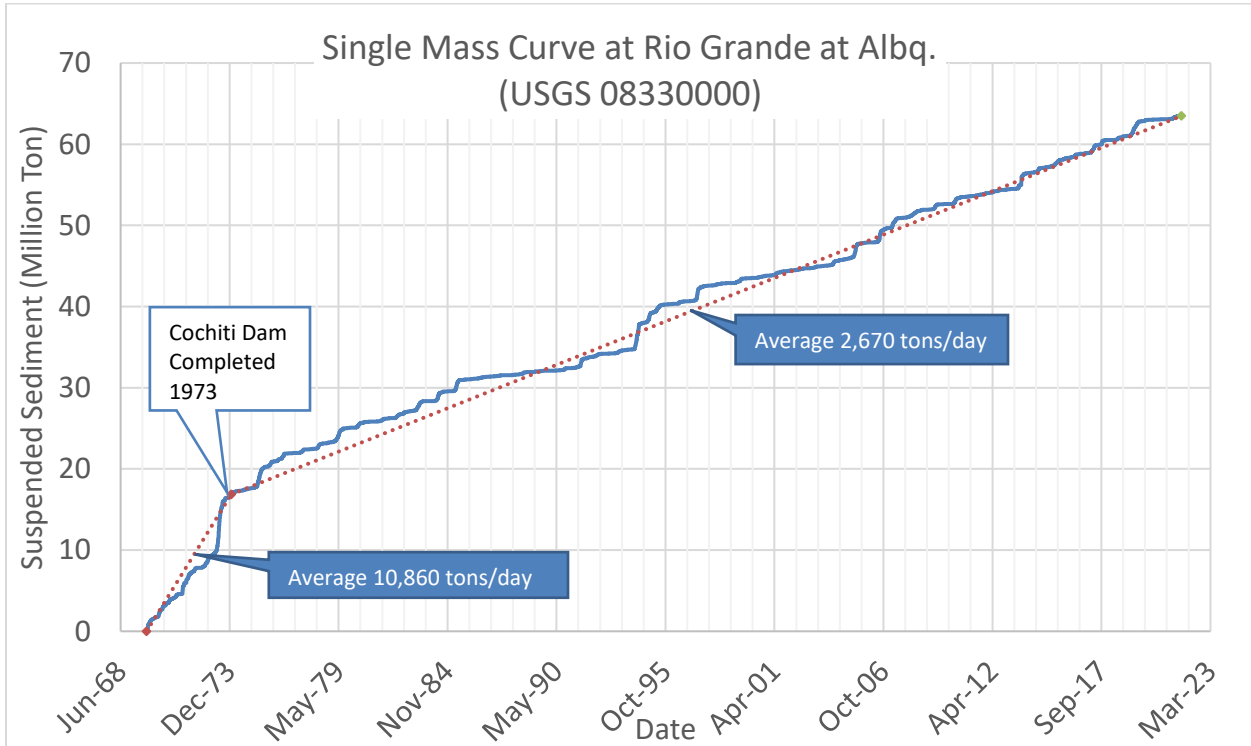


Figure 2-25 Suspended sediment discharge single mass curve for USGS gage 08330000 at Rio Grande at Albuquerque, NM

2.3.2 Double Mass Curve

Double mass curves show how suspended sediment volume relates to the daily discharge volume. The slope of the double mass curve represents the mean sediment concentration. The double mass curve in **Figure 2-26** is for USGS gage Rio Grande at Albuquerque (USGS 08330000).

Figure 2-27 relates the cumulative average monthly suspended sediment at the Rio Grande at Albuquerque (USGS 08330000) gage (located just downstream of Montañó Road) to the cumulative precipitation at the Alameda Precipitation gage. The vertical steps show an increase in suspended sediment occurring without an increase in precipitation. The horizontal steps show an increase in precipitation without an increase in suspended sediment. This stair-step trend shows that at most times, there is not a significant correlation between precipitation and suspended sediment. However, there are monsoonal events that impact the suspended sediment in the Bernalillo and Montañó Reaches. The sections of steep slopes between the stair-step pattern indicate an increase in suspended sediment that is correlated with an increase in precipitation. These represent monsoonal events, such as the monsoonal events that occurred in August 2006 and September 2013.

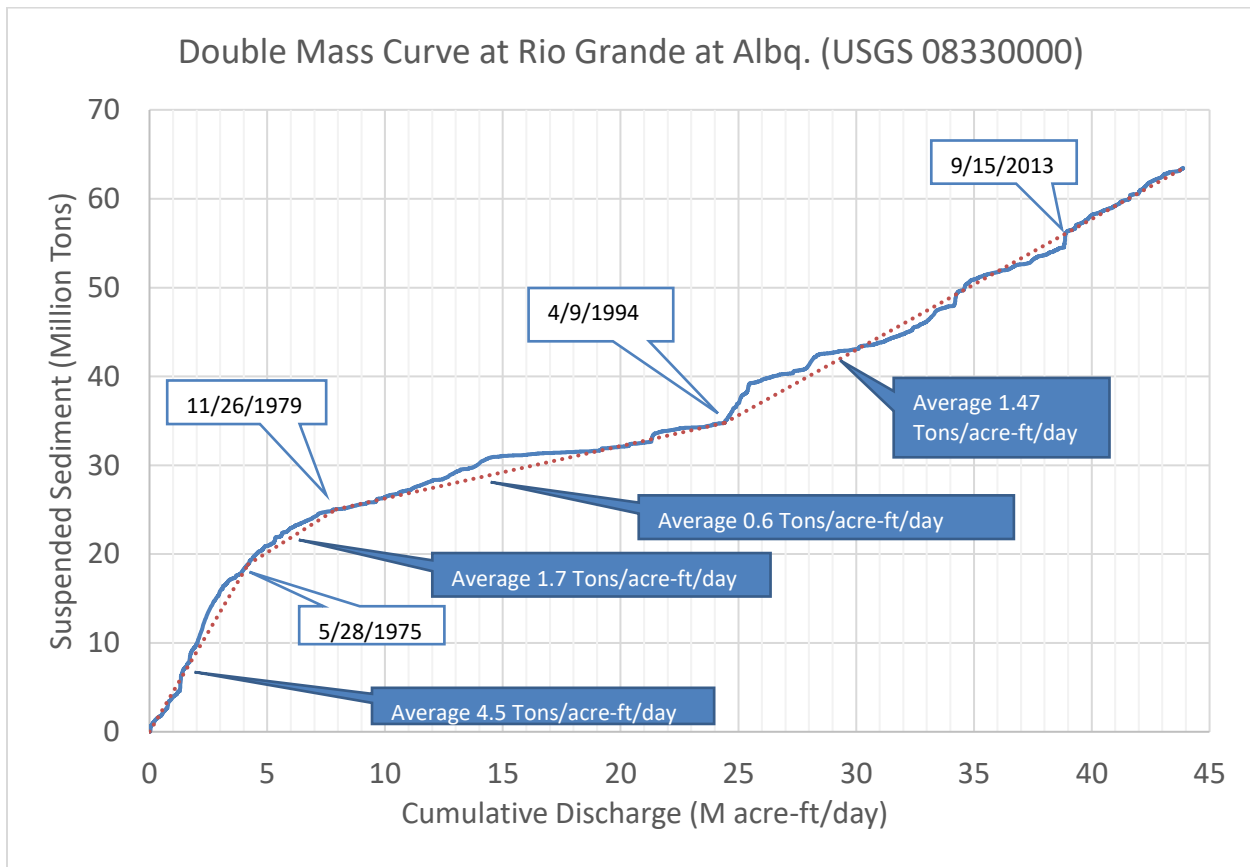


Figure 2-26 Double mass curve for USGS gage 08329500 at Rio Grande Near Bernalillo, NM

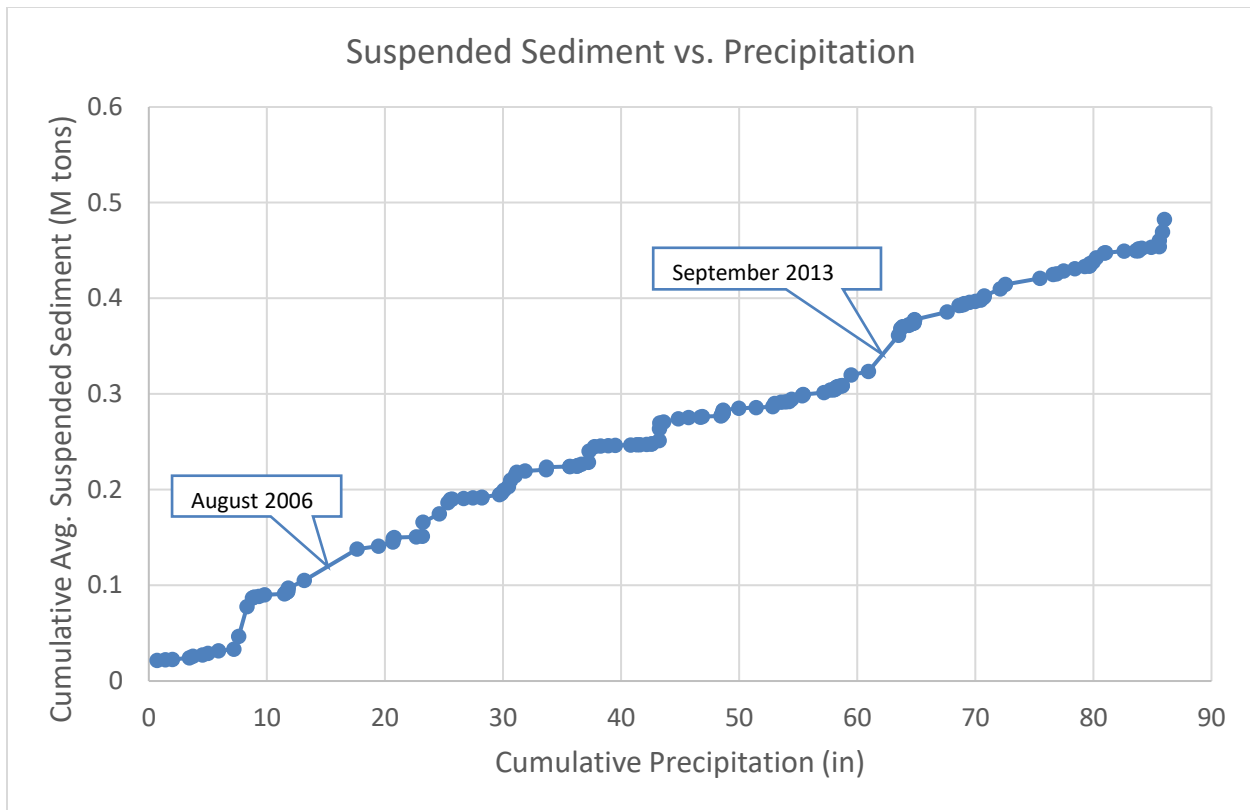


Figure 2-27 Cumulative suspended sediment (data from the Rio Grande at Albuquerque (USGS 08330000) gage) versus cumulative precipitation at the Alameda gage.

2.3.3 Monthly Sediment Variation

Plots of monthly average discharge and suspended sediment was created for the Jemez River (USGS 08329000), Rio Grande Below Cochiti (USGS 08317400), Rio Grande Near Bernalillo (USGS 08329500), and Rio Grande at Albuquerque (USGS 08330000) gages are shown in **Figure 2-28** to **Figure 2-35**, to help reveal any important seasonal trends. These figures show the seasonal trends of suspended sediment load and concentration, respectively, along with the discharges that correspond with the years. The spring snowmelt brings some of the larger flow rates associated with the larger quantities of sediment. However, the increased flows from the monsoonal storm events in the summer months were associated with the higher spikes in sediment concentration. There also peaks in suspended sediment from flood events that occurred prior to the construction of Cochiti Dam and from the 2013 flood. As shown in the figures below, a majority of the sediment flux is occurring during spring runoff associated with seasonal snowmelt in the region. Monsoonal events affect the sediment flux but are not the driving force for sediment movement in the Bernalillo and Montano Reaches of the MRG.

The primary sediment input into the MRG through the Bernalillo and Montano reaches is due to ephemeral tributaries (Fitzner 2018). The spring runoff brings sediment from these tributaries into the MRG. However, the sediment load at the Rio Grande Below Cochiti (USGS 08317400) shows the sediment being in phase with the flow and relatively lower sediment discharges and concentrations compared to the other gages. There are no uncontrolled ephemeral tributaries upstream of Cochiti, so the sediment and flow from Cochiti are both controlled by dam releases. A SEMEP analysis of total sediment load in the MRG was performed for a previous reach report (e.g. Bosque) and a copy can be found in **Appendix B** in that report (e.g. Schied 2021).

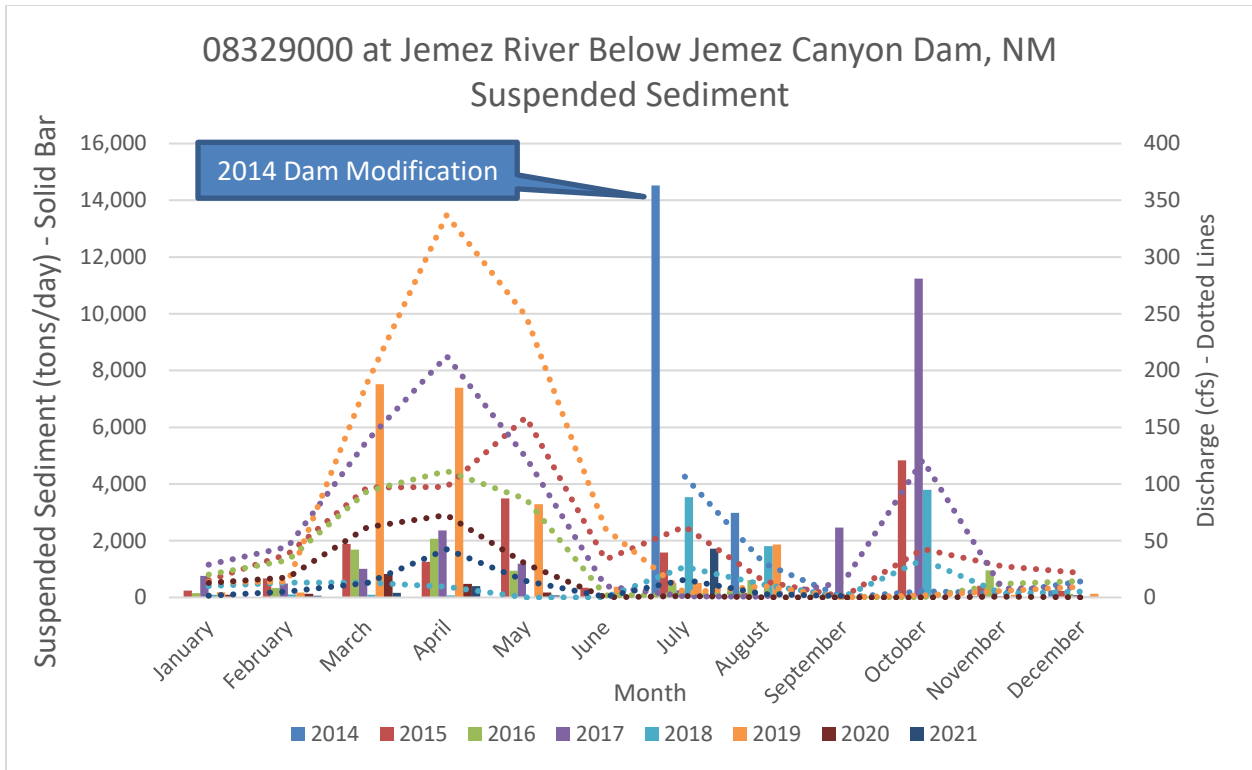


Figure 2-28 Monthly average suspended sediment and water discharge at USGS gage 08329000 at Jemez River Below Jemez Canyon Dam, NM

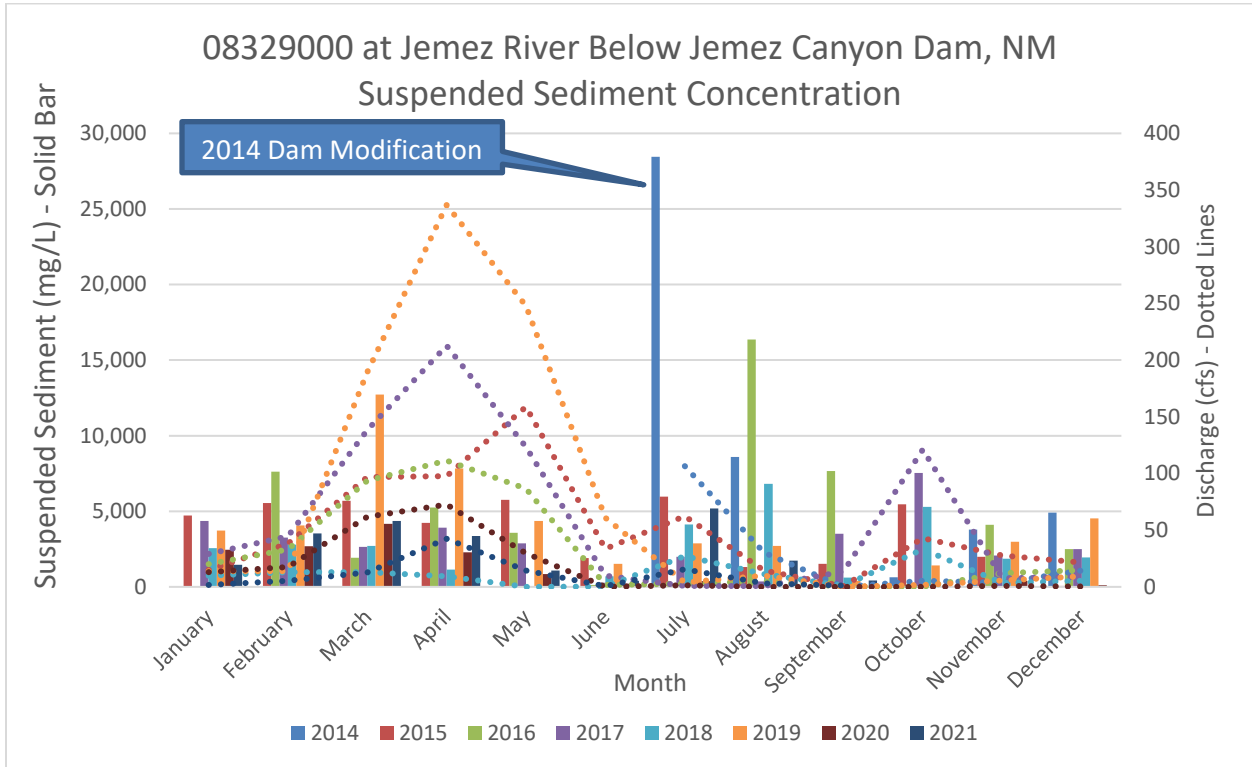


Figure 2-29 Monthly average suspended sediment concentration and water discharge at USGS gage 08329000 at Jemez River Below Jemez Canyon Dam, NM

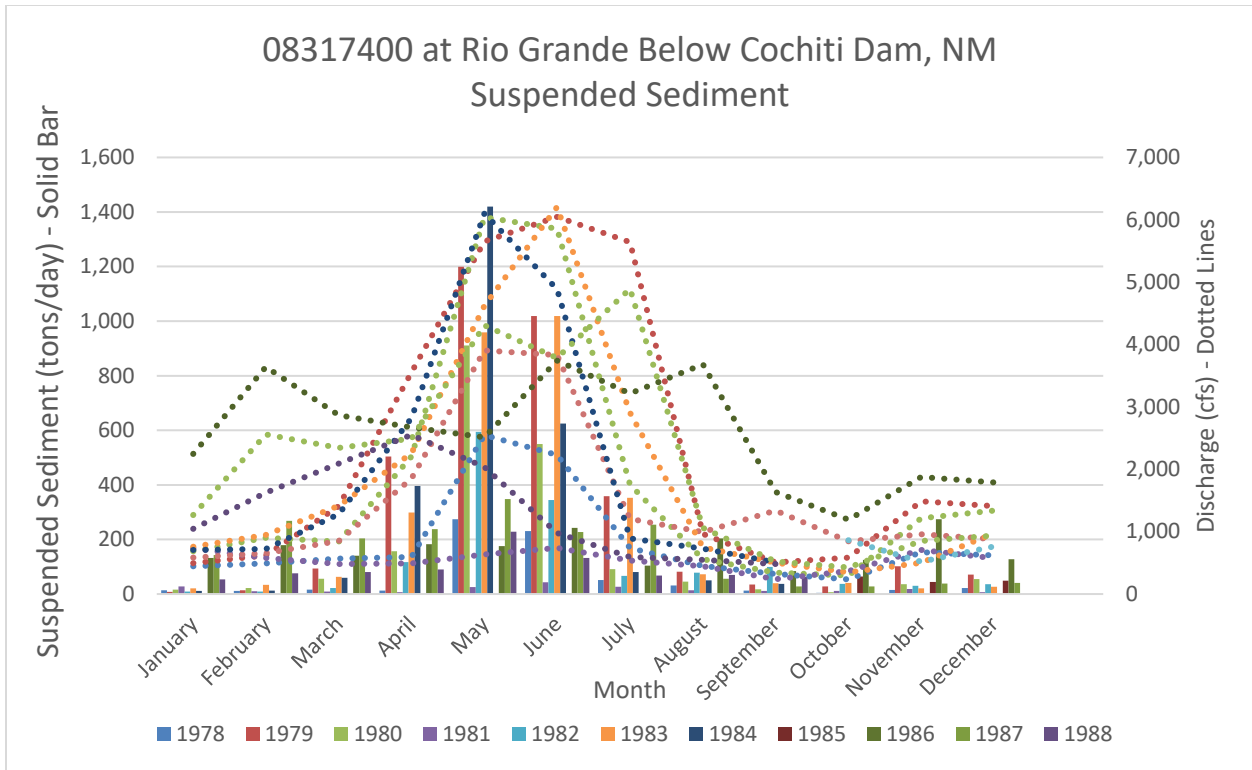


Figure 2-30 Monthly average suspended sediment and water discharge at USGS gage 08317400 at Rio Grande Below Cochiti Dam, NM

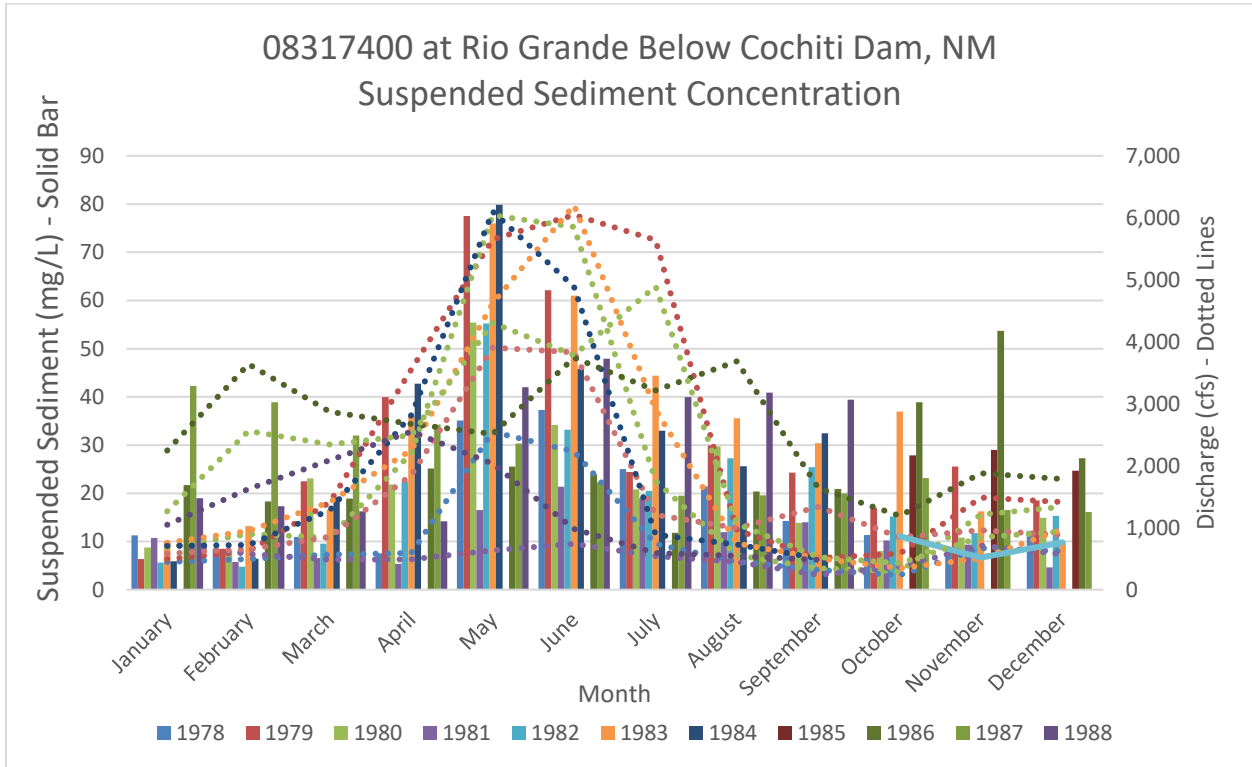


Figure 2-31 Monthly average suspended sediment concentration and water discharge at USGS gage 08317400 at Rio Grande Below Cochiti Dam, NM

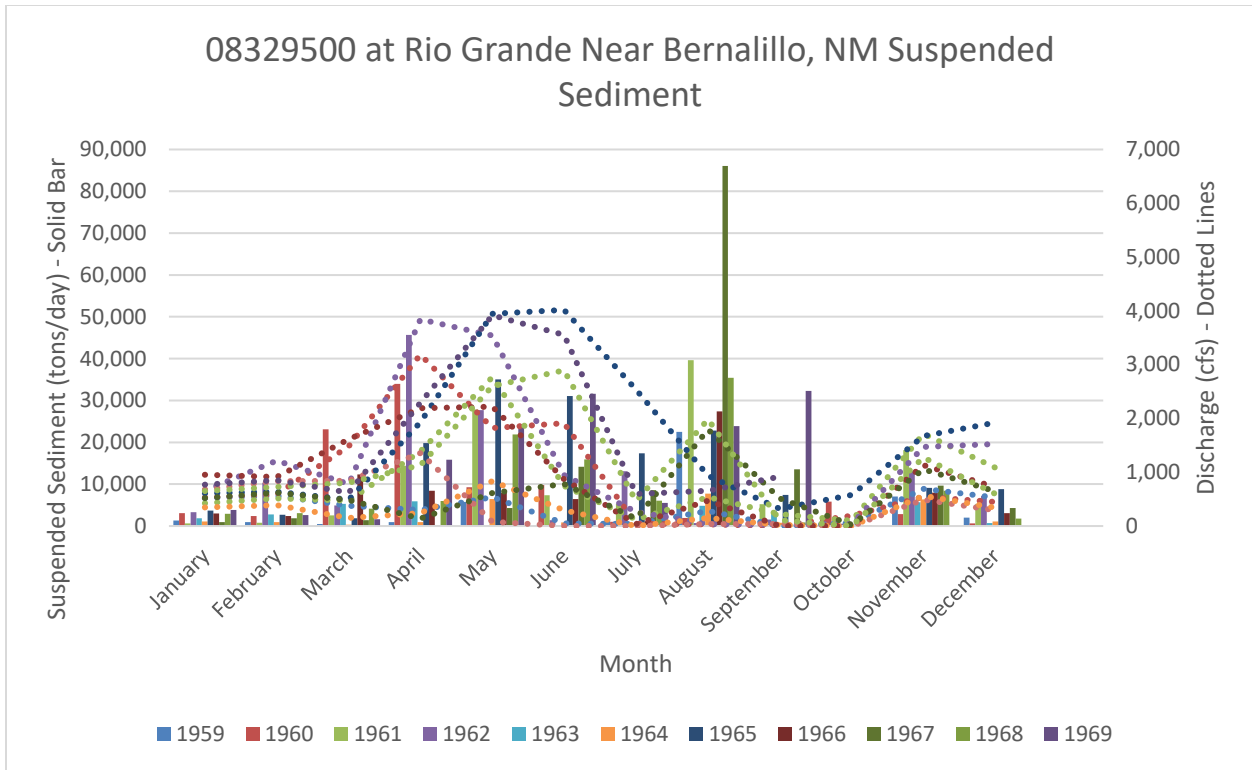


Figure 2-32 Monthly average suspended sediment and water discharge at USGS gage 08329500 at Rio Grande Near Bernalillo, NM

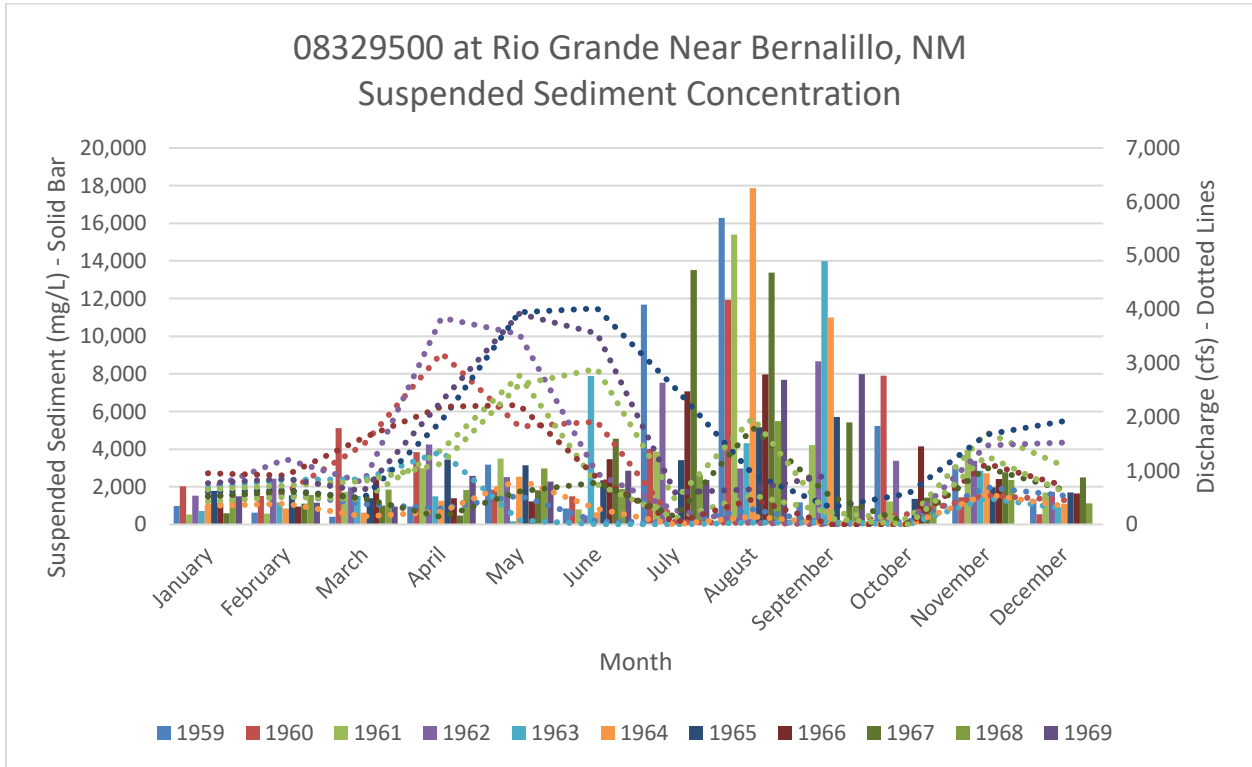


Figure 2-33 Monthly average suspended sediment concentration and water discharge at USGS gage 08329500 at Rio Grande Near Bernalillo, NM

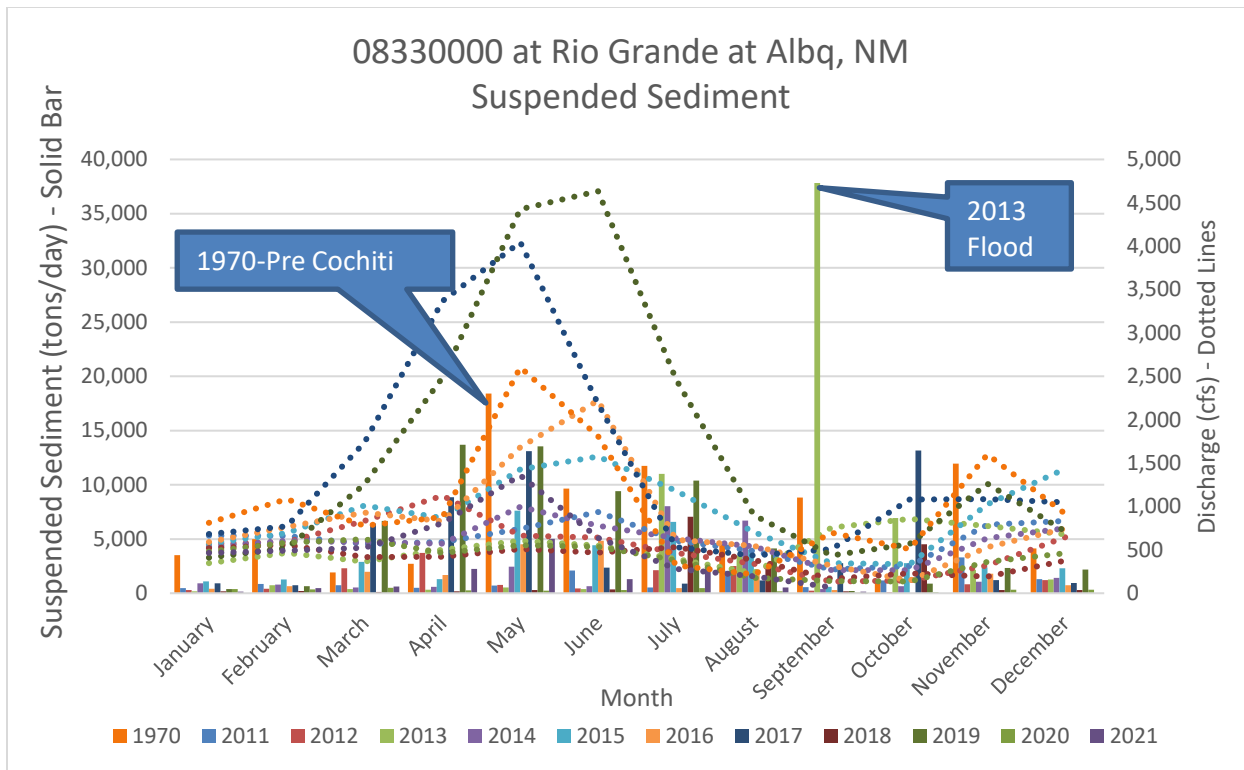


Figure 2-34 Monthly average suspended sediment and water discharge at USGS gage 08330000 at Rio Grande at Albuquerque, NM

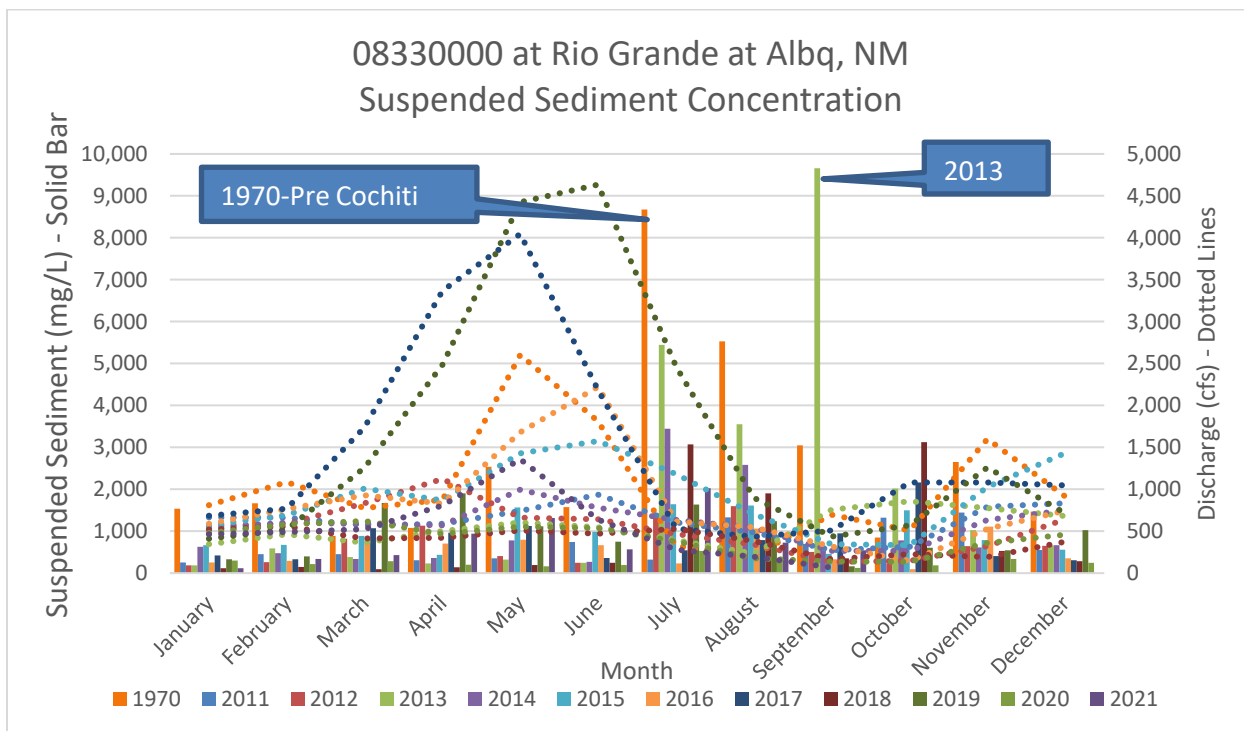


Figure 2-35 Monthly average suspended sediment concentration and water discharge at USGS gage 08330000 at Rio Grande at Albuquerque, NM

3 River Geomorphology

3.1 Wetted Top Width

Wetted top width can provide significant insight into at-a-station hydraulic geometry. Typically, wetted top width in a compound trapezoidal channel would slowly increase as discharge values increase until there is a connection with the floodplain. At this point, the top wetted width would quickly increase as the water spills onto the floodplains. Then, a gradual increase in width would continue after this point. Analysis of the wetted top width can be used to help understand bankfull conditions and how they vary spatially and temporally in the Montano Reach. A HEC-RAS model was created to analyze a variety of top width metrics, flows from 500 cfs up to 10,000 cfs were used in the top width analysis for years: 1962, 1972, 1992, 2002, and 2012. See **Section 4.1** for details on the HEC-RAS model.

Figure 3-1, **Figure 3-3**, and **Figure 3-5** show the moving average of cross section wetted top width at 1,000 cfs, 3,000 cfs, and 5,000 cfs. The top width shown at each Agg/Deg line comes from the moving average from five consecutive cross sections: the identified Agg/Deg line, two upstream Agg/Deg lines, and two downstream Agg/Deg lines. **Figure 3-2**, **Figure 3-4**, and **Figure 3-6** show the respective cumulative top width plots; a steeper slope corresponds to a wider channel and a flatter slope corresponds to a narrower channel.

Figure 3-1 shows a general trend of channel narrowing over time throughout the Montano Reach at 1000 cfs – especially in subreaches M2 through M5. The variation in wetted top widths throughout the Montano Reach have reduced from a range of 700 feet (250 feet to 950 feet) in 1962 to a range of 425 feet (200 feet to 625 feet) in 2012. Generally, across the Montano Reach, a reduction of 275 feet in wetted top width variation has occurred over this 50-year period.

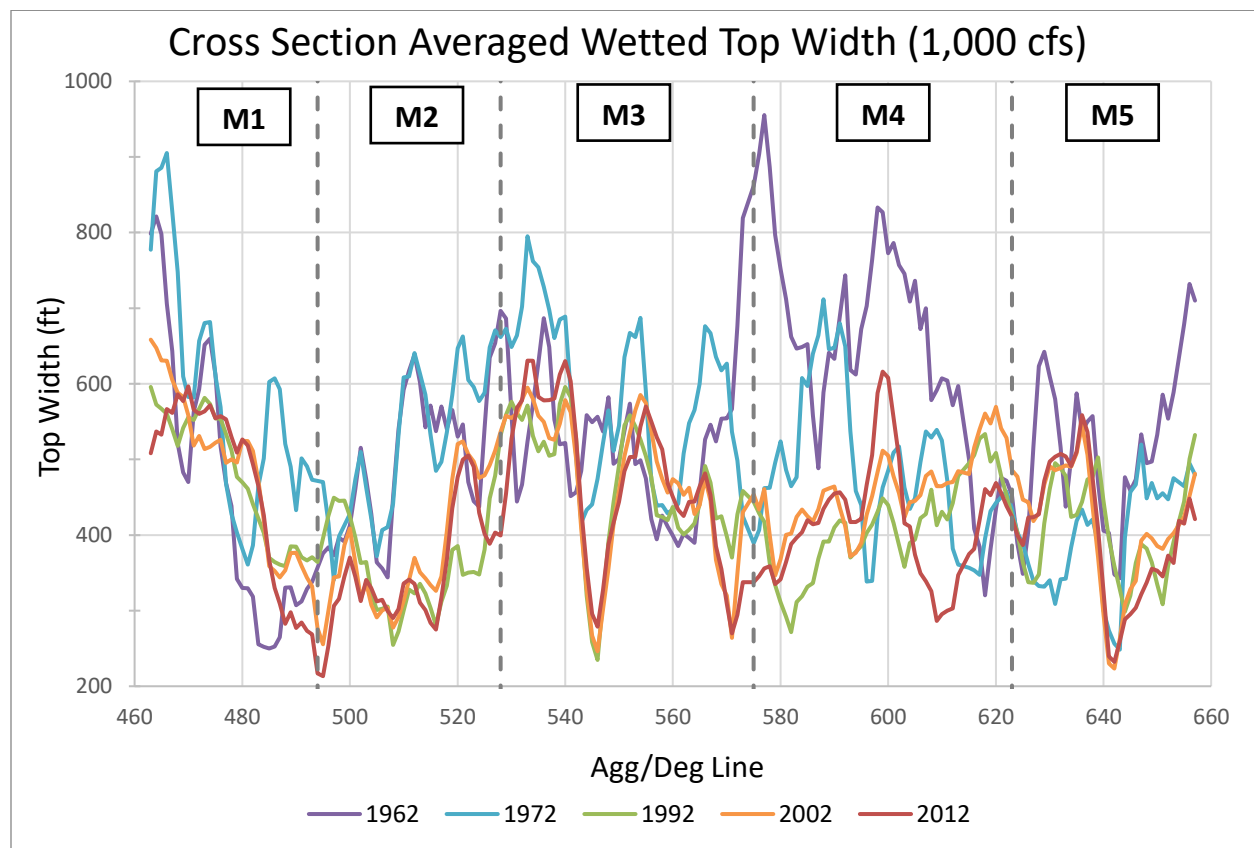


Figure 3-1 Moving cross-sectional average of the wetted top width at a discharge of 1,000 cfs.

Figure 3-2 shows more clearly the narrowing over time and highlights the narrowing in specific subreaches at 1,000 cfs. Subreach M1 remains relatively consistent over time but Subreaches M2 through M5 show significant narrowing, the slope of the 1962 and 1972 lines are much steeper than that in 1992, 2002, and 2012. Note the significant top width decrease at Agg/Deg line 547.

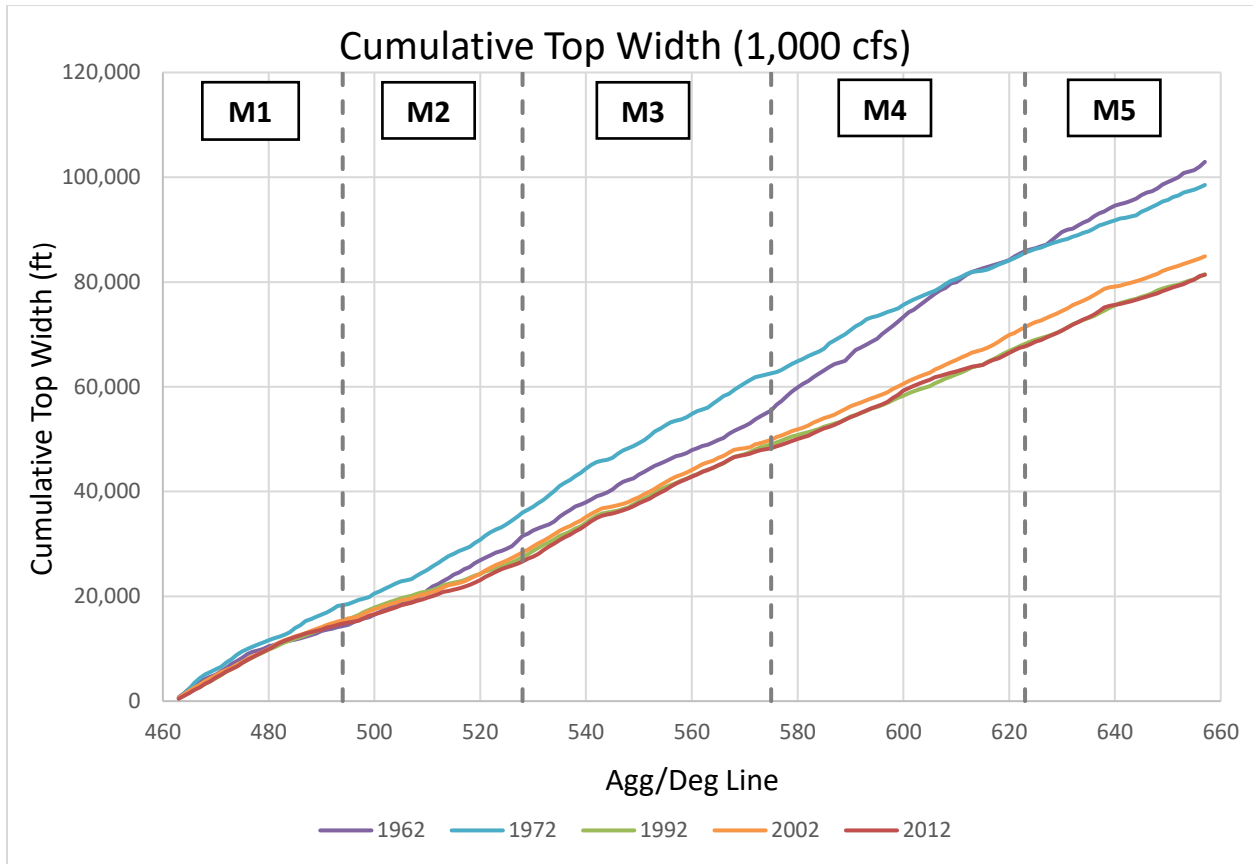


Figure 3-2 Cumulative top width at a discharge at 1,000 cfs.

Figure 3-3 shows a more distinct gap in average wetted top widths between pre (1962 and 1972) and post (1992, 2002, and 2012) Cochiti Dam construction. At 3,000 cfs, 1962 has a wetted top width range of 1150 feet (700 feet to 1850 feet) while 2012 shows a range of 450 feet (300 feet to 750 feet). This would indicate that 3,000 cfs is above the bankfull condition for years pre-Cochiti dam years and below the bankfull condition for the post-Cochiti dam years. A large spike in wetted top width between Agg/Deg lines 635 and 650 is shown across all years. There are physical features that could be causing this. The railroad crossing (constructed prior to 1918), located between Agg/Deg lines 637 and 638, and the Isleta Diversion Dam (Constructed in 1934), located between Agg/Deg lines 655 and 656. The railroad crossing constricts the flow, increasing the flow velocity, at the upstream end while the Isleta Diversion Dam slows and ponds the flow at the downstream end. The floodplain between these physical features is not as restricted, compared to the rest of the Montano Reach, by the riverside drains. A greater top width as discharge increases could be a result of this. The top width returns to a relatively consistent value after the Isleta Diversion Dam where the flow has been hydraulically controlled.

Figure 3-4 highlights the distinction between pre- and post-Cochiti dam top width conditions in the Montano Reach at 3,000 cfs. The slope of the cumulative plots for years 1962 and 1972 is significantly steeper than years 1992, 2002, and 2012 and the gap between them is much greater than that shown at 1,000 cfs. Thus, supporting the results shown and discussed in **Figure 3-3**.

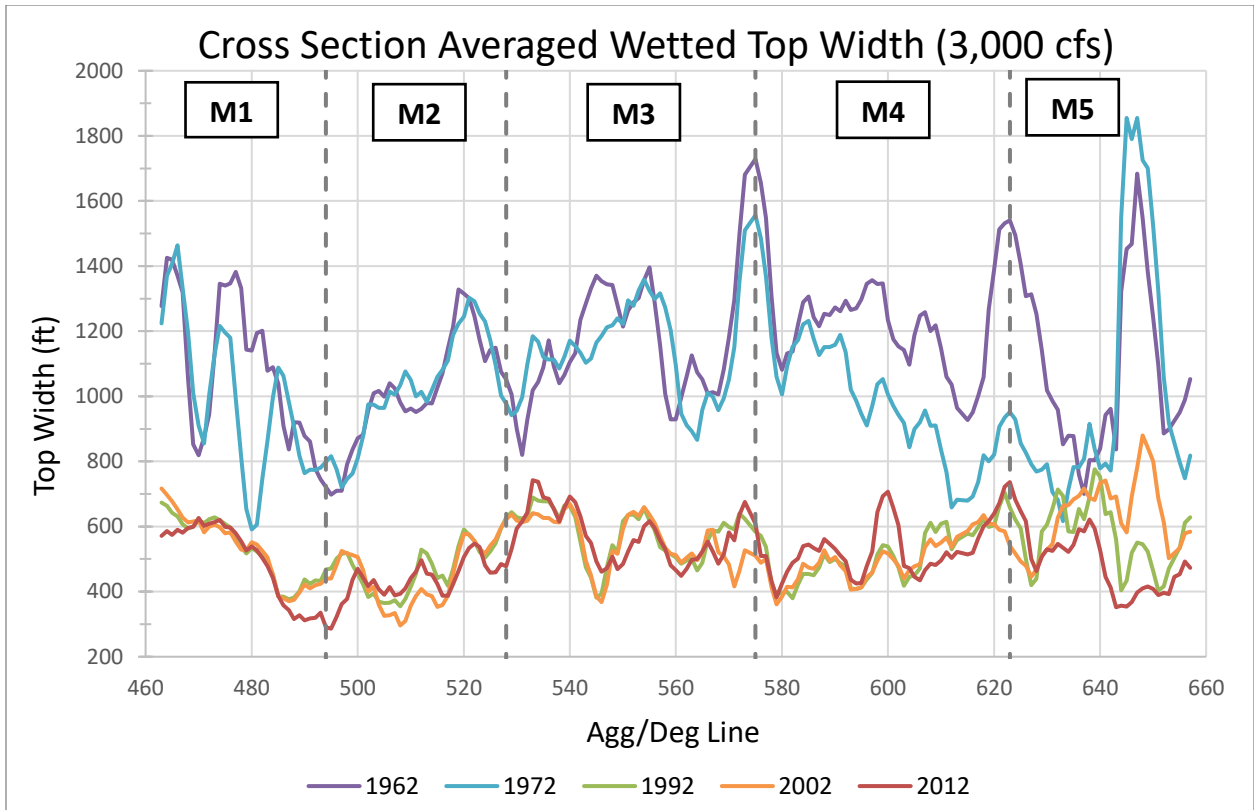


Figure 3-3 Moving cross-sectional average of the wetted top width at a discharge of 3,000 cfs.

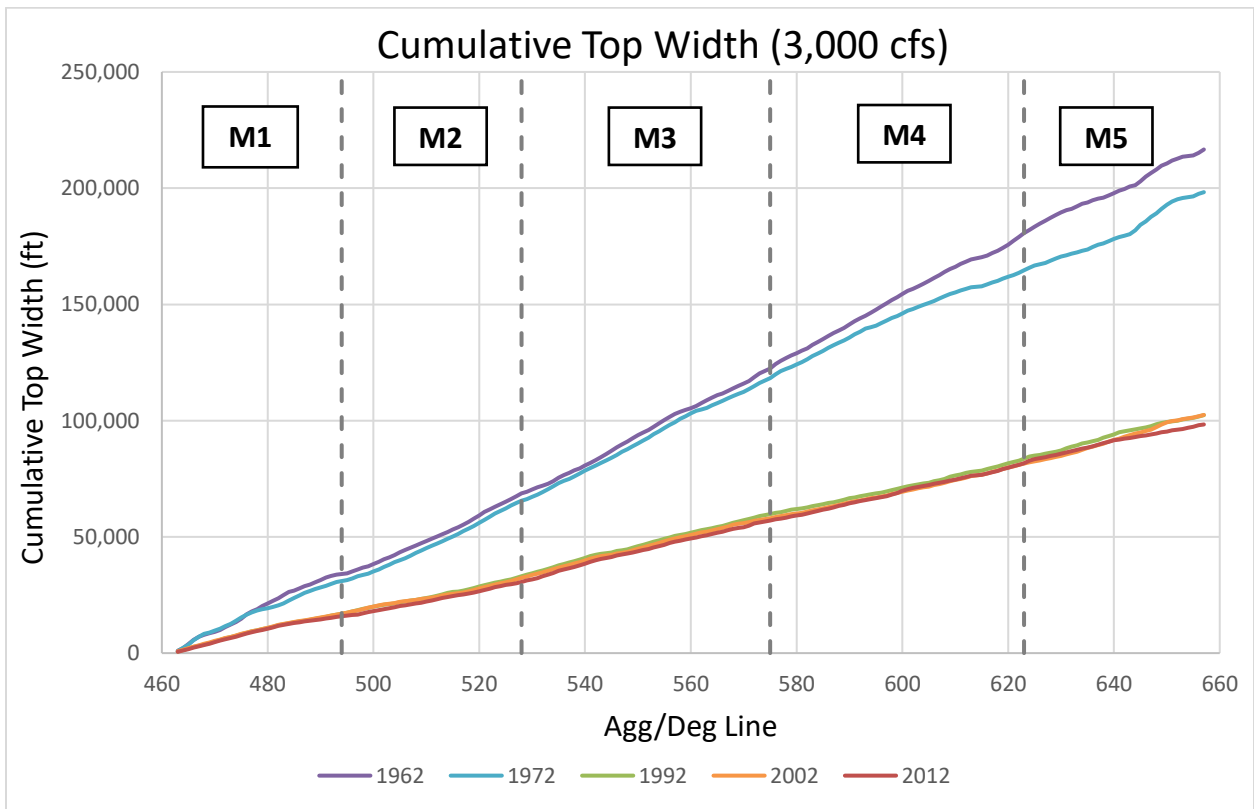


Figure 3-4 Cumulative top width at a discharge of 3,000 cfs.

Figure 3-5 and **Figure 3-6** show the same distinction between the pre- and post-Cochiti dam years as shown for 3,000 cfs. In 2012, some Agg/Deg lines have a significantly increased wetted top width from with the increase in flow magnitude, while other Agg/Deg lines increased only slightly. This would indicate that the bankfull conditions fluctuates throughout the Montaña Reach – 5000 cfs at some locations reactivates previous side channels and inundates the floodplain while at other locations the flow is still contained in the main channel.

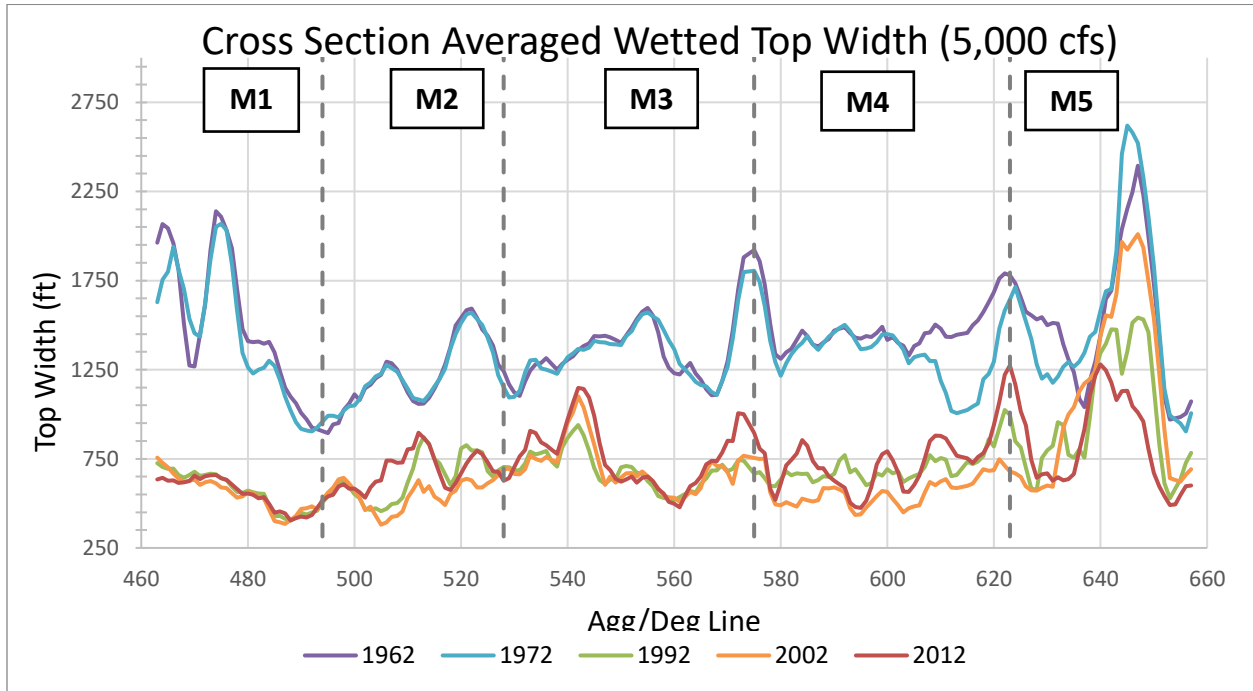


Figure 3-5 Moving cross-sectional average of the wetted top width at a discharge of 5,000 cfs.

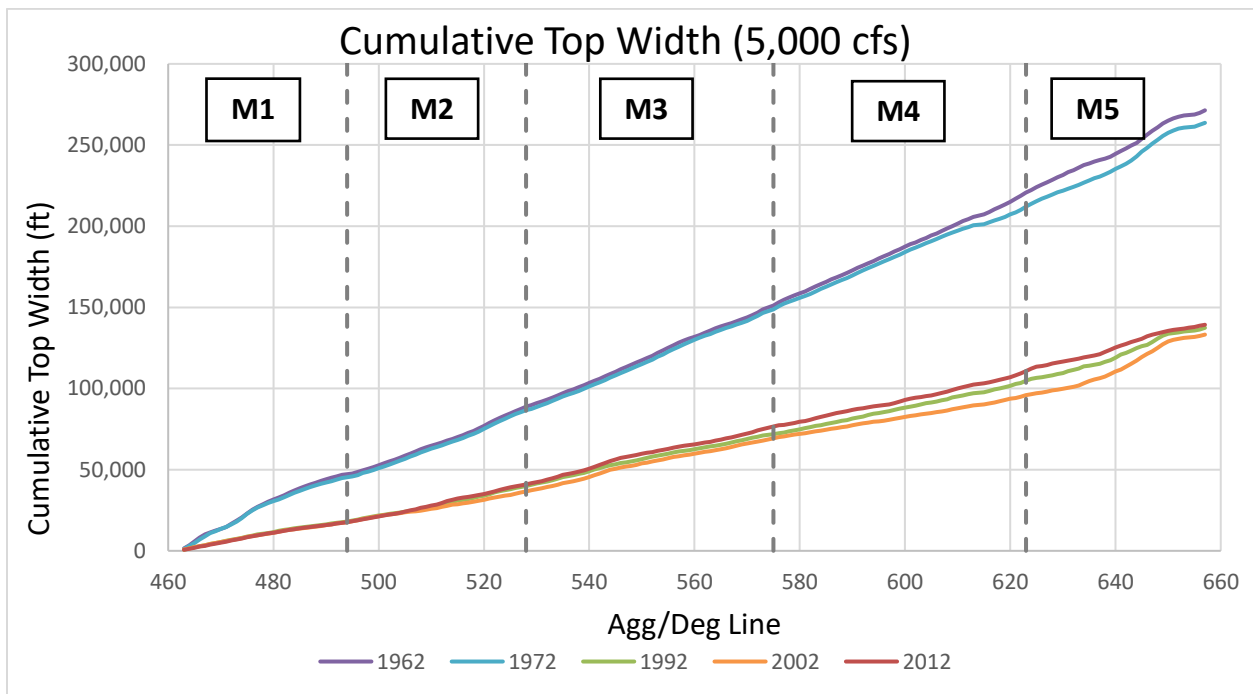


Figure 3-6 Cumulative top width at a discharge of 5,000 cfs

The reduction in wetted top width can mainly be explained by the channelization efforts (e.g. jetty jacks) throughout the Montañó Reach along with the construction of Cochiti dam. The channelization efforts bound the channel to a fixed width and Cochiti Dam significantly reduced peak flows accelerating the channelization efforts. See **Section 3.9** (Geomorphologic Conceptual Model) for more detail on the channel evolution of the Montañó Reach.

The average top width for each subreach was plotted for discharges from 500 cfs to 10,000 cfs is shown in **Figure 3-7**. Pre-Cochiti dam years show significant increases in top width with increasing discharge and then asymptotically approach a “maximum” top width where the entire floodplain has been inundated. This “maximum” top width ranges from 1700 feet to 1300 feet depending on the subreach. For post-Cochiti dam years, slight increases in top width with increasing discharge are shown. When the bankfull discharge (varies depending on the subreach) has been met or exceeded the top width does not spike like the pre-Cochiti dam years. This is most likely because of the channel evolution over time, transitioning from a wide multi thread to a narrow single thread river. As discharge increases, side channels typically reactivate (inundate) before the floodplain, this acts to flatten the top width curve.

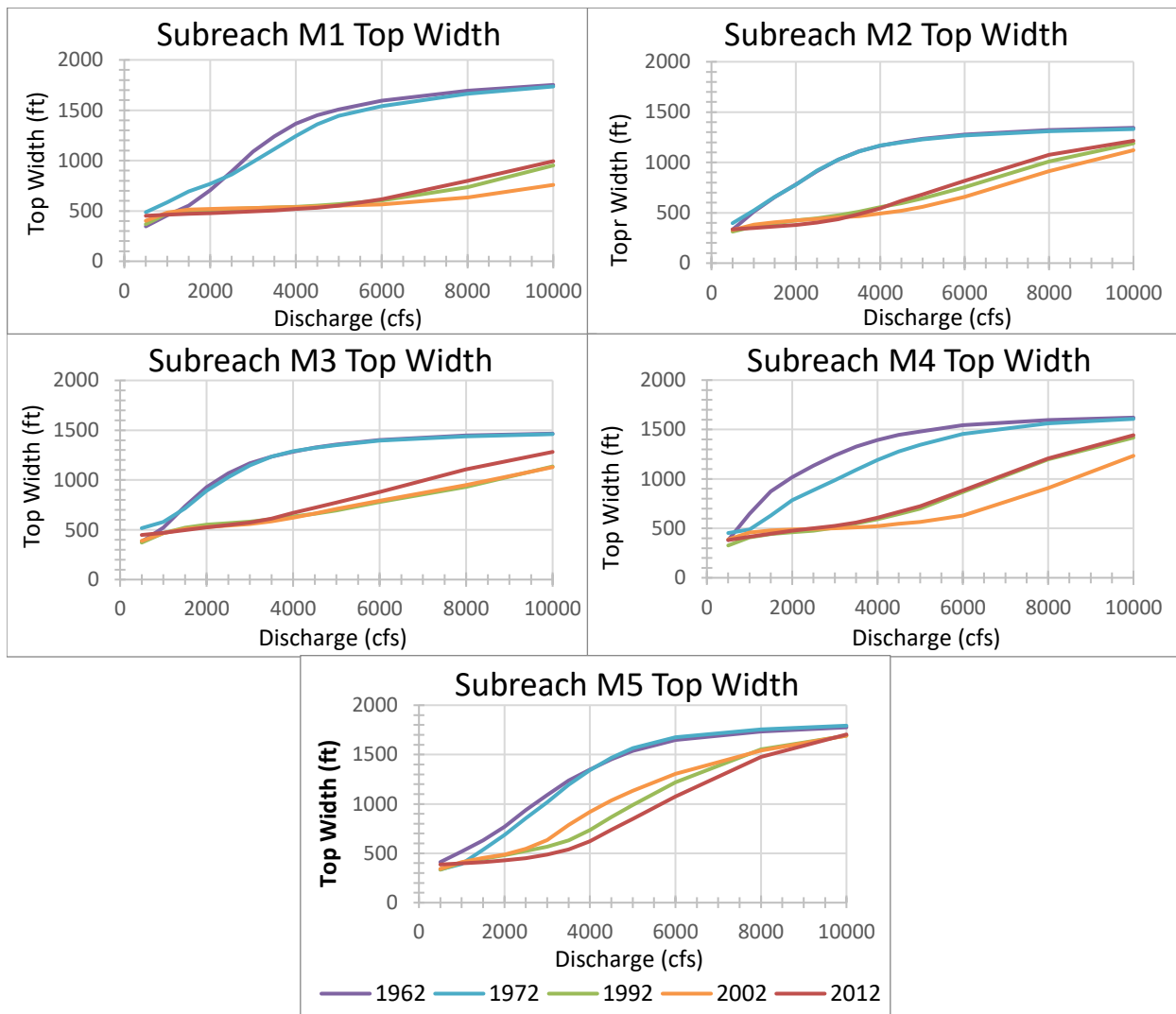


Figure 3-7 Average top width for each subreach at discharges from 500 cfs to 10,000 cfs; M1 (top left), M2 (top right), M3 (middle left), M4 (middle right), M5 (bottom middle).

3.2 Width (Defined by Vegetation)

The width of the active channel was found by clipping the Agg/Deg line to the width of the active channel, defined here as the non-vegetated channel based on aerial imagery. Aerial photographs were provided for years 1918 (digitized sketch), 1935, 1962, 1972, 1992, 2001, 2002, 2004, 2005, 2006, 2008, 2012 and 2019. Additionally, active channel Agg/Deg polygons were provided by Reclamation’s GIS and Remote Sensing Group for the years between 1918 and 1992, for subsequent years the active channel polygons were manually drawn in ArcGIS Pro. The average channel width of each subreach was calculated by averaging the width of all Agg/Deg lines within the subreach. **Figure 3-8** gives a breakdown of the average channel width by subreach.

Throughout the time period of available aerial imagery (1918-2019), the active channel width decreased dramatically, generally from 1200 feet in 1918 to 400 feet in 2019. **Figure 3-8** shows that the active channel width in all subreaches was greatest in 1918 and 1935 before a sharp decrease in width in the following years. During this time, a reduction in spring/summer baseflows from agricultural diversions in addition to changes in land use such as grazing led to dramatic decline in the active channel width of the river between 1918 and 1949 (Scurlock, 1998). An extended period of drought beginning in the 1940s and installation of jetty jacks in the 1950s resulted in additional narrowing of the active channel (Scurlock, 1998). Upstream dams and reservoir storage also lead to a decrease in peak flows throughout this time period. Mowing operations cleared vegetation along the riverbanks from the 1960s to the 1980s (and into the early 1990s in various locations along the MRG), which played a part in a slight widening of the river between 1972 and 1985, in addition to the increased flows as the period of drought came to an end (Makar, 2006). After another period of severe drought from the late 1990s to the late 2000s (though this drought is still on-going), the active channel width of the river has decreased once again and has since remained stable.

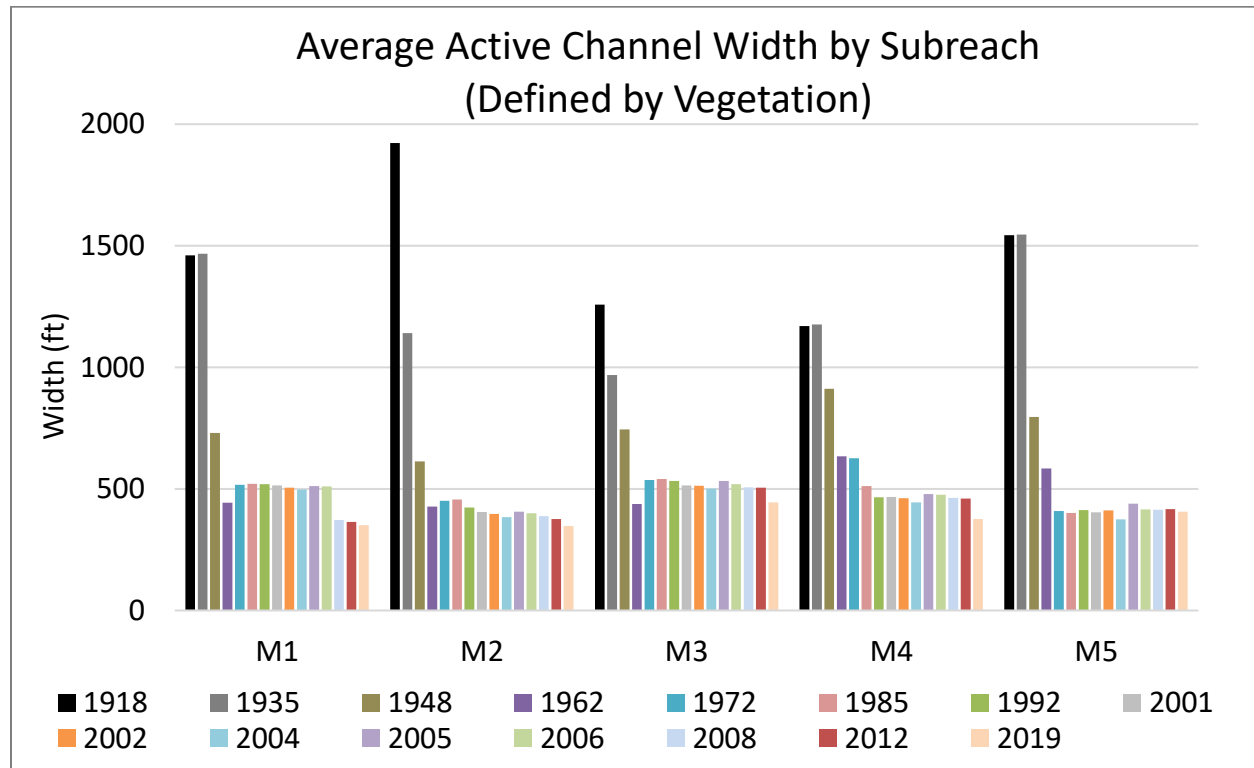


Figure 3-8 Averaged active channel width by subreach from historical imagery (defined by vegetation).

3.3 Bed Elevation

The minimum channel bed elevation is used to evaluate the change in the longitudinal profile of the Montañero Reach. The bed elevation of the channel comes from an estimate generated by HEC-RAS, which is based on the discharge and the water surface elevation on the day of the aerial photography. While the minimum channel elevation points may not be exact, the overall trends can still be identified throughout the Montañero Reach. The minimum channel elevation was obtained at each cross-section from the HEC-RAS geometry files to generate a plot of the bed elevation throughout the reach, as seen in **Figure 3-9**. Overall, the longitudinal profiles show that the Montañero Reach has remained relatively stable over. Small magnitudes of degradation from 1972 to 2002 and aggradation from 2002 to 2012.

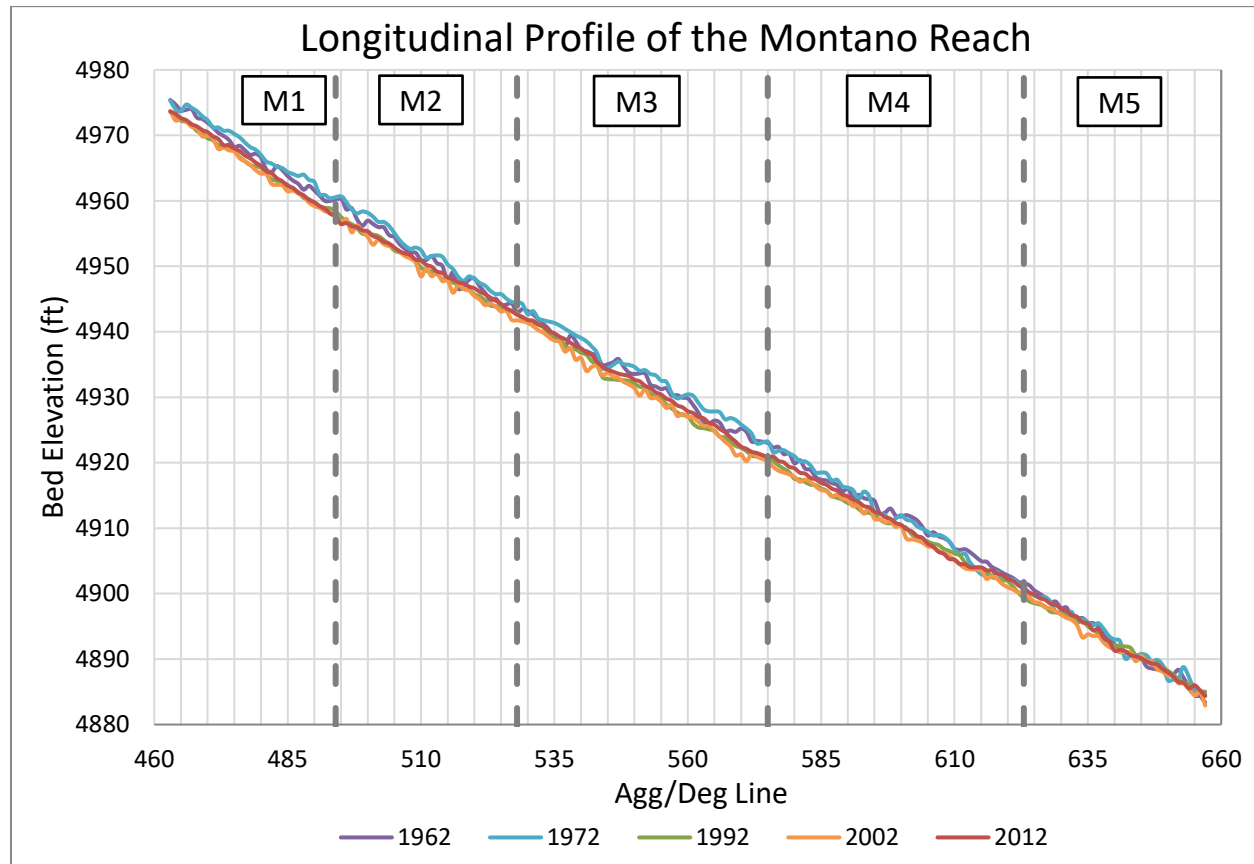


Figure 3-9 Longitudinal bed elevation profile.

The Montañero Reach main channel has experienced similar aggradation and degradation patterns over time as shown in **Figure 3-10**. The aggradation/degradation was determined as an average for each subreach for each time period between data collection (e.g. 1972-1992). The average minimum channel elevation (bed elevation) for each subreach was calculated, the average bed elevation of the earlier year was then subtracted from the later year (e.g. $\text{Min Ch. El.}_{M1:1992} - \text{Min Ch. El.}_{M1:1972} = \text{Deg}$) to calculate the Agg/Deg. A positive number indicates aggradation, and a negative number indicates degradation. This figure visualizes a direct comparison of trends in bed elevation between time intervals within individual subreaches. There is a common pattern observed in the Montañero Reach, from 1962 to 1972 there was aggradation across all subreaches except for Subreach M4. From 1972 to 2002 the channel experienced degradation and from 2002 to 2012 the channel has aggraded. While there is a cycle of aggradation and degradation the magnitude is relatively small, between 0 and 2.5 feet. It is important to note that Subreach M5 has experienced the least amount of aggregation and degradation, this is most likely attributed to the Isleta Diversion Dam, which has been present throughout all the survey years.

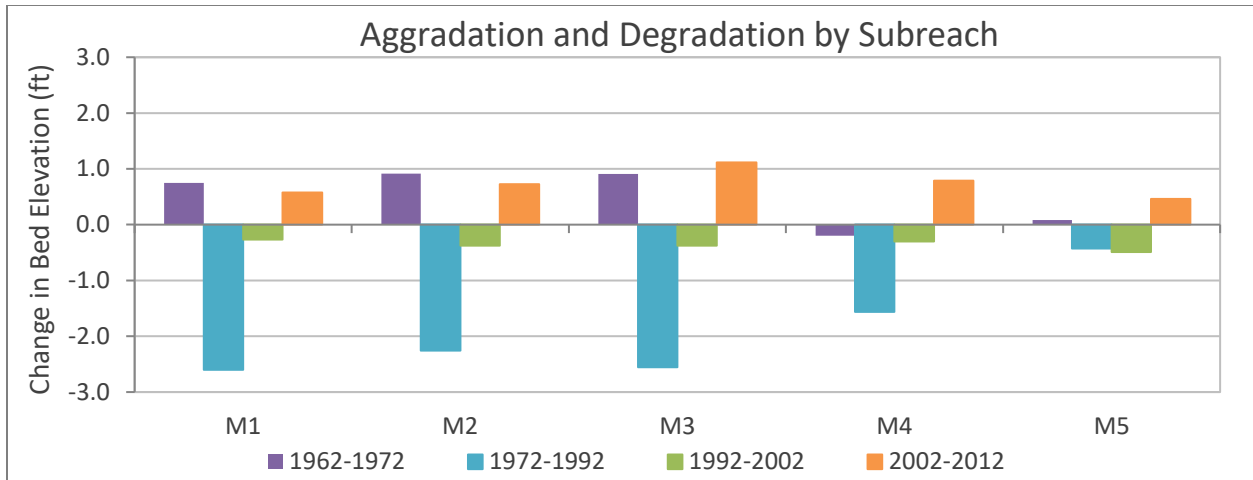


Figure 3-10 Aggradation and degradation by subreach

3.4 Bed Material

Bed material samples were collected at various locations in the river reach denoted by Agg/Deg lines. There are bed material samples available for analysis of the Montañó Reach from the years 1990 to 2014. **Figure 3-11** shows the median grain diameter of each sample versus Agg/Deg line downstream of the Montañó Road bridge crossing (the start of the Montañó Reach). **Figure 3-12** shows the trend of the median grain diameter, D_{50} , over time.

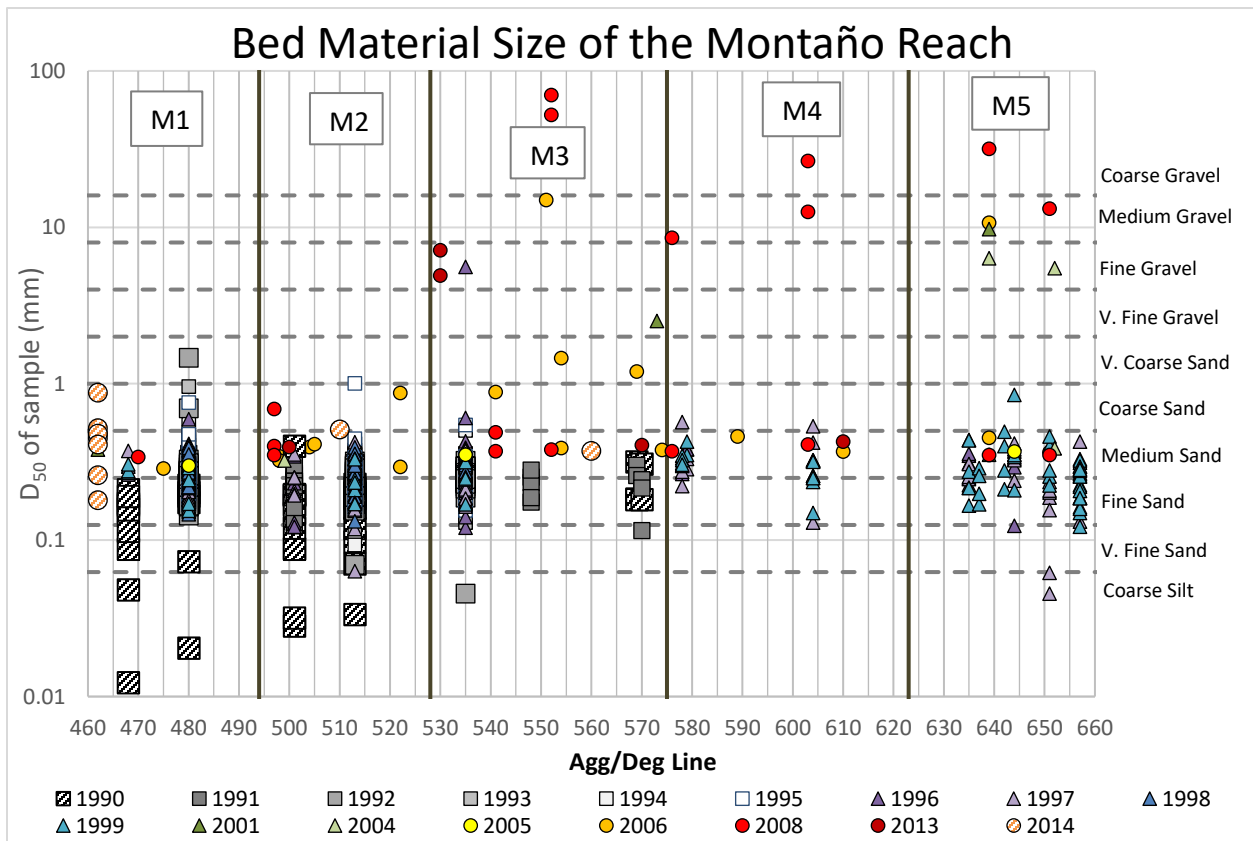


Figure 3-11 Median grain diameter size of samples taken throughout the Montañó Reach. (Circles represent 2014-2005, triangles represent 2004-1996, and squares represent 1995-1990)

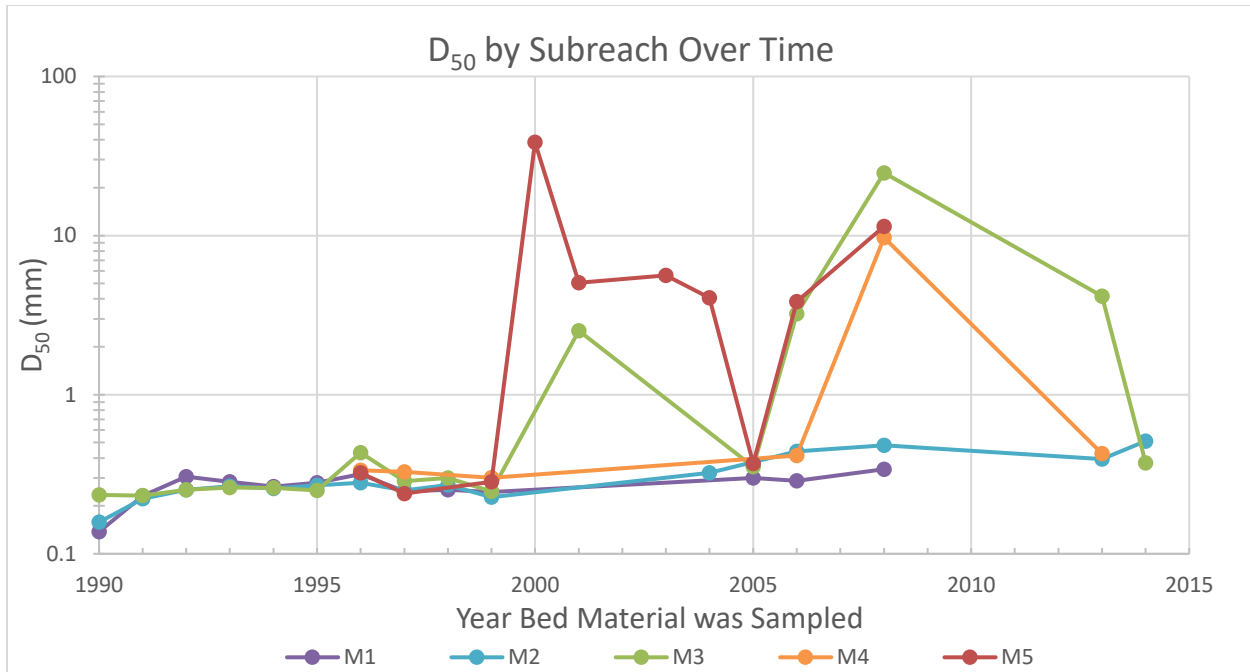


Figure 3-12 Median grain diameter size of samples taken throughout the Montañó reach over time

The beginning of the Montañó reach, Subreaches M1 and M2, show a gradual coarsening of the median grain diameter size; roughly from 0.2 mm to 0.35 mm from 1990 to 2014. Subreaches M3, M4, and M5 all show a spike in median grain size diameter, for the subreaches with data collected in 2014, this extreme coarsening is no longer present and the D₅₀ is at a more similar size of that in Subreaches M1 and M2. The general trend, without spikes, shown in **Figure 3-12** is a gradual coarsening of the bed material. Typically, bed material varies between 0.1 and 2 millimeters for the years in which data were collected. However, larger grain sizes, up to coarse gravel, were found in the downstream reaches, M3 - M5. For a majority of the Montañó Reach the grain size diameters correspond with classifications of fine sand to fine gravel, emphasizing the Montañó Reach as a sand-bed river with some gravel.

3.5 Sinuosity

Channel sinuosity was calculated by dividing the river length by the valley length within each subreach. This was accomplished using historical aerial imagery and digitized channel centerlines provided by Reclamation’s GIS and Remote Sensing Group. Some years that had aerial imagery did not have digitized channel centerlines, for these years the centerlines were manually drawn in ArcGIS Pro; These years are: 2001, 2002, 2004, 2005, 2006, 2008, and 2019. The results of this analysis are presented in **Figure 3-13**.

Generally, the Montañó Reach can be described as straight or as having low sinuosity throughout the last century. A straight channel is classified as having a sinuosity between 1.00 and 1.05, while a low sinuosity channel can be classified as having a sinuosity of 1.06 to 1.3. The average sinuosity in the Montañó Reach varies between 1.01 and 1.16 throughout the years analyzed. There has been a trend of channel sinuosity decreasing over time, but from year to year it is variable. This sinuosity decrease is due to the channelization efforts performed on the MRG.

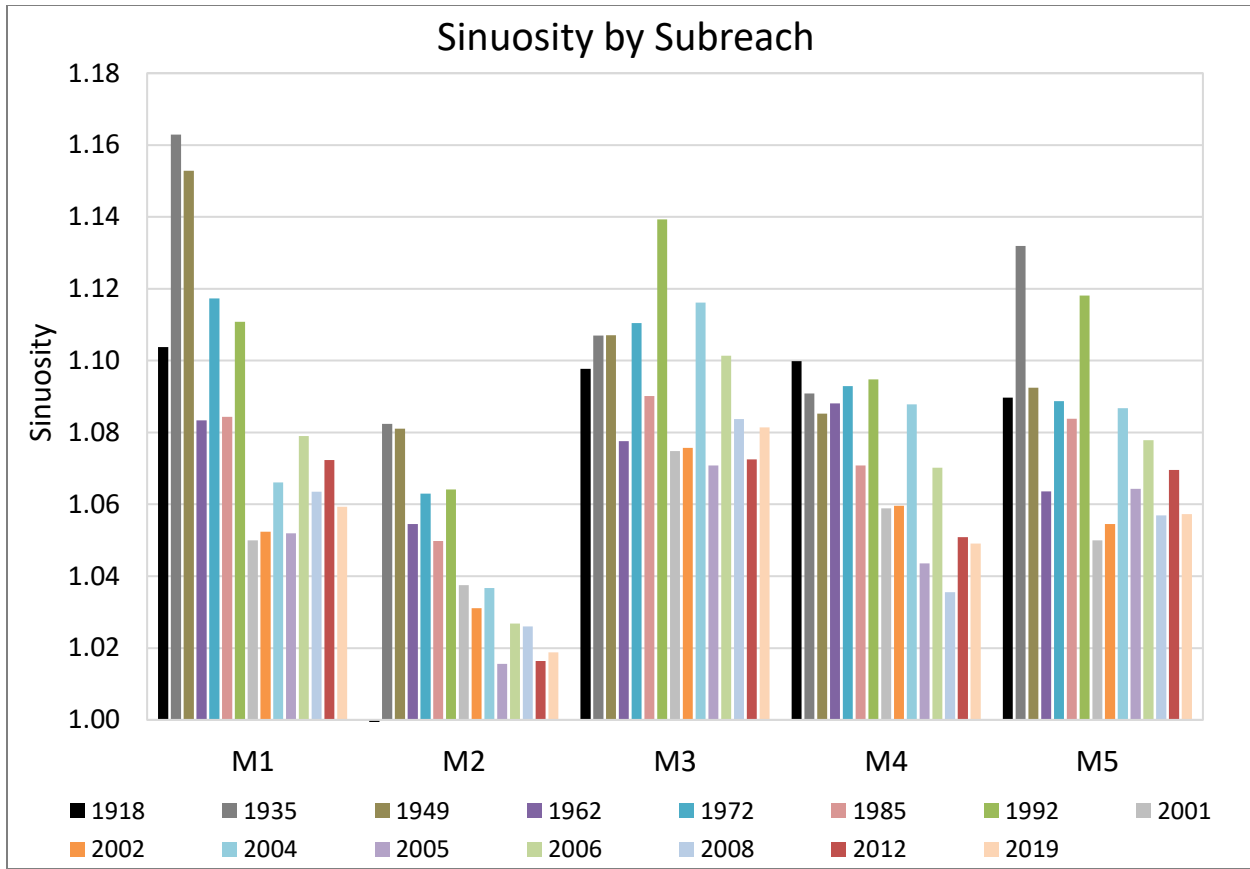


Figure 3-13 Sinuosity by subreach.

3.6 Hydraulic Geometry

Flow depth, velocity, width, wetted perimeter of the main channel, and bed slope are obtained using HEC-RAS 6.2.0 with discharges of 1,000 cfs, 3,000 cfs and 5,000 cfs – an exceedance probability of 33.8%, 9.9% and 3.3% respectively. 1,000 cfs is a common base flow in the MRG. 3,000 cfs is the approximate bankfull condition of previously studied reaches on the MRG and 5,000 cfs is the approximate discharge that represents the bankfull condition in the Bernalillo and Montañero Reaches. Bankfull conditions are the maximum discharges with limited likelihood of overbanking (LaForge et al., 2019 and Yang et al., 2019). It is important to note that, for certain years analyzed, 3,000 cfs and 5,000 cfs do activate the floodplain and is not the bankfull discharge. This can be seen in the Habitat Maps found in **Appendix E**. The hydraulic geometry variables presented in the figures below were averaged by subreach for each year analyzed.

The HEC-RAS results of top width (**Figure 3-14**) confirm general trends that matches shown in **Section 3.1** and **3.2**. At 1,000 cfs, the top width is similar throughout all the subreaches. M1 – M3 show an increase in top width from 1962 to 1972, while M4 and M5 show a decrease. For years 1992-2012, the top width has remained consisted, although there is some variation between the subreaches; M2 has the smallest average top width. At 3,000 cfs, pre-Cochiti dam years display a sharp increase in top width (roughly doubled) while post-Cochiti dam years show a very slight increase. This emphasizes that 3,000 cfs exceeds the bankfull condition for the pre-Cochiti dam years and does not exceed the bankfull condition for the post-Cochiti dam years. At 5,000 cfs, all the years' experience an increase in top width around 300 feet. The most notable increase occurs in M5, and the least amount of top width change occurs in M1.



Figure 3-14 HEC-RAS wetted top width of Montañó Subreaches at 1,000 cfs (top), 3,000 cfs (middle), and 5,000 cfs (bottom).

Top width and hydraulic depth are typically inversely related, it is expected that the hydraulic depth results will have the opposite trend that the wetted top width results showed. **Figure 3-15** shows the hydraulic depths (the cross-sectional area divided by wetted perimeter). At 1,000 cfs, the hydraulic depth varies from 1.0 to 1.4 feet across all years, M2 had the greatest hydraulic depth in 2012. As the flow increases to 3,000 cfs, this inverse relationship is displayed. The sharp increase in top width for years 1962 and 1972 yields a gradual increase in flow depth. While for years 1992-2012, the gradual increase in top width from 1,000 to 3,000 cfs yields a sharp increase in hydraulic depth, nearly doubling the hydraulic depth across all subreaches. M2 continues to have the highest hydraulic depth in 2012, 2.6 feet. This inverse relationship continues at 5,000 cfs. In 2012, at 5,000 cfs, all the subreaches have a similar hydraulic depth around 2.7 feet.

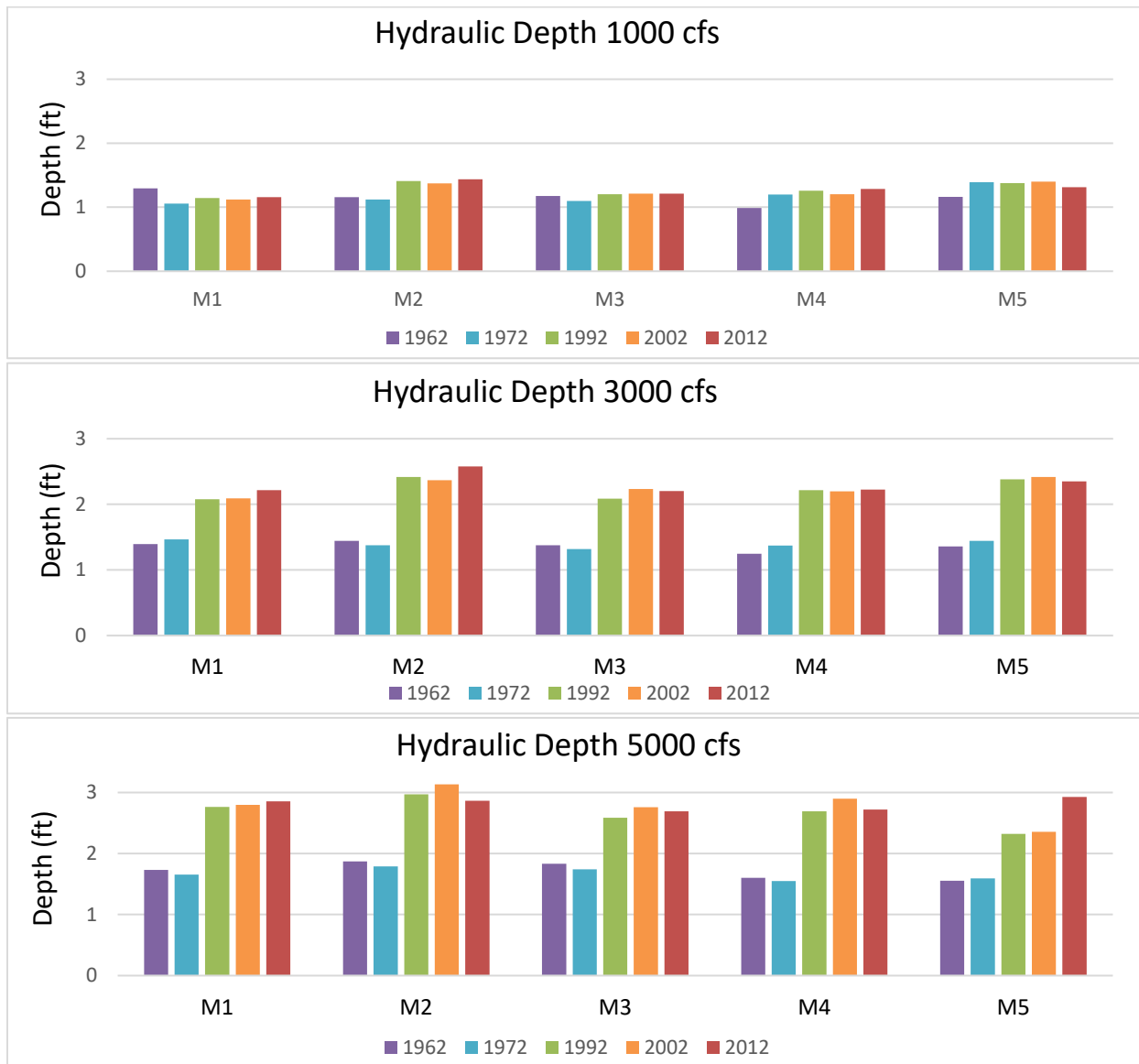


Figure 3-15 HEC-RAS Hydraulic depth of Montañó Subreaches at 1,000 cfs (top), 3,000 cfs (middle), and 5,000 cfs (bottom).

The wetted perimeter of the main channel was also obtained from HEC-RAS for each of the years analyzed, as shown in **Figure 3-16**. In general, for all the analyzed flow rates, the wetted perimeter increases from 1962 to 1972 for subreaches M1-M3 but decreases for M4 and M5. From 1972 to 2012 the wetted perimeter slightly decreases. It is important to note that the wetted perimeter is confined to the main channel and shows how the main channel has changed over time.



Figure 3-16 HEC-RAS main channel wetted perimeter at 1,000 cfs (top), 3,000 cfs (middle), 5,000 cfs (bottom).

The bed slope was calculated by taking the slope of a linear fitted line for each subreach. The bed slope of the linear fitted line is shown in **Table 3-2** and **Figure 3-17**. The left bar chart in **Figure 3-17** shows the bed slope for each subreach. The right bar chart shows the water surface slope calculated from the water surface profile at 500 cfs (HEC-RAS) for each subreach. Both the bed slope and water surface slope have remained relatively stable, varying between 0.0008 and 0.001. Subreach M1 consistently had the steepest slope at 0.001 in 2012. Changes in flow depth and slope often have an inverse relationship. In general, as slope decreases the flow depth increases. This trend can be seen in the Montano Reach throughout all subreaches, as seen in **Figure 3-15** and **Figure 3-17**. It is important to note that these subreaches each have their own characteristics and trends between 1962 and 2012. Those trends are further discussed in **Section 3.3** and **3.9**.

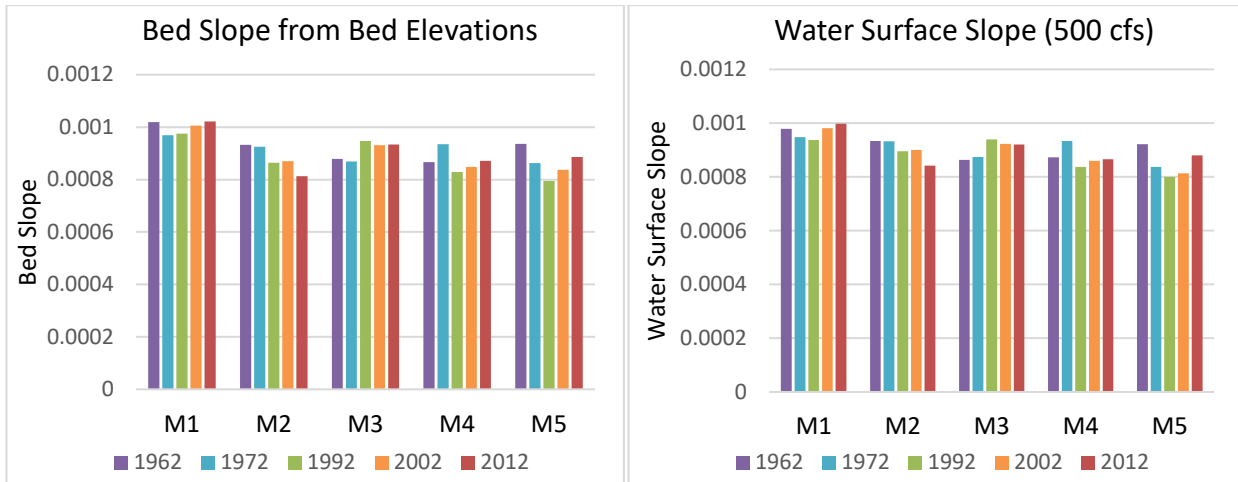


Figure 3-17 Bed Slope from Bed Elevations (left) and Water Surface at 500 cfs (right).

3.7 Mid-Channel Bars and Islands

At low flows, the number of vegetated mid-channel bars and islands at each Agg/Deg line is measured from digitized planforms from aerial photographs provided by the Reclamation. In some locations, multiple channels were present at one Agg/Deg line due to a vegetated bar or island bifurcating the flow. Note that the stage of a river can affect the number of visible islands and bars. A limitation in this analysis is that for some aerial images it is not clear what the discharge was, and as a result, some vegetated islands may be obscured by higher flows. This adds some degree of uncertainty regarding whether the difference between years in terms of number of channels were due to a variation in stage or a change in channel morphology. However, this analysis is still helpful in comparing general trends over a longer time period.

The number of channels at each Agg/Deg line, averaged across each subreach, is presented in **Figure 3-18**. In general, the number of mid-channel bars and islands increased from an average of 1 channel in 1918 to 1.4 channels in 2019 throughout all the subreaches except for subreach M5 which has remained relatively constant at 1 channel.

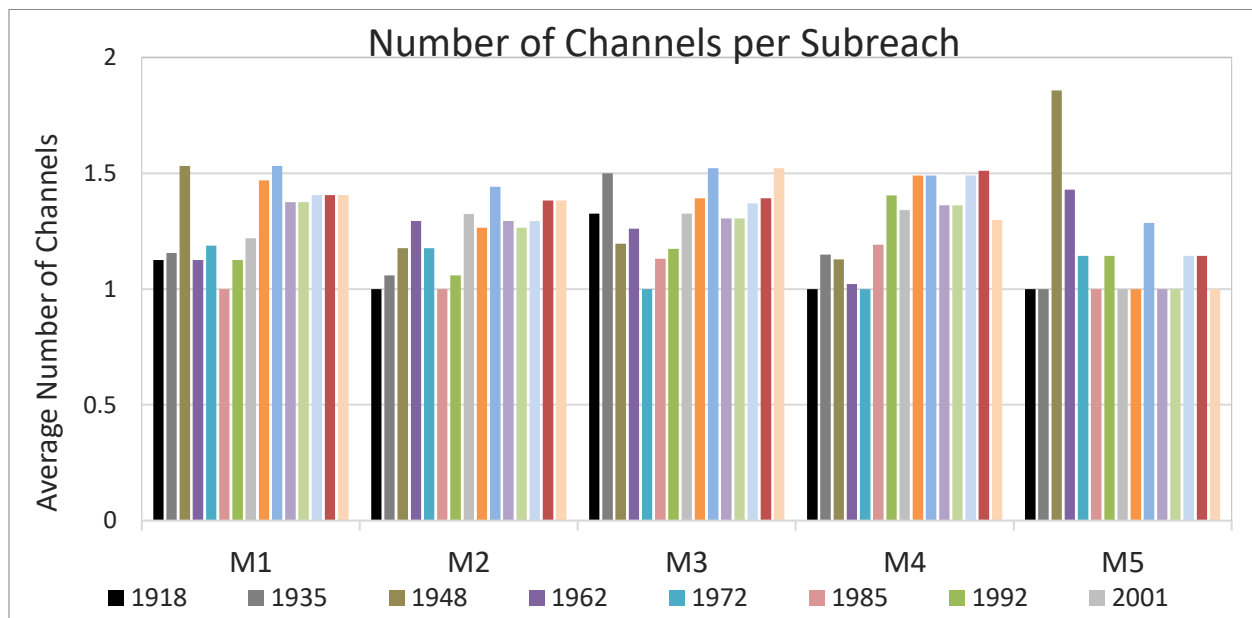


Figure 3-18 Average number of channels at the Agg/Deg lines in each subreach.

Figure 3-19 gives the percentage of Agg/Deg lines with multiple flow paths per year, which gives a rough idea of the percentage of the Montañño Reach that contains multiple channels in any given year. Across all Agg/Deg lines, there were between 1 and 4 channels in any given year. 1935 shows a spike in Agg/Deg lines with multiple channels, with 20% of the Montañño Reach having 2-3 flow paths and 80% having 1 flow path. In 1972, nearly 100% of Agg/Deg lines have a single flow path. The number of Agg/Deg lines crossing multiple channels steadily increases until 2001. This time period during the 1990s coincides with a drought characterized by lower peak flows that were incapable of wiping out the vegetation or re-working the bars and islands. In 2004, about 40% of the Agg/Deg lines have between 2 and 4 flow paths. This number of paths declines to around 30% in 2006, coinciding with a return to normal flows that facilitated denser vegetation growth but also likely wiped out some of the islands. The percentage of Agg/Deg lines trended upwards in 2012 and back to around 30% in 2019.

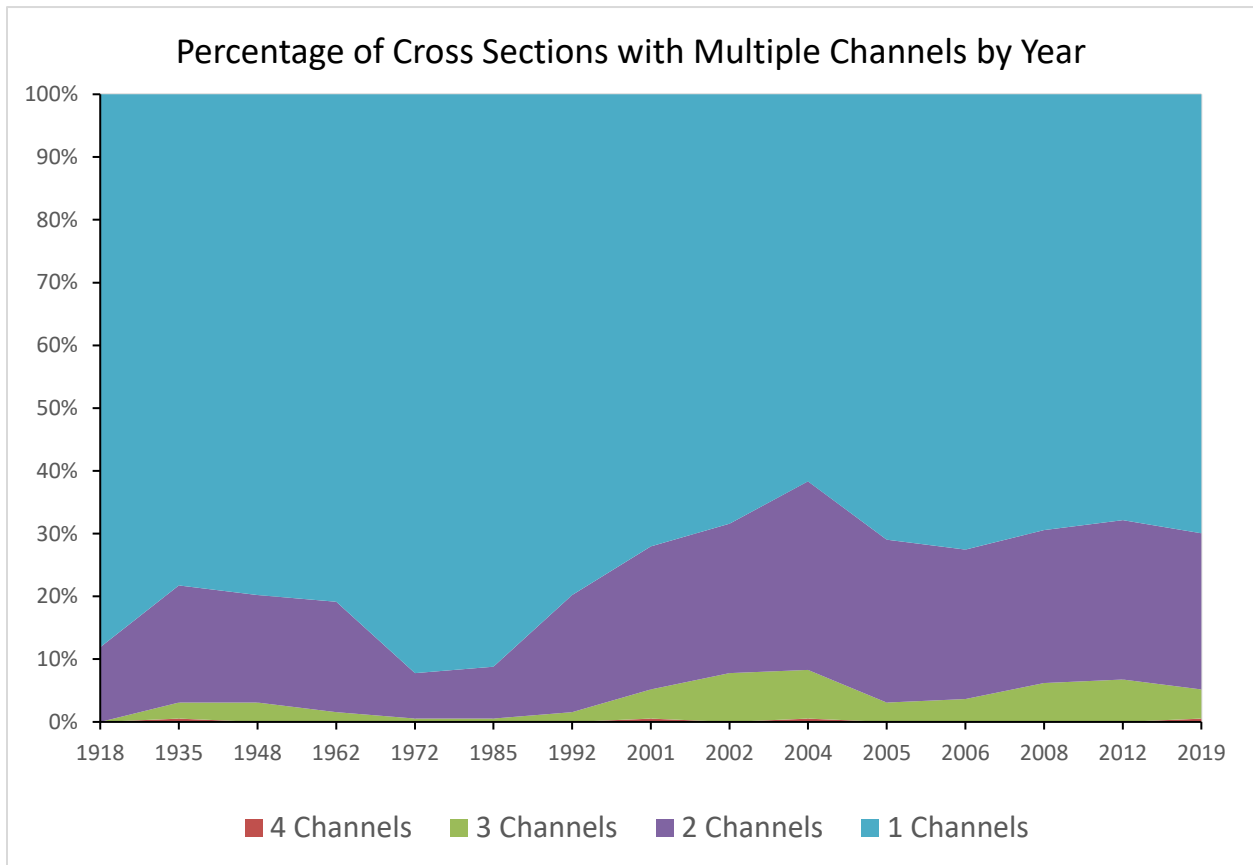


Figure 3-19 Percentage of Agg/Deg lines with multiple channels, by year, segregated by number of channels between 1 and 4.

3.8 Channel Response Models

The Julien and Wargadalam (JW) equations were used to predict the downstream hydraulic geometry of rivers (Julien and Wargadalam, 1995). These equations were based on empirical analysis of over 700 single-threaded rivers and channels, and predicted the width and depth likely to result from a given discharge, grain size and slope:

$$h = 0.2Q^{\frac{2}{6m+5}}D_s^{\frac{6m}{6m+5}}S^{\frac{-1}{6m+5}}$$

$$W = 1.33Q^{\frac{4m+2}{6m+5}}D_s^{\frac{-4m}{6m+5}}S^{\frac{-1-2m}{6m+5}}$$

Where $m = 1/\left[2.3 \log\left(\frac{2h}{D_s}\right)\right]$, h is the flow depth, W is the channel width, Q is the flow discharge, D_s is the median grain size, and S is the slope. A discharge of 3,000 cfs, the same discharge as in the previous HEC-RAS analysis, was used. The values for slope and grain size were obtained from **Section 3.6/3.9** and **Section 3.4**, respectively. The results are compared to the observed active channel widths (from the GIS analysis of the digitized planforms) in **Table 3-1** and plotted in **Figure 3-20**. Due to missing grain size data for every year, the median D_{50} with a (*) symbol indicates data that does not match the specified year. The percent difference was calculated as:

$$\text{Percent Difference} = 100 * \left(\frac{\text{predicted width} - \text{observed width}}{\text{observed width}} \right)$$

Table 3-1 Julien-Wargadalam channel width prediction

Year	Subreach	Ds (mm)	Slope	Predicted Width (ft)	Observed Width (ft)	Percent Difference
1992	M1	0.306	0.0010	255	520	-51%
	M2	0.253	0.0009	261	424	-38%
	M3	0.252	0.0009	256	532	-52%
	M4	0.335*	0.0008	264	466	-43%
	M5	0.323*	0.0008	253	412	-39%
2002	M1	0.245*	0.0010	253	505	-50%
	M2	0.227*	0.0009	260	397	-35%
	M3	0.247*	0.0009	257	513	-50%
	M4	0.300*	0.0008	262	461	-43%
	M5	0.283*	0.0008	265	411	-36%
2012	M1	0.340*	0.0010	253	364	-30%
	M2	0.394*	0.0008	265	376	-29%
	M3	4.161*	0.0009	266	505	-47%
	M4	0.427*	0.0009	262	461	-43%
	M5	11.430*	0.0009	275	416	-34%

*See Table B-1 in Appendix B for specific years used for Ds values.

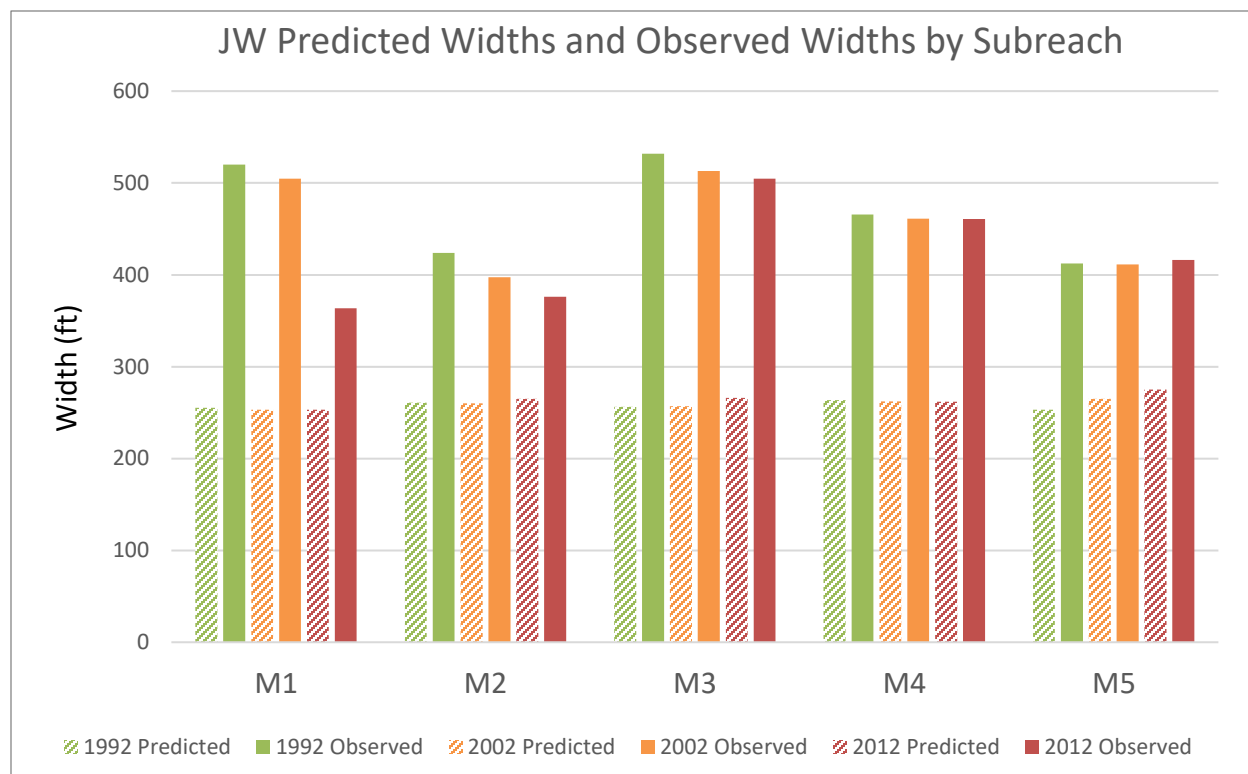


Figure 3-20 Julien and Wargadalam predicted widths and observed widths of the channel

The predicted JW widths are narrower than the observed widths for all subreaches in the Montaña Reach. The JW equations predict that the channel width for all subreaches should be narrower, 250 to 275 feet, than observed. When calculating the predicted width, the bankfull discharge was used, when varying discharges would be occurring in the river. This could lead to the greater variability in the observed width values. It is important to note that the JW equations represent a river whose morphodynamics are in equilibrium. The morphodynamic equilibrium is assuming there would be no aggradation nor degradation occurring. The Montaña Reach has been going through cycles of aggradation and degradation showing that the river is not in equilibrium and is continuously changing.

3.9 Geomorphic Conceptual Model

Massong et al. (2010) developed a channel planform evolution model for the MRG based on historical observations. The sequence of planform evolution is outlined in **Figure 3-21**. Stage 1 describes a wide, shallow channel with a high sediment load and large floods, which results in an active channel with constantly changing bars and dunes and little vegetation encroachment. The evolution from these more transient dunes and bars to more stable, higher relief bars and islands transitions the river into Stage 2. This transition generally occurred throughout the MRG between 1999 and 2004, which was characterized by sparse flooding and dry summer months. As the islands and bars become vegetated, they stabilize and begin to act more like floodplains, indicating that the river is transitioning to Stage 3. This transition occurred following a return to higher flows in 2005 and 2006. During this time, flow was high enough to inundate and erode some of the bars that had formed during the preceding 5-year dry period, but most of the bars survived and became well-vegetated during these wetter years.

The sediment transport capacity then becomes the determining factor of the future course of the river to either an aggrading river or a migrating river. A deficiency in sediment transport capacity, meaning the sediment supply is exceeding the transport capacity, leads to *aggradation* in the main channel and the flow eventually shifts onto the lower surrounding floodplain (Stages A4-A6). This typically forms in areas where

the reach slopes are less than 0.0007 ft/ft. When the sediment transport capacity exceeds the sediment supply, bank material erodes both laterally and vertically, leading to a *meandering* river (Stages M-4 to M-8). This typically happens where average channel slopes are larger than 0.0009 ft/ft. Transitions or complex combinations between the M stages and the A stages can occur, typically in areas where the average channel slope adjusts or in areas where neither A nor M stages dominate (typically where slopes are between 0.0007 ft/ft and 0.0009 ft/ft). However, a reset to Stage 1 always requires a large, prolonged flood to overcome the vegetation encroachment and widen the floodplain (Massong et al., 2010).

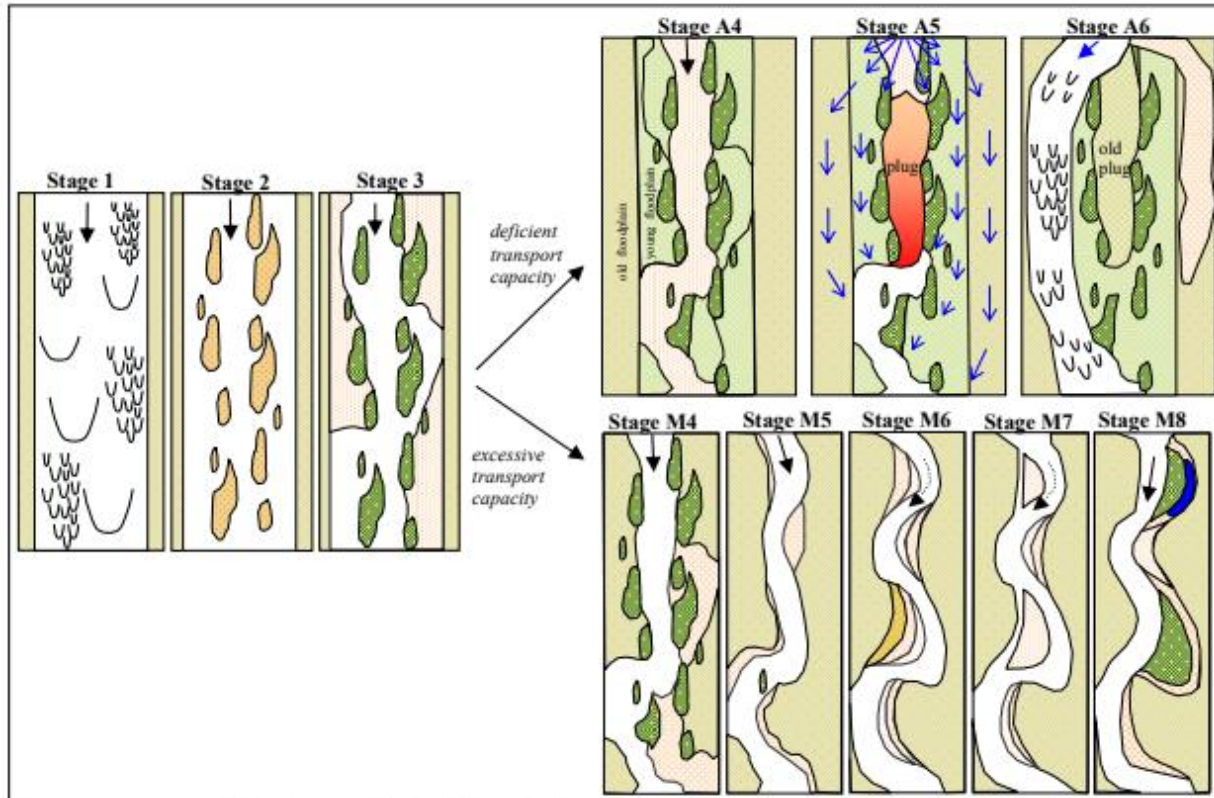


Figure 3-21 Planform evolution model from Massong et al. (2010). The river undergoes stages 1-3 first and then continues to stages A4-A6 or stages M4-M8 depending on the sediment transport capacity.

The reach-averaged slope for the Montañño Reach has adjusted through-out the years as a result of incision, particularly in Subreach M2, flattening significantly between 1962 and 2012 from 0.00093 to 0.00081. Between 1962 and 2012 the slope for M1 has remained relatively steep and stable, ranging between 0.00097 and 0.00102. Other reaches generally saw less significant and unpredictable changes (increasing and decreasing variably) in slope between 1962 and 2012. Refer to **Table 3-2** (below) and **Figure 3-17** (Section 3.6) for more detailed values of bed slope over the years for each subreach.

Table 3-2. Channel bed slope by subreach

Subreach	1962	1972	1992	2002	2012
M1	0.00102	0.00097	0.00098	0.00101	0.00102
M2	0.00093	0.00093	0.00086	0.00087	0.00081
M3	0.00088	0.00087	0.00095	0.00093	0.00093
M4	0.00087	0.00094	0.00083	0.00085	0.00087
M5	0.00094	0.00086	0.00080	0.00084	0.00089

In 2012, the bed slope for M1, M2, M3, M4, and M5 are 0.00102, 0.00081, 0.00093, 0.00087, and 0.00089 respectively. According to Massong (2010), Subreach M1, M4, and M5 fall within the grey-area range of bed slopes, where neither the meandering process nor the aggradation process is clearly dominant. Subreaches M3 and M4 fall within the migrating range of bed slopes. However, it is apparent from the available data that the entire Montañó Reach of the MRG has evolved through the meandering planform changes between 1992 and 2012, not the aggrading planform changes. Signs of this evolutionary track towards a meandering river include channel incision and narrowing rather than aggradation, the meander planform is visible within the aerial imagery, and an absence of sediment plugs.

Figure 3-22 shows the plan view of the stages for a meandering river course (Massong 2010) as well as cross-section view. During Stage M4, a dominant channel is typically established, while secondary channels begin to aggrade and will only become inundated during higher flows. Vegetation begins to encroach into these secondary channels, and they begin to transition from a channel to floodplain. During Stage M5, the channel continues to incise until the channel reaches a stable slope or runs into a coarser bed layer. This form is generally single threaded and straight or slightly sinuous. The channel may begin to meander, as shown by Stage M6, if the channel thalweg is below the root zone. This allows for erosion of the bank material beneath the soil layer that is more consolidated by roots. Meanders progress and typically form side channel cuts (chutes) through the point bar on the inside of the bend (Stage M7). These gradually become larger until it eventually able to convey all of the flow, leading to the eventual abandonment of the old channel. The old channel fills with sediment and becomes part of the floodplain (Stage M8).

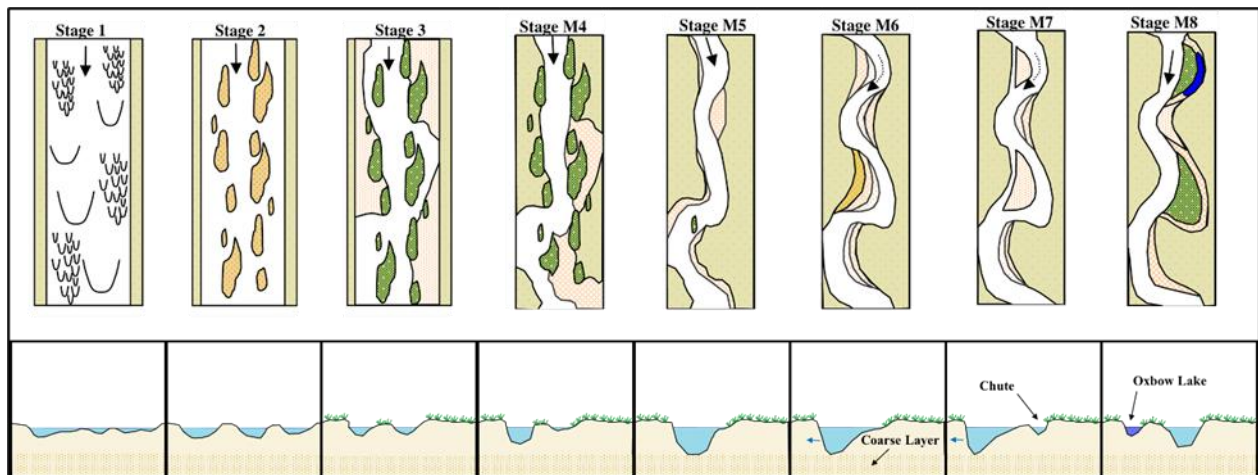


Figure 3-22 Planform evolution model from Massong et al. (2010) applied to channel cross sectional view (modified 2022).

Figure 3-23 shows the evolution of the channel in the upstream-most subreach using a representative cross section at Agg/Deg 483 for the years 1962, 1972, 1992, 2002, and 2012. In Subreach M1 the channel bed elevation remained relatively constant at an elevation of 4965 feet, with an approximate depth of 3.5 feet, between 1962 and 1972. An island with small regions of vegetation developed during this time, this bifurcated the flow. The main channel narrowed from an approximate width of 250 feet to 200 feet and shifted from station 1200 feet to 800 feet – the old main channel of 1962 is now a smaller side channel in 1972. Between 1972 and 1992, the island was mobilized, the one distinguished main channel incised (~2 feet) while the right bank encroached and stabilized with vegetation. From 1992 to 2002 the channel continued to incise (~1 foot). This trend reversed from 2002 to 2012 where the channel aggraded (~1 foot). Subreach M1 shows the greatest net decrease in channel elevation.

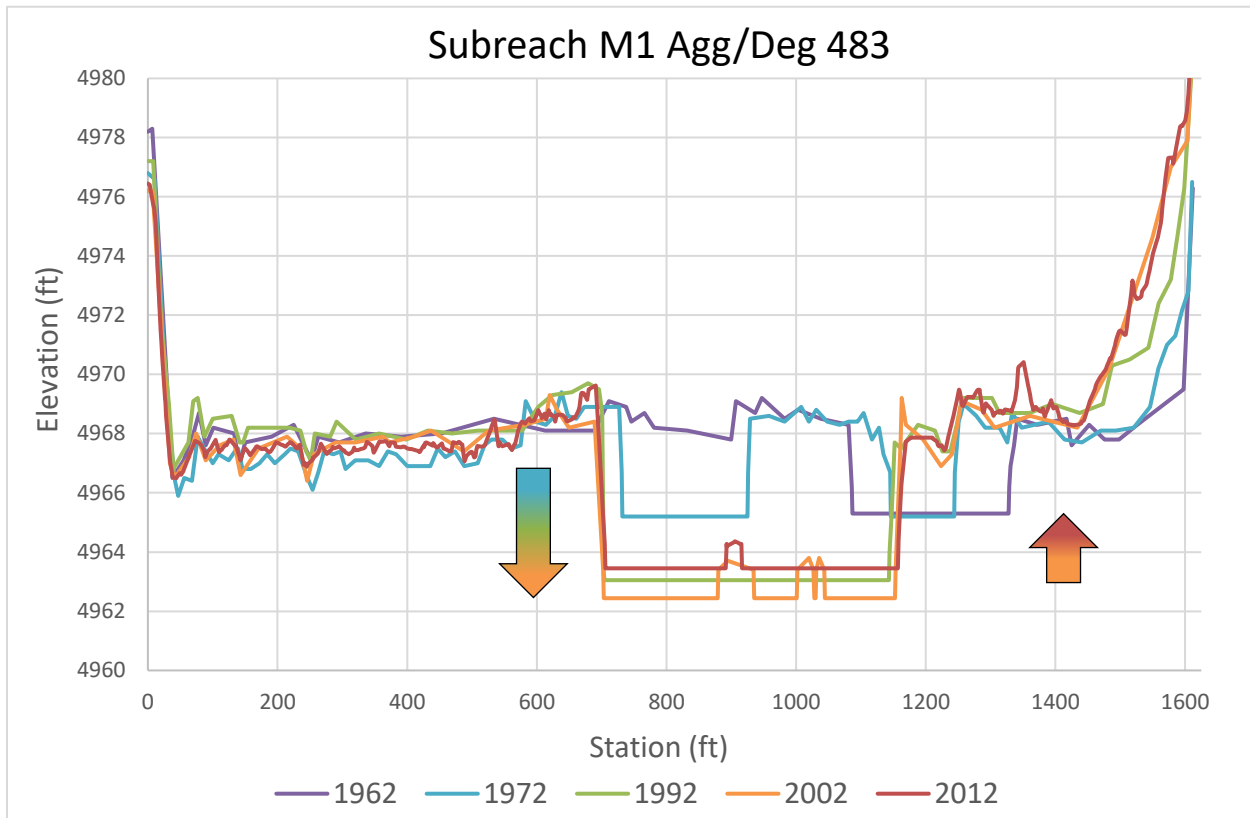


Figure 3-23 Subreach M1: Channel evolution of representative cross section Agg/Deg 483. Displaying a trend of incision from 1962 to 2012.

Figure 3-24 gives a synthesis of the likely channel form based on the Massong classification (left), the channel cross section (center) and aerial imagery (right) for Agg/Deg 483 in Subreach M1 for each evaluated year. River discharge is unknown at the time that the aerial imagery was collected.

Between 1962, Subreach M1 appears to be in Stage 1, with a wide, undefined channel and transient bars and islands. In 1972, the channel had shifted into Stage 2, with some vegetation encroachment along the right side of the channel as well as the formation of more clearly defined bars and islands. In the 20-year period from 1972 to 1992, the previous island is no longer present, the main channel incised while the vegetation has continued to encroach and establish along the banks and islands – indicating that the channel has evolved past Stage 3 and into Stage M4. During this time some grain sorting appears to have occurred, see **Figure 3-11**. From 1992 to 2002 the channel continued to incise, indicating that the channel is still in stage M4. In 2012, the channel appears to have aggraded, while this is not in line with the Massong classification, with the continuation of bed material sorting, armoring, and bed slope stabilization the channel can be classified as Stage M5. According to Massong (2010) Stage M5 can be short lived or a final stage depending on the armoring process and stable slope attainment process. Although the main reason why Subreach M1 cannot move past Stage M5 is because of the channelization efforts of the installation of jetty jacks preventing lateral migration. The underwater prisms developed for the adequate flow conveyance of the channel may underestimate the channel bed elevation leading to this aggradation shown from 2002 to 2012. This aggradation from 2002 to 2012 is a common theme throughout the Montano Reach.

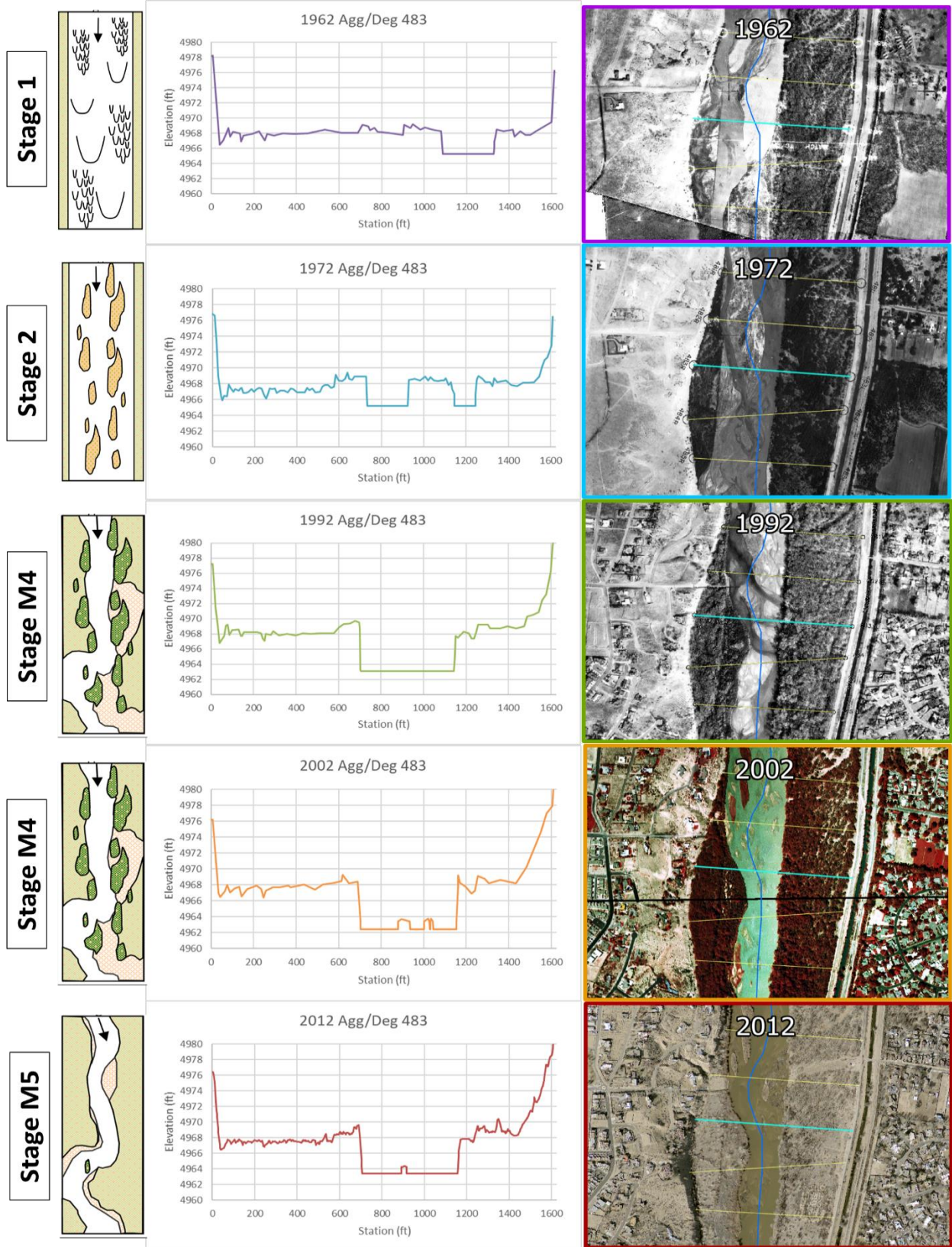


Figure 3-24 Subreach M1: Massong (2012) classification (left), historical cross section profiles (center) and corresponding aerial images (right) at Agg/Deg 483.

Figure 3-25 shows the evolution of the channel in Subreach M2 using a representative cross section at Agg/Deg 515 for the evaluated years.

In Subreach M2, the channel aggraded from a singular channel at low flows to an equal conveyance split channel at low flows from 1962 to 1972. The total width of the channel increased during this period. From 1972 to 1992 the channel greatly narrowed (from ~400 feet to ~215 feet) and incised (~2.5 feet). From 1992 to 2002 the channel incised slightly and in 2012 the channel slightly aggraded (~0.5 feet). A net degradation of 2 feet occurred in the 40 years between 1972 and 2012.

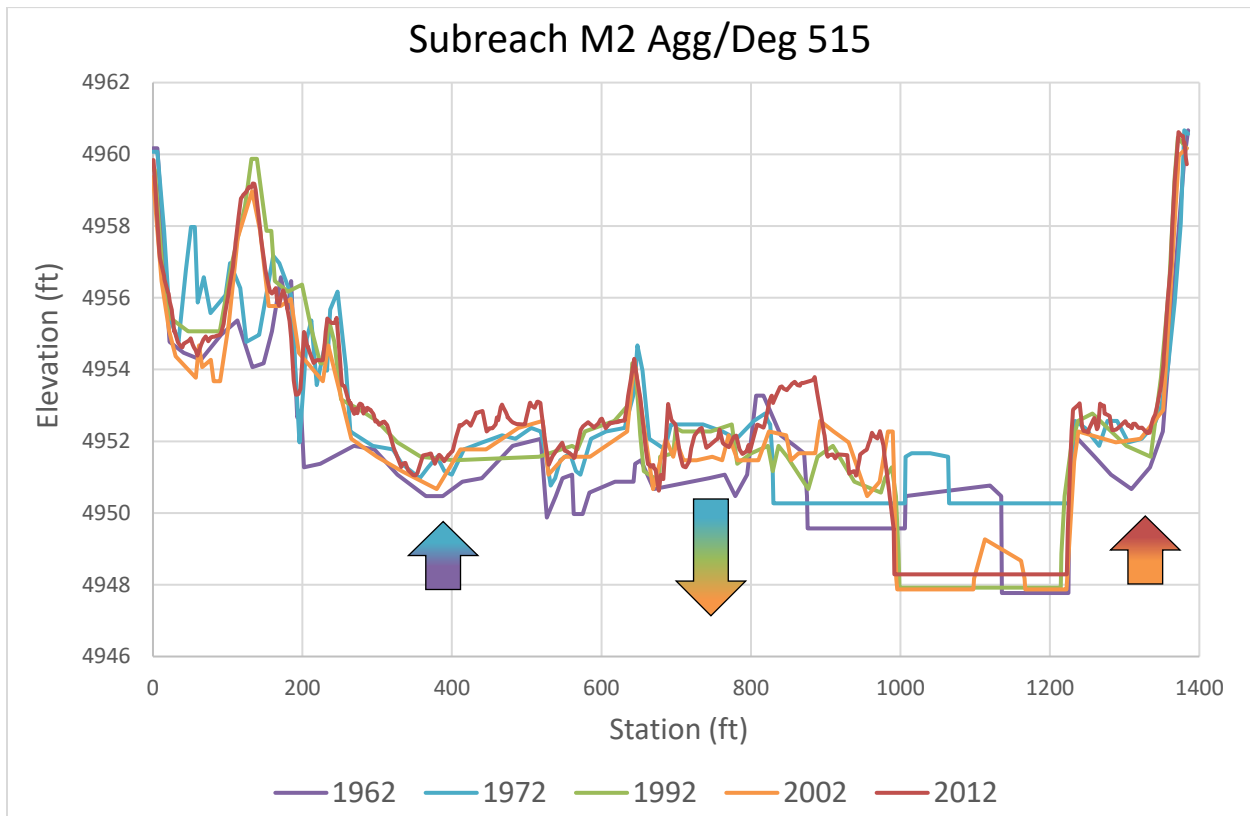


Figure 3-25 Subreach M2: Channel evolution of representative cross section Agg/Deg 515. Significant channel degradation and narrowing occurred between 1972 and 2012.

Figure 3-26 gives a synthesis of the likely channel form based on the Massong classification (left), the channel cross section (center) and aerial imagery (right) for Agg/Deg 515 in Subreach M2 for each evaluated year.

In 1962, Subreach M2 appears to be in Stage 2. A wide channel is present, but one with more clearly defined braids, bars, and islands. Between 1962 and 1972, the channel widened and became shallower, continually adjusting to the jetty jack installation. The islands attached to the banklines, which receded slightly into the floodplain, but also stabilized with more dense vegetation – this classifies as Stage 3. From 1972 to 1992, significant channel narrowing and incision occurred, the channel is in Stage M4. The channel remains in Stage M4 with slight incision occurring in 2002 before transitioning to Stage M5 with slight aggregation in 2012. Stage M5 appears to be the end stage for Subreach M2, the channel cannot meander due to jetty jack installation that now defines the strong, erosion resistant, banklines.

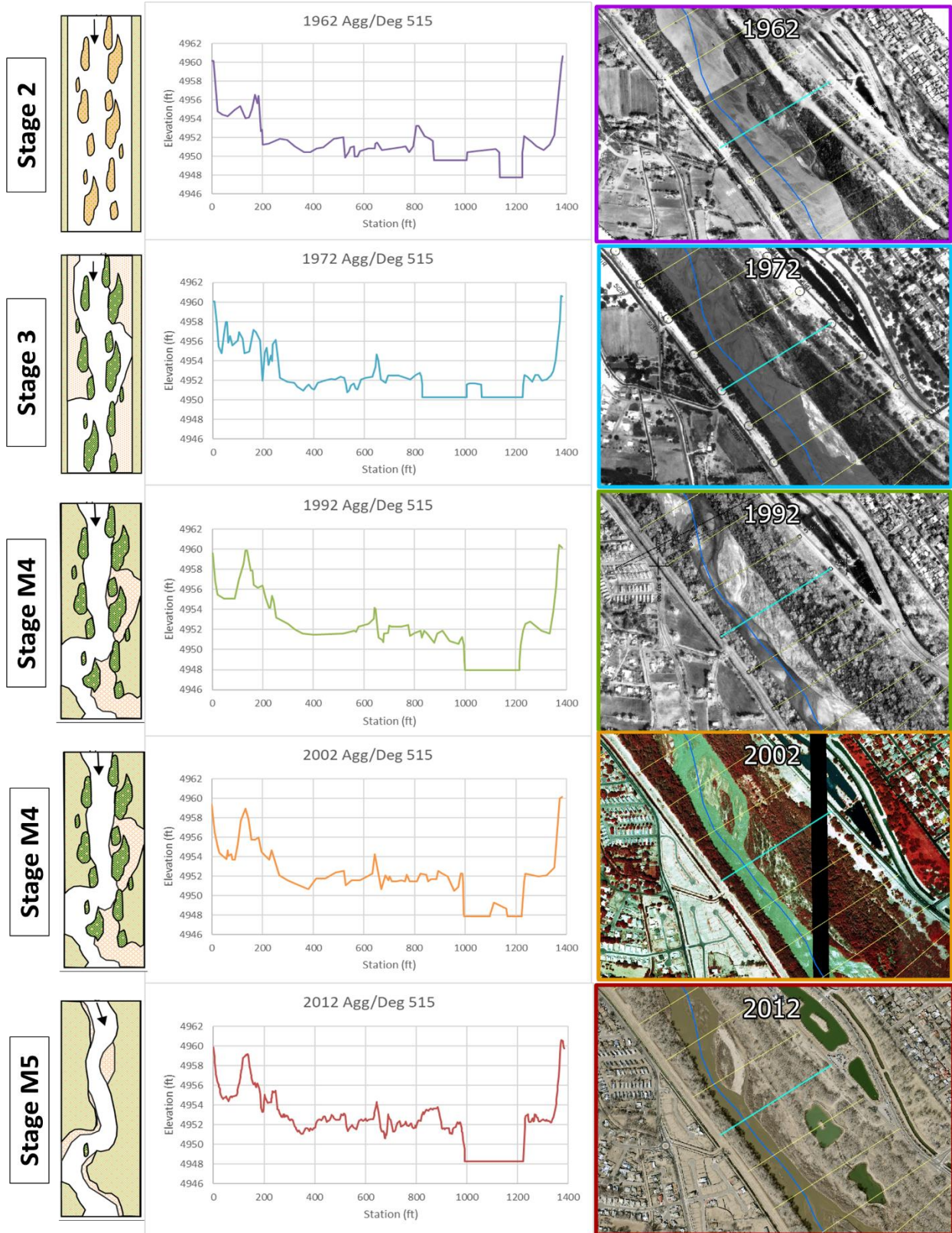


Figure 3-26 Subreach M2: Massong (2010) classification (left), historical cross section profiles (center) and corresponding aerial images (right) at Agg/Deg 515.

Figure 3-27 shows the evolution of the channel in Subreach M3 using a representative cross section at Agg/Deg 554 for the evaluated years.

In Subreach M3, the channel aggraded (~2 feet) from 1962 to 1972 at Agg/Deg 554. It appears the channel has widened significantly (~200 feet) during this period, but this is exaggerated. The flow observed in the aerial imagery in 1962 seems to be much less than that observed in 1972. What looks like the floodplain in 1962 is part of the main channel. By 1972, the channel conforms to the width defined by the jetty jack installation. From 1972 to 1992, significant incision (~3 feet) occurred while the channel width increased slightly. From 1992 to 2002, slight incision and channel narrowing occurred. The channel width remained constant from 2002 to 2012, but the channel bed experienced aggradation (~1 foot).

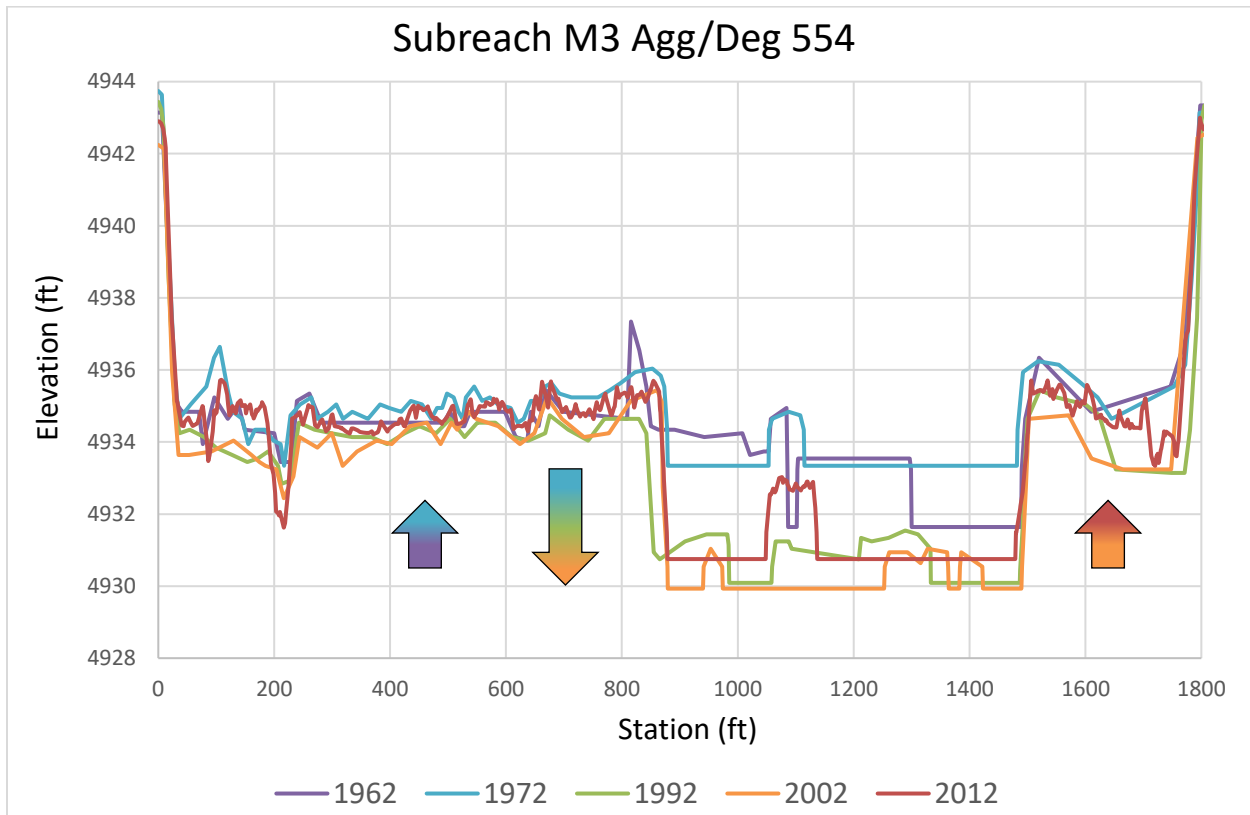


Figure 3-27 Subreach M3: Channel evolution of representative cross section Agg/Deg 554. Significant channel degradation occurring between 1972 and 2012.

Figure 3-28 gives a synthesis of the likely channel form based on the Massong classification (left), the channel cross section (center) and aerial imagery (right) for Agg/Deg 554 in Subreach M3 for each evaluated year.

In 1962, the preceding jetty jack installation had a more immediate channel response, multiple braids/threads were cut off rapidly. This year was difficult to classify, but appears to be in Stage 3, sand dunes and islands shown in 1949 have stabilized with vegetation and attached to the banks in 1962. In 1972, the main channel aggraded, and the side channel degraded to conform to the width defined by the jetty jacks – without vertical incision the channel is still classified as Stage 3. From 1972 to 1992, the channel vertically incised, thus, has transitioned into Stage M4. In 2002, very slight incision occurred along with grain sorting, classifying as Stage M4. The slope seems to have stabilized with the continuation of grain sorting and bed armoring between 2002 and 2012, the channel has transitioned into Stage M5. This will most likely be the end stage for this subreach.

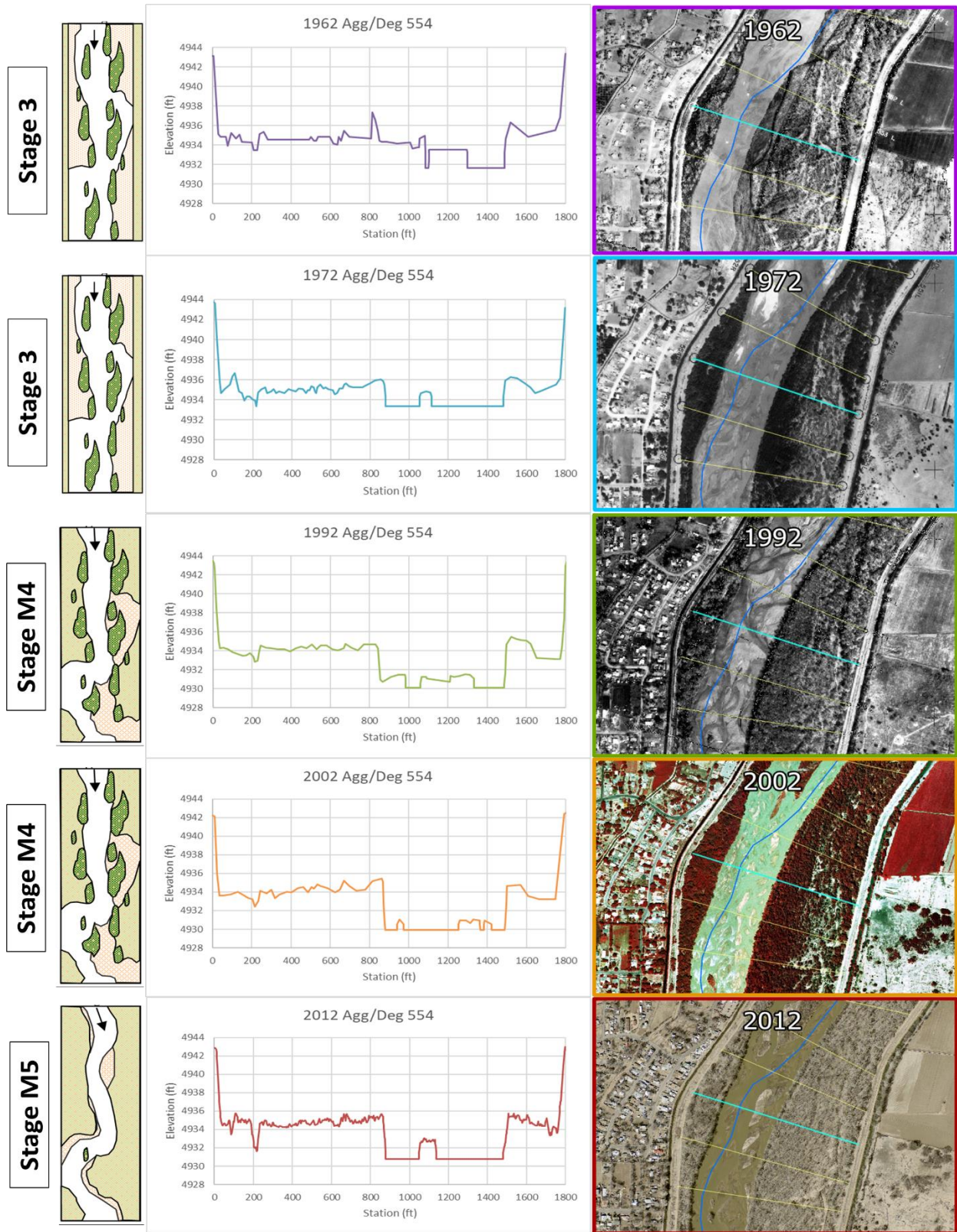


Figure 3-28 Subreach M3: Massong (2010) classification (left), historical cross section profiles (center) and corresponding aerial images (right) at Agg/Deg 554.

Figure 3-29 shows the evolution of the channel in Subreach M4 using a representative cross section at Agg/Deg 596 for the evaluated years.

In Subreach M4, jetty jacks were installed prior to 1962, but the channel was still relatively wide and shallow except for the main low flow channel shown at station 600 feet. From 1962 to 1972, the channel conformed completely to the jetty jack boundaries and incised the entire main channel to an elevation of 4912 feet. The left bank encroached while the right bank did not change. From 1972 to 1992, the channel incised (~1 foot) while the right bank widened slightly. From 1992 to 2002 the channel bed remained constant while the right bank continued to widen slightly. In 2012 both banks remain at their previous locations while the channel bed elevation aggraded (~1 foot), almost identical shape and size of that surveyed in 1972.

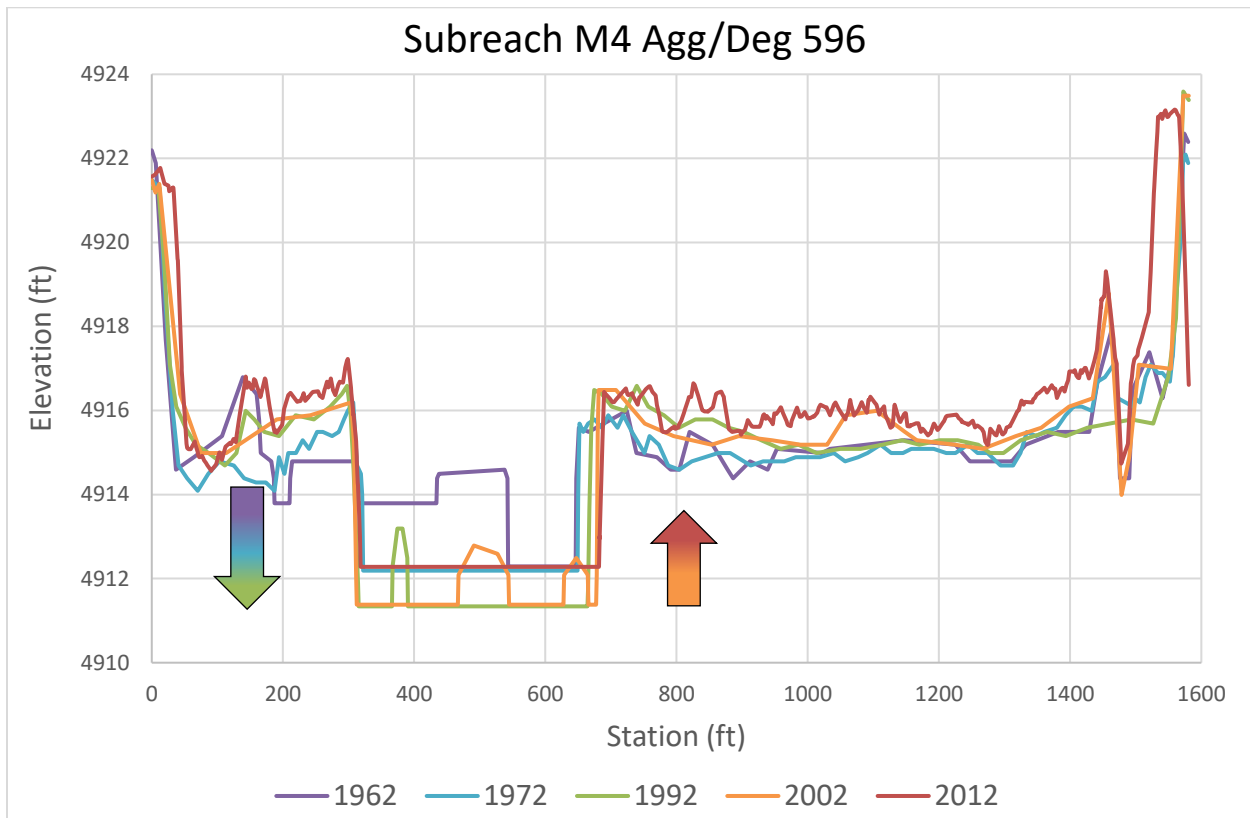


Figure 3-29 Subreach M4: Channel evolution of representative cross section Agg/Deg 596.

Figure 3-30 gives a synthesis of the likely channel form based on the Massong classification (left), the channel cross section (center) and aerial imagery (right) for Agg/Deg 596 in Subreach M4 for each evaluated year.

In 1962 the channel is adjusting to the jetty jack installation, vegetation has encroached, and sand dunes have started to stabilize and attach to the banklines since 1949, classifying as Stage 2. In 1972, the main channel widened conforming to the jetty jack installation (the entire active channel width decreased), the average slope in this Subreach is within the Massong meandering range, although with no incision of the thalweg this classifies as Stage M3. The channel incised from 1972 to 1992, thus Stage M4 is observed. The channel bed elevation remains constant while grain sorting occurs from 1992 to 2002, the average bed slope slightly seems to have stabilized indicating a transition into Stage M5. In 2012 the bed elevation aggraded, along with bed armoring – the channel remains in Stage M5.

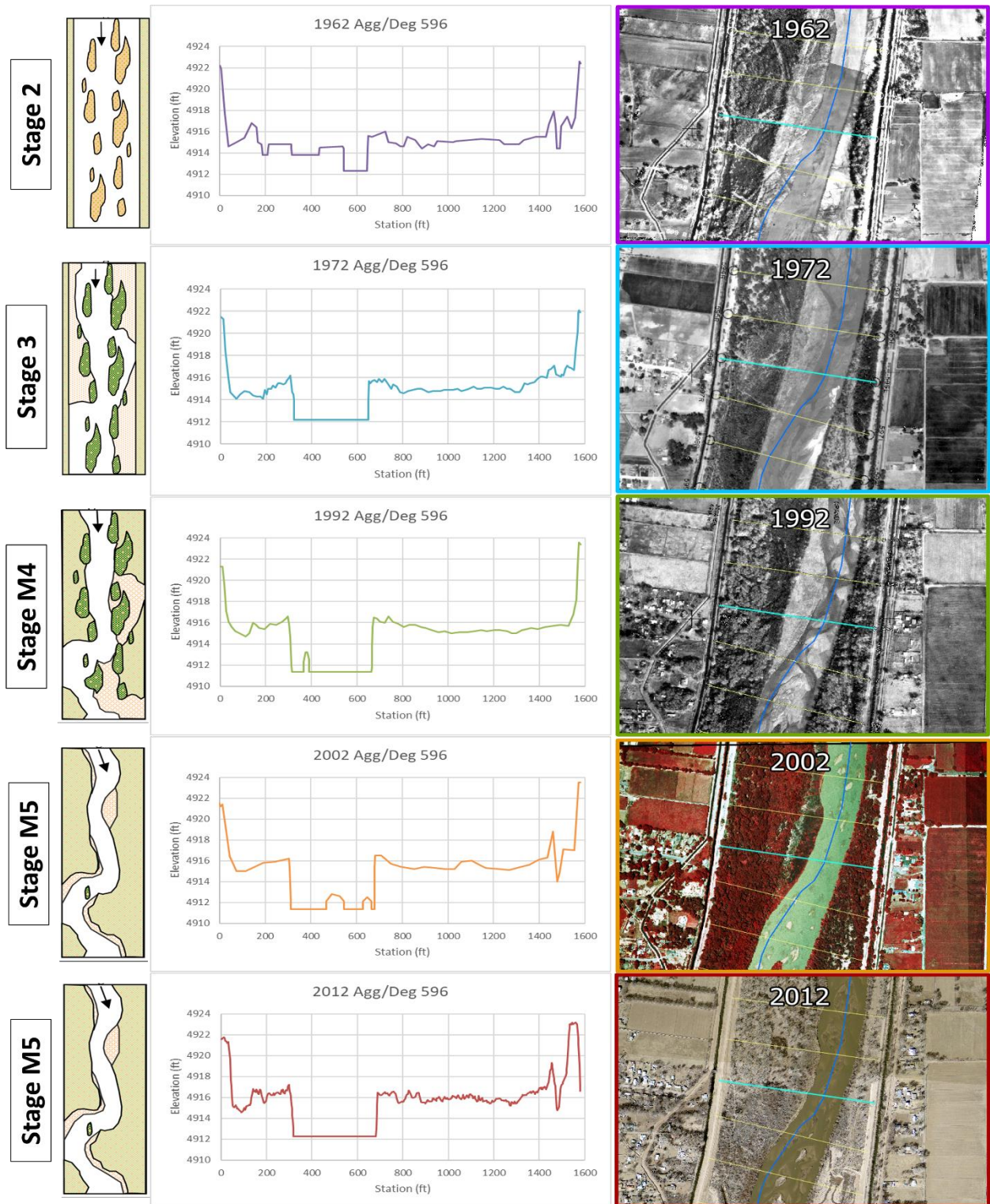


Figure 3-30 Subreach M4: Massong (2010) classification (left), historical cross section profiles (center) and corresponding aerial images (right) at Agg/Deg 596

Figure 3-31 shows the evolution of the channel in Subreach M5 using a representative cross section at Agg/Deg 629 for the evaluated years.

In Subreach M5, the channel significantly narrowed (from ~575 feet to ~225 feet) and incised (~2 feet) from 1962 to 1972. This abrupt change was caused by the installation of jetty jacks just prior to 1962. From 1972 to 1992 the channel widened and shifted from station 1100 feet to 800 feet. The right bank encroached while the left bank remained stable. From 1992 to 2002 the channel geometry did not change; the formation of dunes is observed from the aerial imagery (low flow compared to the other years). From 2002 to 2012, the channel bed elevation aggraded (~1 foot), while the geometry remained constant.

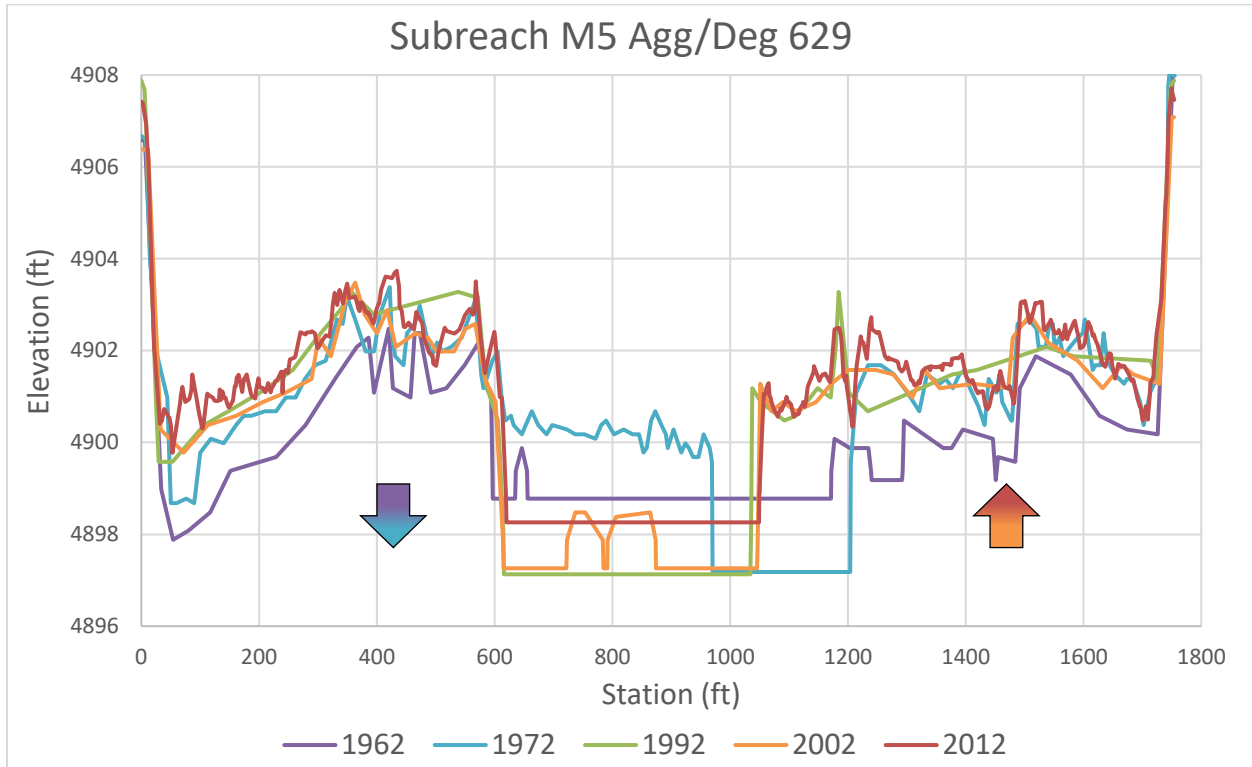


Figure 3-31 Subreach M5: Channel evolution of representative cross section Agg/Deg 629.

Figure 3-32 gives a synthesis of the likely channel form based on the Massong classification (left), the channel cross section (center) and aerial imagery (right) for Agg/Deg 629 in Subreach M5 for each evaluated year.

Although the channel in 1962 is wide compared to the following years, it is much narrower when compared to 1949. The installation of jetty jacks just prior to 1962 induced a channel response suggesting Stage 2 – where parts of the active channel have stabilized with vegetation, specifically the left bank. In 1972, the channel appears to be in Stage 3, although it has incised, the conveyance capacity of the main channel is like that of 1962. In 1992, the channel widened significantly and shifted locations, increasing its channel size, thus Stage M4. The channel slightly aggraded from 1992 to 2002, some grain sorting and bed armoring occurred indicating a transition into M5. The channel aggraded from 2002 to 2012, although this type of response is not outlined in Massong (2010) the channel is assumed to remain in Stage M5, its final stage.

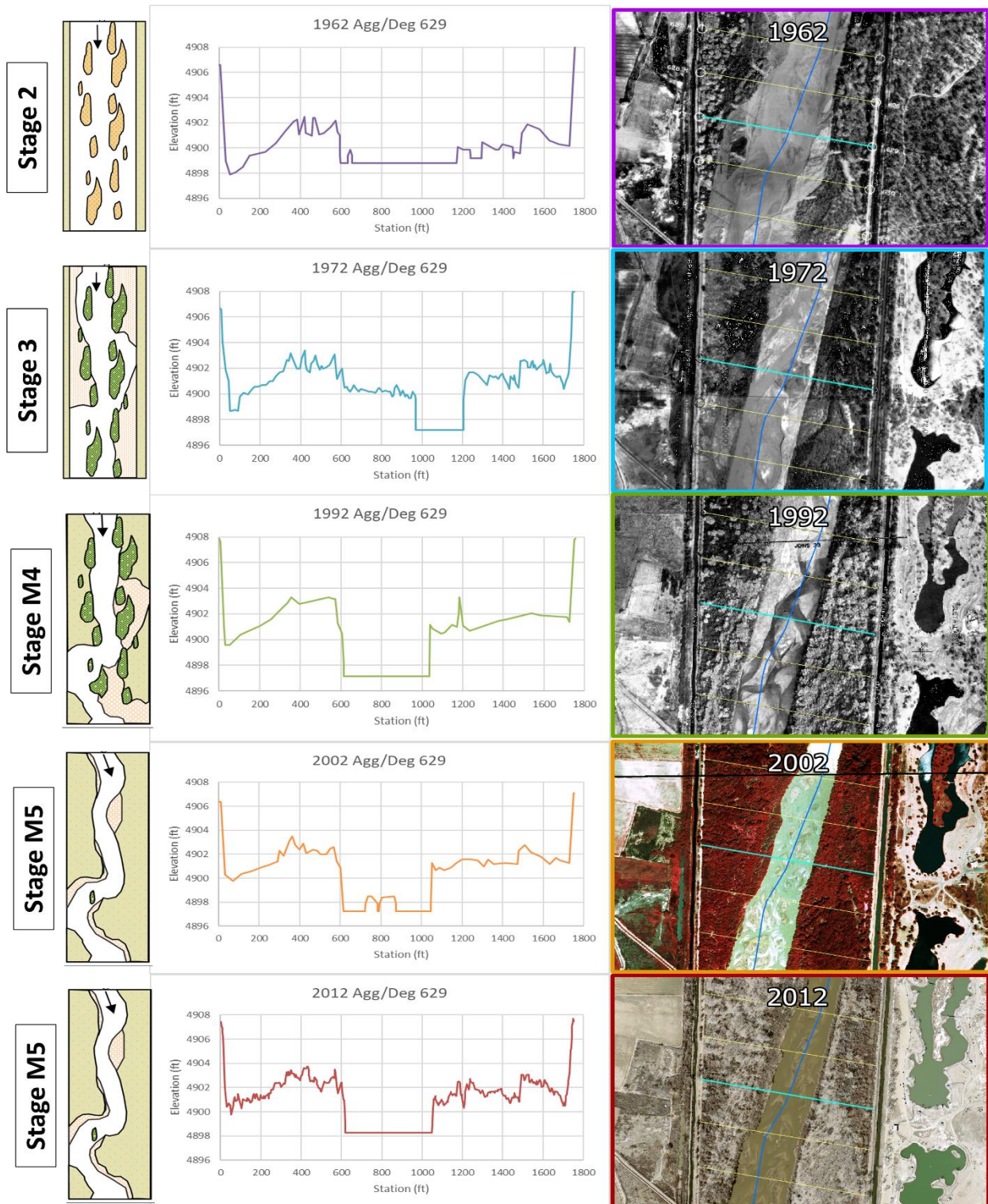


Figure 3-32 Subreach M5: Massong (2010) classification (left), historical cross section profiles (center) and corresponding aerial images (right) at Agg/Deg 629.

4 HEC-RAS Modeling for Silvery Minnow Habitat

The Rio Grande Silvery Minnow (RGSM or silvery minnow) is an endangered fish species that is native to the Middle Rio Grande. Currently, it occupies only about seven percent of its historic range (U.S. Fish and Wildlife Service, 2010). It was listed on the Endangered Species List by the US Fish and Wildlife Service in 1994.

One of the most important aspects of silvery minnow habitat is the connection of the main channel to the floodplain. Spawning is stimulated by peak flows in late April to early June. These flows should create shallow water conditions on the floodplains, which is ideal nursery habitat for the silvery minnow (Mortensen et al., 2019). Silvery minnows require specific velocity and depth ranges depending on the life stage that the fish is in. **Table 4-1** outlines these velocity and depth guidelines. Fish population counts are available prior to 1993 to the present. Therefore, analysis of silvery minnow habitat will not begin prior to 1992. In preparation for the process linkage report, figures relating the geomorphology of the river and RGSM habitat availability are included in **Appendix F**.

Table 4-1 Rio Grande Silvery Minnow habitat velocity and depth range requirements (from Mortensen et al., 2019)

	Velocity (cm/s)	Velocity (ft/s)	Depth (cm)	Depth (ft)
Adult Habitat	<40	<1.31	>5 and <60	>0.16 and <1.97
Juvenile Habitat	<30	<0.98	>1 and <50	>0.03 and <1.64
Larvae Habitat	<5	<0.16	<15	<0.49

4.1 Modeling Data and Background

The data available to develop these models varies year by year. Cross section geometry was available for the years 1962, 1972, 1992, 2002, and 2012. In 2012, additional LiDAR data of the floodplain was available, which allowed the development of a terrain for RAS-Mapper. Therefore, RAS-Mapper was used in 2012 only, while comparisons across years are done using 1-D techniques.

4.1.1 Ineffective Flow Analysis

HEC-RAS distributes water by adding water to a cross section from the lowest elevation upwards. Much of the MRG is either perched or has been altered with levees, so this can lead to inaccurate predictions of the flow distribution within the cross sections (overpredicting water in the floodplains), therefore, overpredicting hydraulically suitable habitat.

The Montaña Reach does not experience a significant amount of channel perching, where the floodplain has a lower elevation than the main channel. Therefore, the use of computational levees and the accompanying freeboard analysis, as done in previous reach reports (e.g. Elephant Butte), was not necessary. Although, the large amount of channelization efforts performed on the MRG (jetty jacks, spoil levees, etc.) modeling the flow is atypical and there is a need to restrict the HEC-RAS model from adding water at locations in specific cross sections throughout the Montaña Reach.

The spoil levees, when constructed, were not engineered. Often, they were placed at locations of most convenience – this resulted in inconsistencies, discontinuities, and failures along the spoil levee’s alignment. Furthermore, the MRG, specifically the Montaña Reach, has largely transitioned from a wide and shallow braided multi-threaded river to a narrow and deep single thread river over time. The Montaña Reach has cut off many of its side channels over time, these tend to reactivate at higher discharges before the floodplain starts to inundate. Because of the channelization efforts and the change in channel morphology there is a need to restrict the flow within the main channel until an overtopping water surface

elevation has been exceeded at site specific locations. To model this adequately in HEC-RAS, ineffective flow areas were implemented.

Ineffective flow areas are not the same as computational levees but serve a similar purpose. Ineffective flow areas identify areas of zero-velocity, regions in a cross section that should not have flow conveyance until a trigger water surface elevation has been met. Once this WSE has been met or exceeded the flow is modeled without the consideration of the ineffective flow areas, see **Figure 4-1** for an example cross section. The advantage of using ineffective flow areas over computational levees is that you can set ineffective flow areas at multiple locations at varying elevations, this allows to model the atypical flow paths and inundation patterns of the Montañó Reach more accurately. With computational levees, the implementation is more ridged, HEC-RAS limits levee placement to a singular location on each side (left of bank and/or right of bank) of the channel cross section.

Ineffective flow areas were typically set at the average minimum floodplain elevation for the respective bank. Historical side channels were typically free of ineffective flow areas or had one placed below that of the average floodplain elevation to simulate the reactivation of these side channels before the floodplain. Ineffective flow areas were implemented for years 1992, 2002, and 2012 but not for 1962 and 1972. This is because in 1962 and 1972 the channel was wide, shallow, and braided.

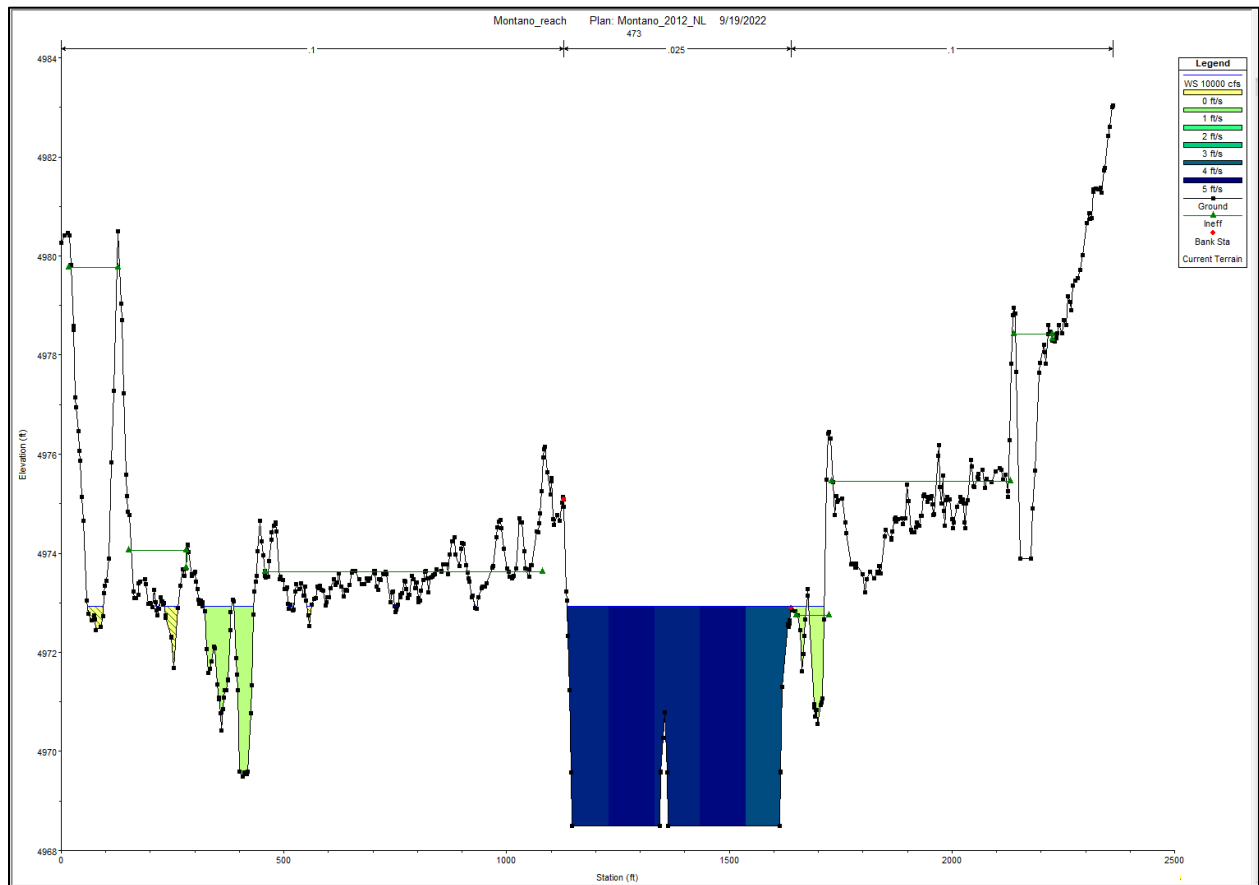


Figure 4-1 Example cross section with ineffective flow areas at 10,000 cfs, hatched areas are those below the trigger elevation and will not convey water in the model.

4.2 Width Slices Methodology

Without a terrain for 2002 and 1992, additional methods had to be considered to determine a metric of fish habitat in area per distance and in length of river. HEC-RAS has the capability to perform a flow distribution analysis to calculate the laterally varying velocities, discharges, and depths throughout a cross section as described in chapter 4 of the HEC-RAS Hydraulic Reference Manual (US Army Corps of Engineers, 2016). HEC-RAS allows each cross-section to be divided into 45 slices. The Montañero Reach is more incised compared to other river reaches along the MRG, therefore the bankfull discharge is greater. The greatest flow modeled for habitat mapping was 5,000 cfs, see **Section 4.4** for more details on habitat mapping. For the greatest resolution for accessible RSGM habitat the 45 slices distributed 10 to right of bank, 25 to main channel, and 10 to left of bank. An example of the flow distribution in a cross-section is shown in **Figure 4-2**. The velocity and depth of each slice were analyzed to determine the total width at each Agg/Deg line that meets the RSGM larval, juvenile, and adult criteria. Because the Agg/Deg lines are spaced approximately 500 feet apart, the hydraulically suitable widths were multiplied by 500 feet to obtain an area of hydraulically suitable habitat per length of river. For areas outside of the main channel, a Manning’s roughness of 0.1 was used, and for inside the main channel 0.025 was used.

As mentioned in **Section 4.1.1** (above), HEC-RAS designates ineffective flow areas as areas of ponding water (zero velocity regions), which are typically disconnected from the main channel. To remove these regions a criterion of “velocity > 0 ” was added within the Microsoft Excel spreadsheet calculations. HEC-RAS calculates velocities to the hundredth decimal place (e.g. 0.01), therefore the overestimation of flow inundation does not become an underestimation with this criterion. This is consistent with the habitat maps discussed the following sections. criteria which were calculated neglecting zero velocity regions as suitable habitat.

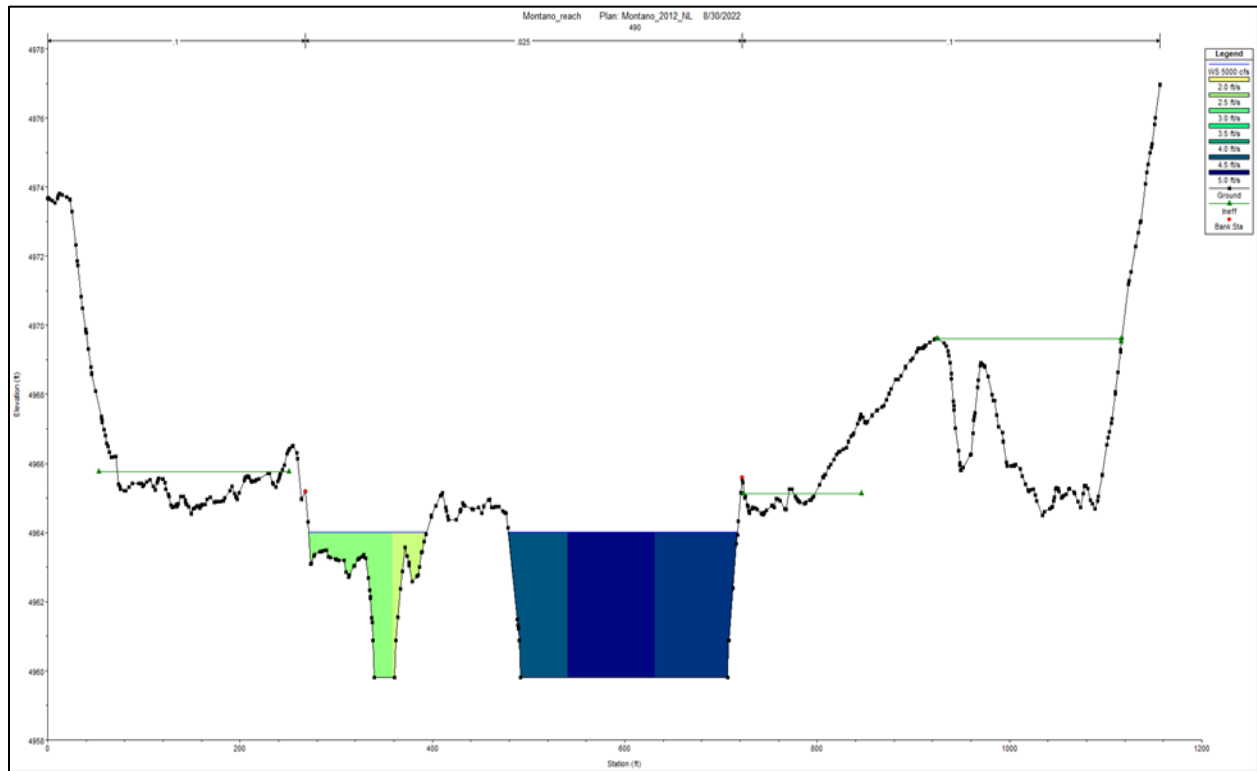


Figure 4-2 Cross section at a discharge of 5,000 cfs with the flow distribution from HEC-RAS of 20 vertical slices in the floodplain (10 ROB and 10 LOB) and 25 vertical slices in the main channel. The slices are small enough that the discrete color changes look more like a gradient.

4.3 Width Slices Habitat Results

The width slices method was first used to analyze the habitat availability throughout the Montaña Reach at a reach scale for the years of 1962, 1972, 1992, 2002 and 2012. For the discharges at which the water is contained in the main channel, there is less habitat availability. In general, when the discharge sufficiently increases to where the water can reactivate side channels and/or spill out onto the floodplains, there is suddenly an increase in area where the depth and velocity criteria are met, as shown in **Figure 4-3** to **Figure 4-5** below.

Throughout the Montaña Reach, the results follow a similar trend for larvae, juvenile, and adult life stage habitat. There was more habitat availability during the years of 1962 and 1972. There is a dramatic decrease in habitat between 1972 and 1992, which corresponds to the degradation and the decrease in active top width that the reach experiences during that time frame. See **Section 3** for more information on the change in channel characteristics between time periods. There is limited available larvae habitat in comparison to the juvenile and adult available habitats, it does slightly increase as the flow increases and side channels, mid-channel islands, and the floodplain start to inundate. The Montaña Reach generally shows less overall habitat availability compared with other reaches of the MRG. As a basis for comparison, the Bosque reach shows roughly 50 times more larval habitat and 20 times more juvenile and adult habitat at 3,000 cfs than the Montaña reach in 2012 (Schied 2022). For the Montaña Reach, the floodplain rarely inundates at typical flows experienced throughout the MRG. The main channel, reactivated side channels, or mid-channel islands provide the only opportunities for RSGM habitat at these flows whereas the floodplain contributed to the large amount of available habitat in previously studied reaches (Sperry 2022 and Schied 2022).

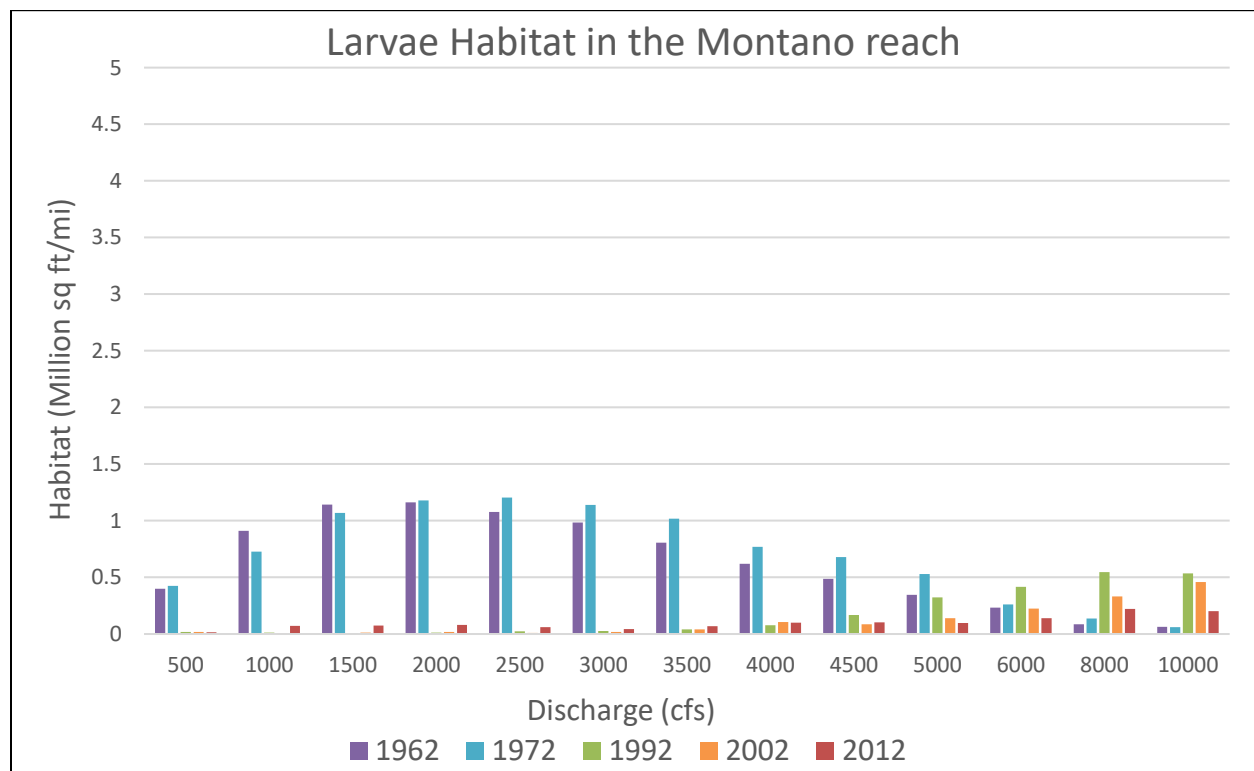


Figure 4-3 Larval RSGM habitat availability throughout the Montaña Reach

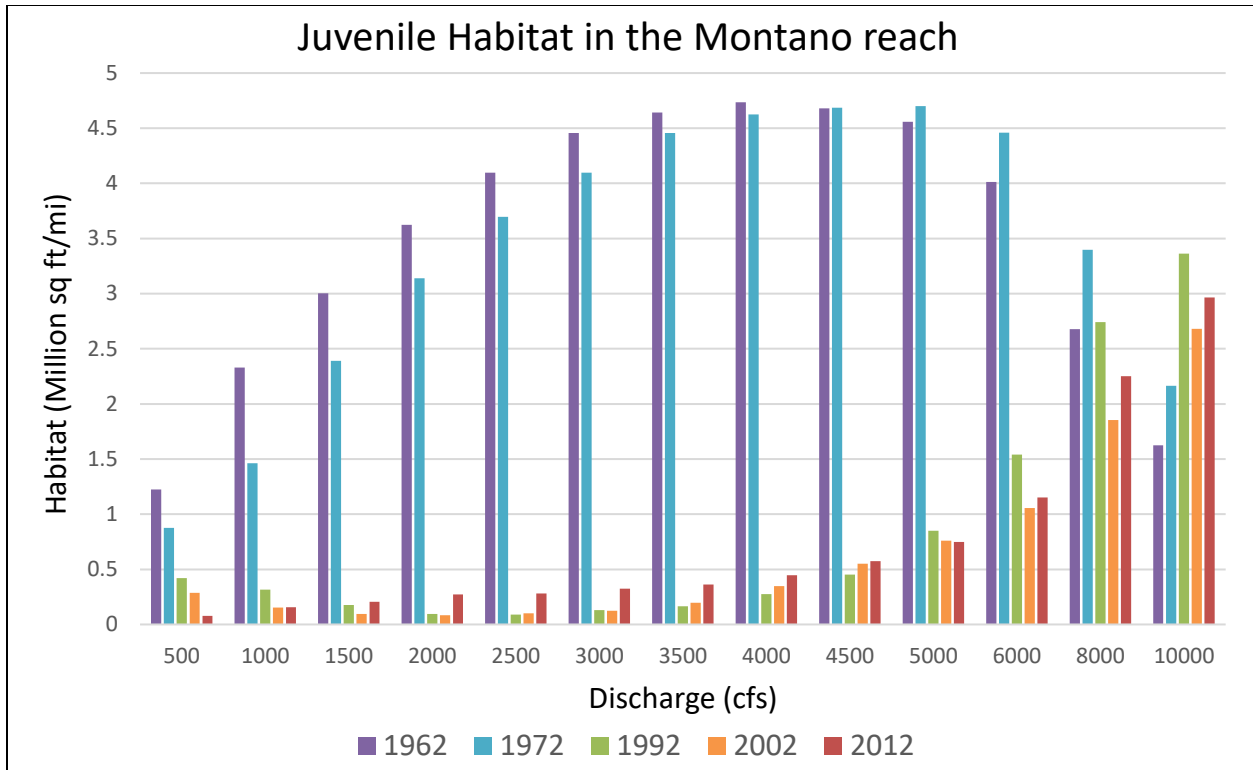


Figure 4-4 Juvenile RSGM habitat availability throughout the Montano Reach

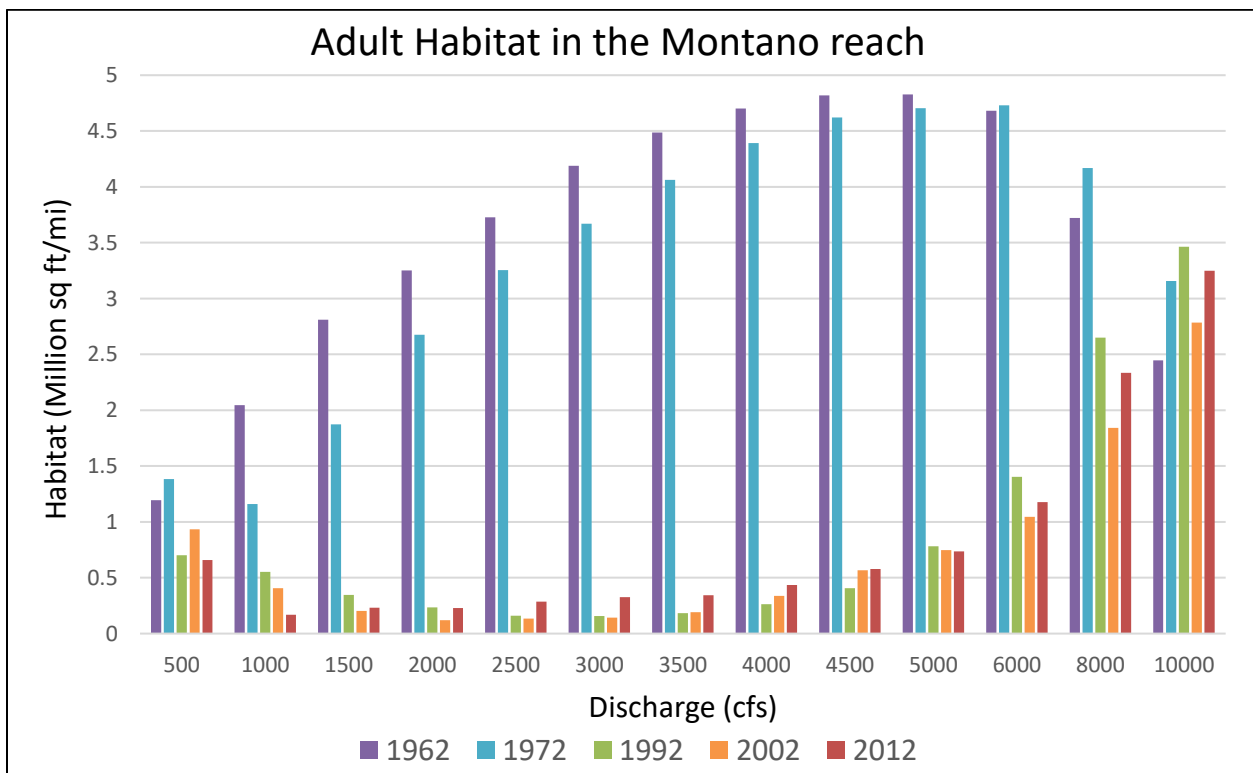
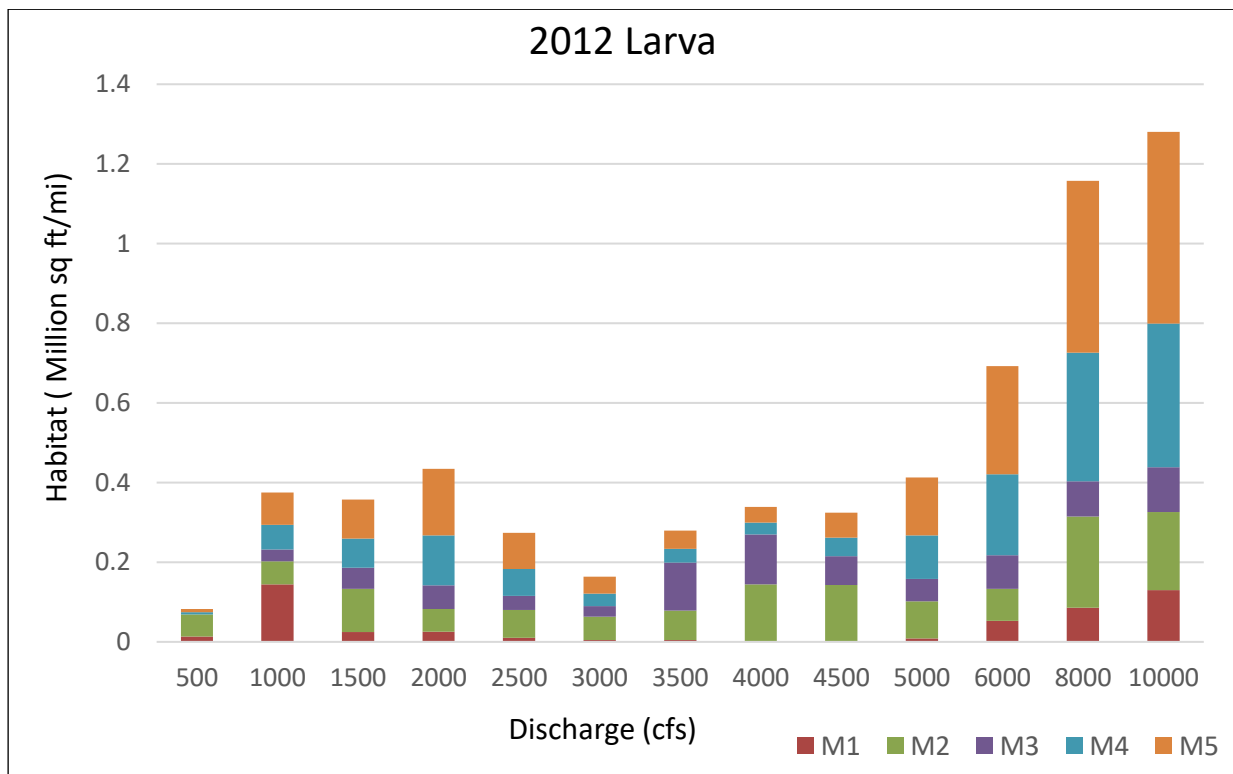


Figure 4-5 Adult RSGM habitat availability throughout the Montano Reach

The width slices method was also used to analyze the habitat availability throughout the Montañño Reach at a subreach level. Stacked habitat bar charts were created to portray the spatial variation of hydraulically suitable habitat of the RGSM throughout the Montañño Reach. The bar charts display the width of habitat at different discharges for 2012. To convert the hydraulically suitable habitat to an area, these values would be multiplied by 500 feet, which is the approximate distance between each Agg/Deg line. **Figure 4-6** shows the 2012 habitat availability from 500 cfs to 10,000 cfs for subreaches M1 through M5.

Based on this method, applied to the 2012 data, subreaches M4 and M5 consistently had the most hydraulically suitable habitat for larvae, juvenile, and adult life stages across all the discharges. Juvenile and adult habitat distributions are consistent with a slight increase in habitat with the increase in discharge until 5000 cfs, then a sharp increase is observed. The larvae distribution shows a bit more of an irregular pattern, increases in habitat between 1000 cfs and 2000 cfs, then a decrease from 2500 cfs to 3000 cfs, then a continued increase until 10000 cfs. Note the different scales between the figures, overall, the magnitude of larvae habitat is significantly less than that of the other life stages, especially at higher discharges.



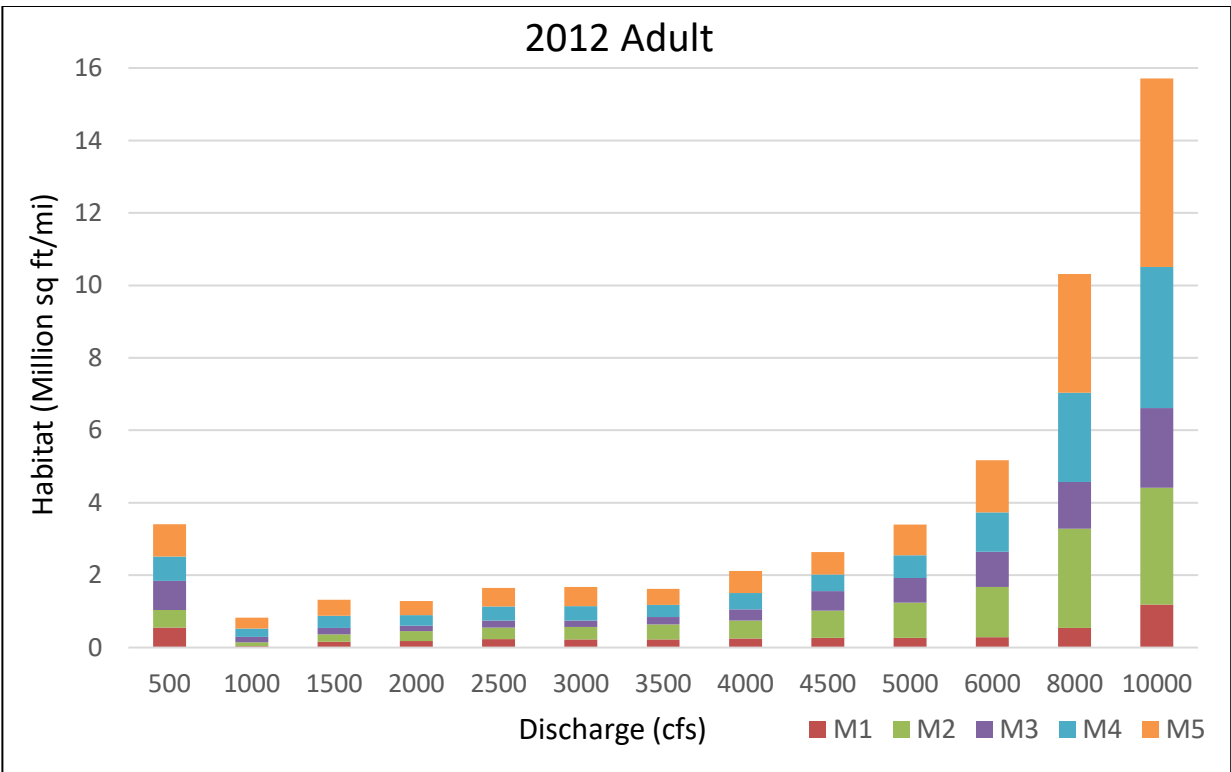
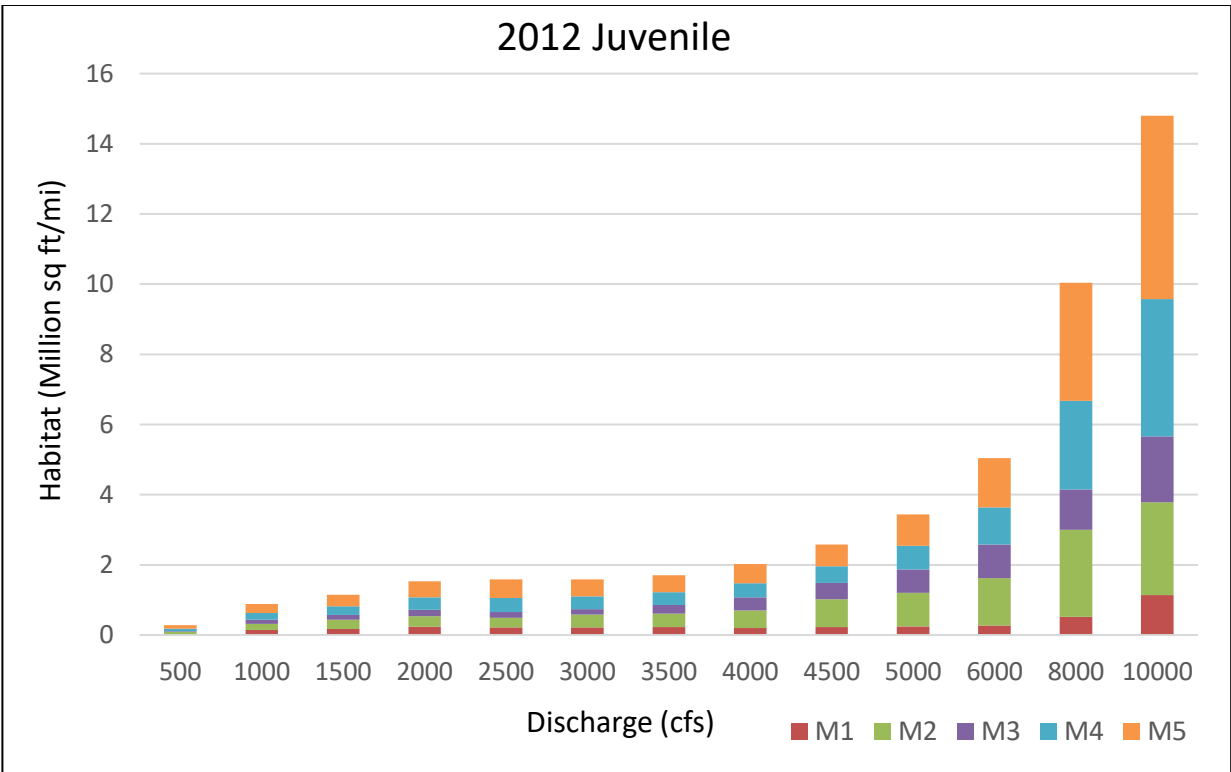


Figure 4-6 Stacked habitat charts at different scales to display spatial variations of habitat throughout the Montañó Reach in 2012

4.4 RAS-Mapper Methodology

By using RAS-Mapper, the goal was to transform the 1-D habitat estimates into pseudo two-dimensional (2-D) results. RAS-Mapper overlays the water onto a prescribed terrain and interpolates the water surface elevation to create an estimate of the location of water inundation, which can then be used to predict locations of hydraulically suitable habitat for the Silvery Minnow.

The HEC-RAS geometry data that was necessary for the RAS-Mapper analysis (geo-referenced cross-sections and a LiDAR surface to generate a terrain) was available only for the year 2012. Therefore, only 2012 results were processed in RAS-Mapper. The original 2012 LiDAR data was used to develop a raster on ArcMap software (intellectual property of ESRI), which could be imported as a terrain in RAS-Mapper. The RAS-Mapper application distributes the water throughout the terrain, interpolating between the cross-sections, which results in a more accurate understanding of where water is present in a channel.

RAS-Mapper will also predict the flow depth and velocity at a given discharge. It should be noted that while the cross-sectional data has a low-flow channel stamped into each cross section, the LiDAR surface used for mapping does not include channel data below the water surface. As a result, the water depth in the channel generated from RAS-Mapper underestimates the flow depth by around 2 feet throughout the entire reach and will not show accurate habitat mapping within the main channel. Given that suitable habitat is generally found in the floodplain, this was not as great of a concern. Additionally, the habitat graphs discussed in **Sections 4.2** and **4.3** account for the low flow channel and are therefore not subject to this same error.

ArcGIS Pro was used to combine the RAS-Mapper generated raster datasets for velocity and depth so that the RGSM depth and velocity criteria could be applied to identify the areas of suitable habitat. The results were used to create maps that show the areas of hydraulically suitable habitat for each life stage of the RGSM throughout the Montañó Reach. As mentioned in **Section 4.1.1** (above), HEC-RAS designates ineffective flow areas as areas of ponding water (zero velocity regions). During the habitat map generation, these areas are shown as inundated areas, typically disconnected from the main channel. To account for this, the regions of zero velocity (WSE below the ineffective flow elevation) were removed by adding a “velocity > 0” criterion within ArcGIS Pro. HEC-RAS calculates velocities to the hundredth decimal place (e.g. 0.01), therefore the overestimation of flow inundation does not become an underestimation of RSGM habitat with this criterion. This is consistent with the methods used to generate the habitat curves discussed in **Section 4.2**.

4.5 RAS-Mapper Habitat Results in 2012

While the width slice method quantitatively determined areas with increased potential for habitat, RAS-Mapper was used to spatially depict these areas of potential RGSM habitat throughout the Montañó Reach of the MRG and display the results on a map of the river. The hydraulically suitable habitat for each life stage was mapped at discharges of 1,500 cfs, 3,000 cfs, and 5,000 cfs, which have post Cochiti dam daily exceedance probabilities of around 20.2%, 9.9%, and 3.3%, respectively (**Figure 2-17**). The habitat maps for the reach at these discharges are available in **Appendix E**.

At lower flow magnitudes the hydraulically suitable habitat is primarily seen in the side channels for all life stages and near island and bank boundaries for the juvenile and adult life stages where velocities are slower and channel depths are smaller. From the RAS-Mapper results and the habitat graphs (**Figure 4-6**), there is more hydraulically suitable habitat for all life stages in Subreaches M5, M4, and M2 than there is in M1 and M3. This is because these subreaches experience more floodplain inundation and side channel activation at lower flow magnitudes than the other subreaches.

While the more frequent 1,500 cfs magnitude flood event does not provide significant hydraulically suitable habitat for the juvenile and adult life stages when compared to the 3,000 and 5,000 cfs events. There is an increase in available larvae habitat in the 1,000 cfs to 2,000 cfs range of flows, most of the larvae habitat is shown along the various slightly inundated side channels along subreach M2. Suitable habitat for the larval life stage generally reduces as flow depth increases within the side channels up to 3,000 cfs, then a trend upward is shown increasing the flood magnitude to 5,000 cfs where the flow has inundated various locations of the floodplain. Suitable habitat for juveniles and adults generally increases with increased flood magnitude, especially along midchannel islands and bars that become fully inundated.

It is likely that the model is over predicting side channel activation at 1,500 cfs, underpredicting at 3,000 cfs, and over predicting floodplain inundation at 5,000 cfs. Therefore, the results would be overestimating habitat at 1,500 cfs and 5,000 cfs while 3,000 cfs is underestimating habitat availability in the habitat maps and stacked habitat charts, **Figure 4-7**, **Figure 4-8**, and **Figure 4-9** show an example of this.

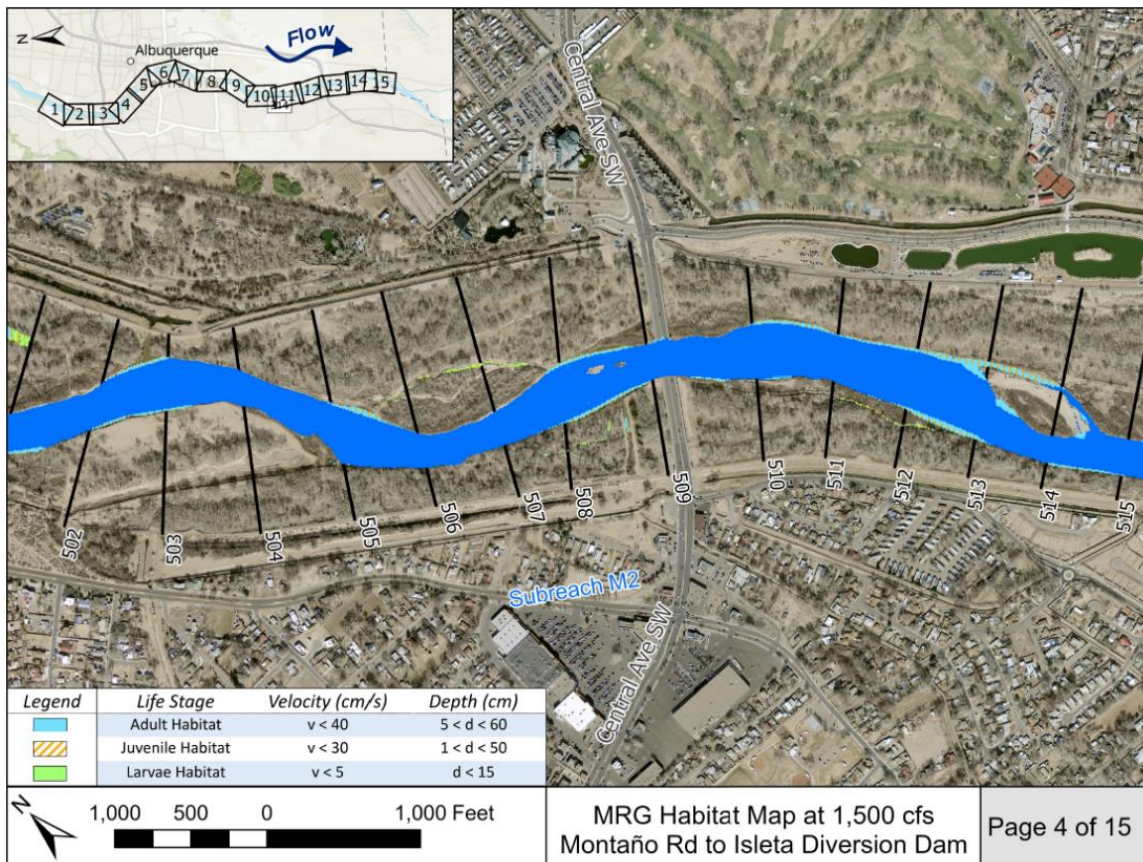


Figure 4-7 Suitable habitat in 2012 for each life stage at 1,500 cfs in Subreach M2.

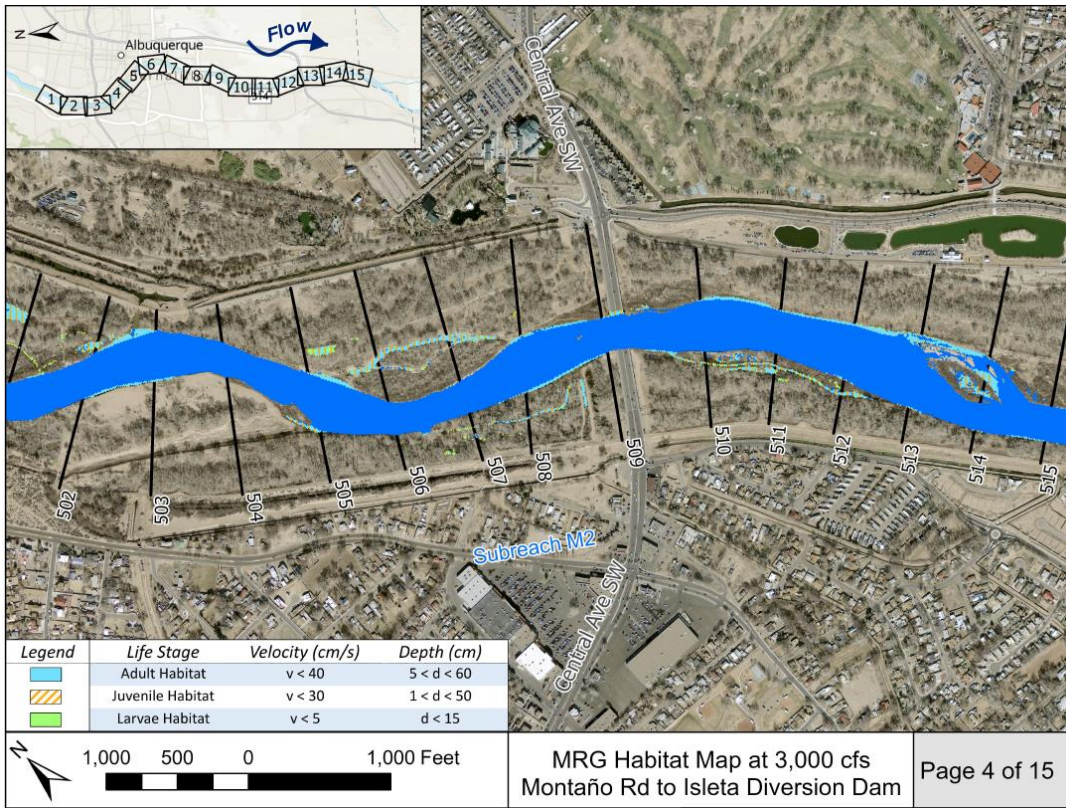


Figure 4-8 Suitable habitat in 2012 for each life stage at 3,000 cfs in Subreach M2.

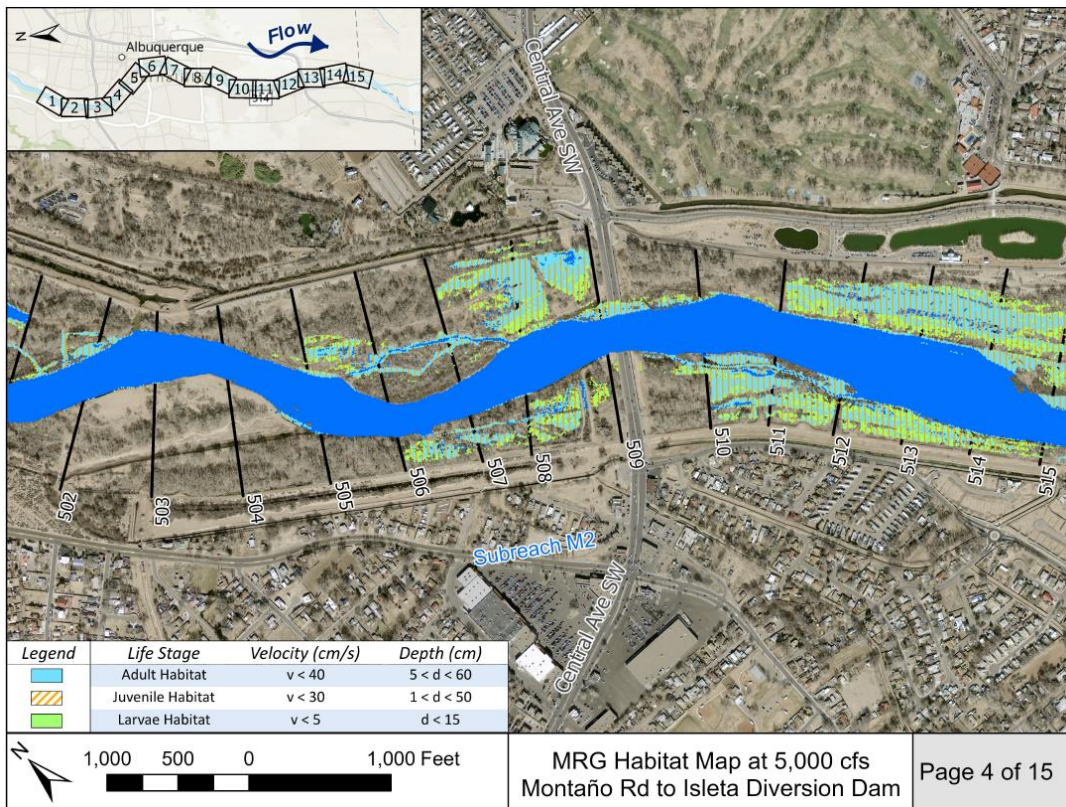


Figure 4-9 Suitable habitat for each life stage at 5,000 cfs in Subreach M2.

4.6 Disconnected Areas

RAS-Mapper provides the opportunity to identify areas that likely meet the velocity and depth requirements of the RGSM at specified discharges. RAS-Mapper may also be beneficial for identifying areas throughout the reach that may contain water but are not connected to the main channel. These may be possible areas of focus for restoration efforts. By connecting several of these disconnected areas, the Silvery Minnow may gain a great amount of possible habitat. **Figure 4-10** shows one instance of a disconnected area in Subreach M5. The disconnected area is emphasized by the red rectangle. These low-laying areas appear to contain side channels that historically became inundated at lower magnitude flood events, but over time have become disconnected from the main channel due to aggradation. The disconnected areas could identify problem areas for the RGSM by indicating that there are areas where fish may become stranded in months when the river contains less water and disconnected areas form. Conversely, these areas could become possible restoration sites leading to an increase in hydraulically suitable RGSM habitat.

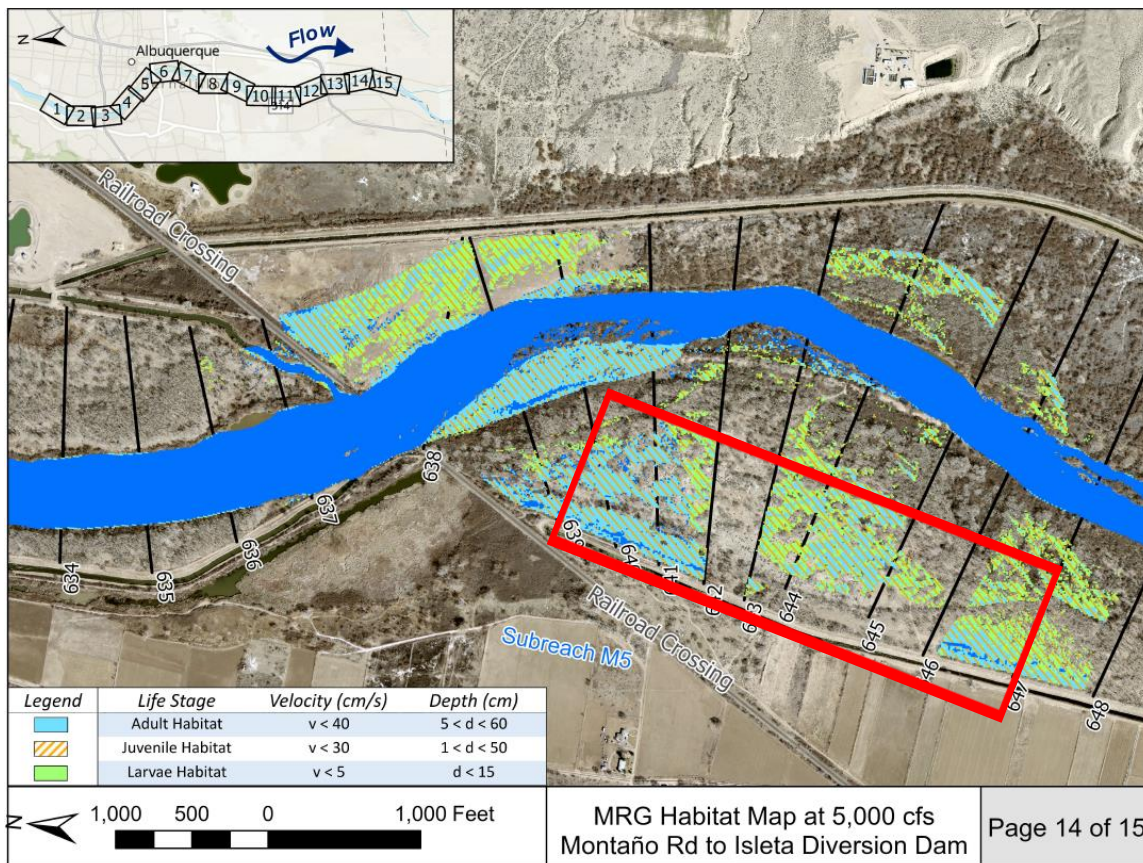


Figure 4-10 Disconnected low-laying areas that are no longer connected to the main channel at 5,000 cfs in Subreach M5.

5 Conclusions

The Montaña Reach spans about 19 miles from the Montaña bridge crossing Albuquerque, New Mexico, to the Isleta Diversion Dam. The purpose of this report is to analyze the hydrologic, hydraulic, and geomorphic trends between 1918 and 2021. HEC-RAS and ArcGIS were used to find geomorphic and river characteristics such as sinuosity, width, bed elevation, and other hydraulic parameters. In addition, hydraulically suitable RSGM habitat was determined quantitatively and spatially throughout the river reach.

Major findings of this study include:

- The construction of upstream dams, most notably Cochiti Dam in 1973, has impacted the hydrograph for the Montaña Reach. Before the dam construction, there was a greater frequency and magnitude of large flood events. These flow events with a daily exceedance probability of less than 10% have been most impacted. Climate has also impacted the hydrograph - the climate region containing the MRG cycles through dry and wet periods and is currently in a dry period.
- Spring snowmelt typically supplies the greatest water and sediment discharge volumes. Occasional monsoonal thunderstorms transport the greatest concentrations of suspended sediment, but only for short periods of time. The sediment flux into the river is primarily driven by snowmelt that drains into ephemeral tributaries and nearby arroyos, which transport sediment into the MRG.
- The Montaña Reach narrowed significantly between 1918 and 1962 from an average width (defined by vegetation) of 1470 feet to 500 feet. The channel has continued to narrow gradually from 1962 to 2019 to an average of 375 ft. This narrowing results from channelization efforts (e.g., jetty jacks and levees), construction of Cochiti dam (reduced peak flows), and dry periods.
- The Montaña Reach experienced net degradation between 1962 and 2012. Most of the incision occurred between 1972 and 1992. As a result, the slope of the Montaña Reach has flattened slightly – the Isleta Diversion Dam at the downstream boundary acts as a grade control. Slight aggradation occurred from 2002-2012.
- Median grain diameter measurements from 1990 to 2014 show a trend grain sorting and bed arming, especially in Subreaches M3, M4, and M5. Large spikes in median grain diameter, up to coarse gravel, was observed. Although, slight coarsening over time is the general trend, from 0.2 to 0.37 mm.
- Sinuosity has remained low but relatively variable from 1918 to 2019. The trend has been a decrease in sinuosity over time resulting from channelization efforts (e.g. jetty jacks) performed on the MRG.
- Between 1962 and 2012, the Montaña Reach appears to be progressing through the meandering (M) planform stages of the Massong geomorphic conceptual model. This indicates that the Montaña Reach tends to have excess transport capacity, meaning that the channel will degrade. In 2012, the entire Montaña Reach is classified as Stage M5, where the channel has found a relative equilibrium between grain size, slope, and sediment supply/transport.
- From the Habitat analyses, Subreaches M2, M4, and M5 may be more efficient at providing RSGM habitat for all life stages in the Montaña Reach. In general, the Montaña Reach has a relatively low potential for RSGM habitat. In comparison with the Bosque del Apache Reach (Shied, 2022), the Montaña Reach has roughly 50 times less larvae habitat potential and 20 times less juvenile and adult habitat potential at 3,000 cfs.

6 Bibliography

- Beckwith, T and Julien, P.Y. (2020) “Middle Rio Grande Escondida Reach Report: Morpho-dynamic Processes and Silvery Minnow Habitat from Escondida Bridge to US-380 Bridge (1918-2018.)” Colorado State University, Fort Collins, CO.
- Bovee, K.D., Waddle, T.J., and Spears, J.M. (2008). “Streamflow and endangered species habitat in the lower Isleta reach of the middle Rio Grande.” *U.S. Geological Survey Open-File Report 2008-1323*.
- Corsi, B., Chelsey, R., and Julien, P.Y. (2022). Draft Report. “Middle Rio Grande Montañño Reach Report: Morpho-dynamic Processes and Silvery Minnow Habitat from Hwy 550 Bridge to Montañño Road Bridge,” Submitted to the U.S. Bureau of Reclamation, Albuquerque, New Mexico.
- Fogarty, C and Julien, P.Y. (2020). *Linking Morphodynamic Processes and Silvery Minnow Habitat Conditions in the Middle Rio Grande – Isleta Reach, New Mexico*. Colorado State University, Fort Collins, CO.
- Doidge, S and Julien, P.Y. (2019). Draft Report. *Middle Rio Grande San Acacia Reach: Morphodynamic Processes and Silvery Minnow Habitat from San Acacia Diversion Dam to Escondida Bridge*, Colorado State University, Fort Collins, CO.
- Fitzner, A. (2018). Draft Report “Reclamation Managing Water in the West.” *Bureau of Reclamation Draft Lower Reach Plan*, Albuquerque Area Office, Albuquerque, NM, 36 p.
- Greimann B., and Holste N. (2018). “Analysis and Design Recommendations of Rio Grande Width”, *Technical Service Center, Sedimentation and River Hydraulic Group, U.S. Bureau of Reclamation, Denver, CO*
- Holste, N. (2020) “One-Dimensional Numerical Modeling of Perched Channels.” *U.S. Bureau of Reclamation, Denver, CO*.
- Julien, P.Y. (2002). *River Mechanics*, Cambridge University Press, New York
- Julien, P. Y., and Wargadalam, J. (1995). “Alluvial channel geometry: theory and applications.” *Journal of Hydraulic Engineering*, American Society of Civil Engineers, 121(4), 312–325.
- Klein, M., Herrington, C., AuBuchon, J., and Lampert, T. (2018a). *Isleta to San Acacia Geomorphic Analysis*, U.S. Bureau of Reclamation, Reclamation River Analysis Group, Albuquerque, New Mexico.
- Klein, M., Herrington, C., AuBuchon, J., and Lampert, T. (2018b). *Isleta to San Acacia Hydraulic Modeling Report*, U.S. Bureau of Reclamation, Reclamation River Analysis Group, Albuquerque, New Mexico.
- LaForge, K., Yang, C.Y., Julien, P.Y., and Doidge, S. (2019). Draft Report. *Rio Puerco Reach: Hydraulic Modeling and Silvery Minnow Habitat Analysis*, Colorado State University, Fort Collins, CO.
- Larsen, A. (2007). *Hydraulic modeling Analysis of the Middle Rio Grande-Escondida Reach, New Mexico*. M.S thesis, Civil Engineering Department, Colorado State University, Fort Collins, CO.
- Makar, P. (2006). “Channel Widths Changes Along the Middle Rio Grande, NM.” *Proceedings of the Eight Federal Interagency Sedimentation Conference*, Bureau Of Reclamation, Denver, CO. 943 p.
- Makar, P., Massong, T., and Bauer, T. (2006). “Channel Widths Change Along the Middle Rio Grande, NM.” *Joint 8th Federal Interagency Sedimentation Conference, Reno, NV, April 2 -April6, 2006*.
- Massong, T., Paula, M., and Bauer, T. (2010). “Planform Evolution Model for the Middle Rio Grande, NM.” *2nd Joint Federal Interagency Conference, Las Vegas, NV, June 27 - July 1, 2010*.
- MEI. (2002). *Geomorphic and Sedimentologic Investigations of the Middle Rio Grande between Cochiti Dam and Elephant Butte Reservoir*, Mussetter Engineering, Inc., Fort Collins, CO, 220 p.

- Mortensen, J.G., Dudley, R.K., Platania, S.P., and Turner, T.F. (2019). Draft report. *Rio Grande Silvery Minnow Habitat Synthesis*, University of New Mexico with American Southwest Ichthyological Researchers, Albuquerque, NM.
- Mortensen, J.G., Dudley, R.K., Platania, S.P., White, G.C., and Turner, T.F., Julien, P.Y., Doidge, S., Beckwith, T., Fogarty, C. (2020). Draft Report. *Linking Morpho-Dynamics and Bio-Habitat Conditions on the Middle Rio Grande: Linkage Report 1- Isleta Reach Analyses*. Submitted to the U.S. Bureau of Reclamation, Albuquerque, New Mexico.
- Pinson, A.O., Scissons, S.K., Brown, S.W., Walther, D.E. (2014). Post Flood Report: Record Rainfall and Flooding Events during September 2013 in New Mexico, Southeastern Colorado and Far West Texas, U.S. Army Corps of Engineers, Albuquerque, New Mexico.
- Pinson, A.O., Scissons, S.K., Brown, S.W., Walther, D.E. (2014). *Post Flood Report: Record Rainfall and Flooding Events during September 2013 in New Mexico, Southeastern Colorado and Far West Texas*, U.S. Army Corps of Engineers, Albuquerque, New Mexico
- Posner, A. J. (2017). Draft report. *Channel conditions and dynamics of the Middle Rio Grande River*, U.S. Bureau of Reclamation, Albuquerque, New Mexico.
- Scurlock, D. (1998). "From the Rio to the Sierra: an environmental history of the Middle Rio Grande Basin." *General Technical Report RMRS-GTR-5*. Fort Collins, CO: US Department of Agriculture, Forest Service, Rocky Mountain Research Station, 440 p.
- Schied, A., Sperry, D. J., and Julien, P.Y. (2022). *Middle Rio Grande Bosque Reach Report: Morpho-dynamic Processes and Silvery Minnow Habitat from US-380 Bridge to Southern Boundary of Bosque Del Apache National Wildlife Refuge (BDANWR)*. Final report prepared for the United States Bureau of Reclamation. Colorado State University, Fort Collins, CO.
- Sperry, D.J., Schied, A., and Julien, P.Y. (2022). *Middle Rio Grande Elephant Butte Reach Report: Morpho-dynamic Processes and Silvery Minnow Habitat from the Southern Boundary of the Bosque Del Apache National Wildlife Refuge to Elephant Butte Reservoir*. Final report prepared for the United States Bureau of Reclamation. Colorado State University, Fort Collins, CO.
- Towne, L. (2007). "Infrastructure and Management of the Middle Rio Grande." *The Middle Rio Grande Today*, Bureau of Reclamation, 17 p.
- U.S. Bureau of Reclamation. (2012). "Middle Rio Grande River Maintenance Program - Comprehensive Plan and Guide." Albuquerque Area Office, Albuquerque, New Mexico, 202p.
- U.S. Bureau of Reclamation. (2021). "Water Operations: Historic Data." Online Resource. <https://www.usbr.gov/rsvrWater/HistoricalApp.html>
- U.S. Fish and Wildlife Service. (2007). "Rio Grande Silvery Minnow (*Hybognathus amarus*)." Draft Revised Recovery Plan, Albuquerque, New Mexico, 174 p.
- Varyu, D. (2013). *Aggradation / Degradation Volume Calculations: 2002-2012*. U.S. Department of the Interior, Bureau of Reclamation, Technical Services Center, Sedimentation and River Hydraulics Group. Denver, CO.
- Varyu, D. (2016). *SRH-1D Numerical Model for the Middle Rio Grande: Isleta Diversion Dam to San Acacia Diversion Dam*. U.S. Department of the Interior, Bureau of Reclamation, Technical Services Center, Sedimentation and River Hydraulics Group. Denver, CO.
- Yang, C.Y., LaForge, K., Julien, P.Y., and Doidge, S. (2019). Draft Report. *Isleta Reach: Hydraulic Modeling and Silvery Minnow Habitat Analysis*, Colorado State University, Fort Collins, CO.

Appendix A

Cumulative Plots used in the Subreach Delineation, Aerial Imagery with Agg/Deg Line Labels

Montaño Subreach Delineation Report

Reach Definition

The Montaño Reach spans approximately 19 miles and begins just upstream of the Montaño Bridge in Albuquerque, NM (Agg/Deg Line 463) and ends just downstream of the Isleta diversion dam (Agg/Deg 657). This river reach is located within an urban river corridor. For purposes of hydraulic analysis, the Montaño reach was delineated into five subreaches based on notable urban features such as bridge crossings or drainage outlets. **Table A-1** below summarizes each subreach.

Table A-1 Montaño Subreach Delineation

Subreach Name	Agg/Deg Lines	Approximate Distance	Description
M1	463 – 494	3.0 miles	Montaño Bridge to Coronado Fwy (I-40)
M2	494 – 528	3.5 miles	Coronado Fwy (I-40) to Bridge Blvd
M3	528 – 575	4.5 miles	Bridge Blvd to Tijeras Arroyo (tributary)
M4	575 – 623	4.5 miles	Tijeras Arroyo to I-25 Bridge
M5	623 – 657	3.5 miles	I-25 Bridge to Isleta Diversion Dam

An analysis of the flood widths at a discharge of 3,000 cfs (**Figure A-1** and **Figure A-3**) as well as channel widths identified by the bank stationing (**Figure A-2** and **Figure A-4**) were considered. Other analyses performed include the longitudinal profile of the reach (**Figure A-5**) and the particle distribution through the reach (**Figure A-6**). All analyses performed identified boundaries consistent with the subreach delineation.

An overview map of the subreach delineation is shown in **Figure A-7**. Aerial imagery of each Montaño subreach is shown in **Figures A-8** through **A-12**.

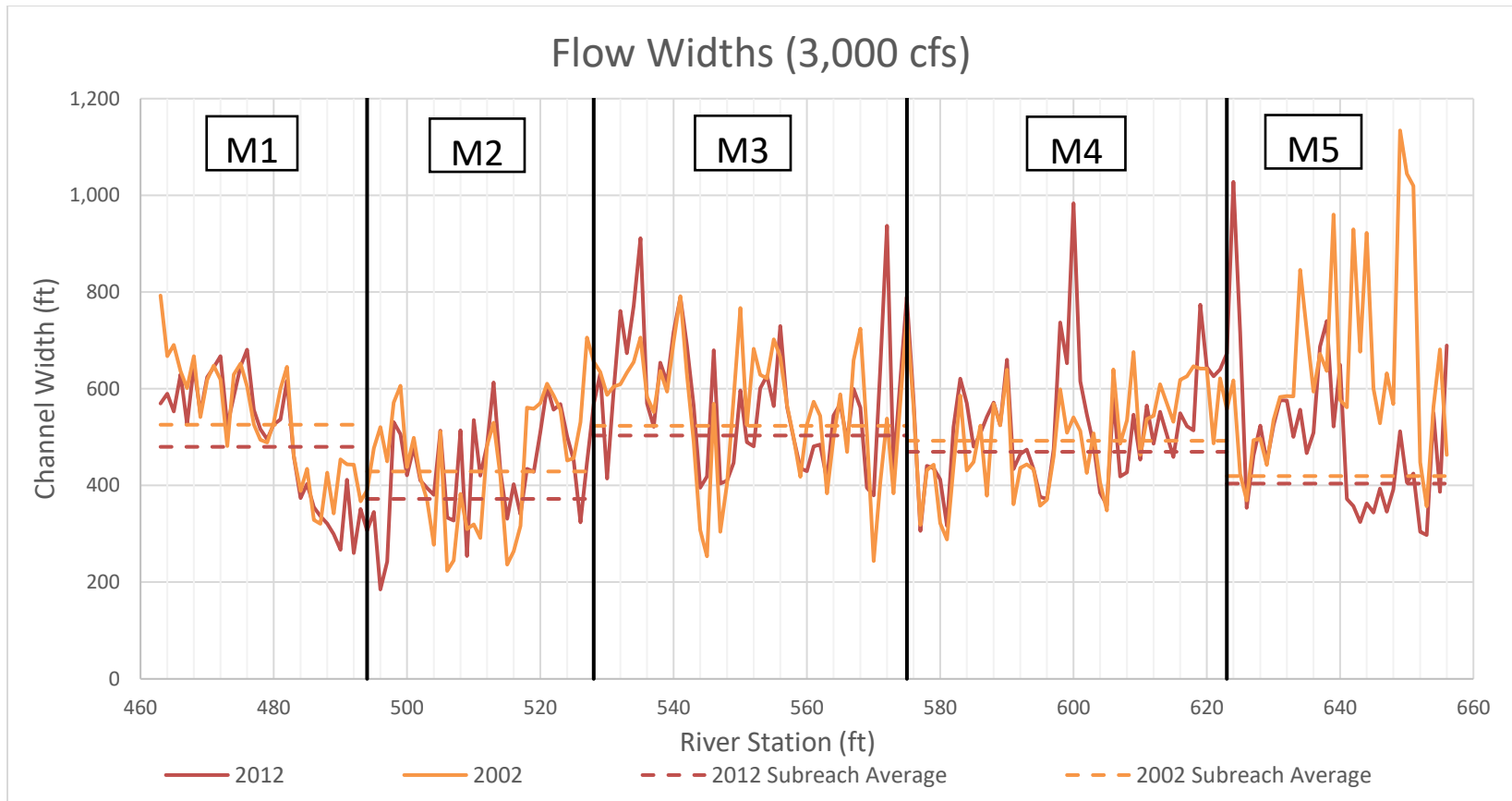


Figure A-1 Average Flow widths at 3,000 cfs for survey years 2002 and 2012.

2002		
Subreach	Average Flow Width, ft	Standard Deviation
M1	529.2	120.5
M2	451.1	127.3
M3	560.6	129.8
M4	504.8	106.0
M5	641.9	194.5

2012		
Subreach	Average Flow Width, ft	Standard Deviation
M1	494.8	128.4
M2	431.4	104.1
M3	573.0	136.1
M4	531.3	127.8
M5	499.3	154.9

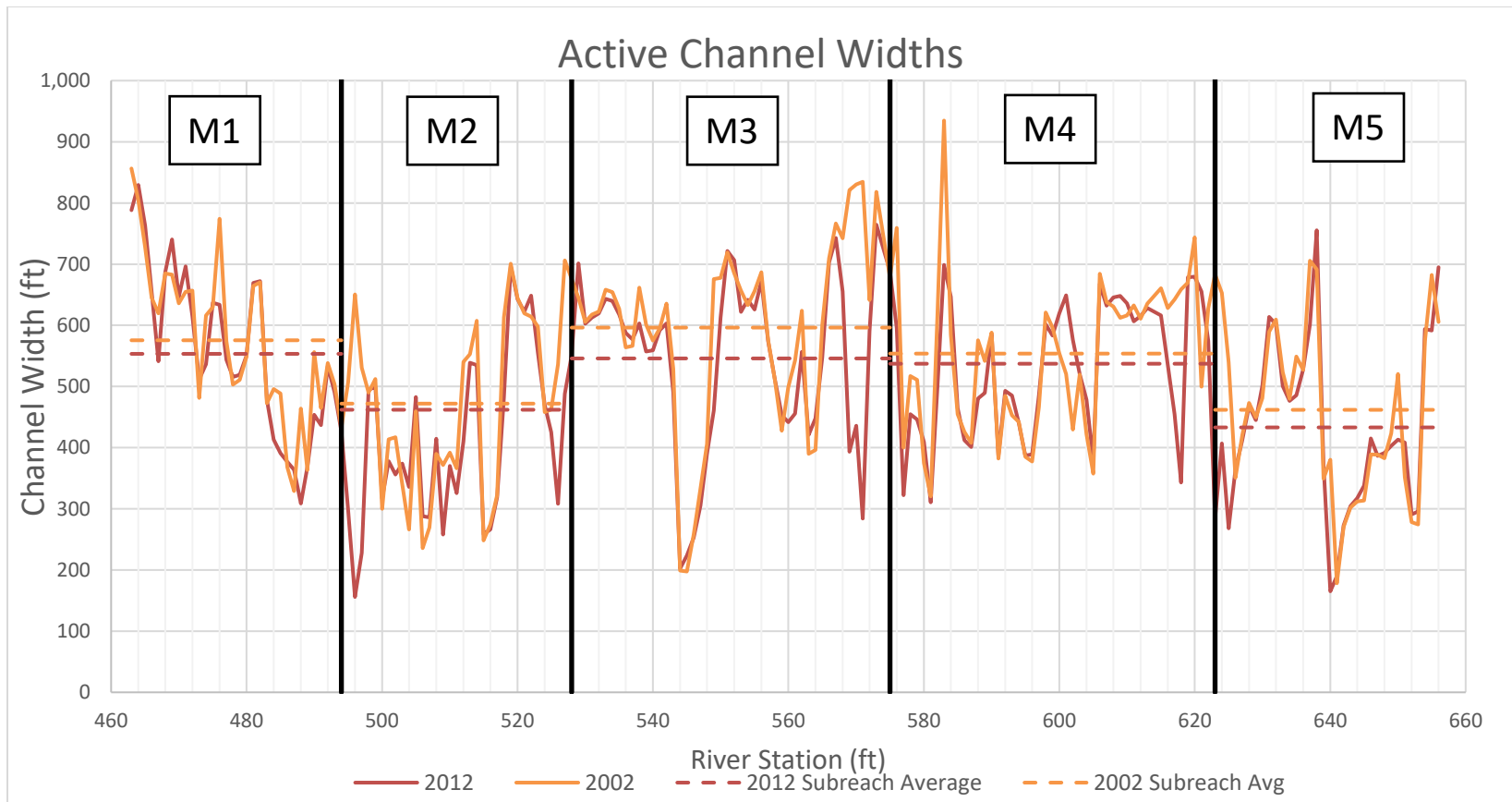


Figure A-2 Active Channel widths defined by bank stations.

2002		
Subreach	Average Active Channel Width, ft	Standard Deviation
M1	575.6	125.8
M2	472.0	138.2
M3	596.3	148.4
M4	553.7	124.1
M5	461.8	139.7

2012		
Subreach	Average Active Channel Width, ft	Standard Deviation
M1	556.0	133.9
M2	414.4	131.0
M3	546.0	136.5
M4	526.7	114.2
M5	428.1	136.8

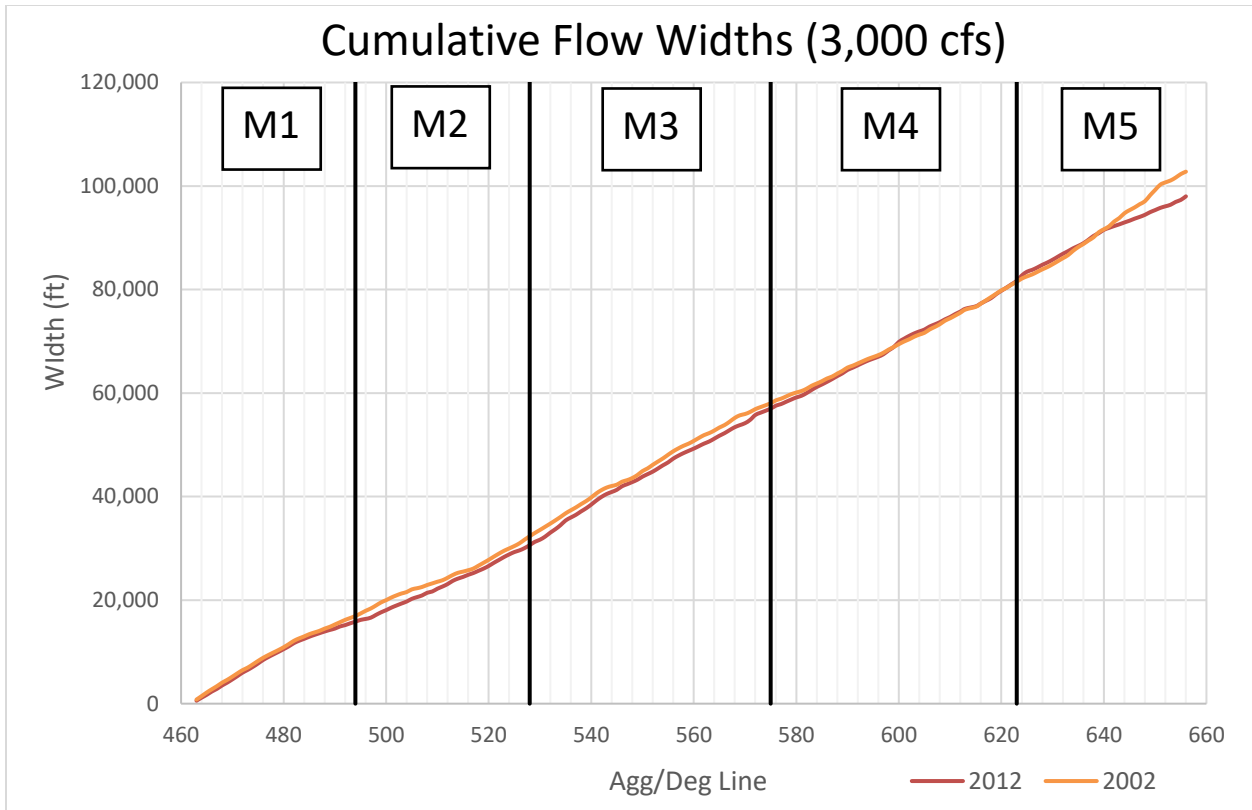


Figure A-3 Cumulative flow widths at 3,000 cfs.

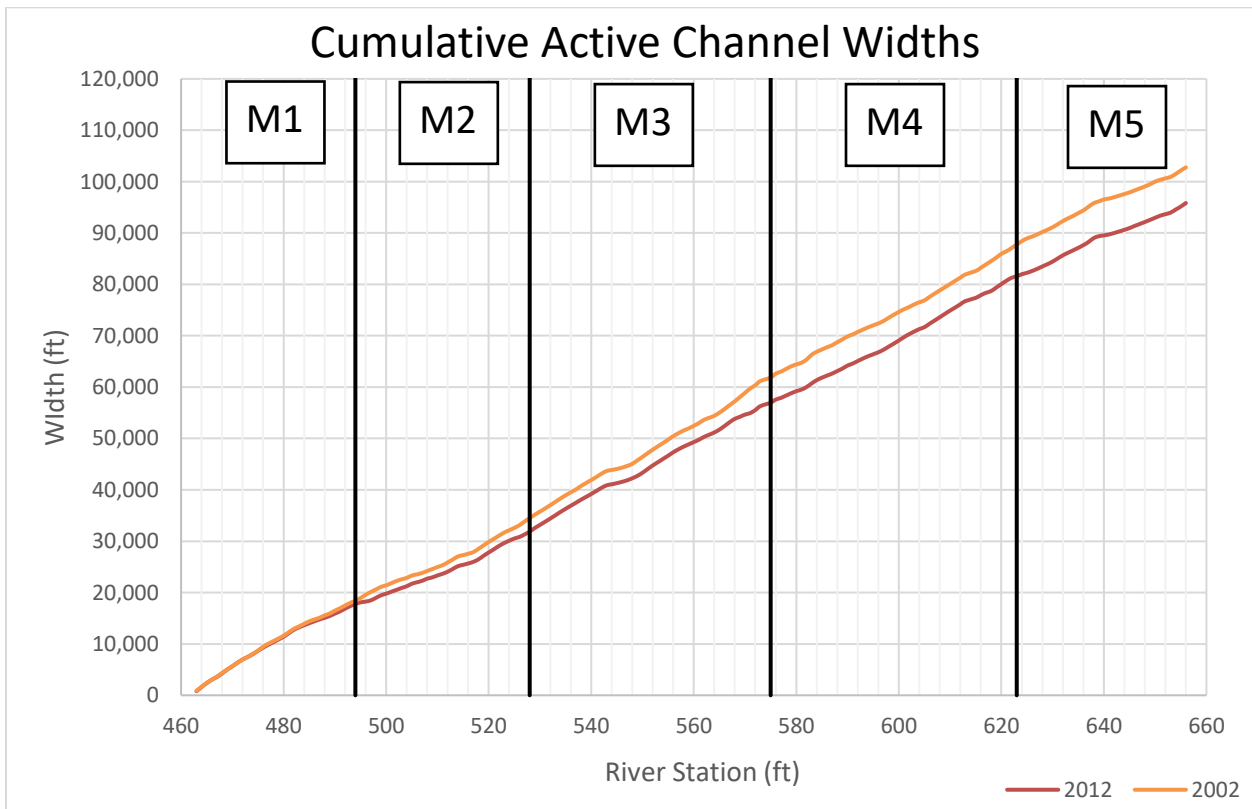


Figure A-4 Cumulative active channel widths defined by banklines.

Longitudinal Profile of the Montano Reach

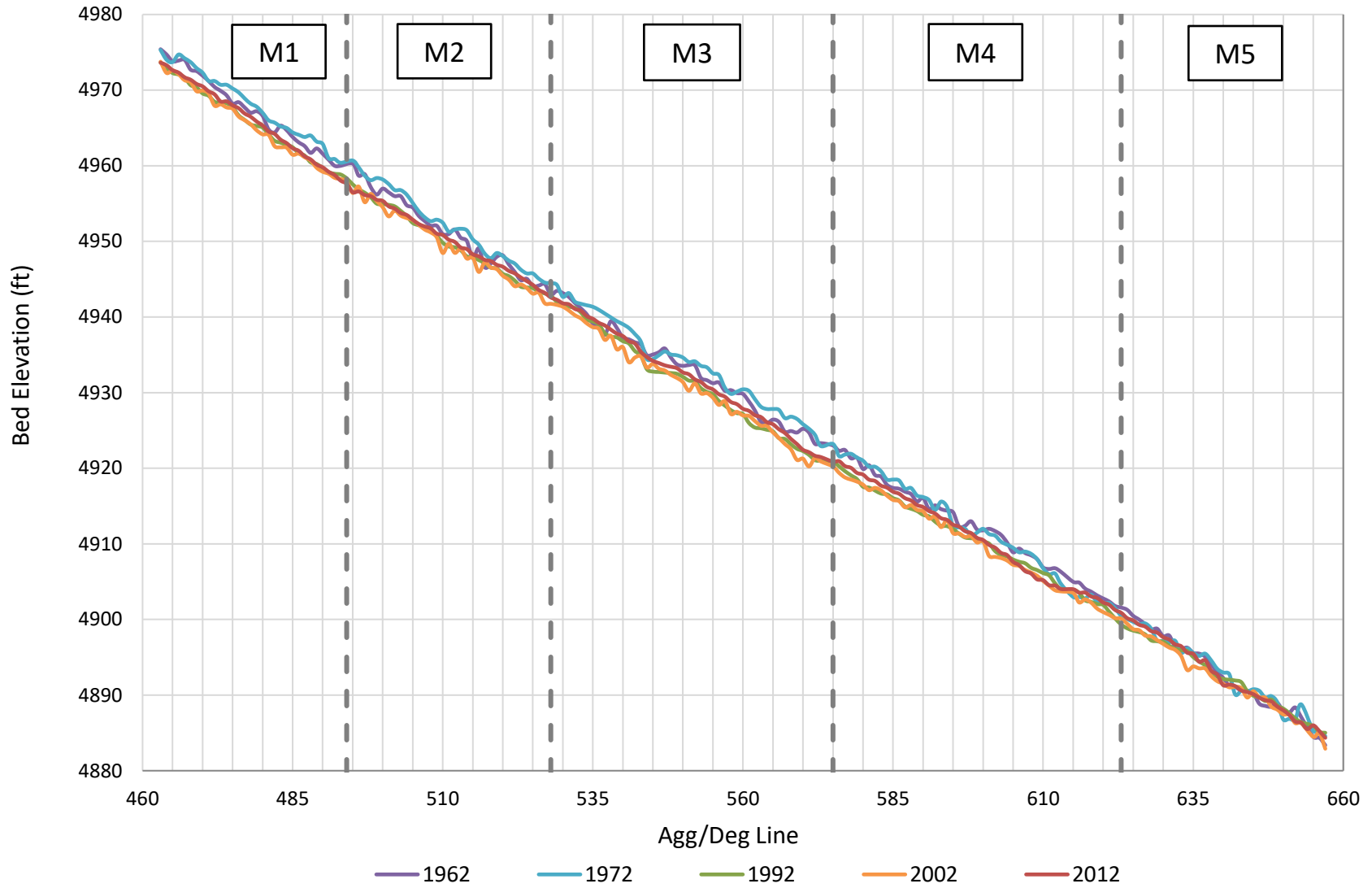


Figure A-5 Longitudinal profile of the Montano reach.

Bed Material Size of the Montaña Reach

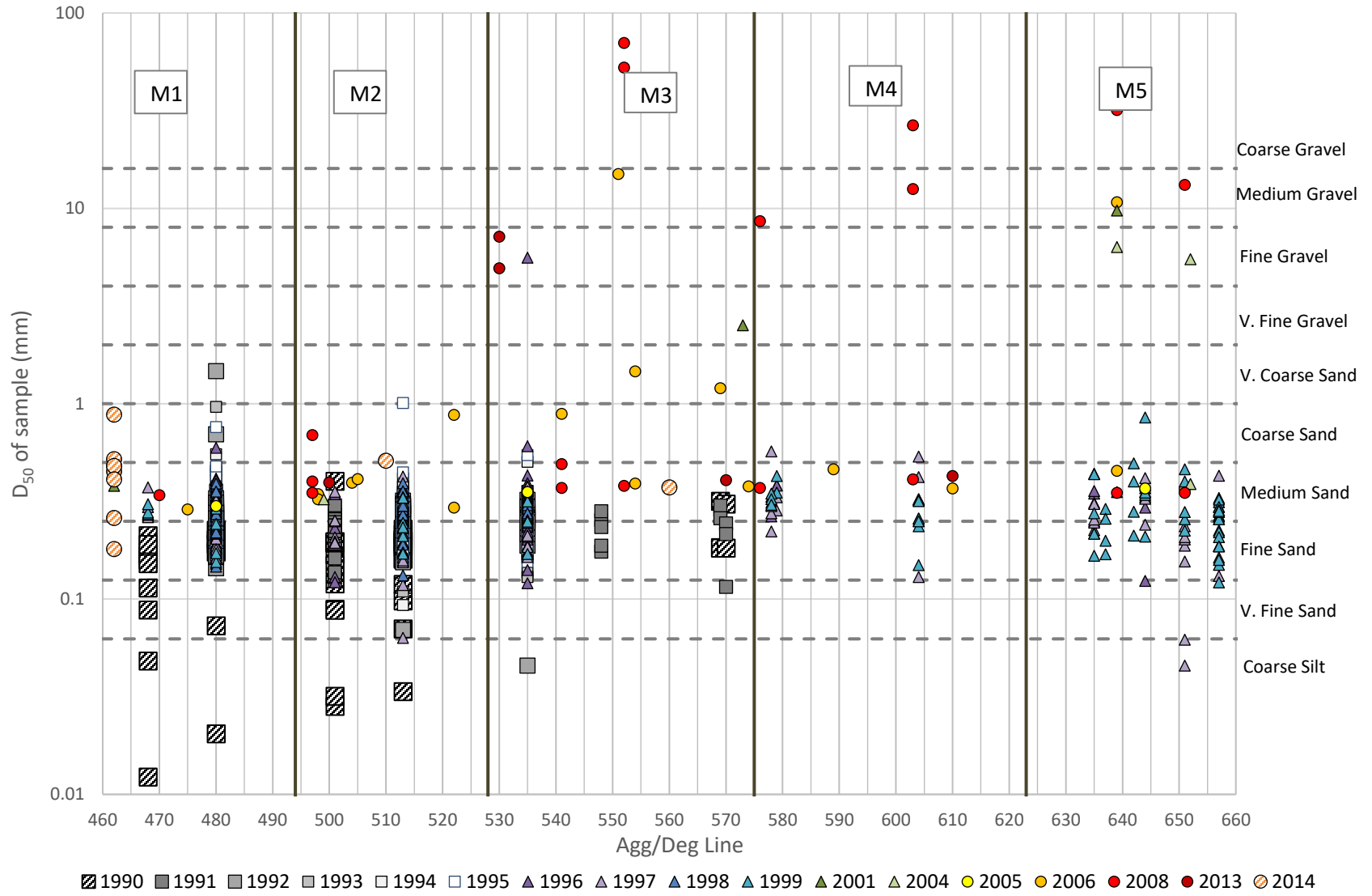


Figure A-6 Average grain size throughout the Montaña reach from 1990 to 2014.

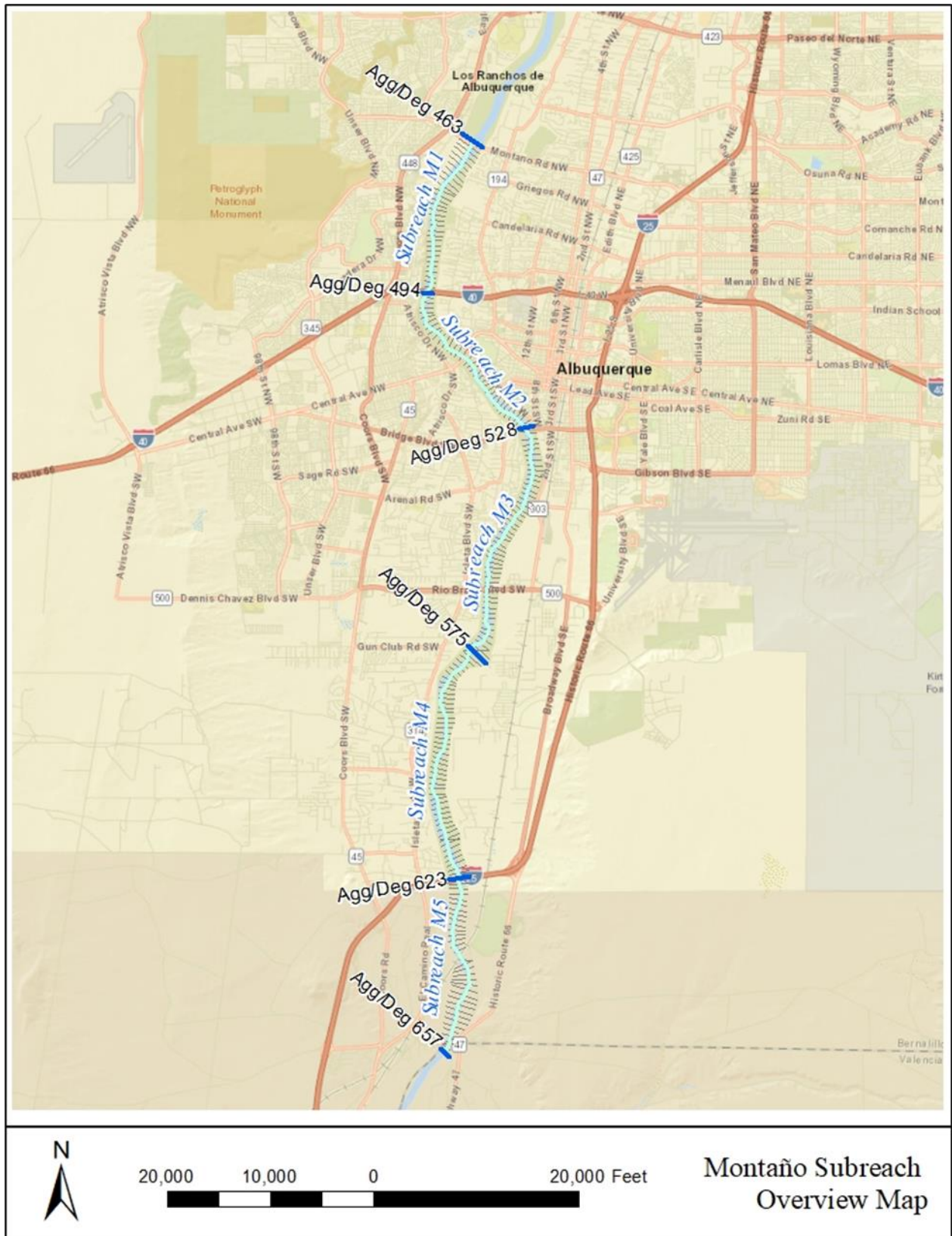


Figure A-7 Montañito Subreach Delineation Overview Map.

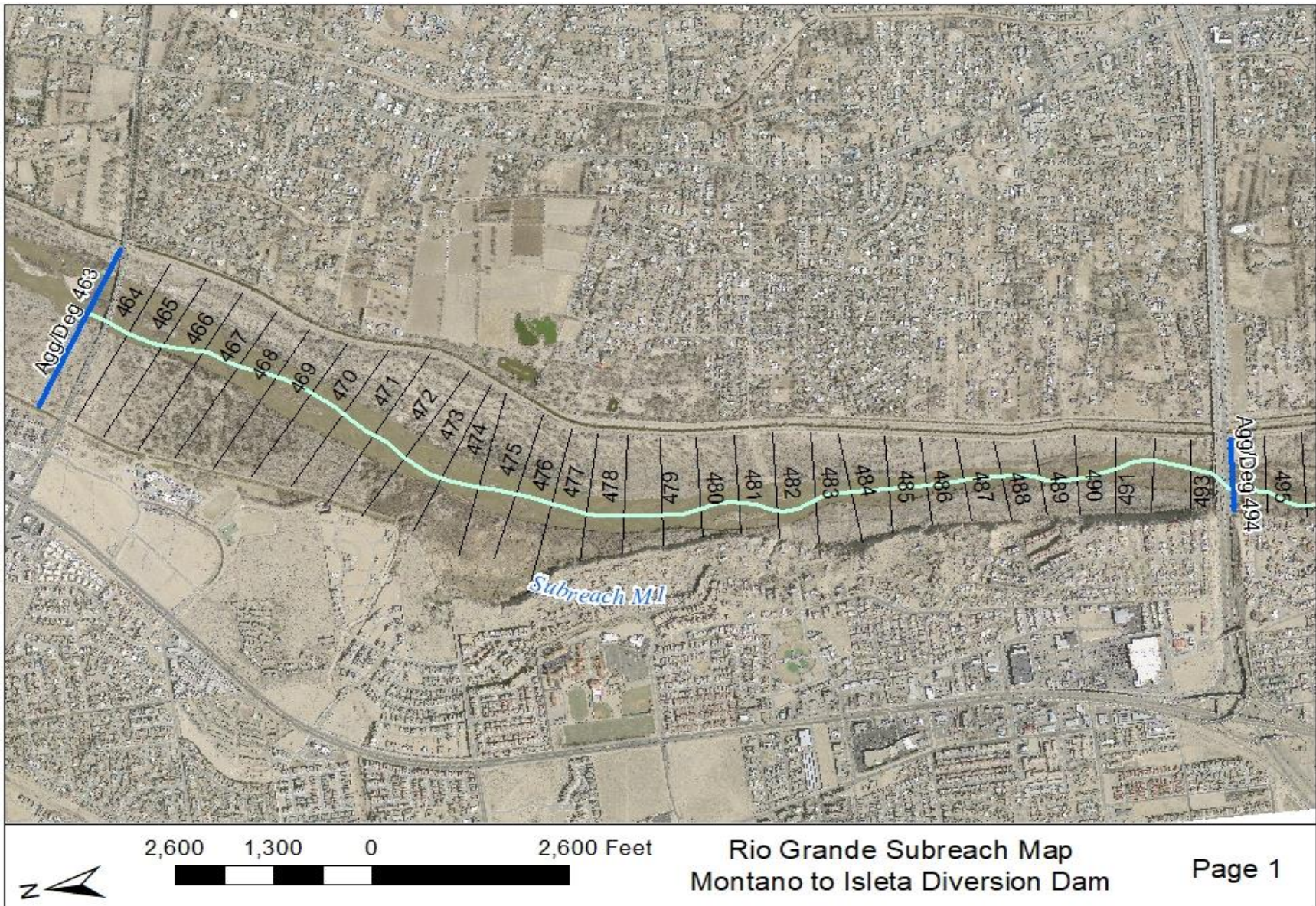


Figure A-8 Subreach delineation with aerial imagery of Subreach M1.

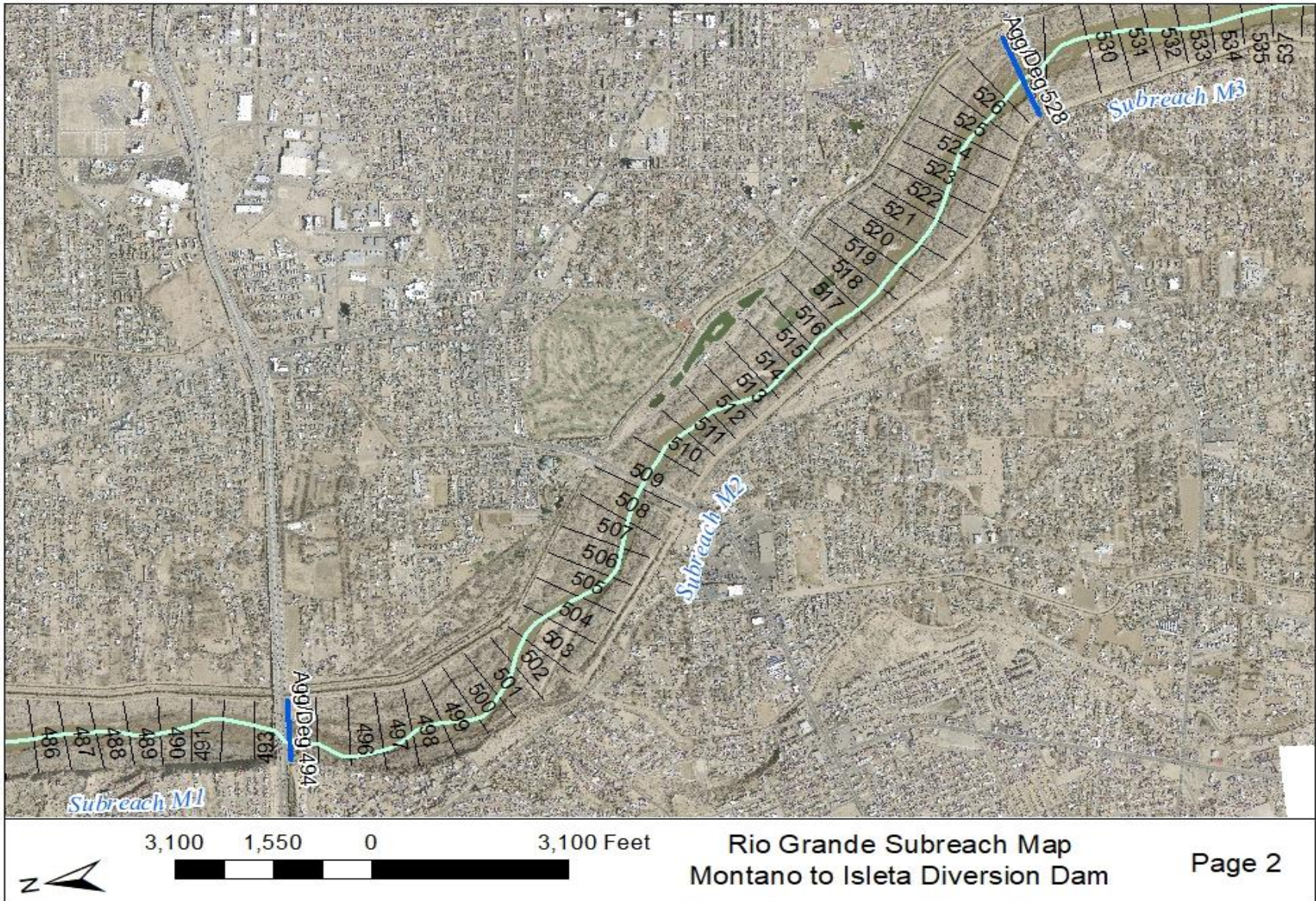


Figure A-9 Subreach delineation with aerial imagery of Subreach M2.

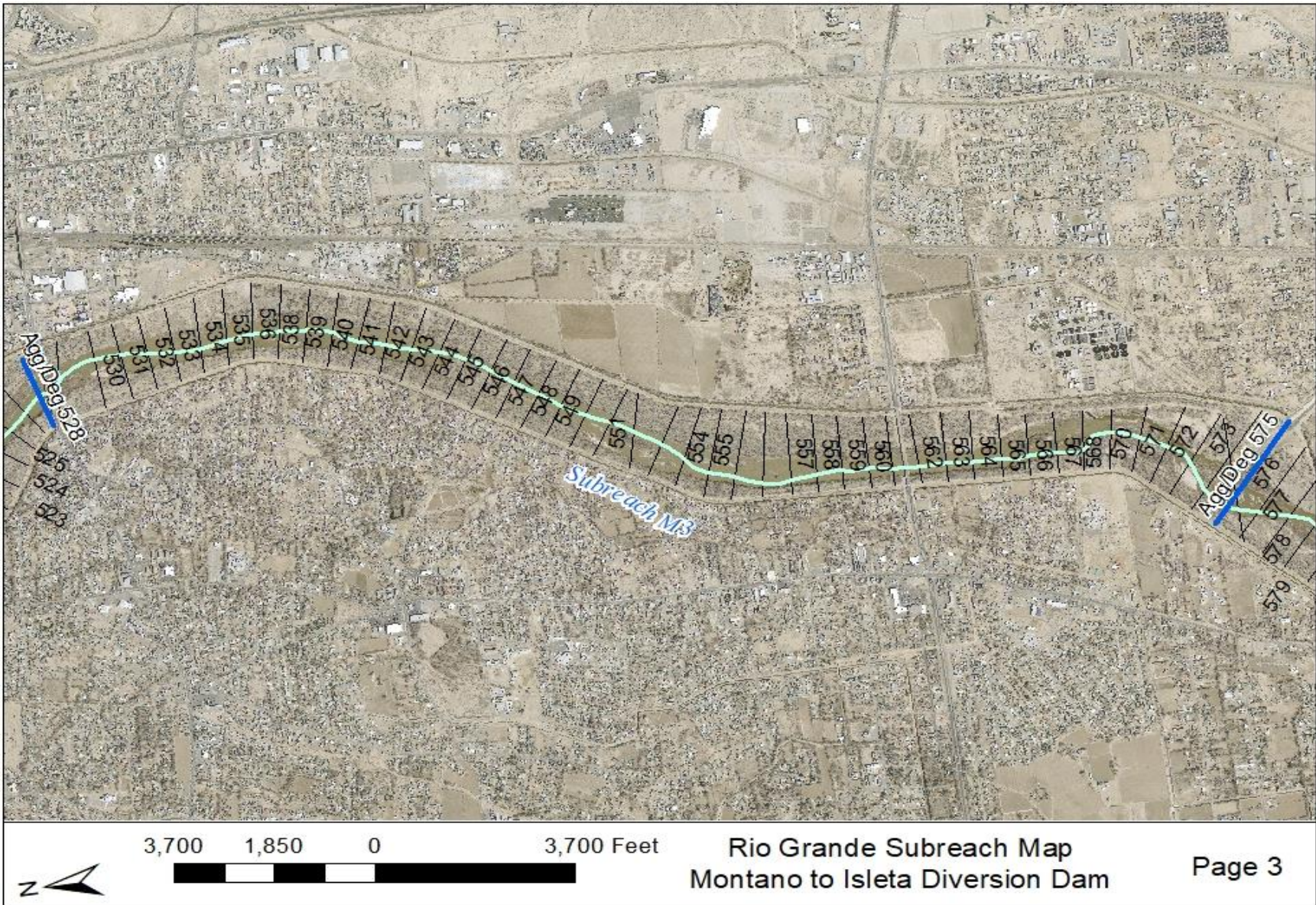


Figure A-10 Subreach delineation with aerial imagery of Subreach M3.

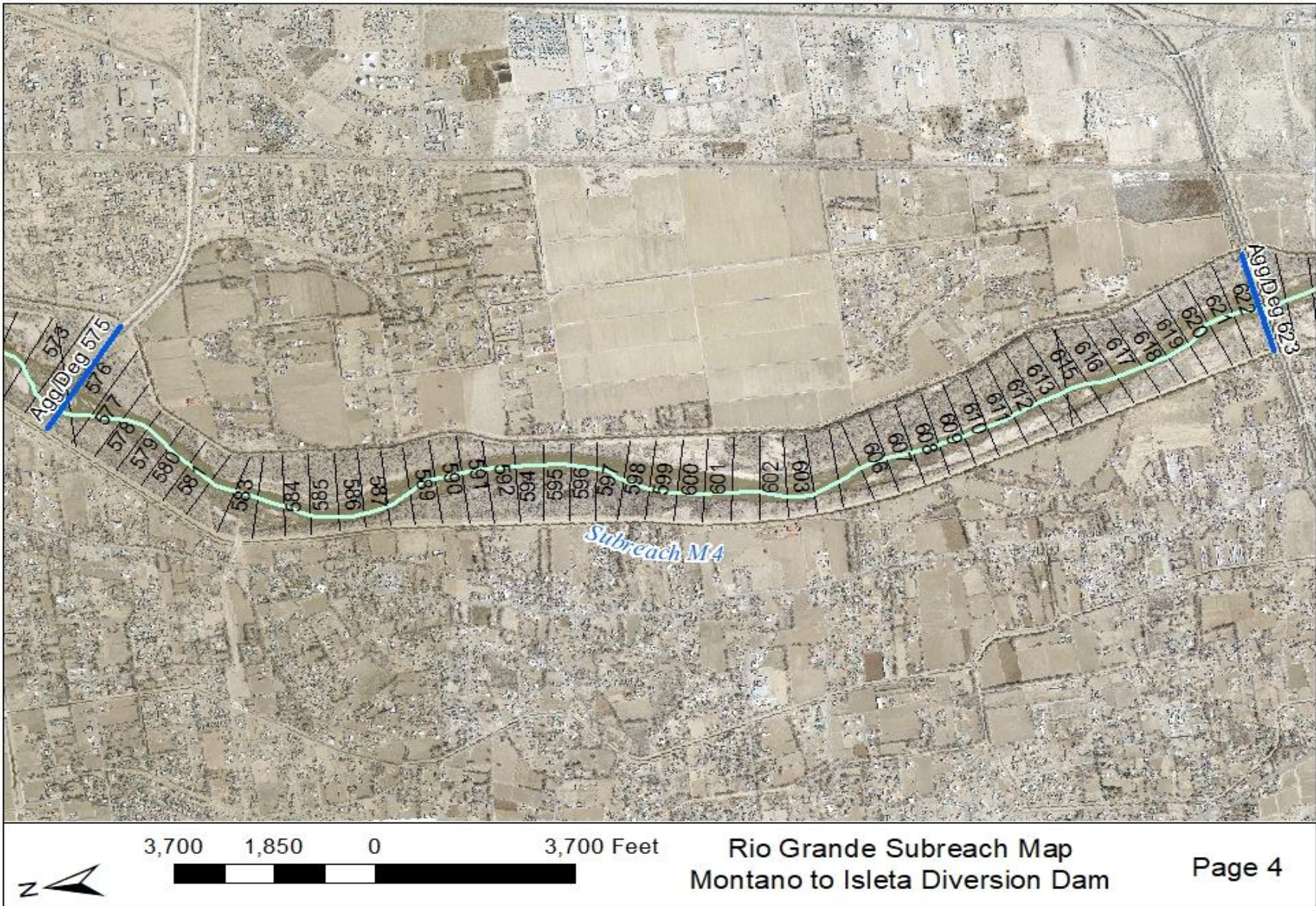


Figure A-11 Subreach delineation with aerial imagery of Subreach M4.

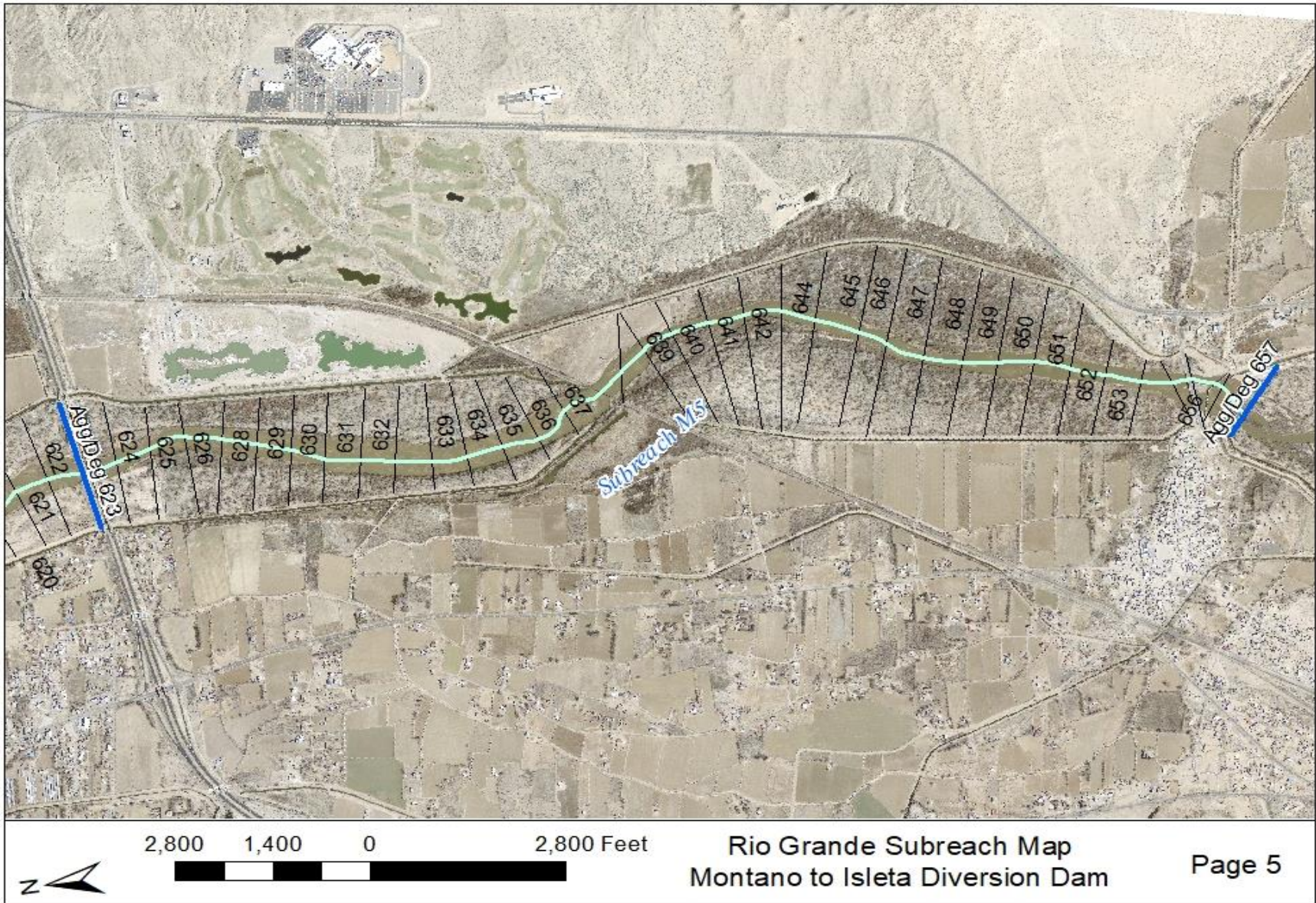


Figure A-12 Subreach delineation with aerial imagery of Subreach M5.

Appendix B

Years used in JW Calculations for D50

Table B-1 Years used in JW Calculations for D50

Year Analyzed	Subreach	Year Used
1992	M1	1992
	M2	1992
	M3	1992
	M4	1996
	M5	1996
2002	M1	1999
	M2	1999
	M3	1999
	M4	1999
	M5	1999
2012	M1	2008
	M2	2013
	M3	2013
	M4	2013
	M5	2008

Appendix C

Additional Figures from Geomorphology Analyses

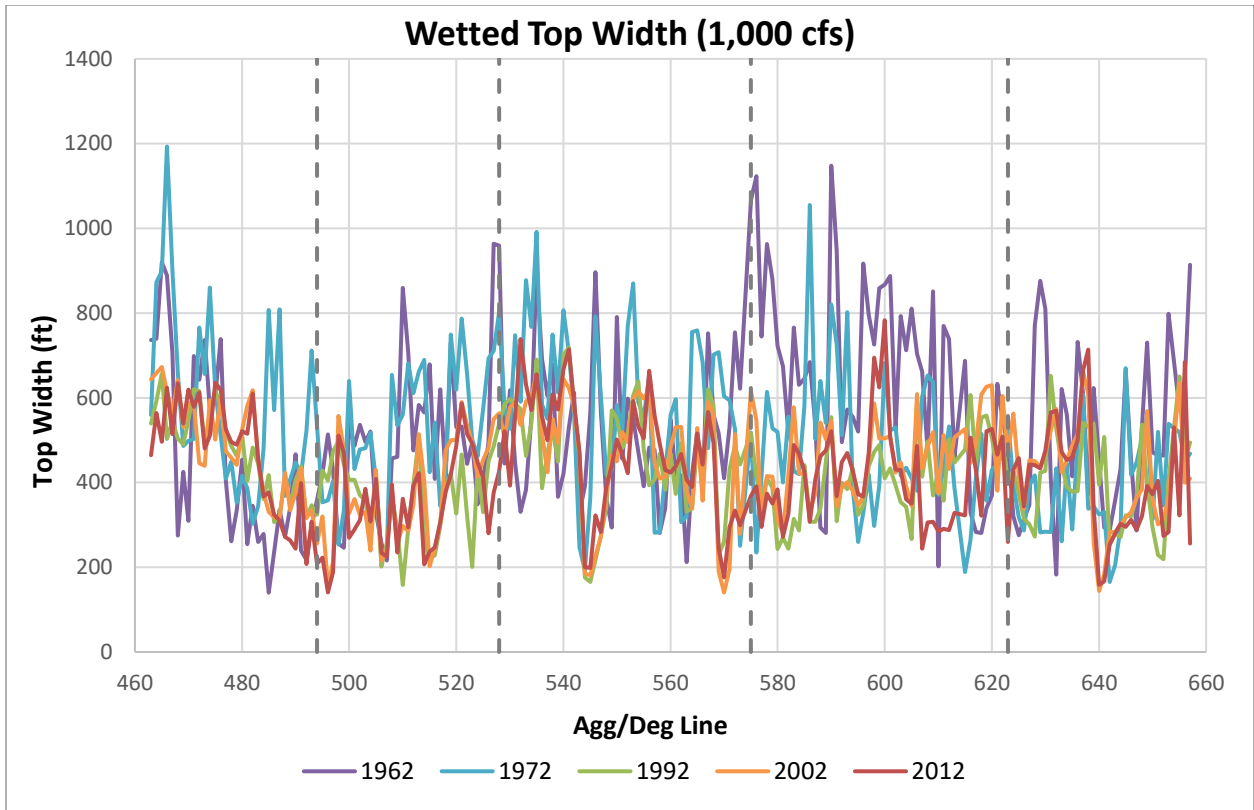


Figure C-1 Wetted top width at each Agg/Deg line in the Montano reach at a discharge of 1,000 cfs

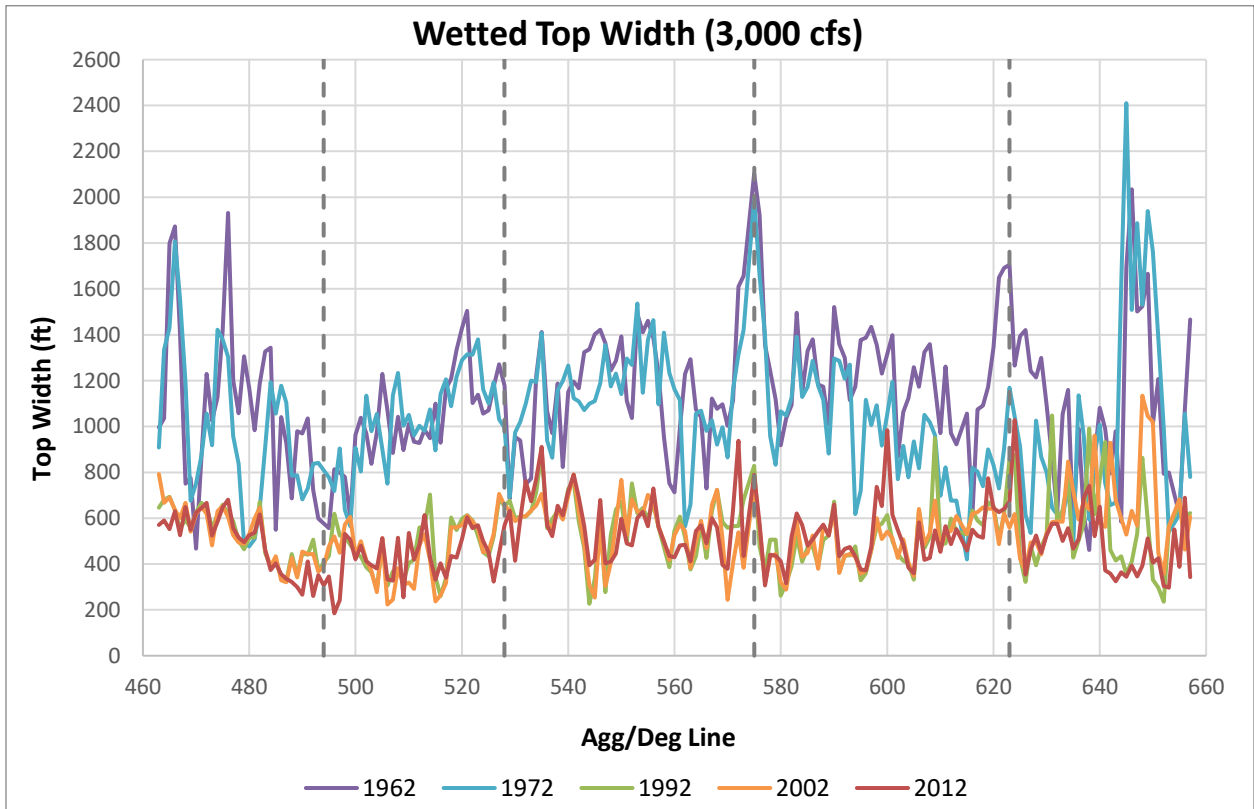


Figure C-2 Wetted top width at each Agg/Deg line in the Montano reach at a discharge of 3,000 cfs

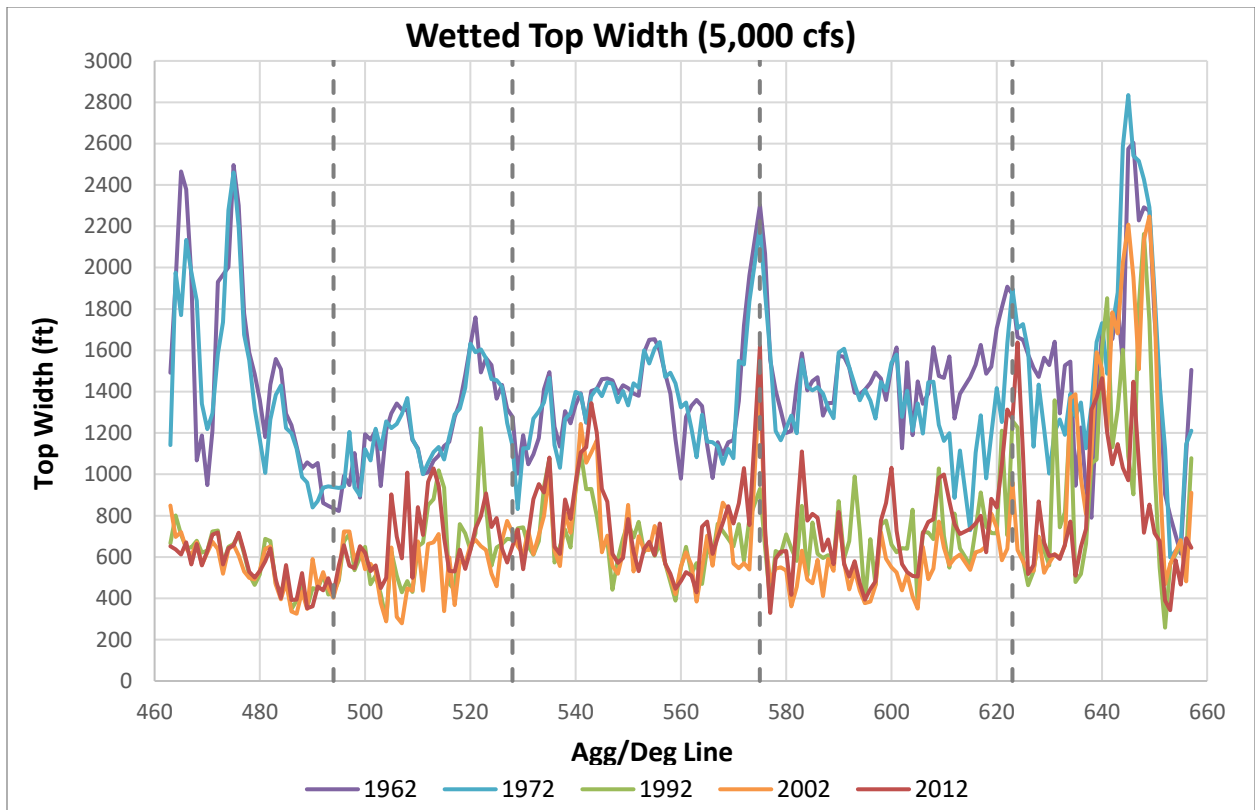


Figure C-3 Wetted top width at each Agg/Deg line in the Montano reach at a discharge of 5,000 cfs

Appendix D

Additional Figures from Habitat Analyses

(Habitat Charts by Subreach, Spatially Varying Habitat Charts, Habitat Curves)

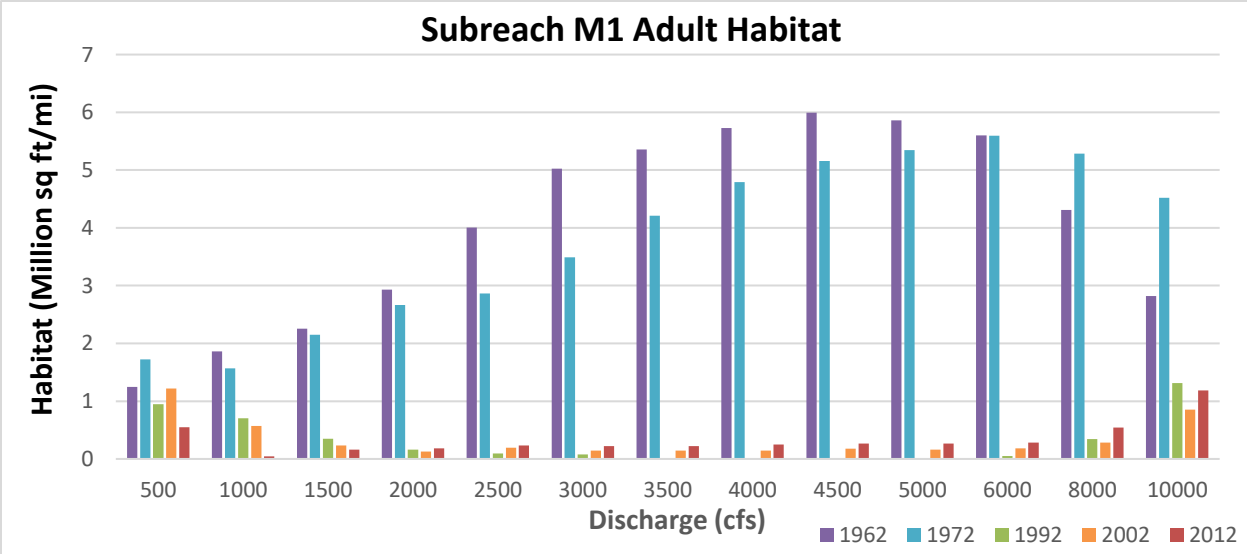
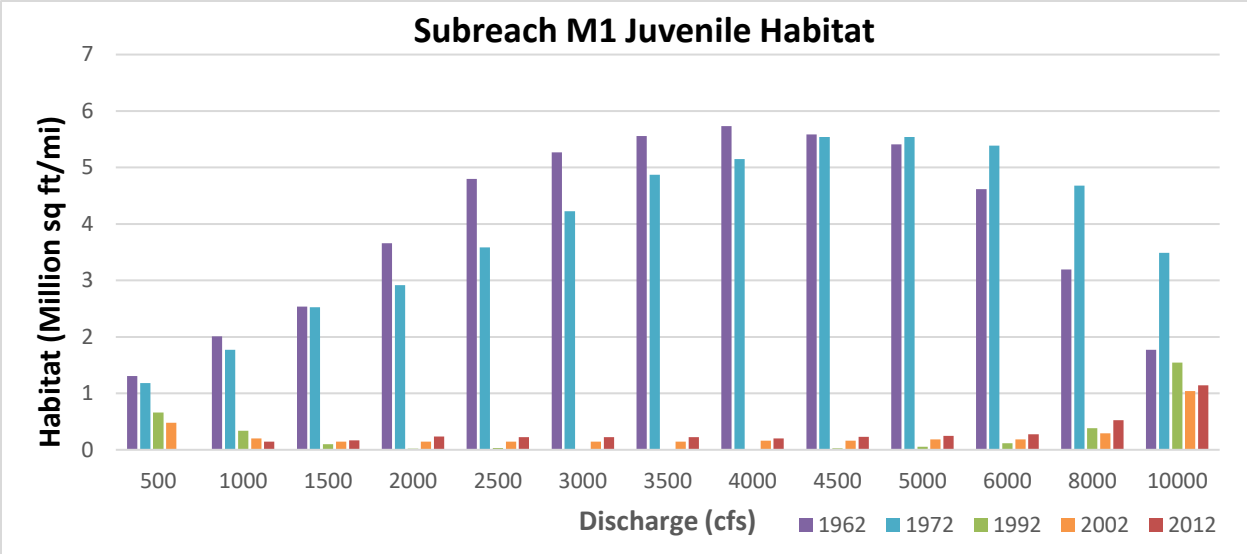
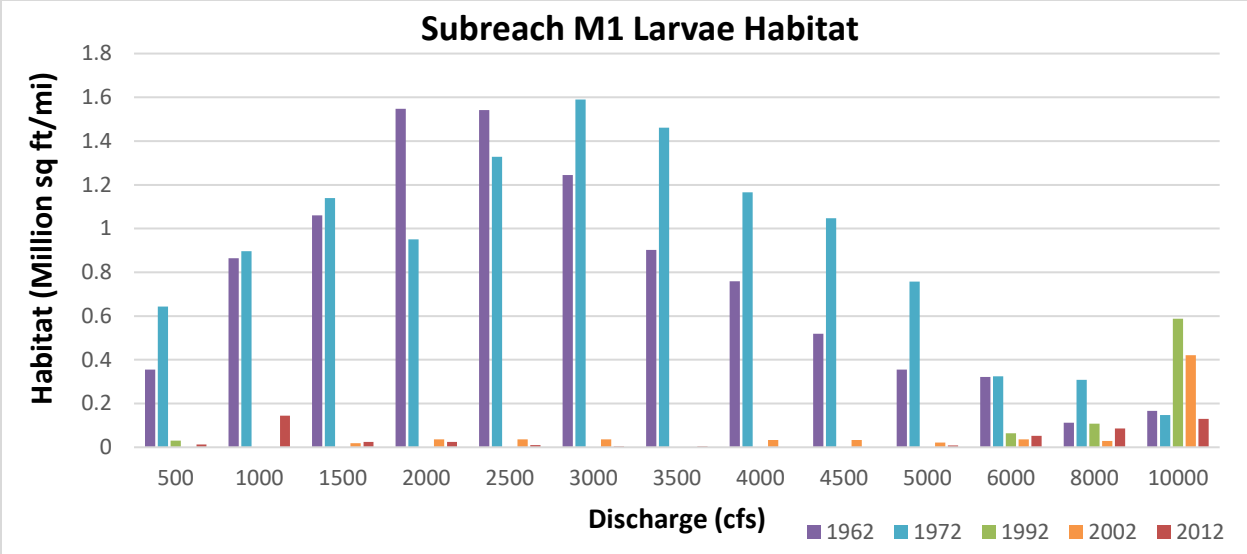


Figure D-1 RGSM habitat availability in Montano Subreach M1

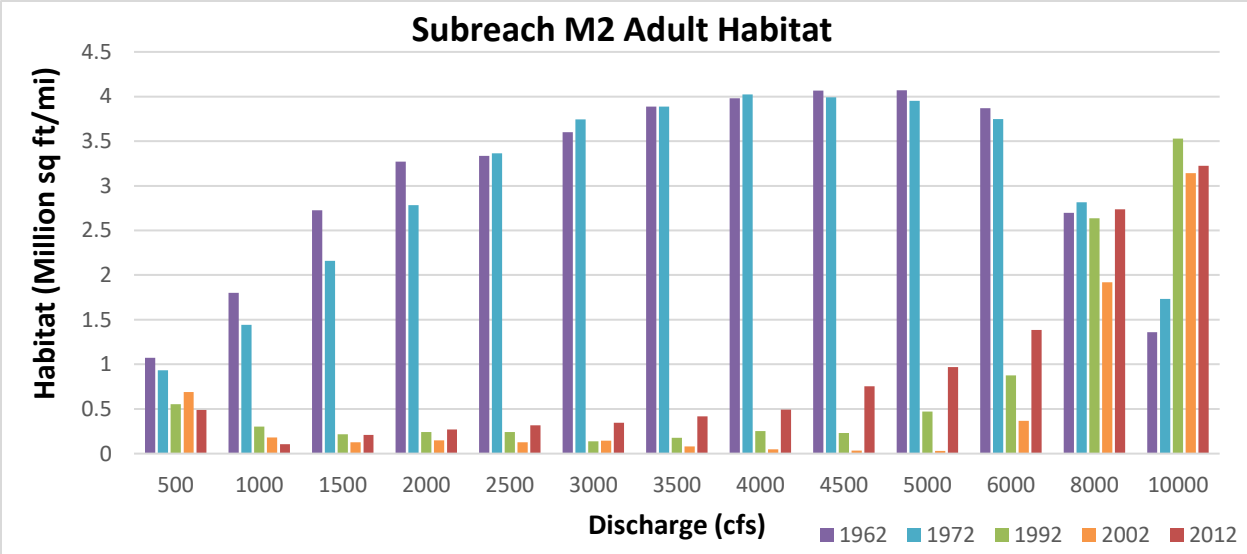
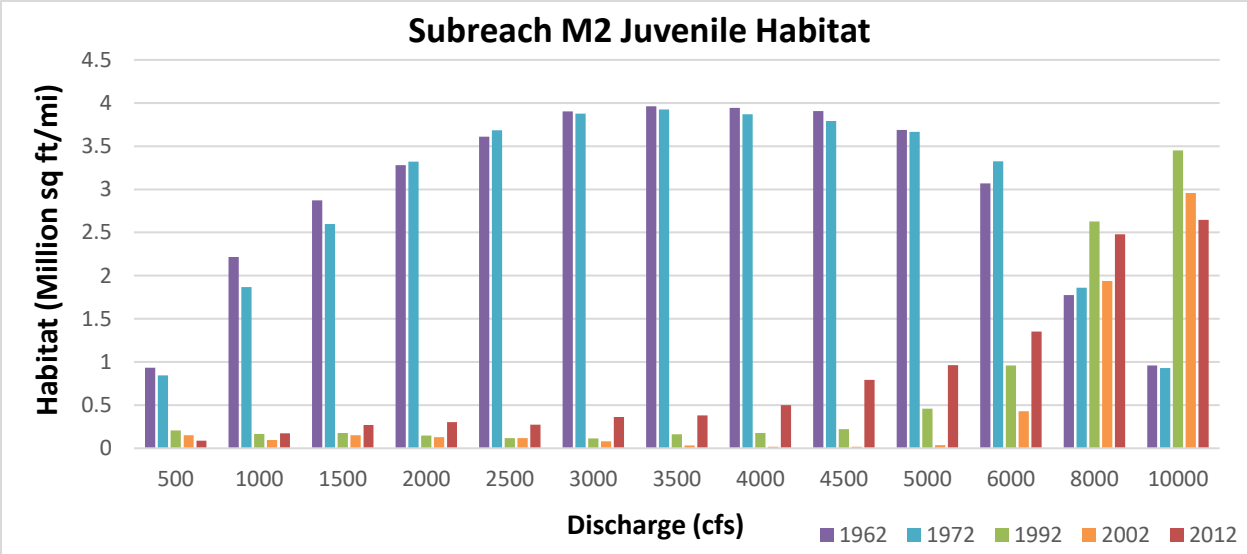
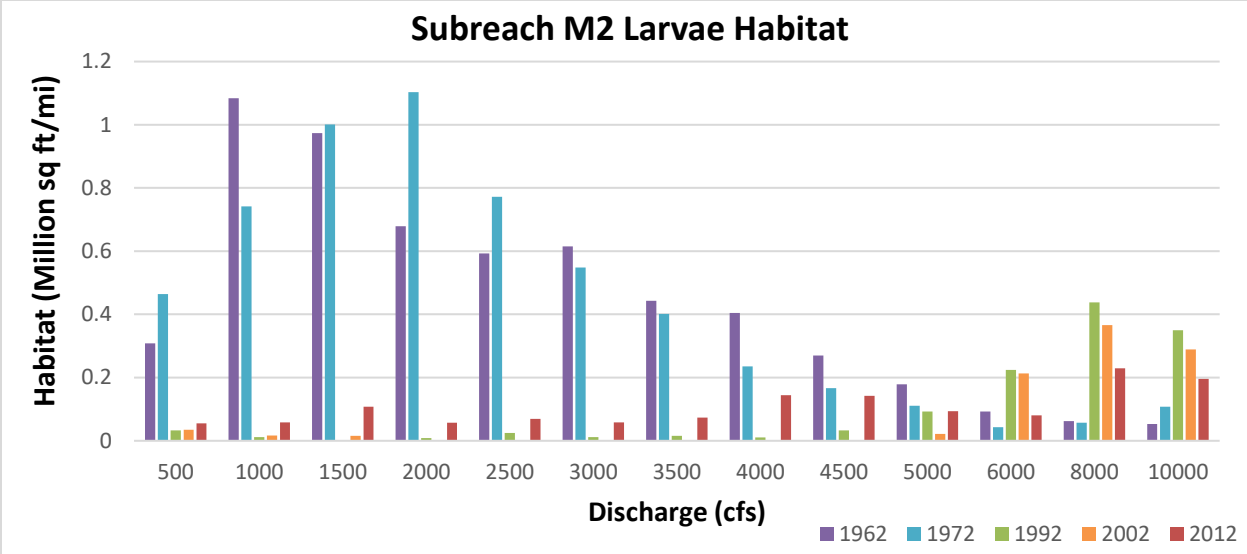


Figure D-2 RGSM habitat availability in Montano Subreach M2

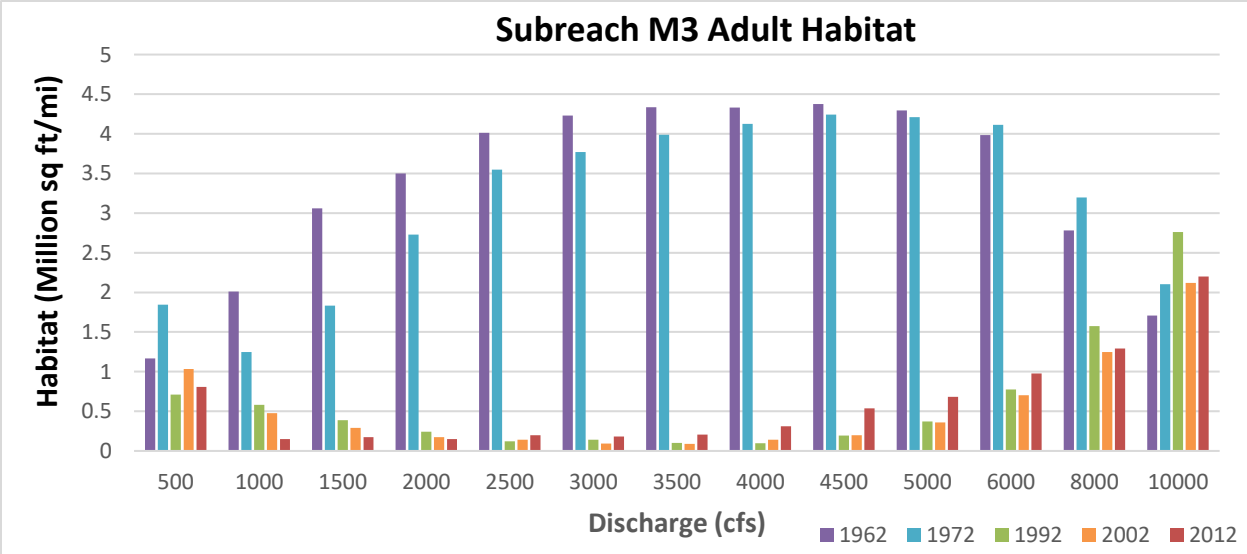
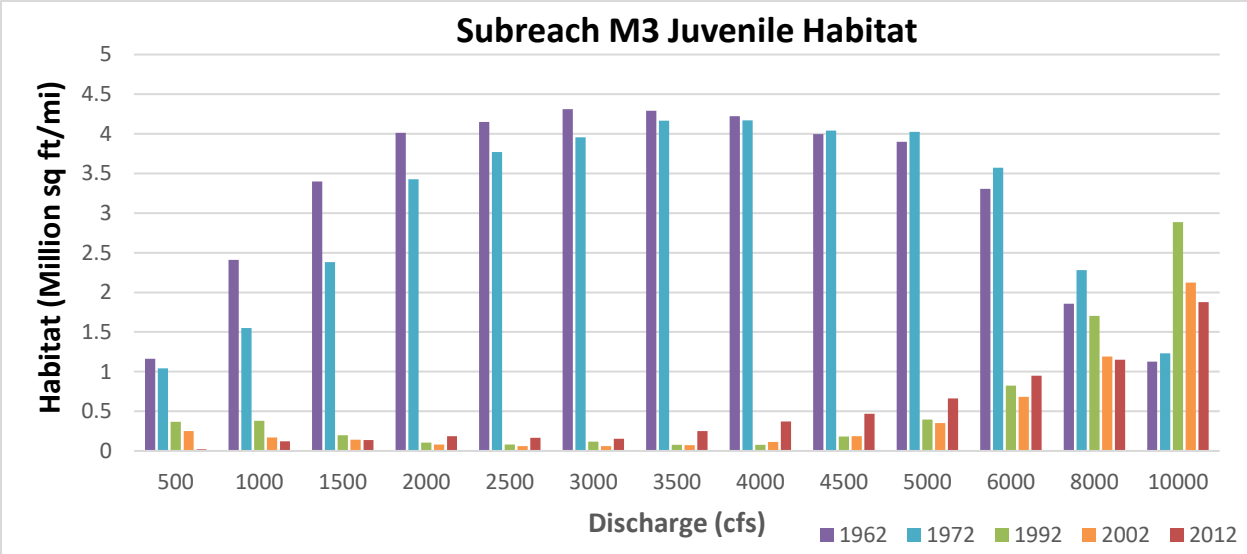
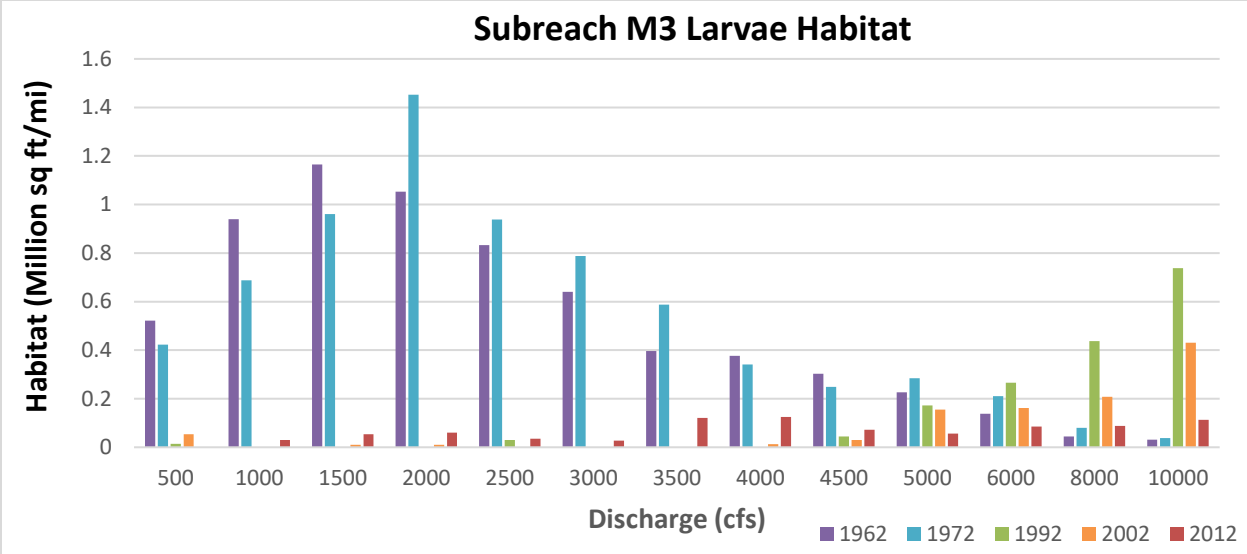


Figure D-3 RGSM habitat availability in Montano Subreach M3

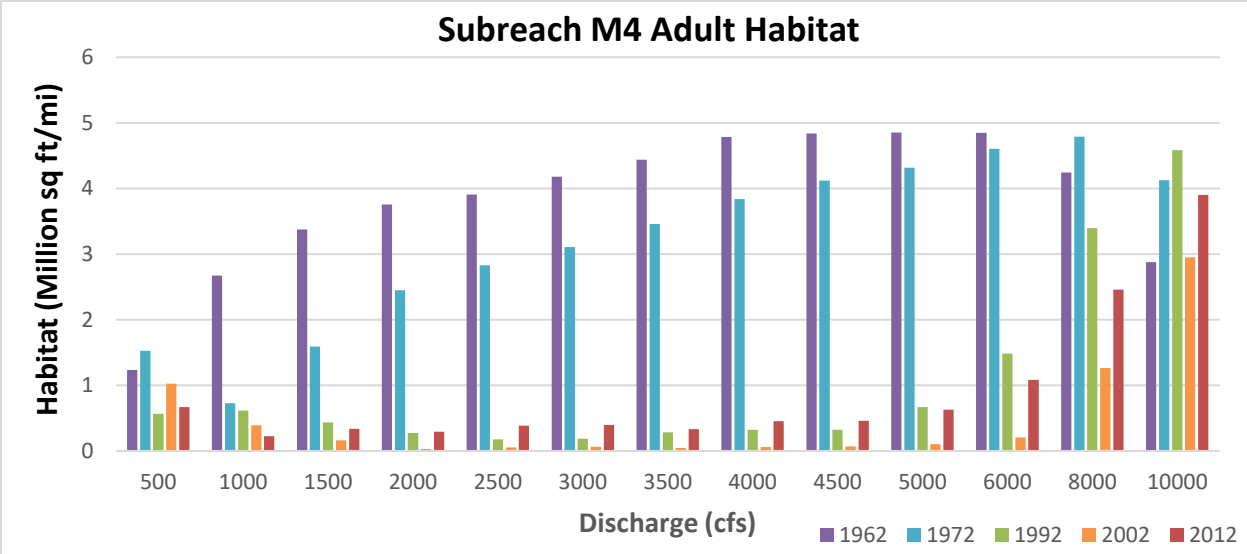
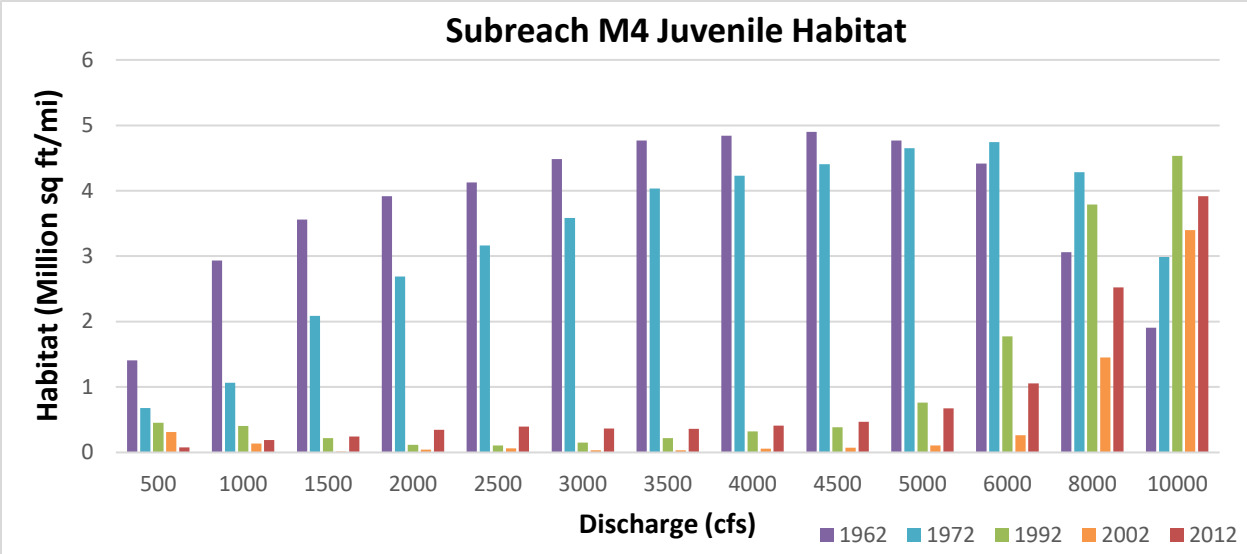
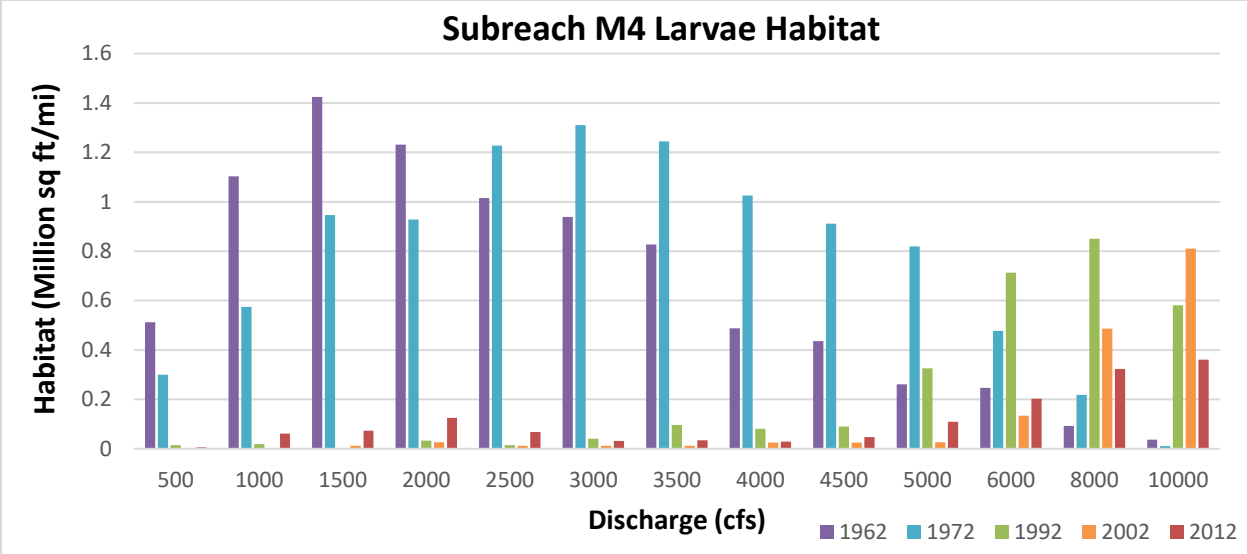


Figure D-4 RGSM habitat availability in Montano Subreach M4

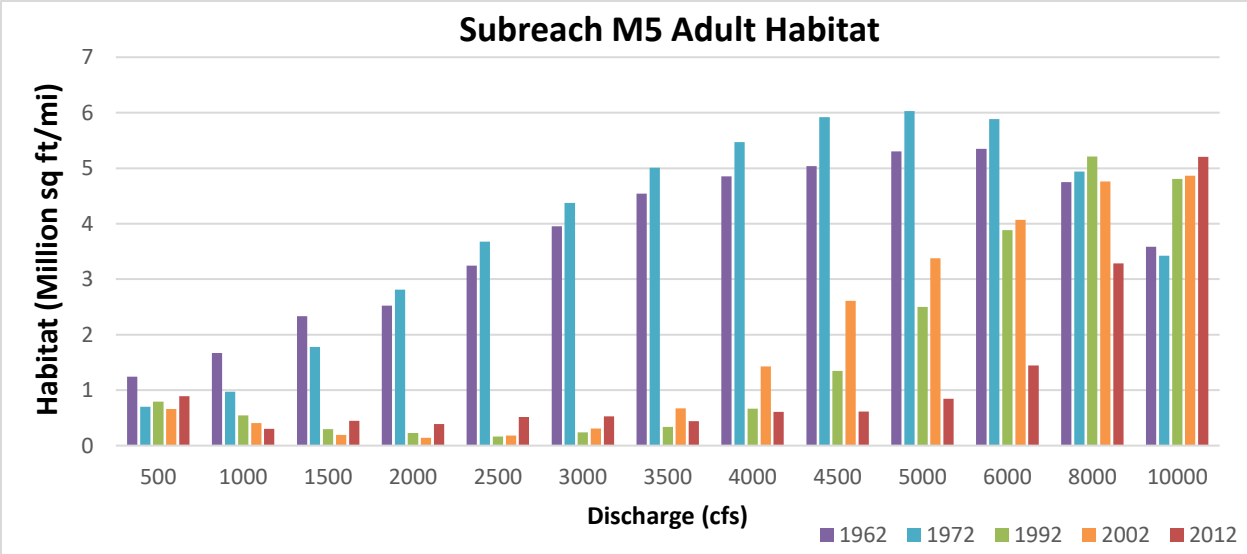
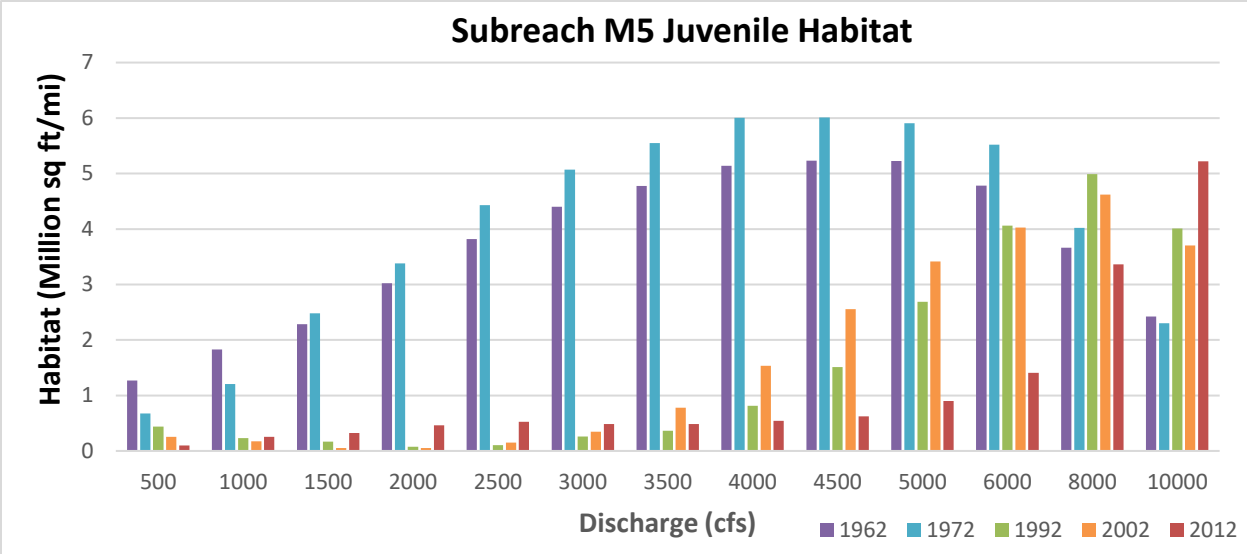
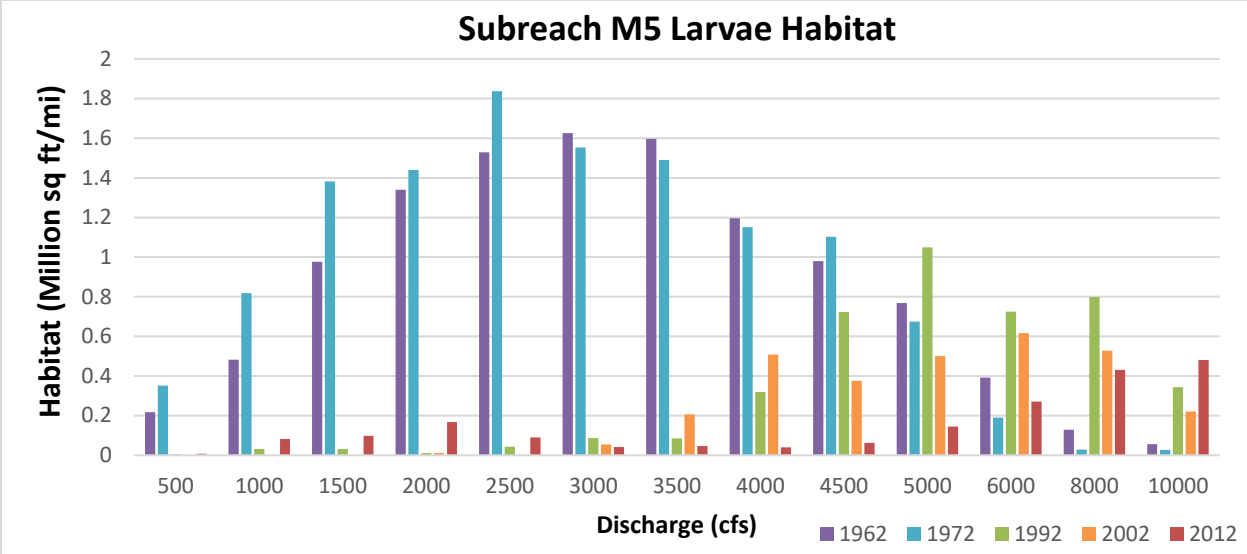


Figure D-5 RGSM habitat availability in Montano Subreach M5

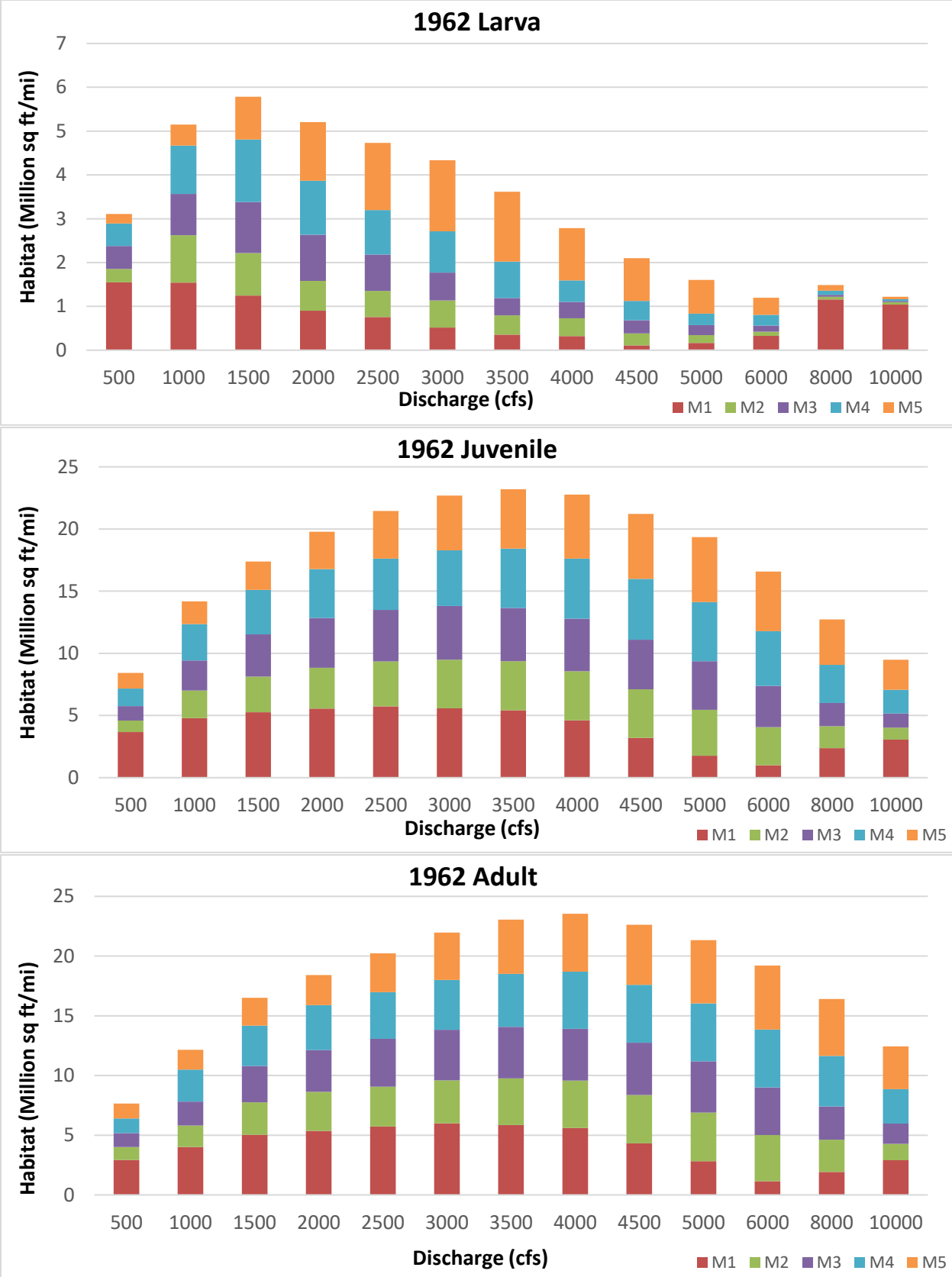


Figure D-6 Stacked habitat charts to display spatial variations of habitat throughout the Montano reach in 1962

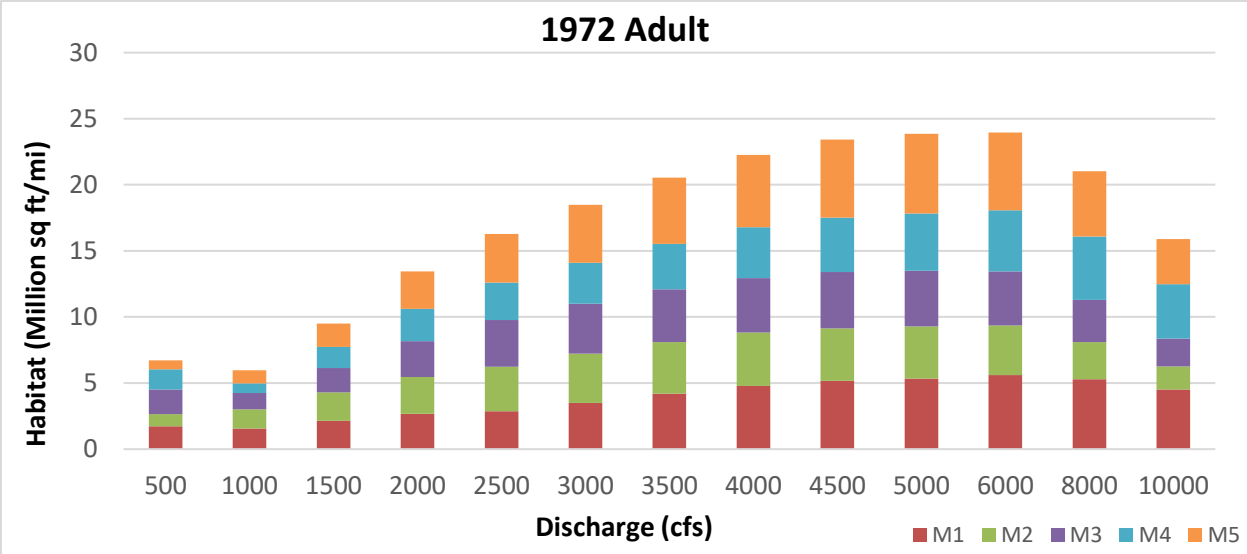
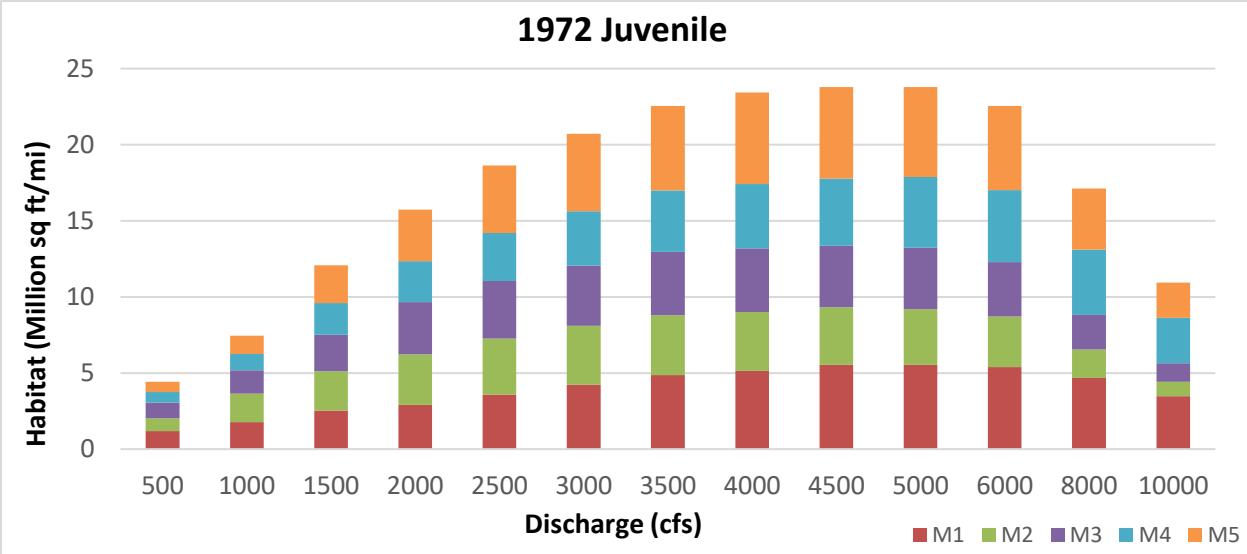
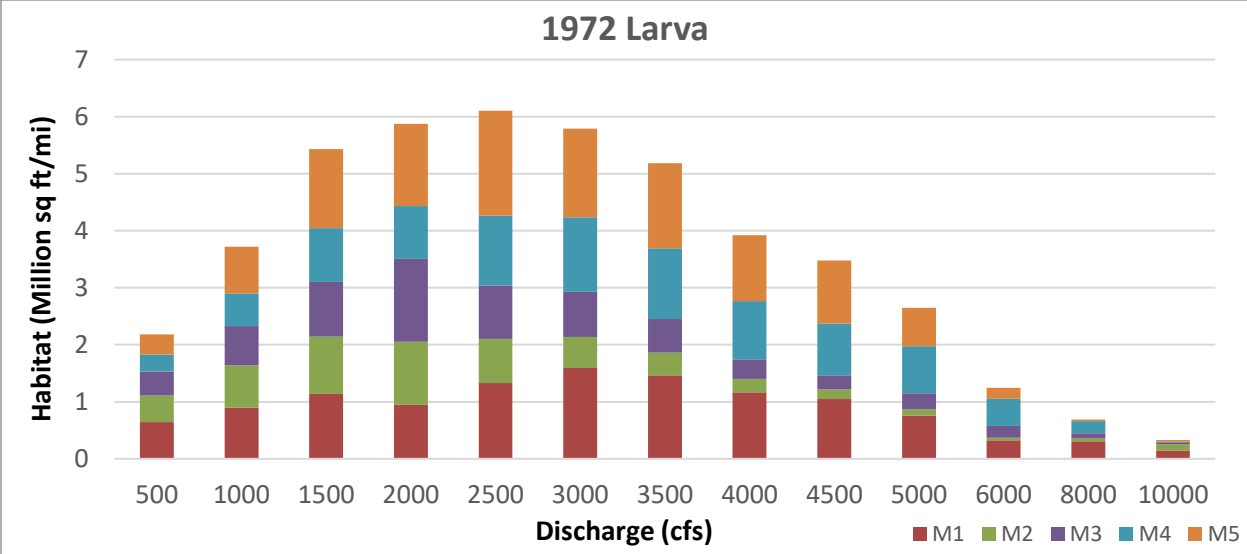


Figure D-7 Stacked habitat charts to display spatial variations of habitat throughout the Montano reach in 1972

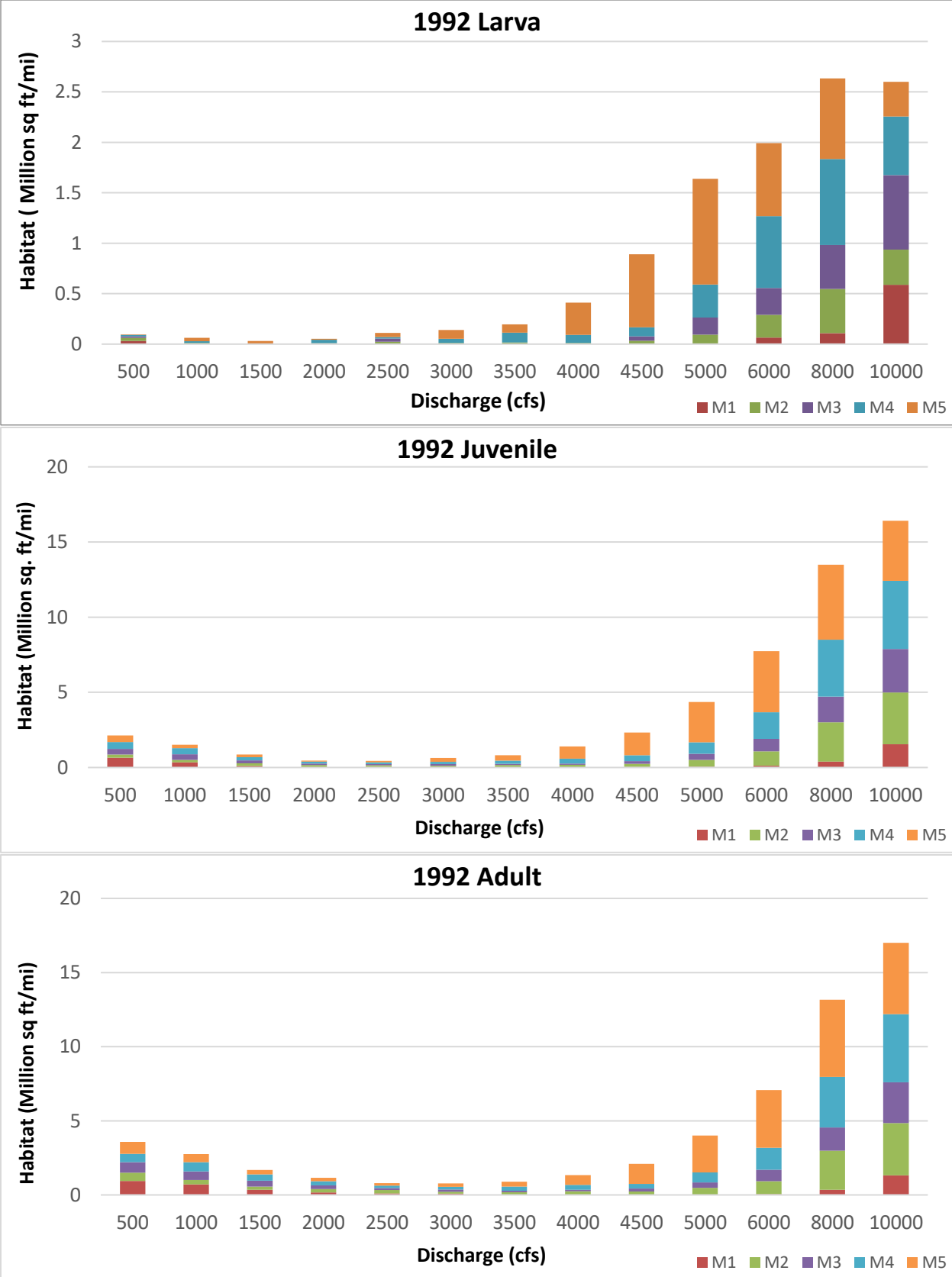


Figure D-8 Stacked habitat charts to display spatial variations of habitat throughout the Montano reach in 1992

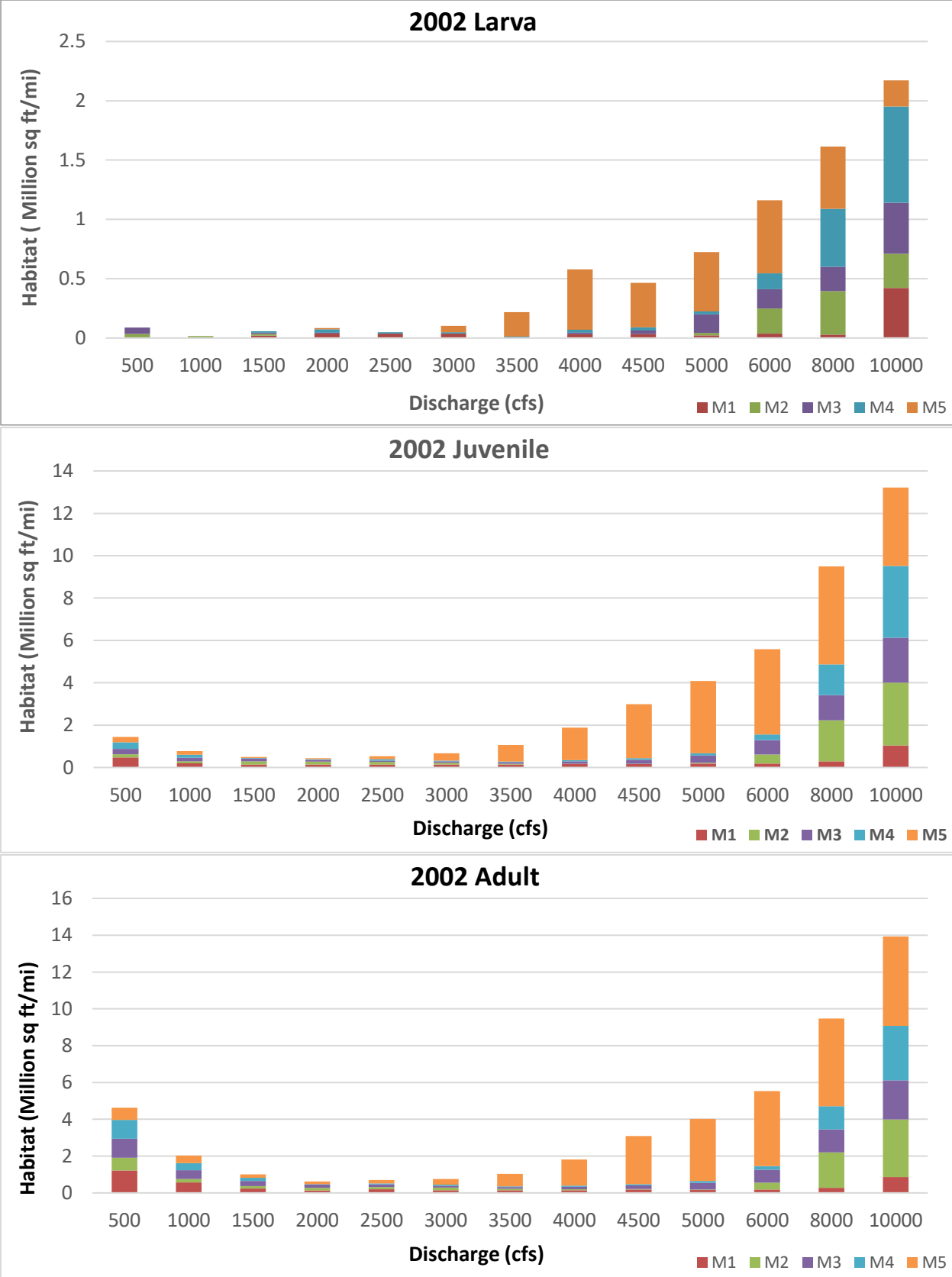


Figure D-9 Stacked habitat charts to display spatial variations of habitat throughout the Montano reach in 2002

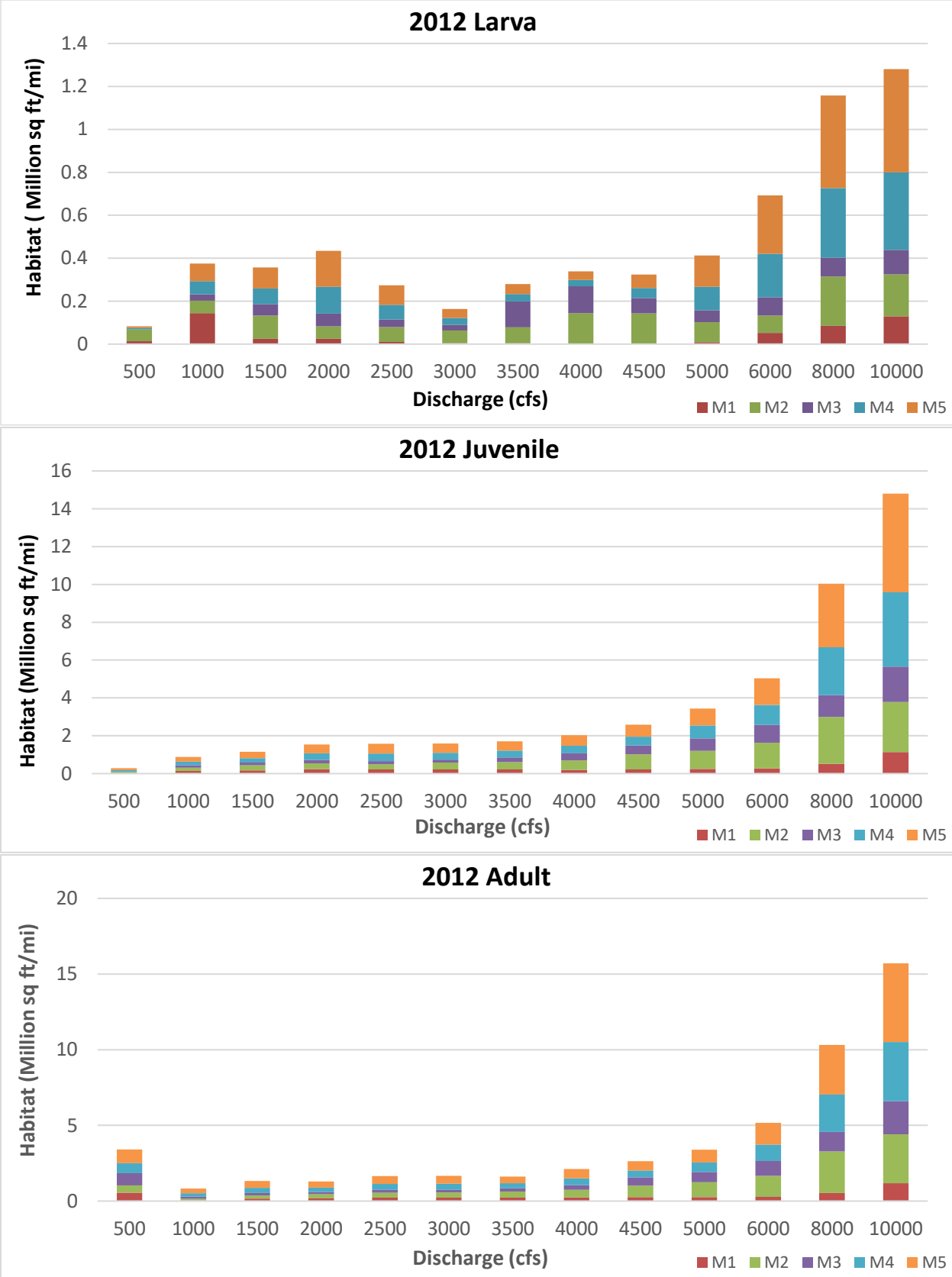
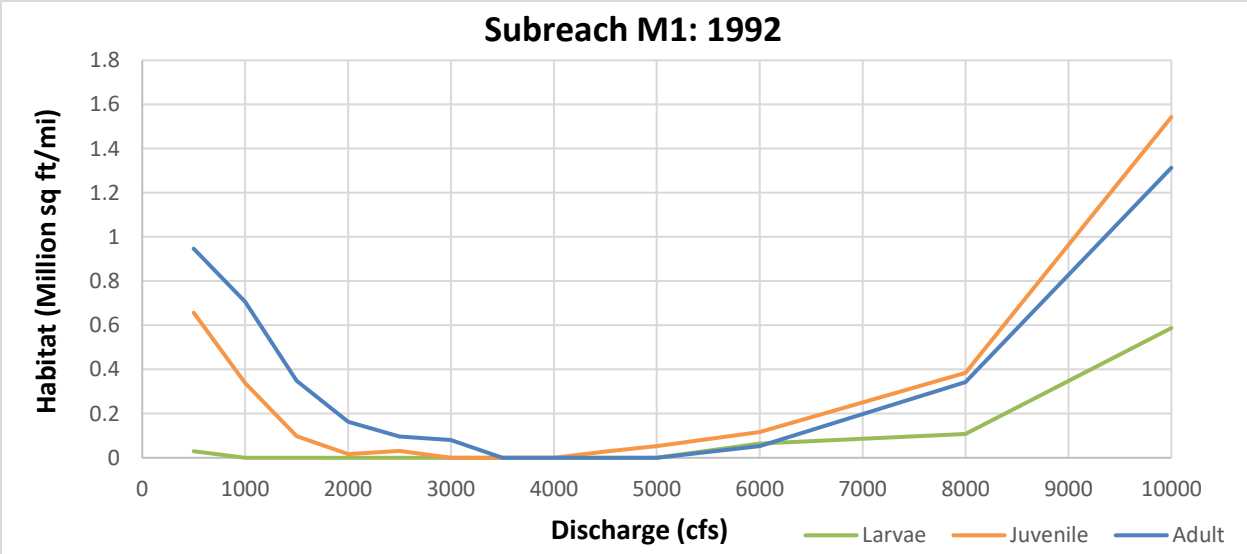
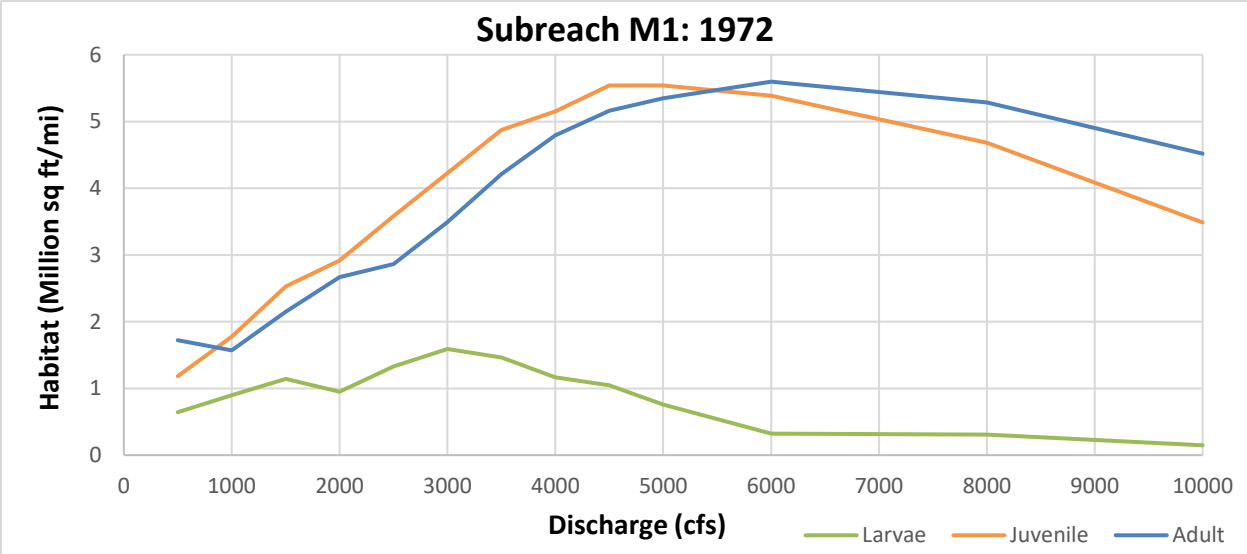
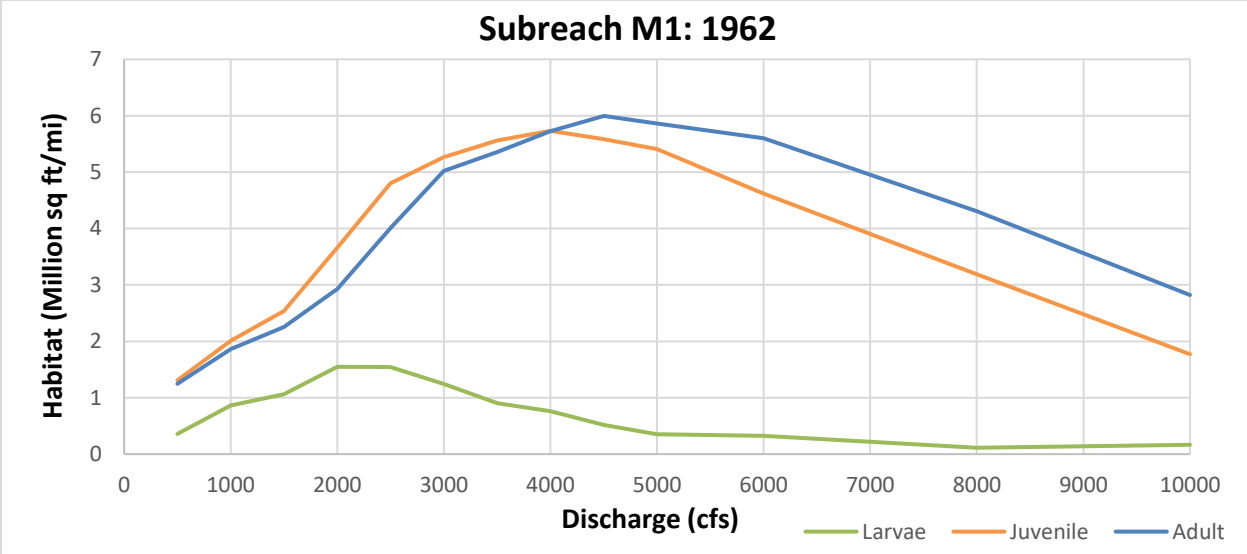


Figure D-10 Stacked habitat charts to display spatial variations of habitat throughout the Montano reach in 2012



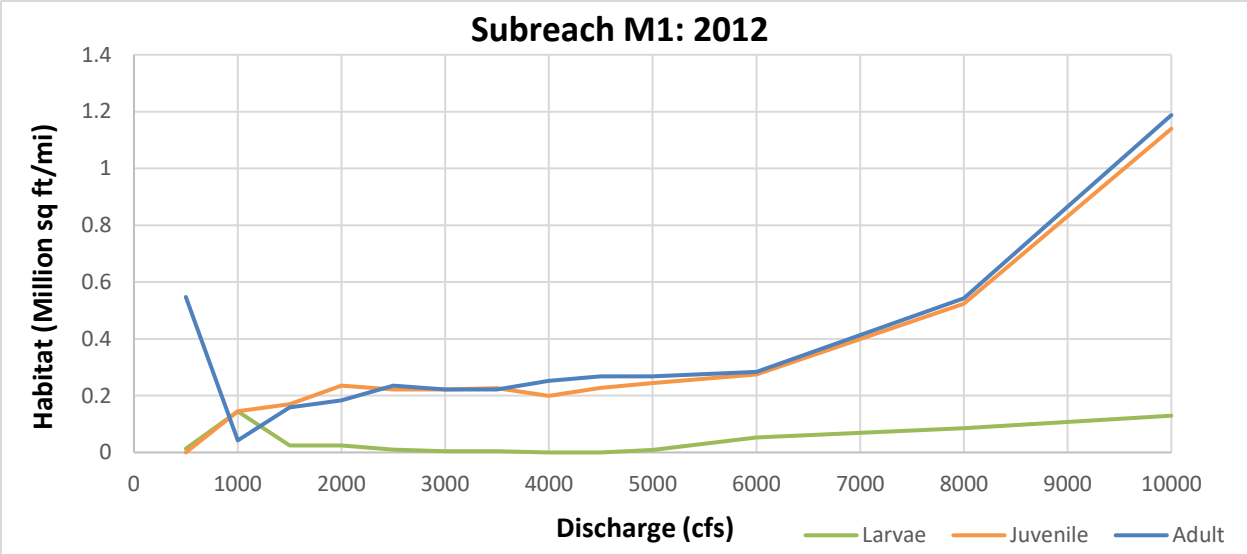
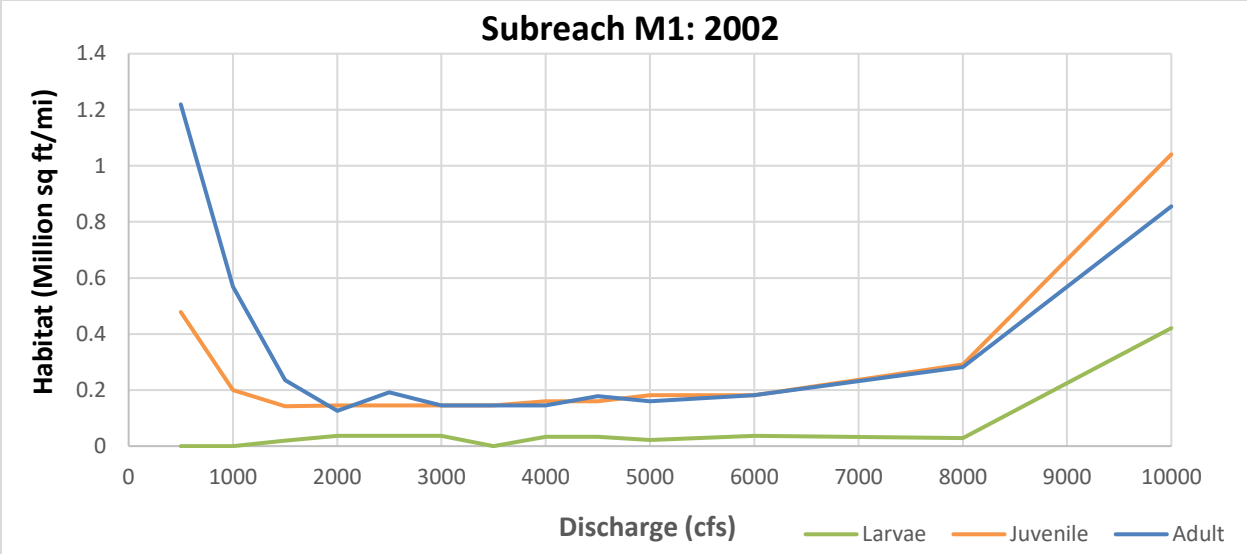
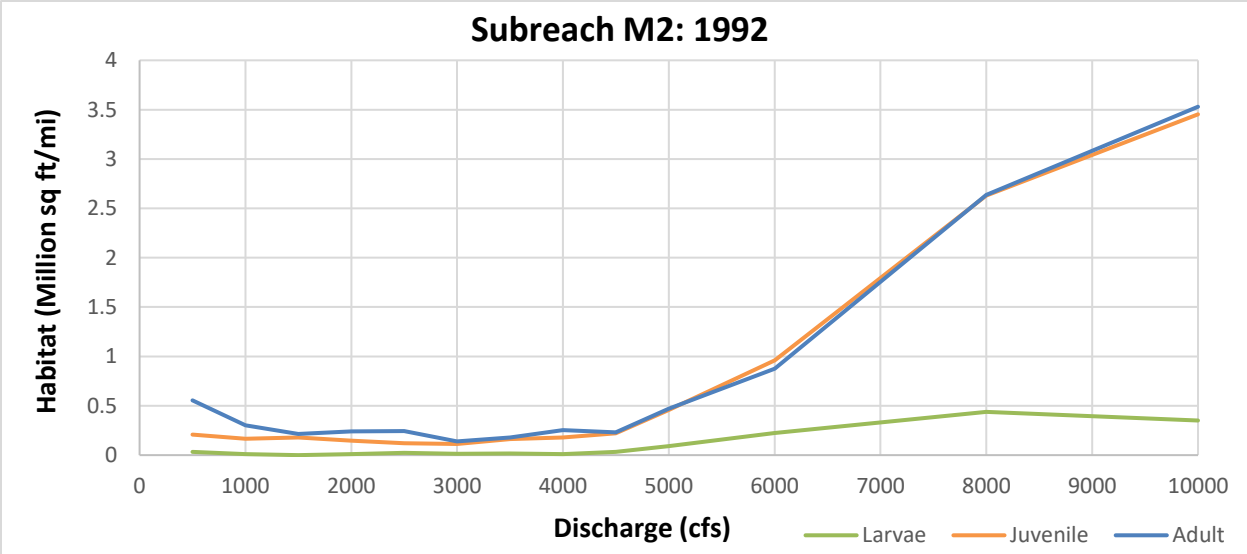
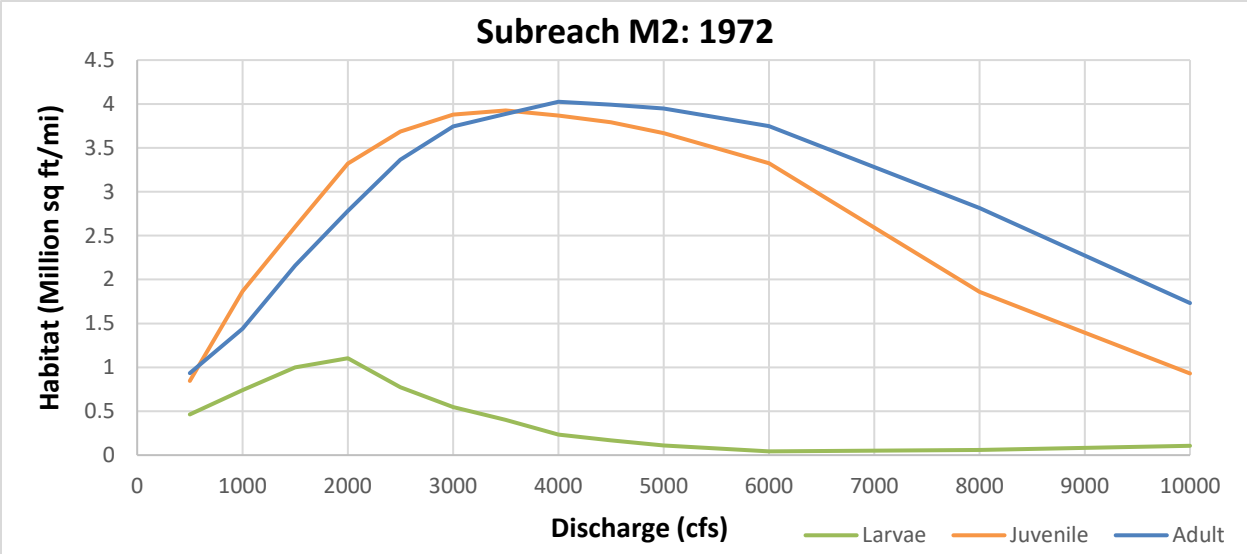
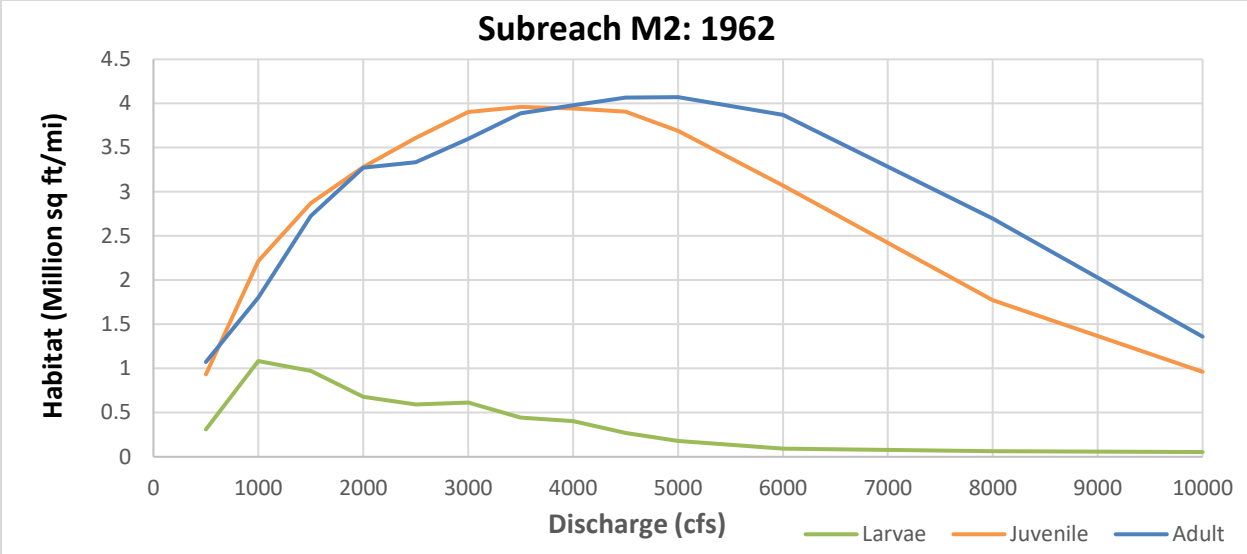


Figure D-11 Life stage habitat curves for subreach M1



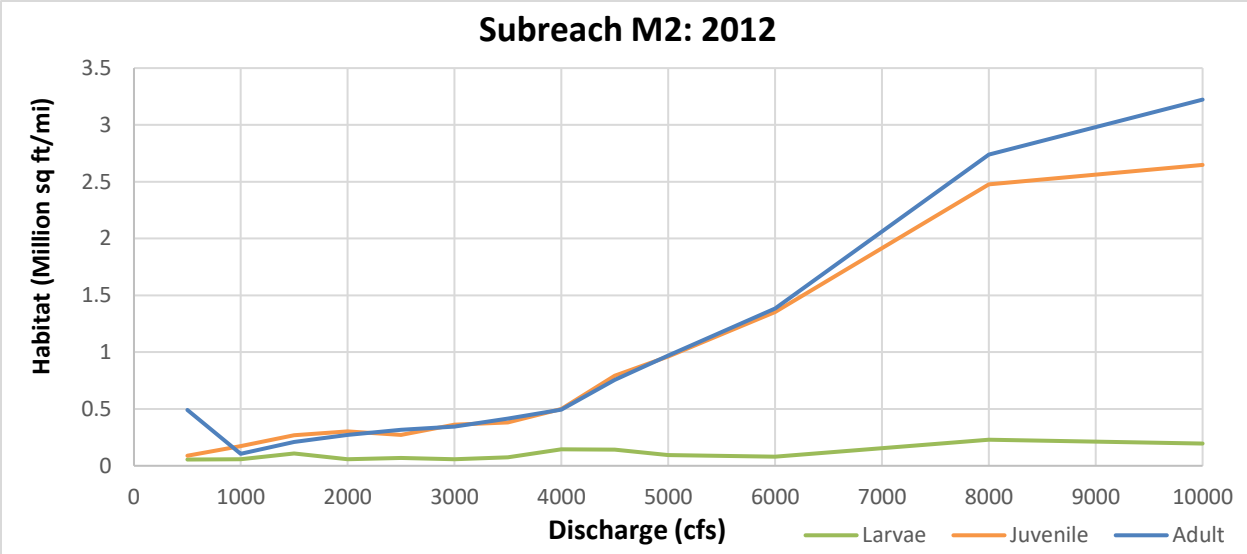
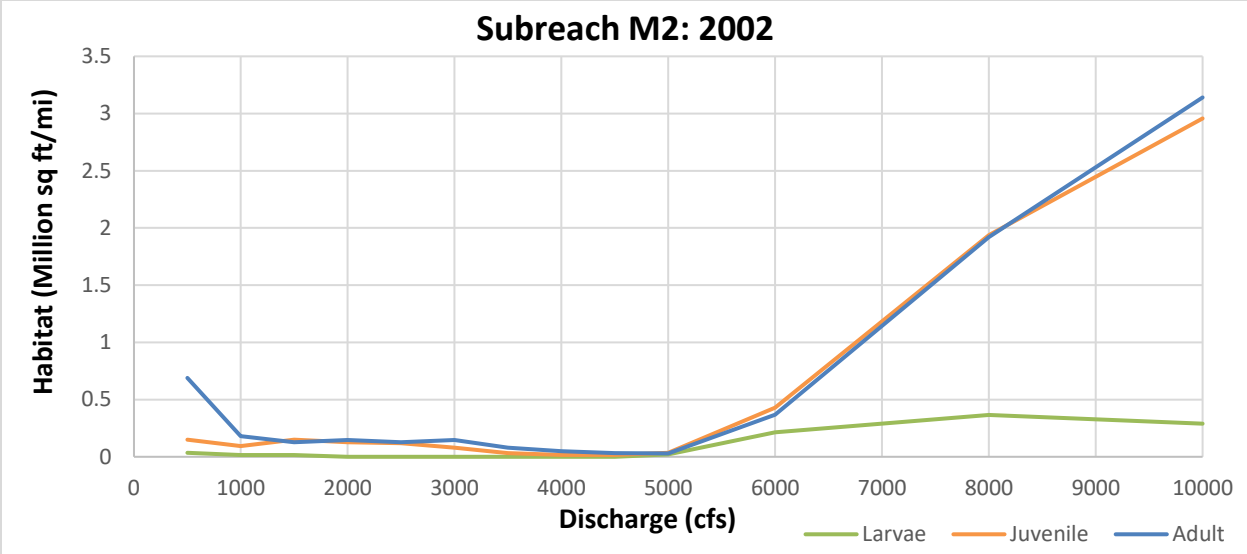
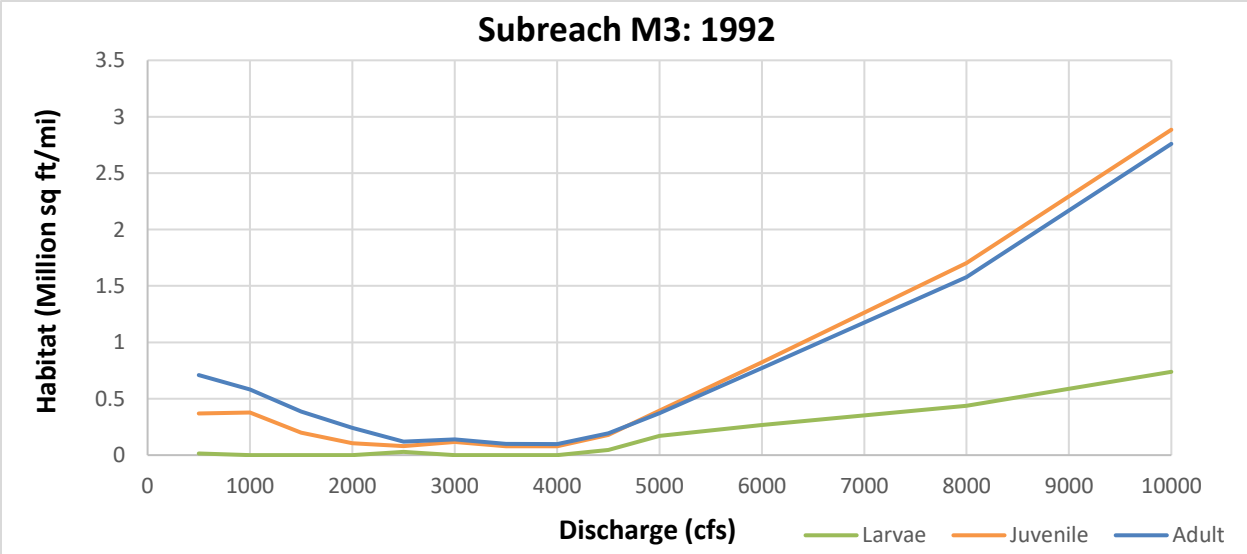
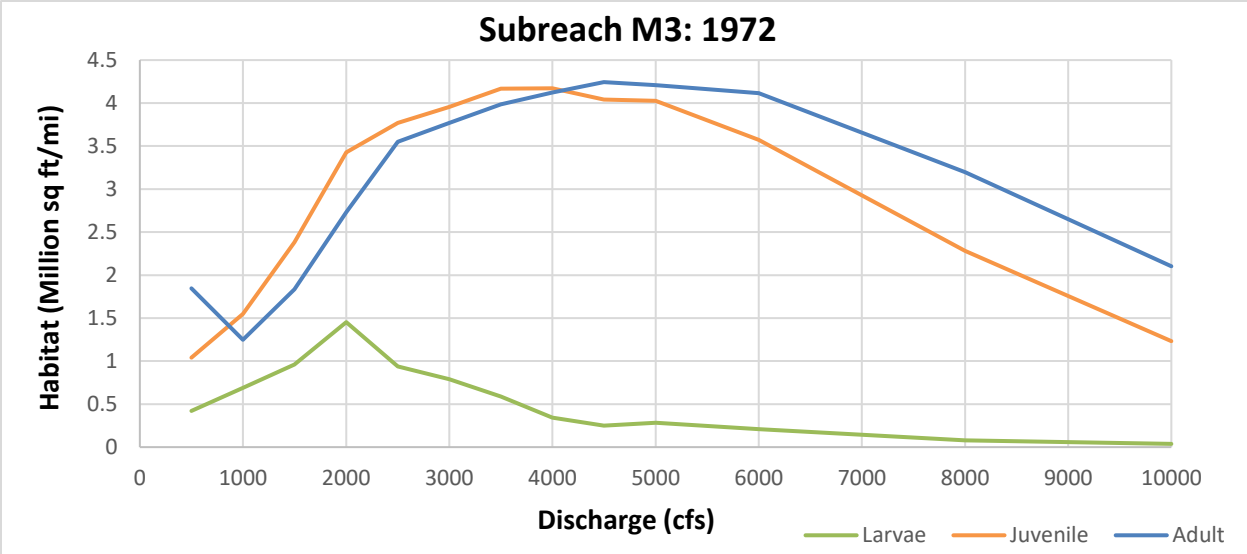
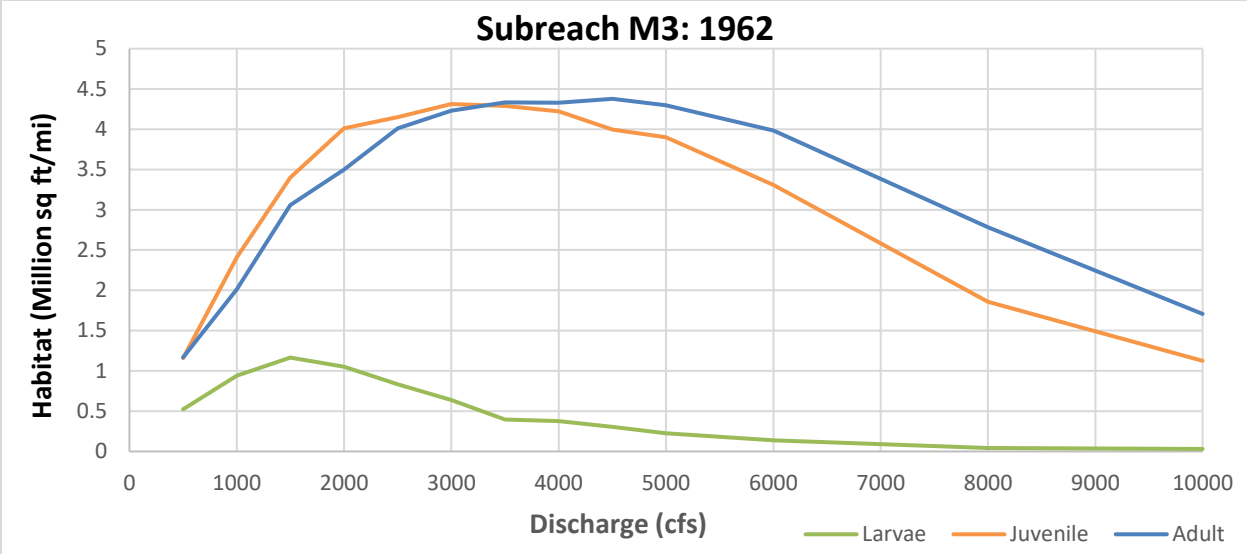


Figure D-12 Life stage habitat curves for subreach M2



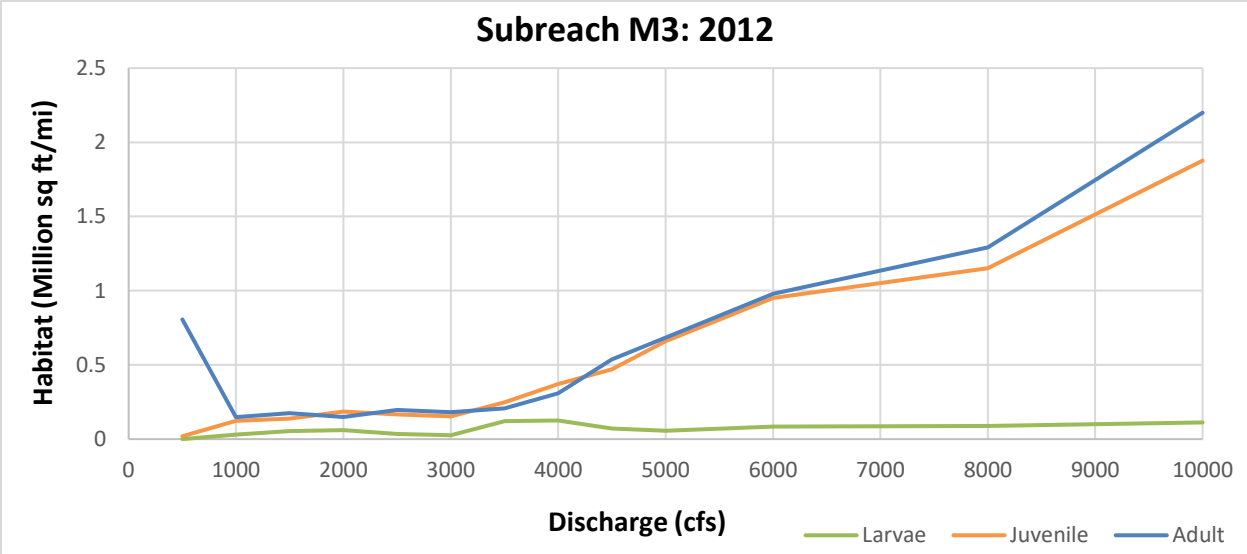
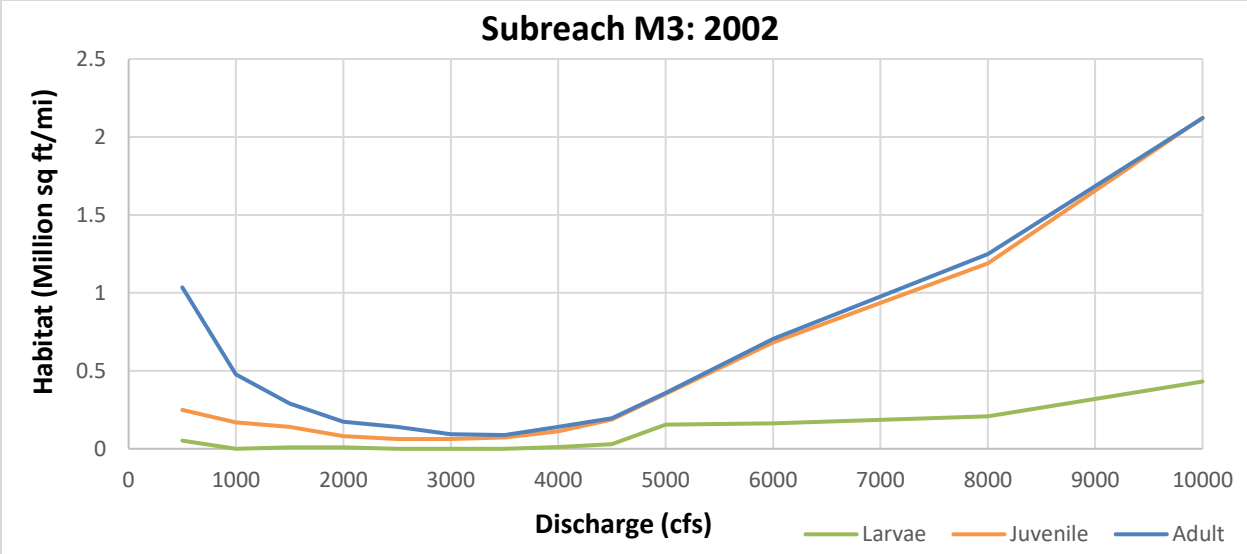
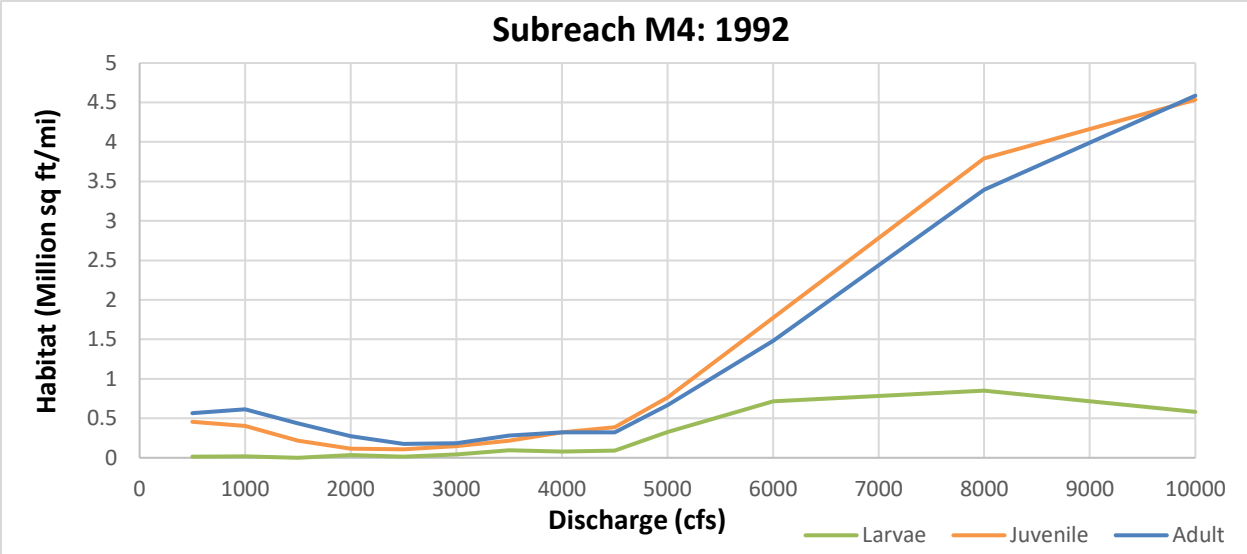
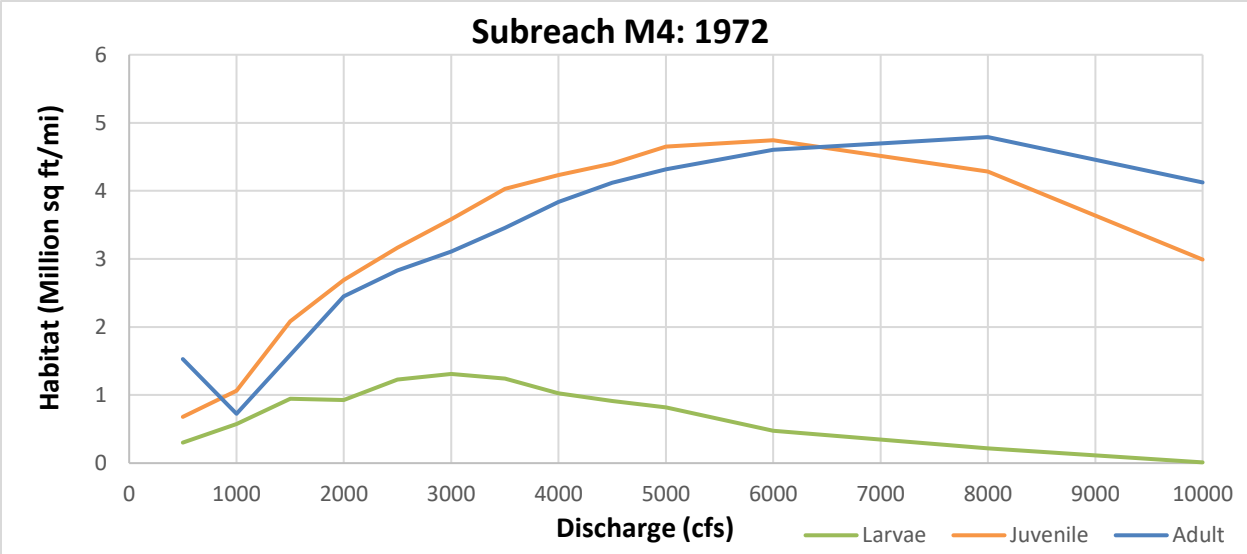
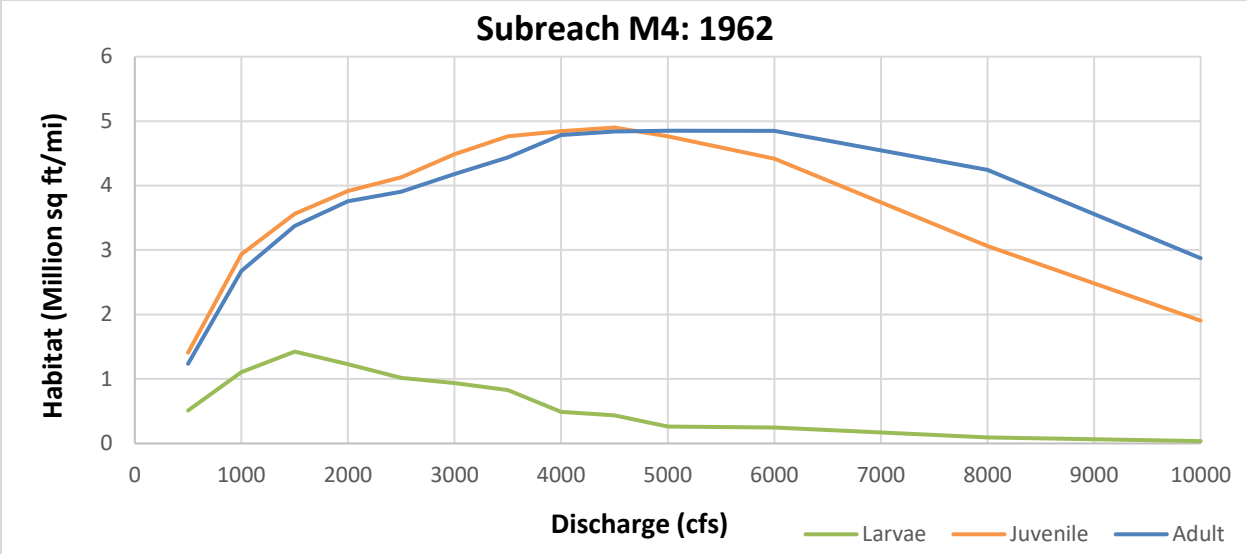


Figure D-13 Life stage habitat curves for subreach M3



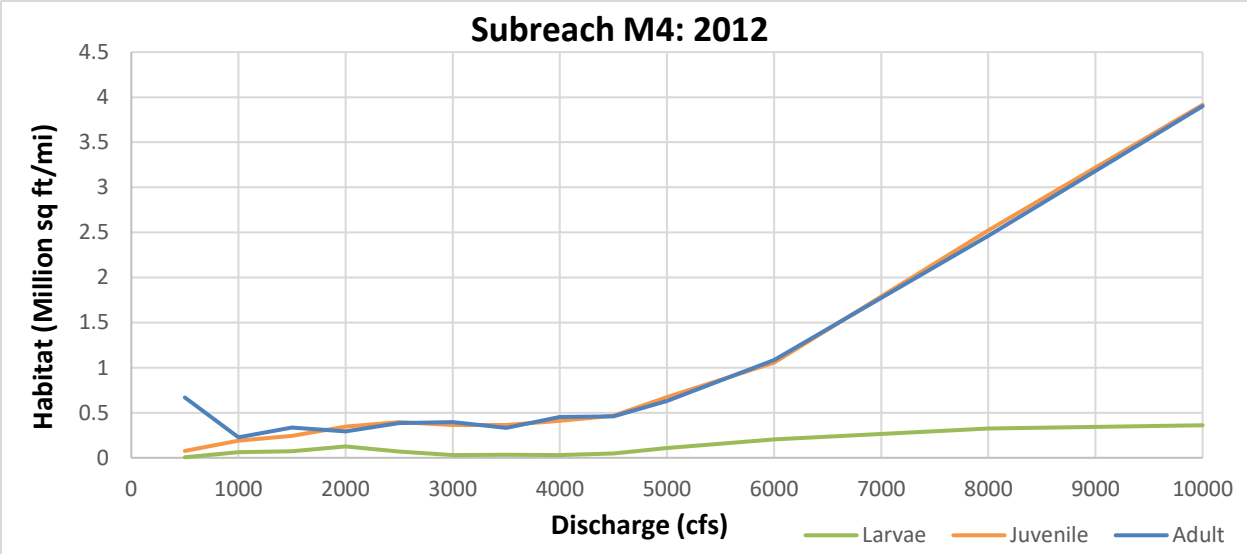
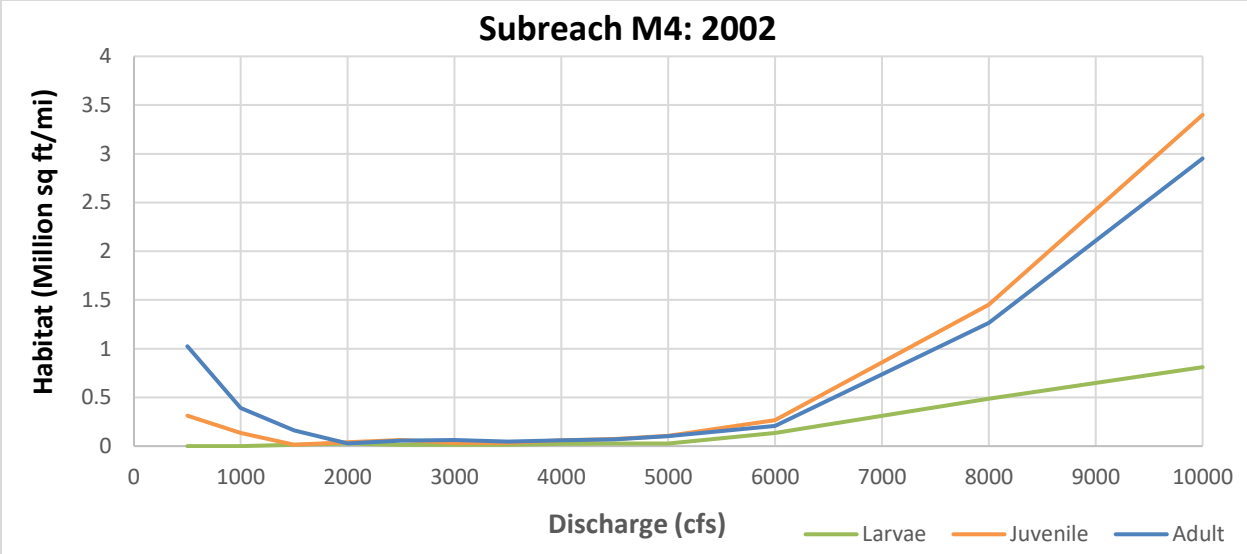
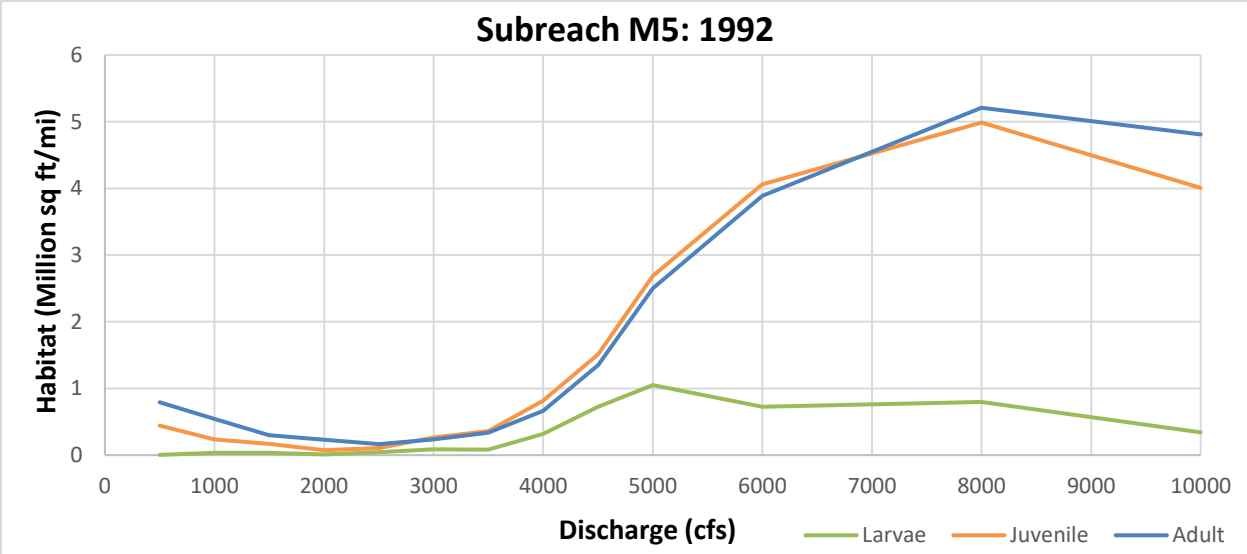
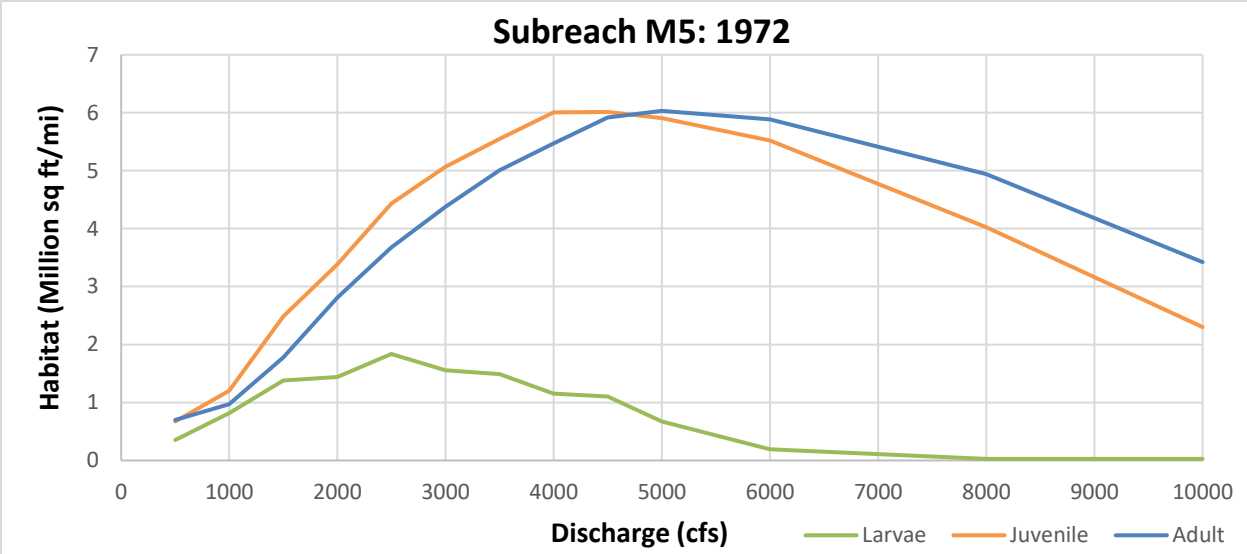
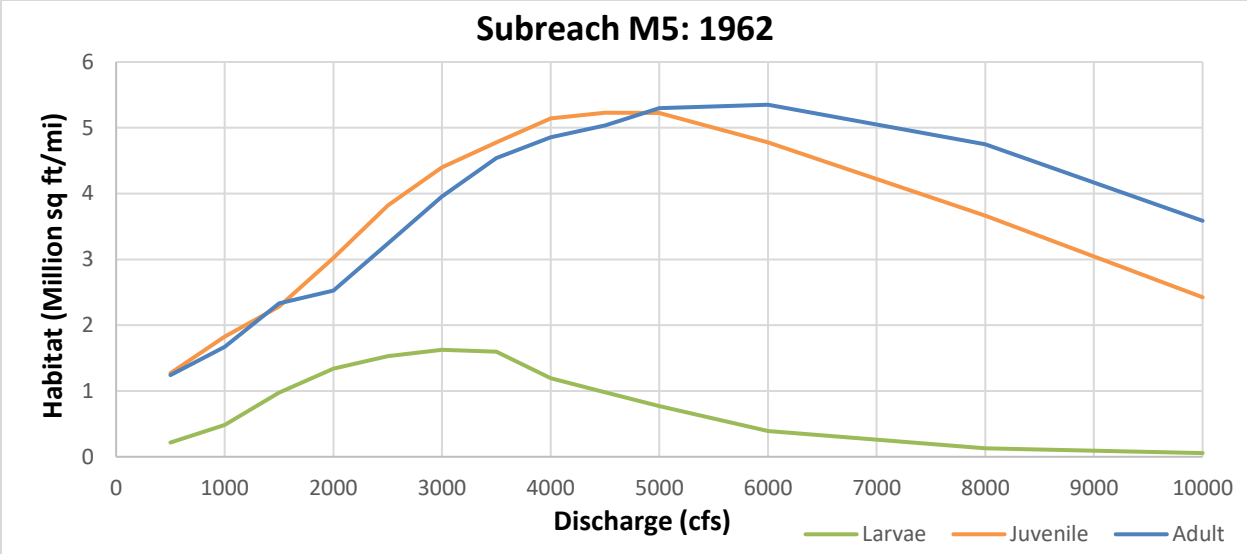


Figure D-14 Life stage habitat curves for subreach M4



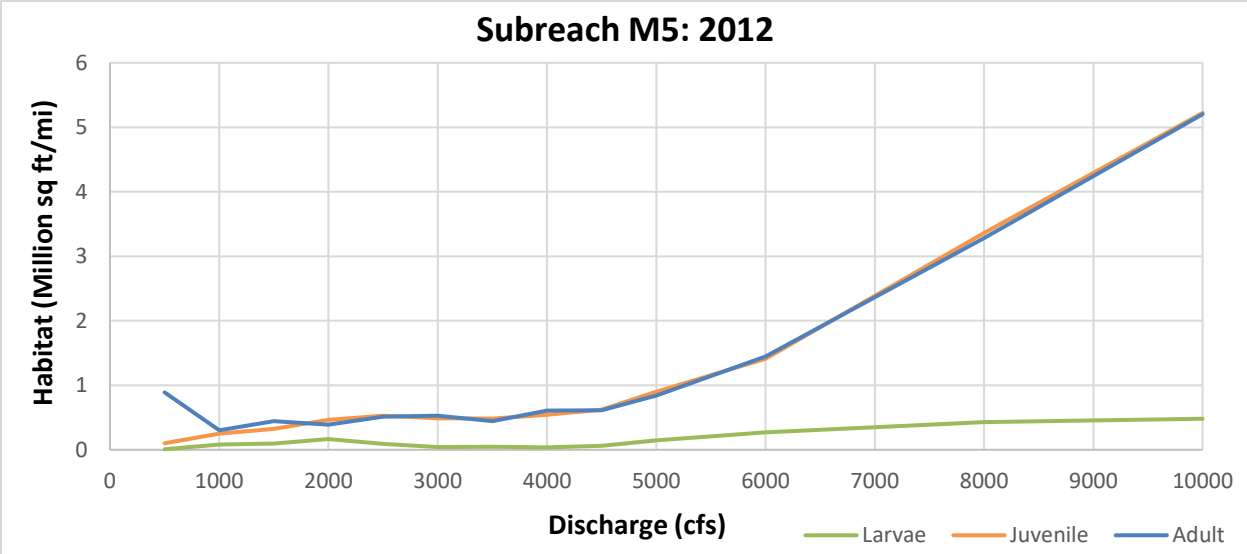
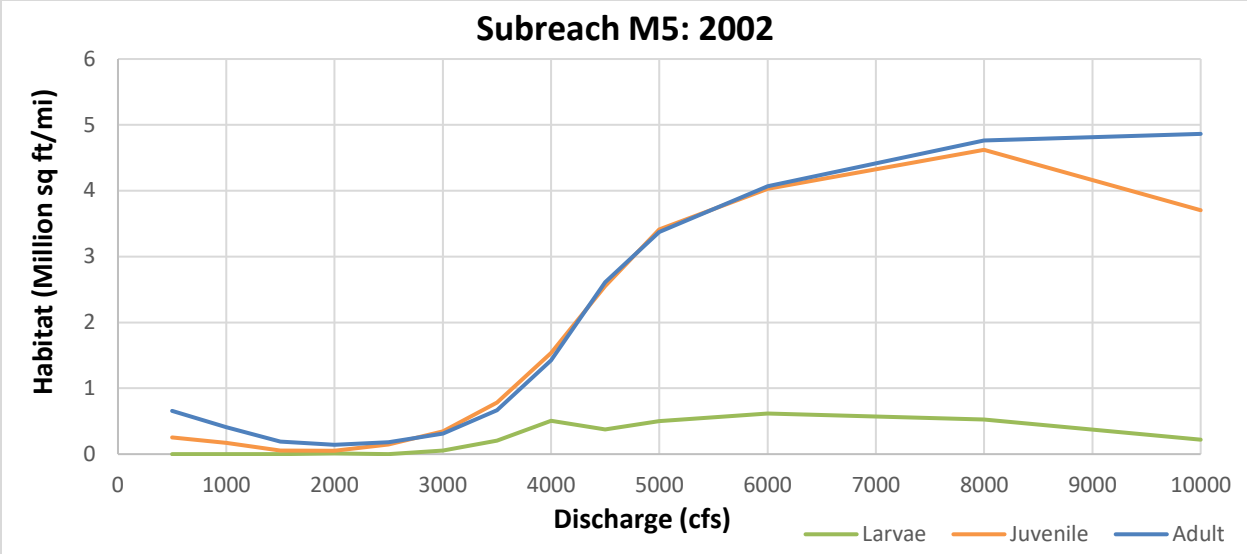
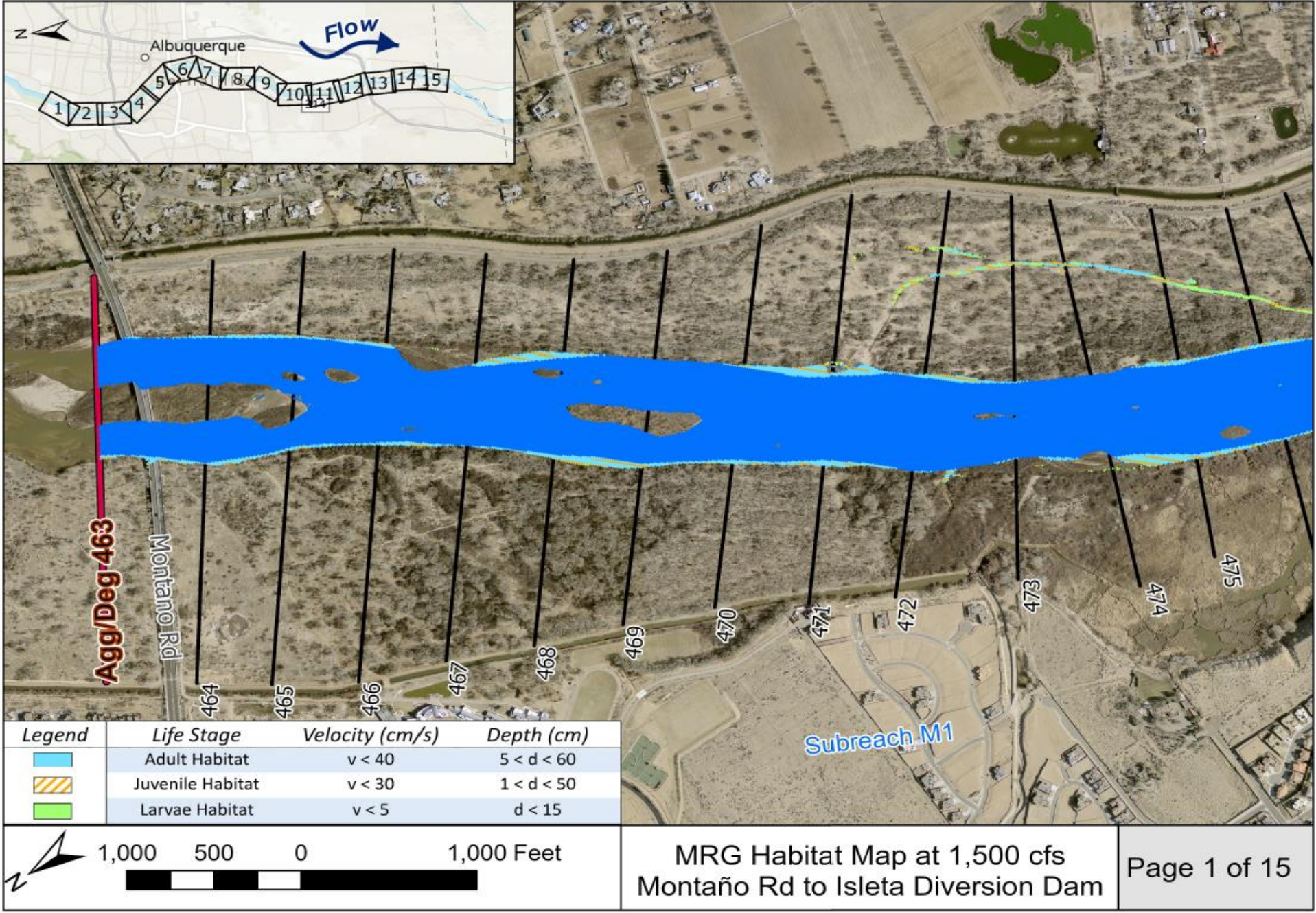
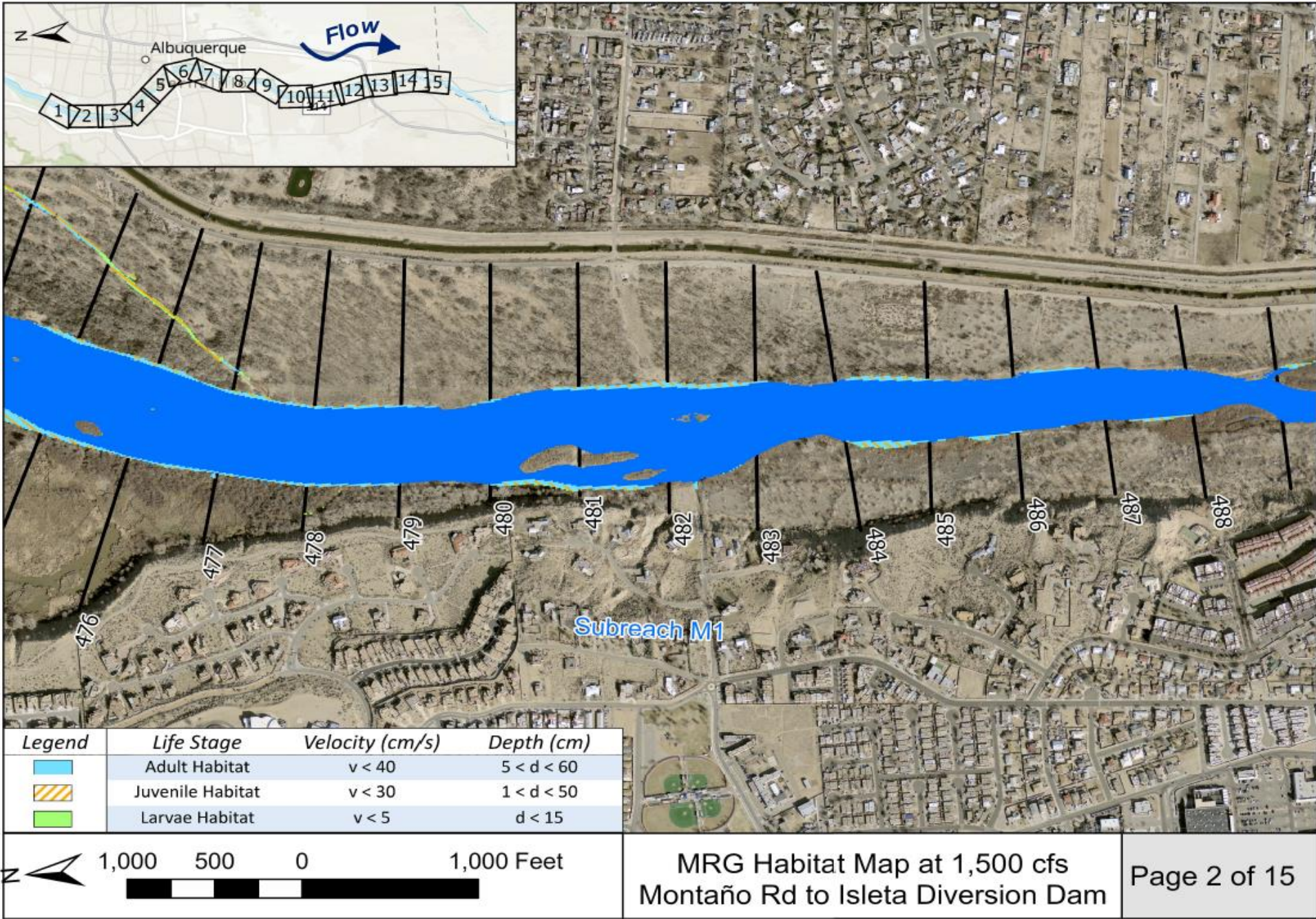


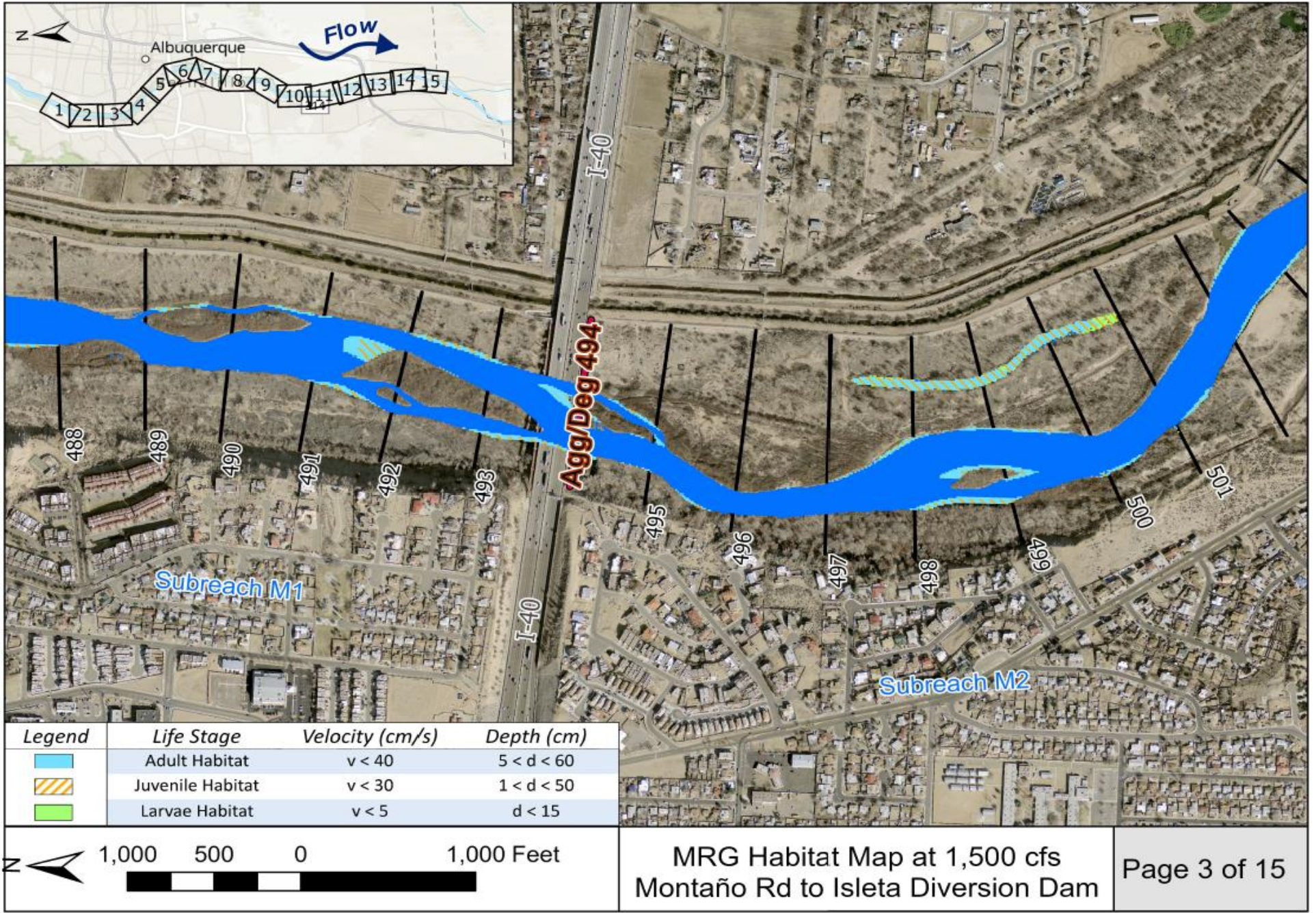
Figure D-15 Life stage habitat curves for subreach M5

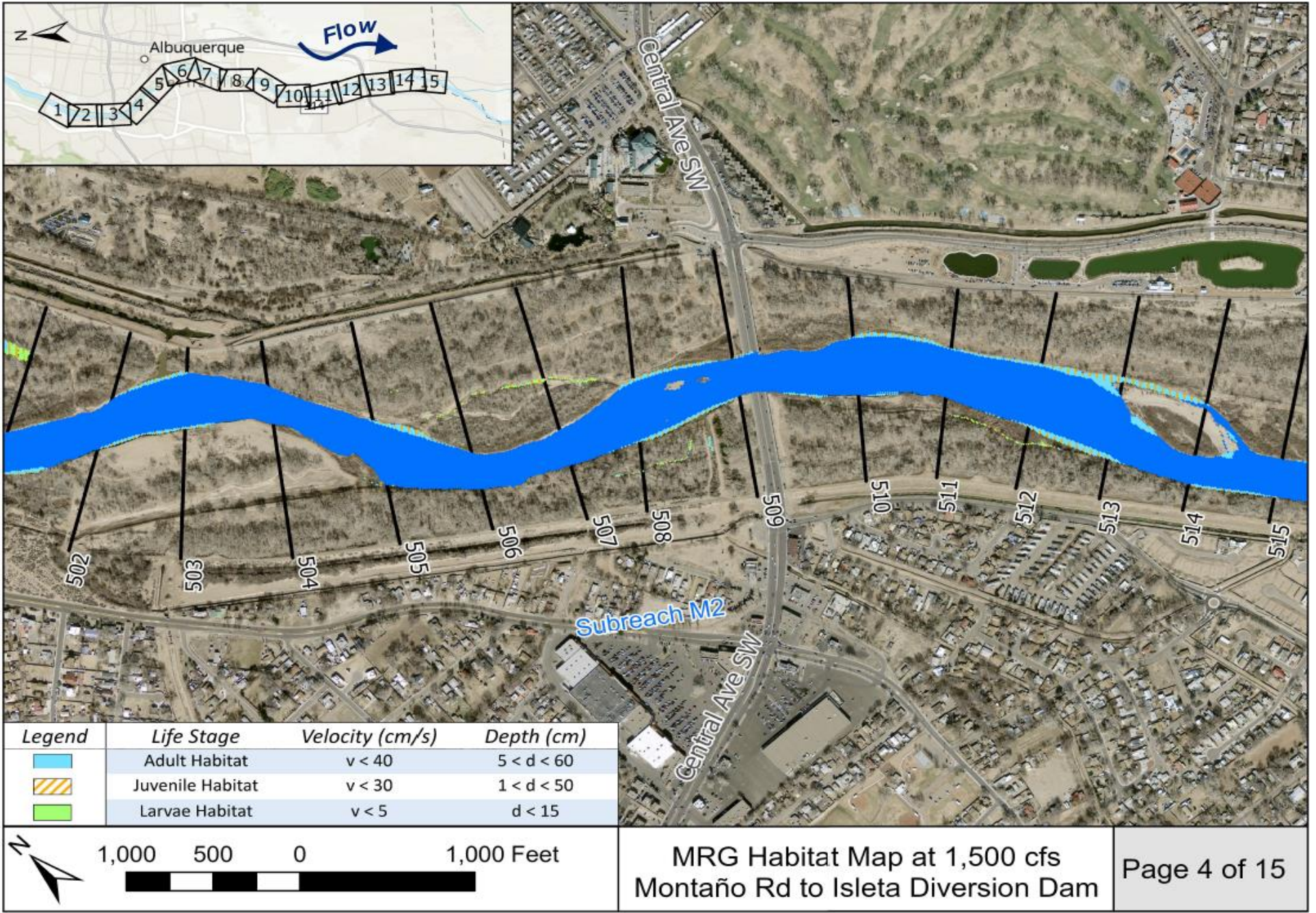
Appendix E

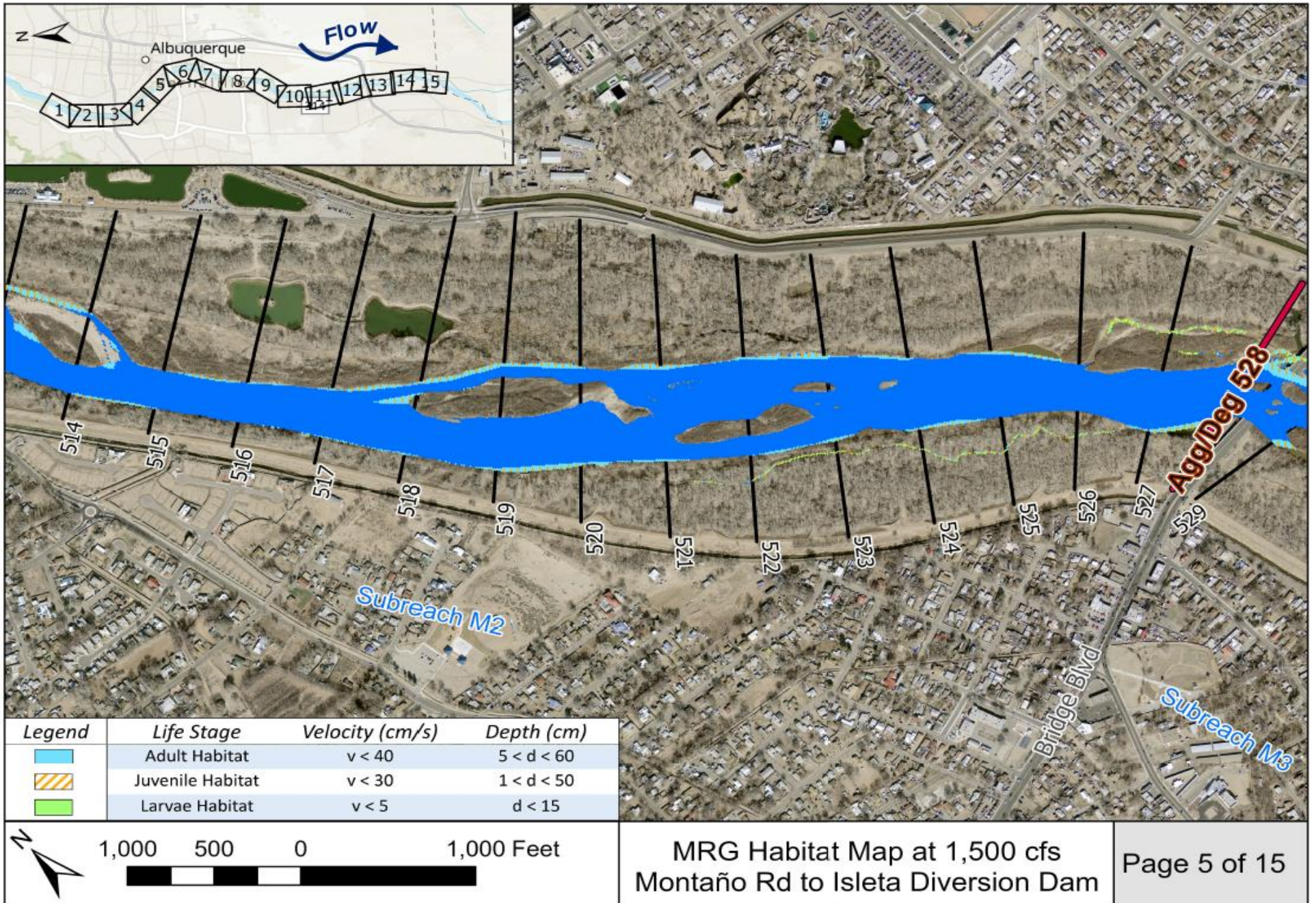
Habitat Maps, Table of Disconnected Areas of Hydraulically Suitable Habitat

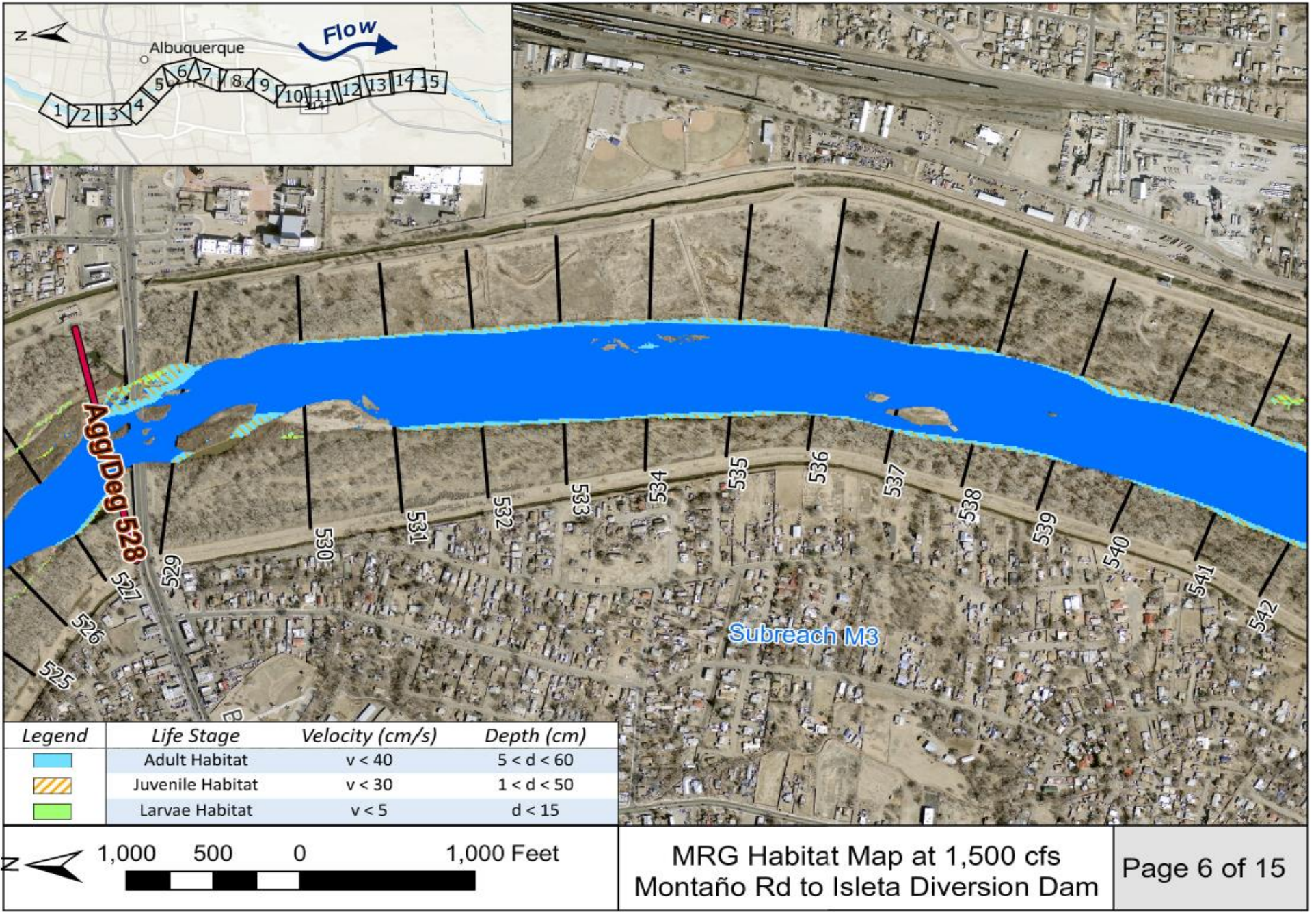


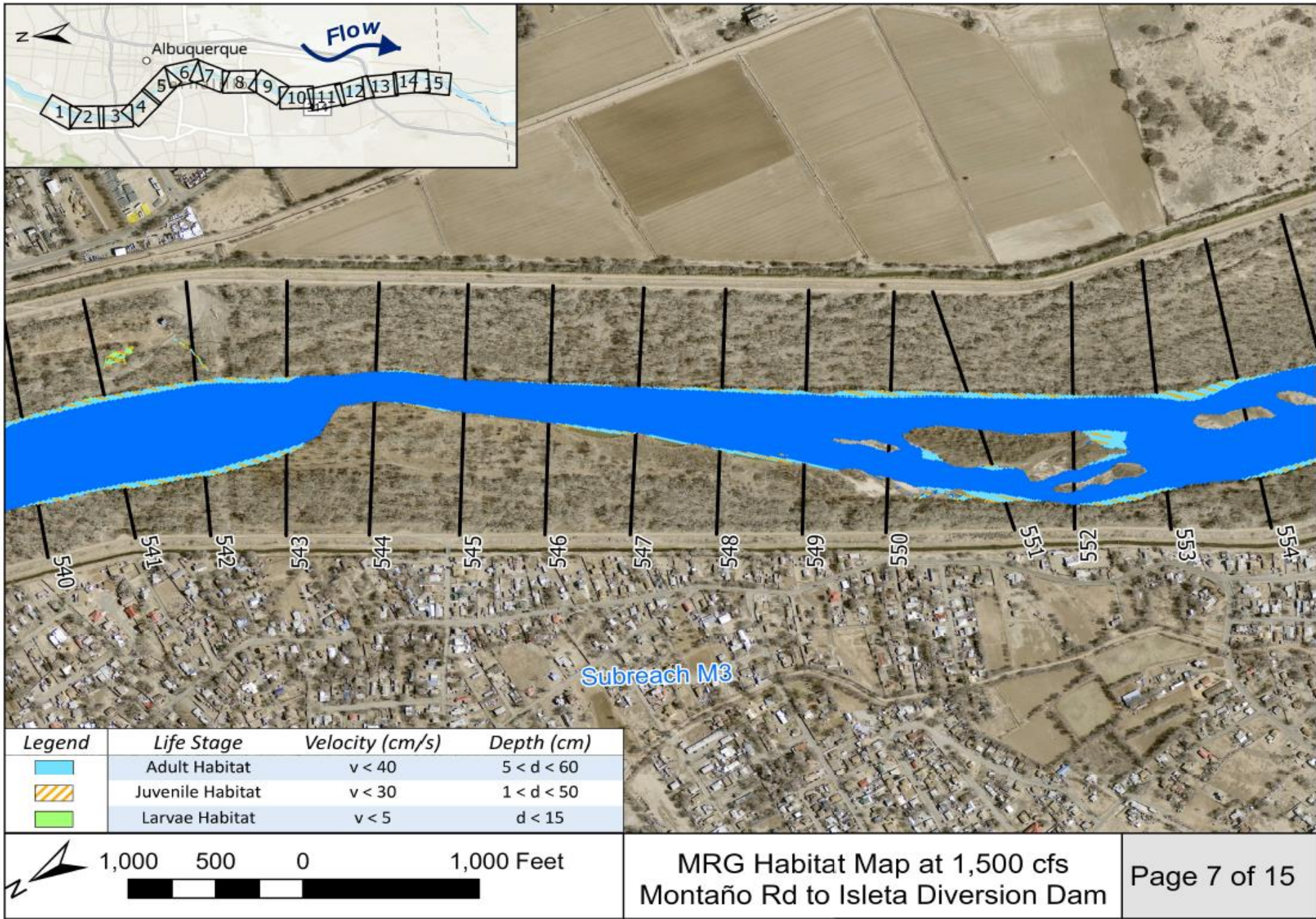


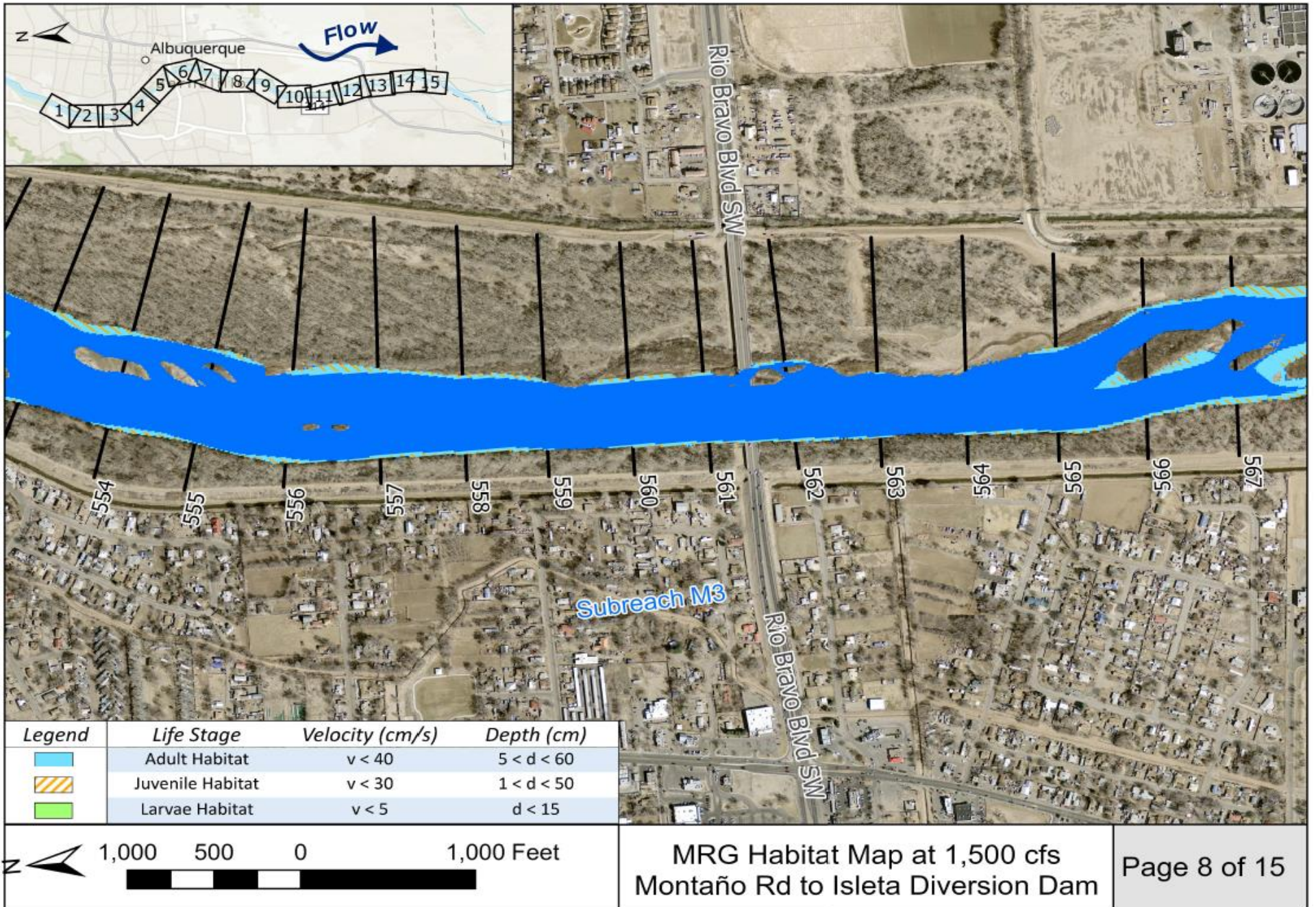


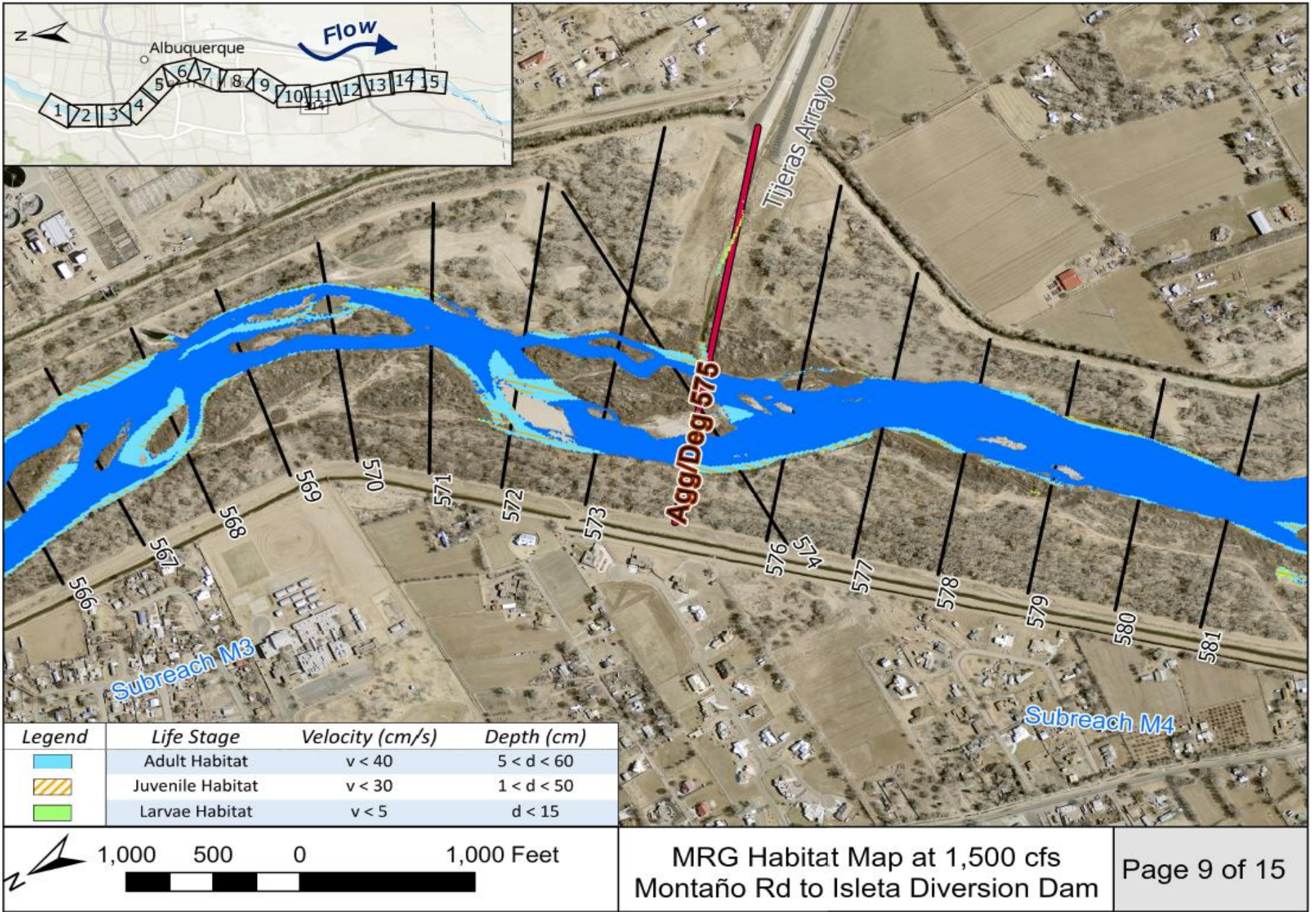


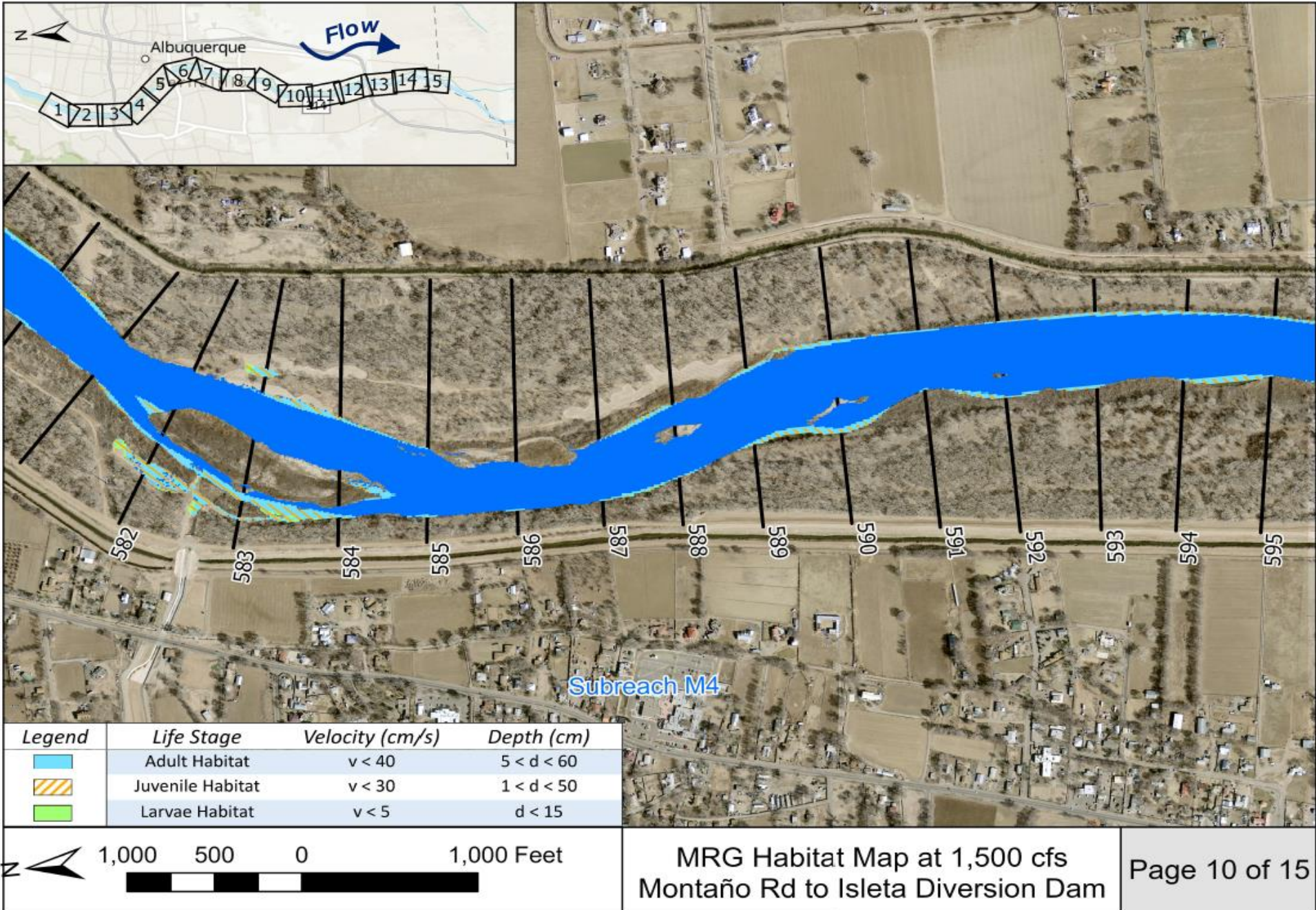


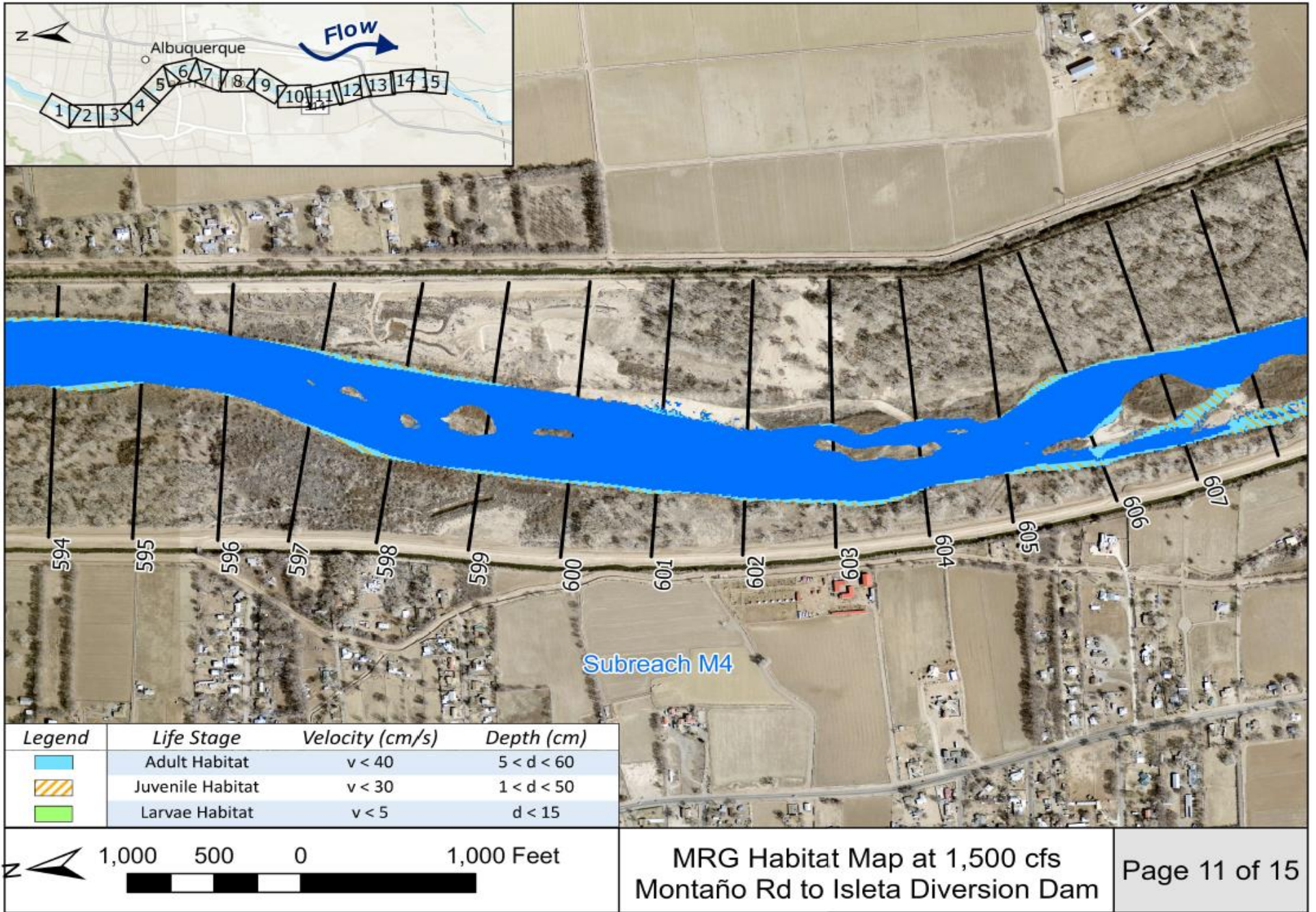


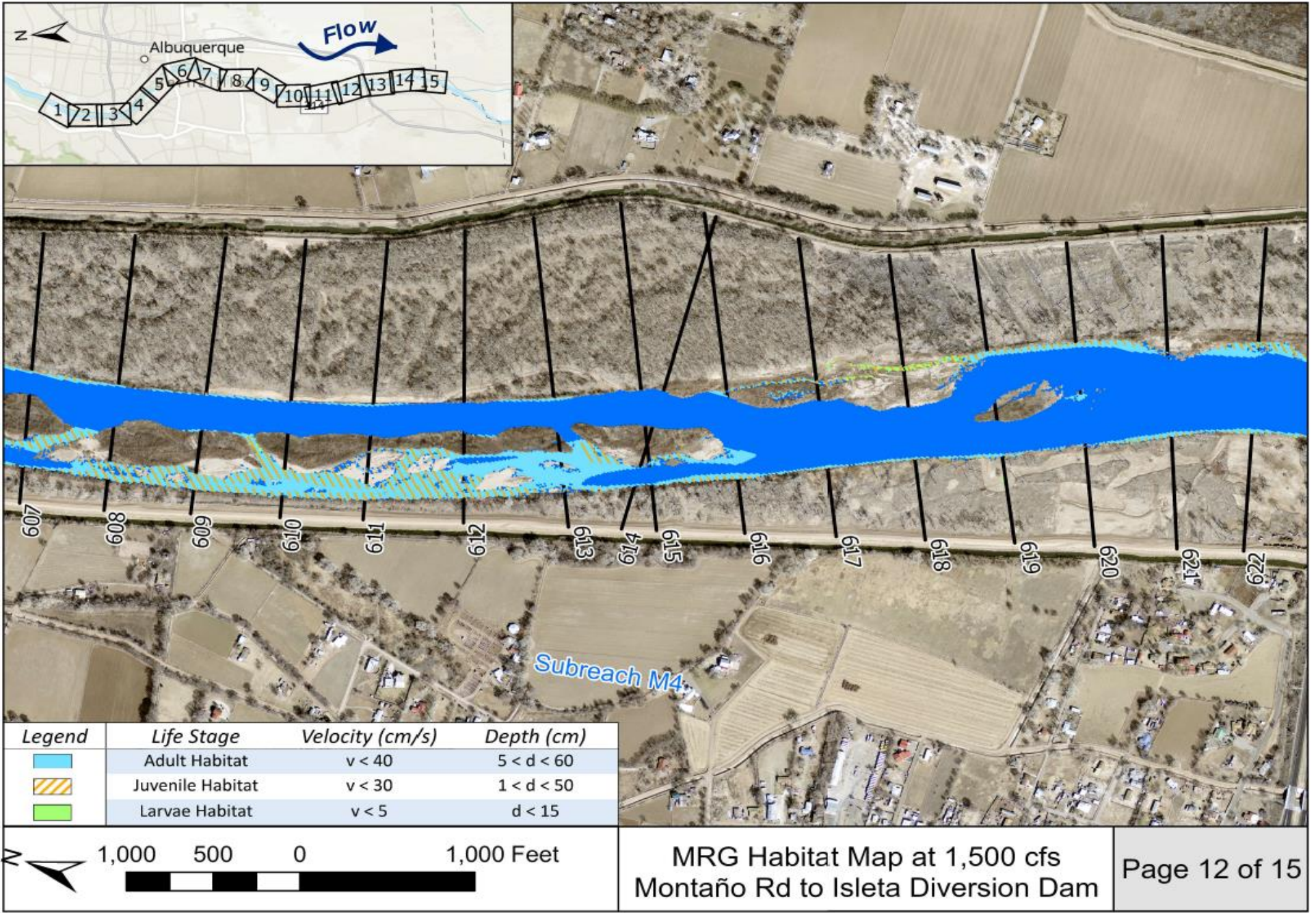


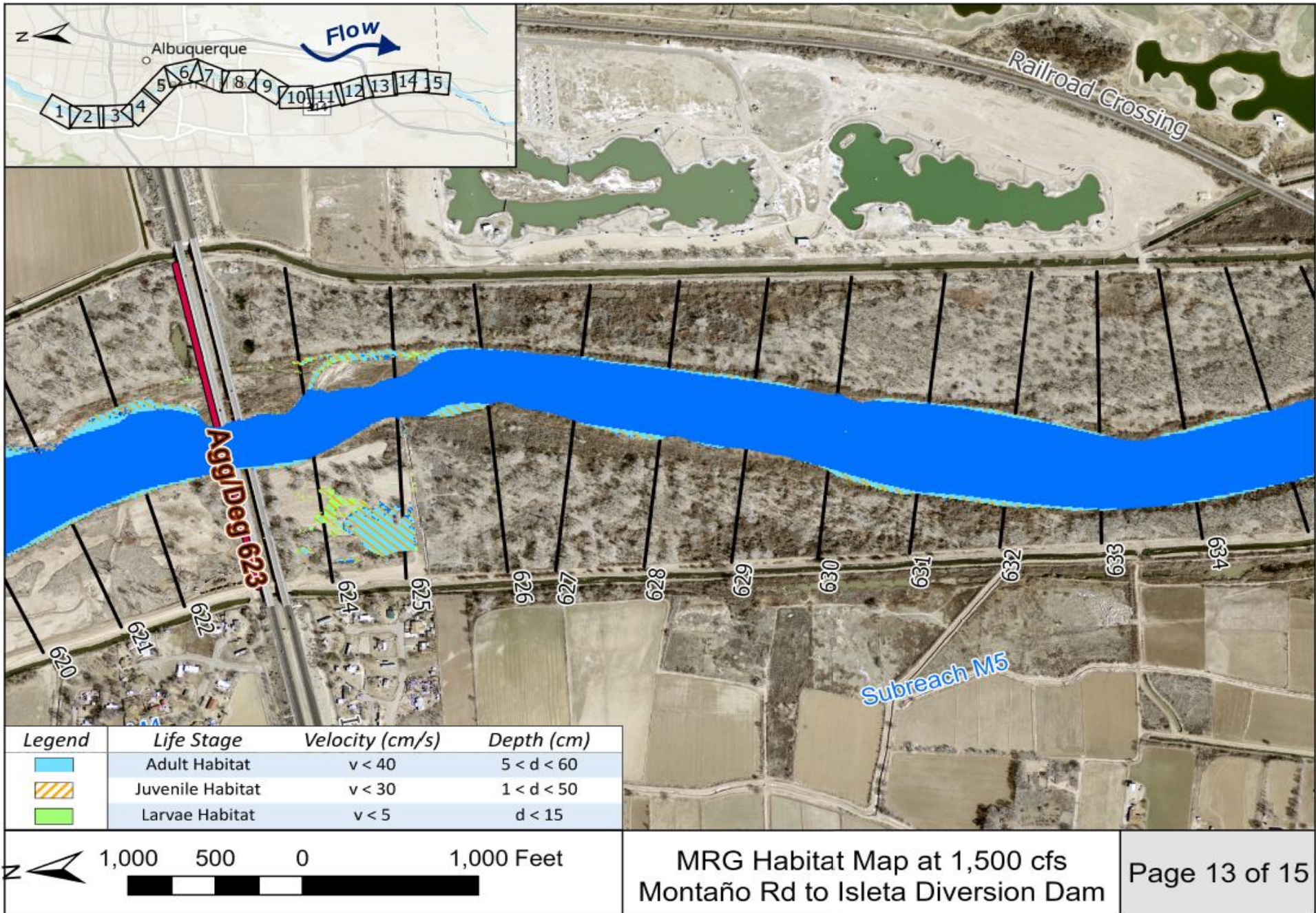


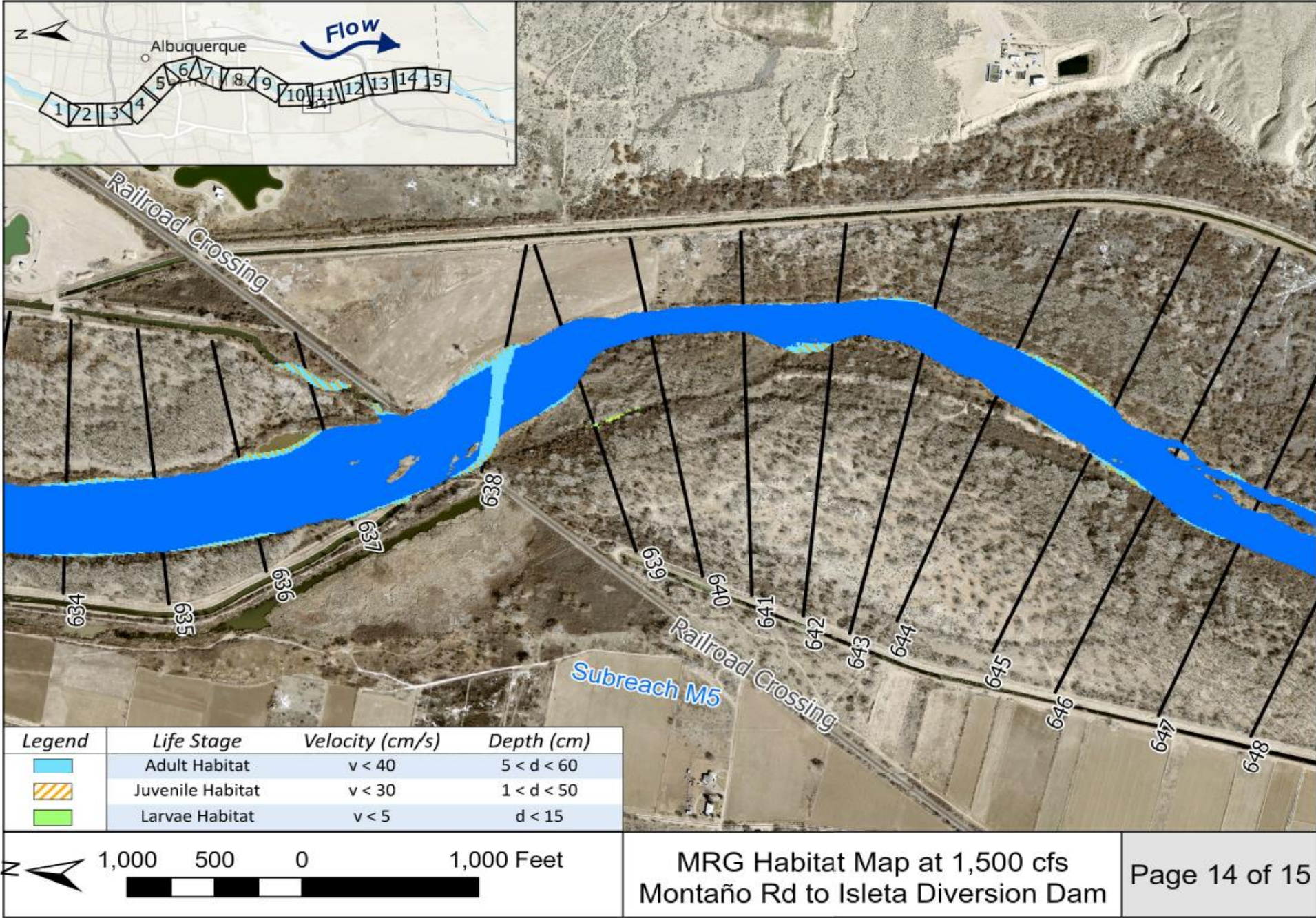


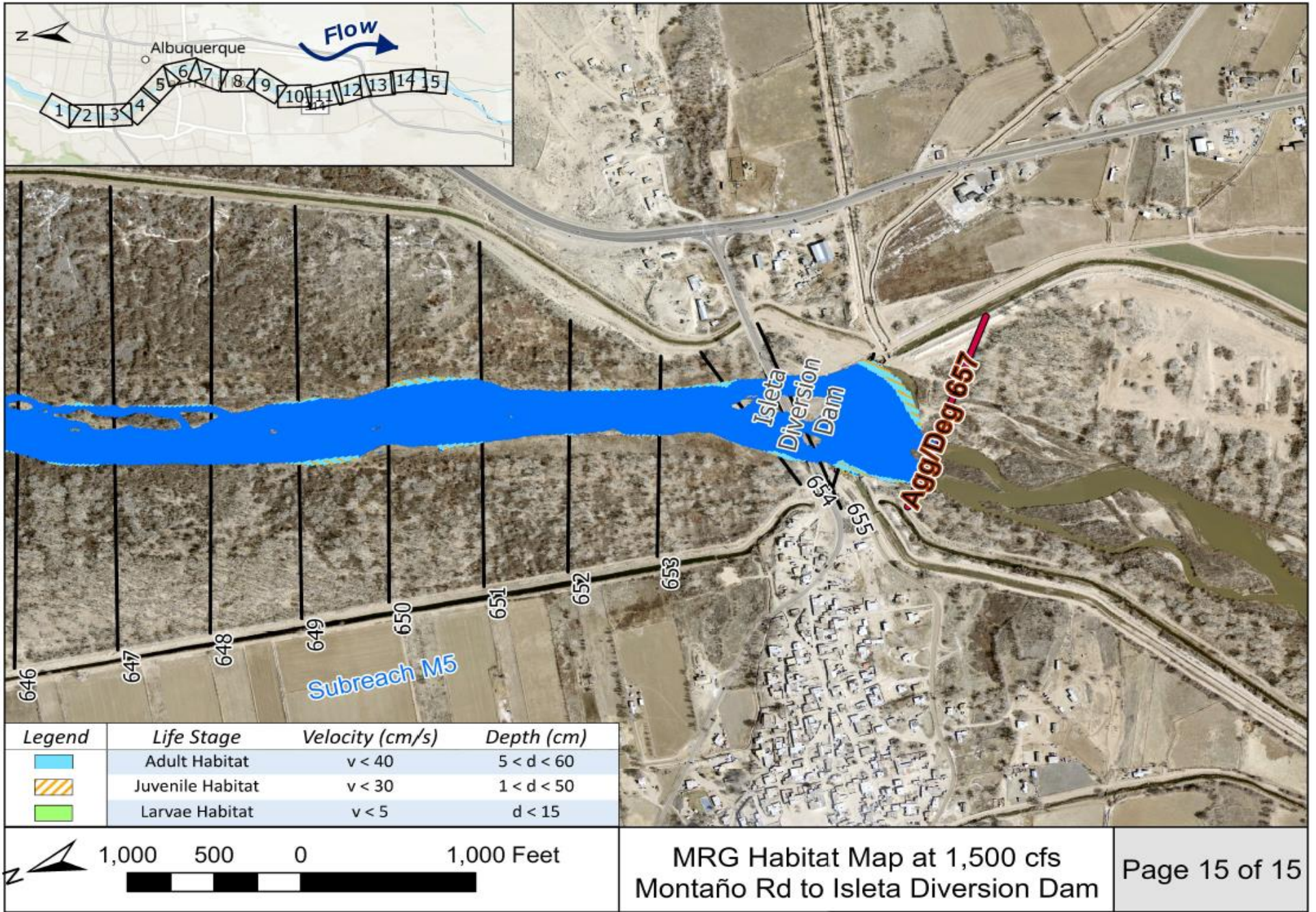


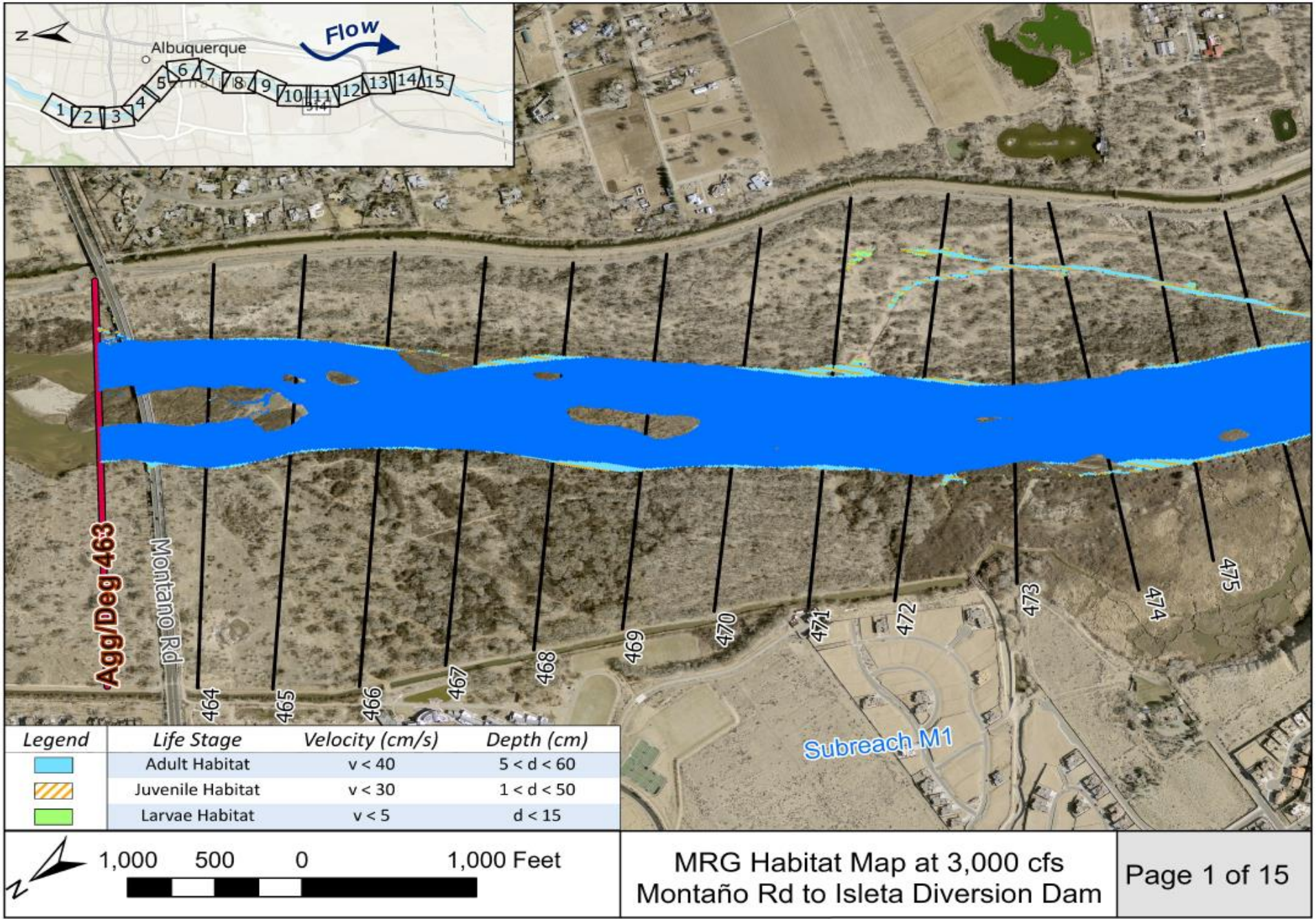


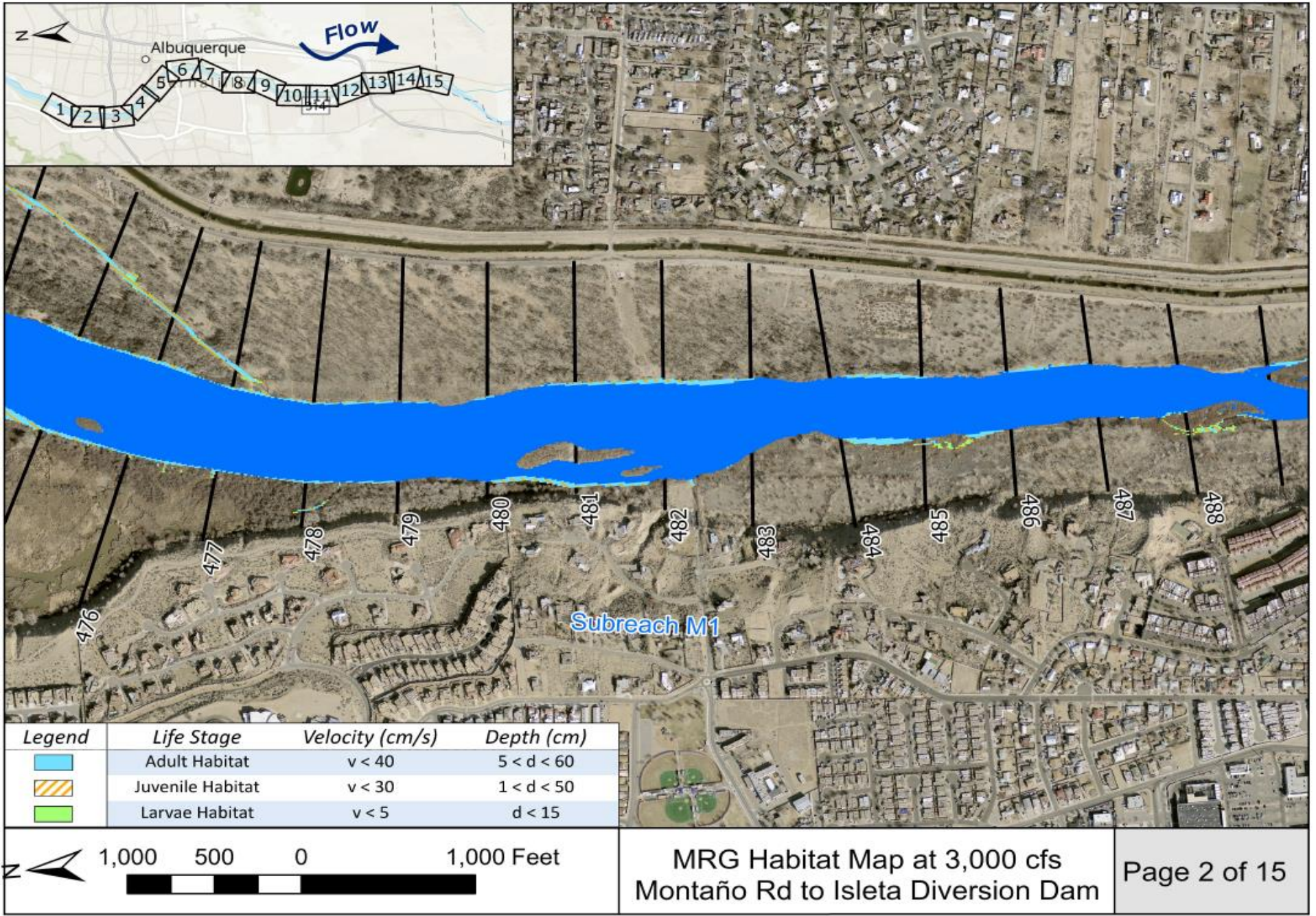


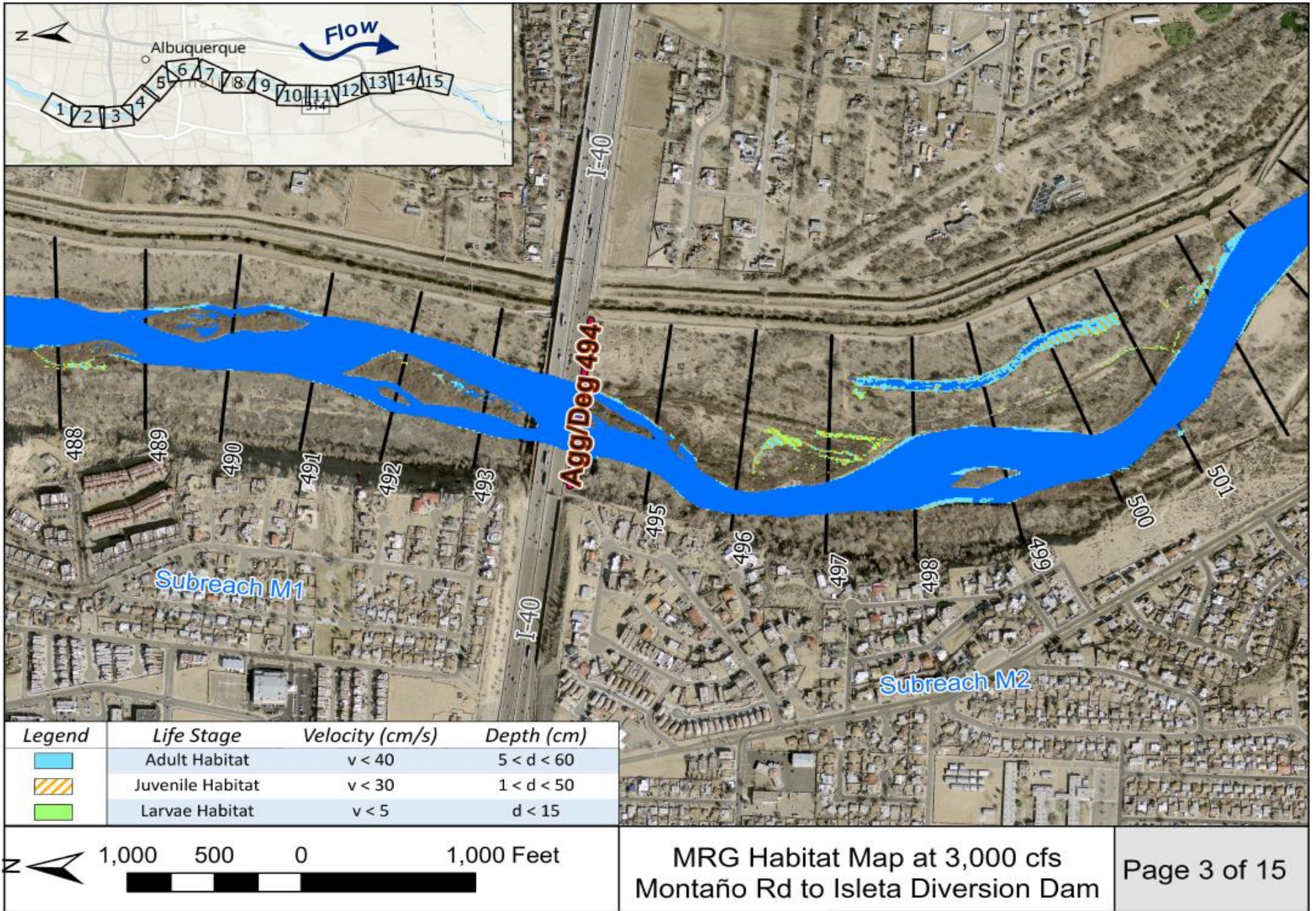


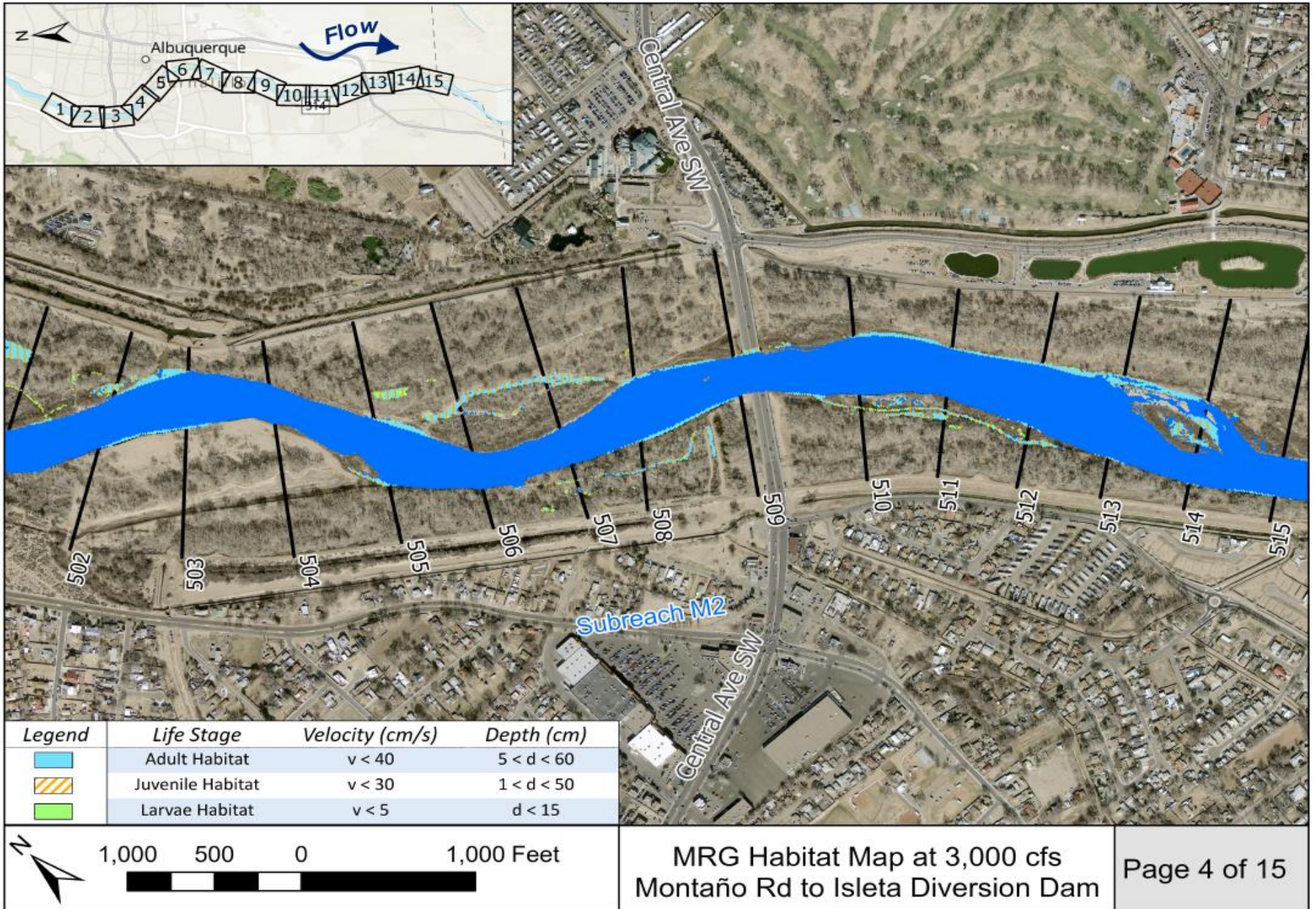


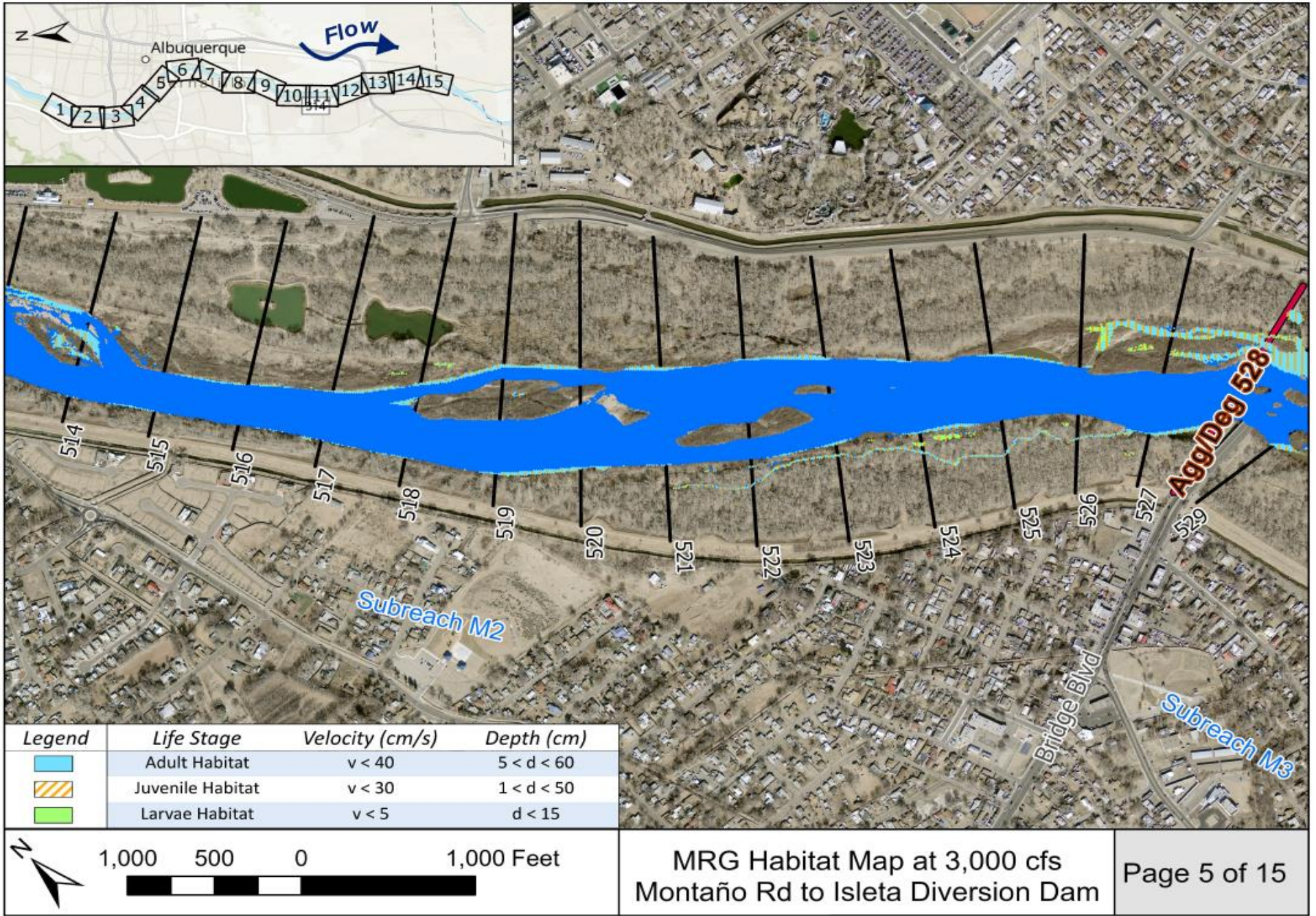


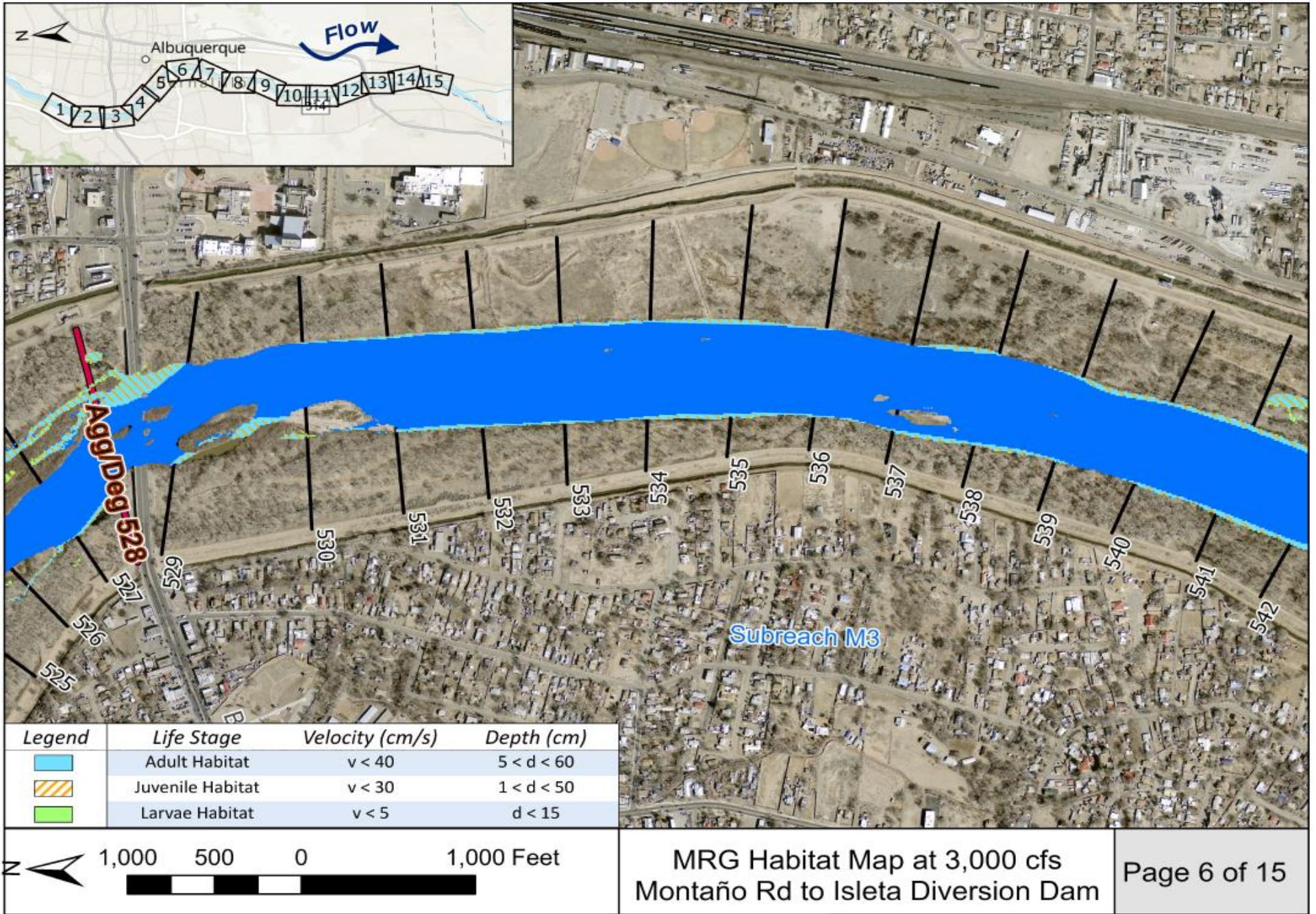


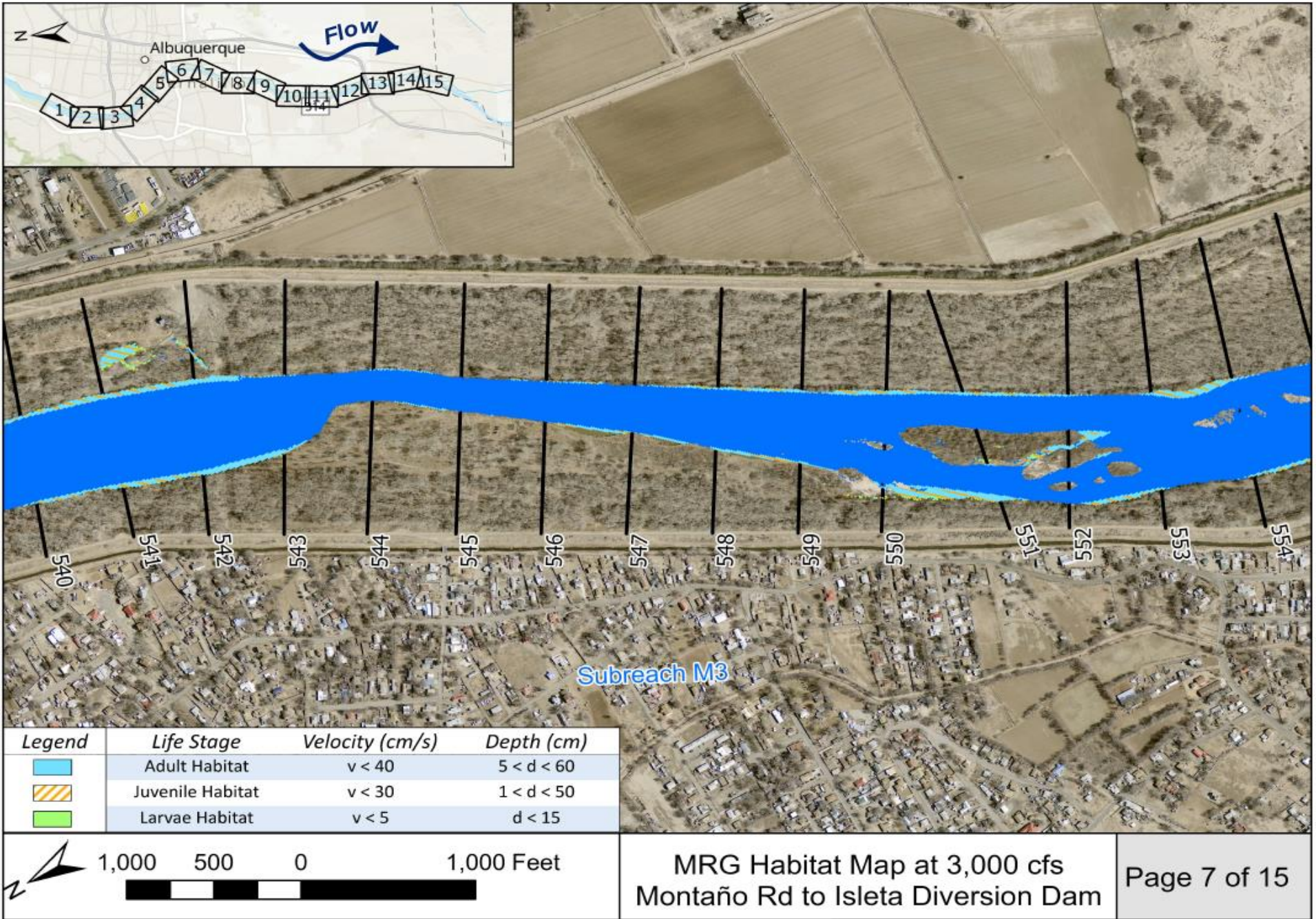


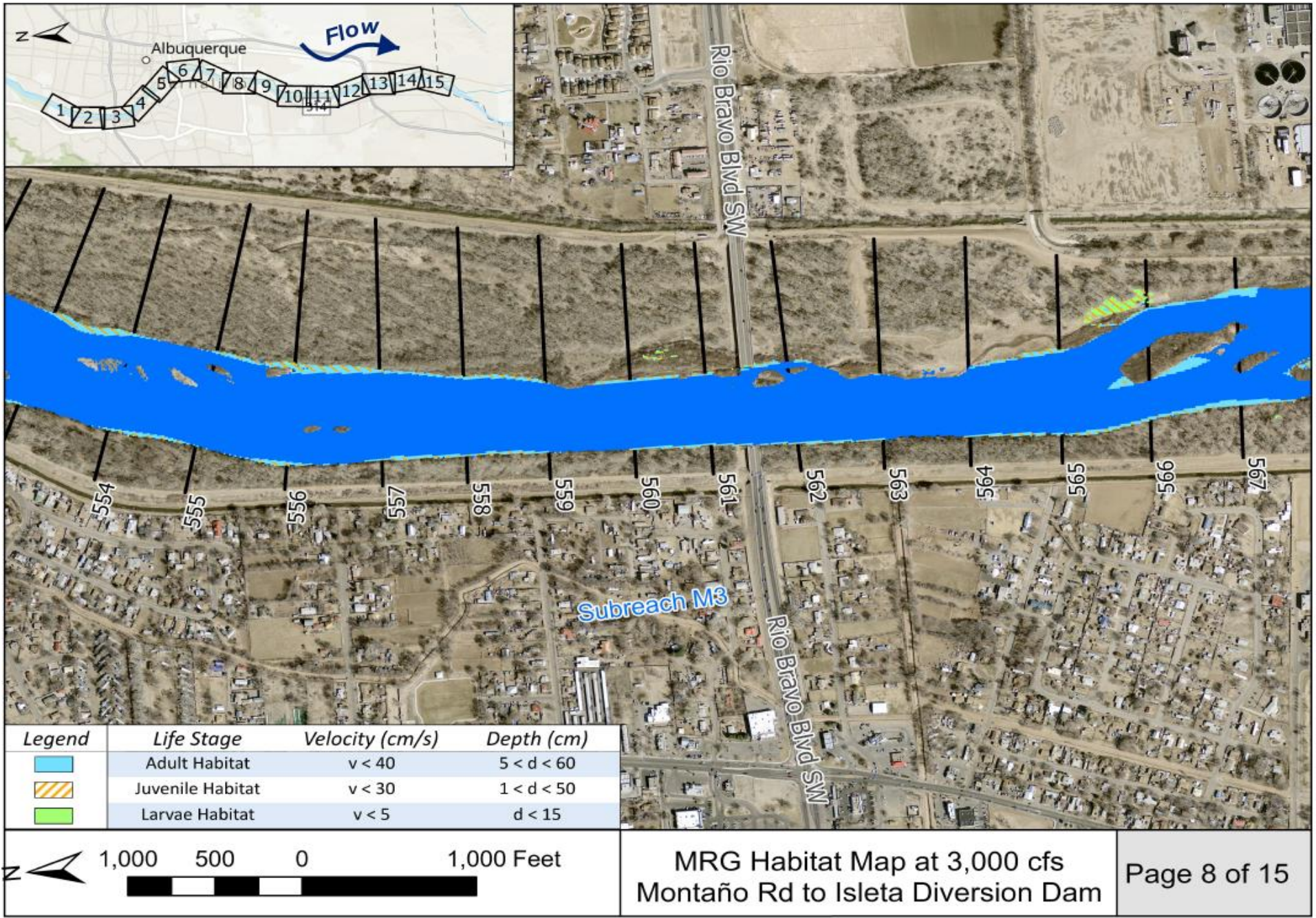


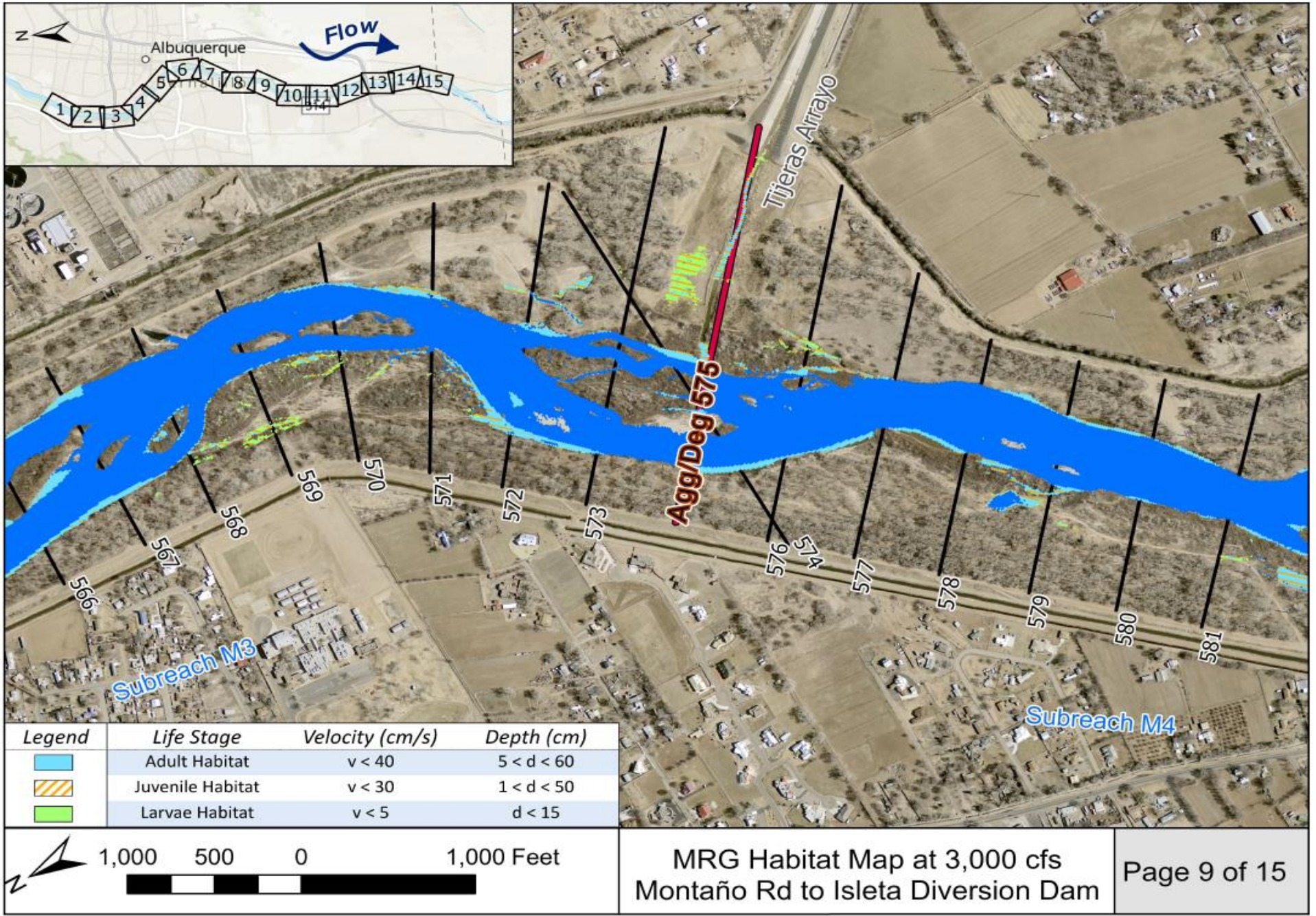




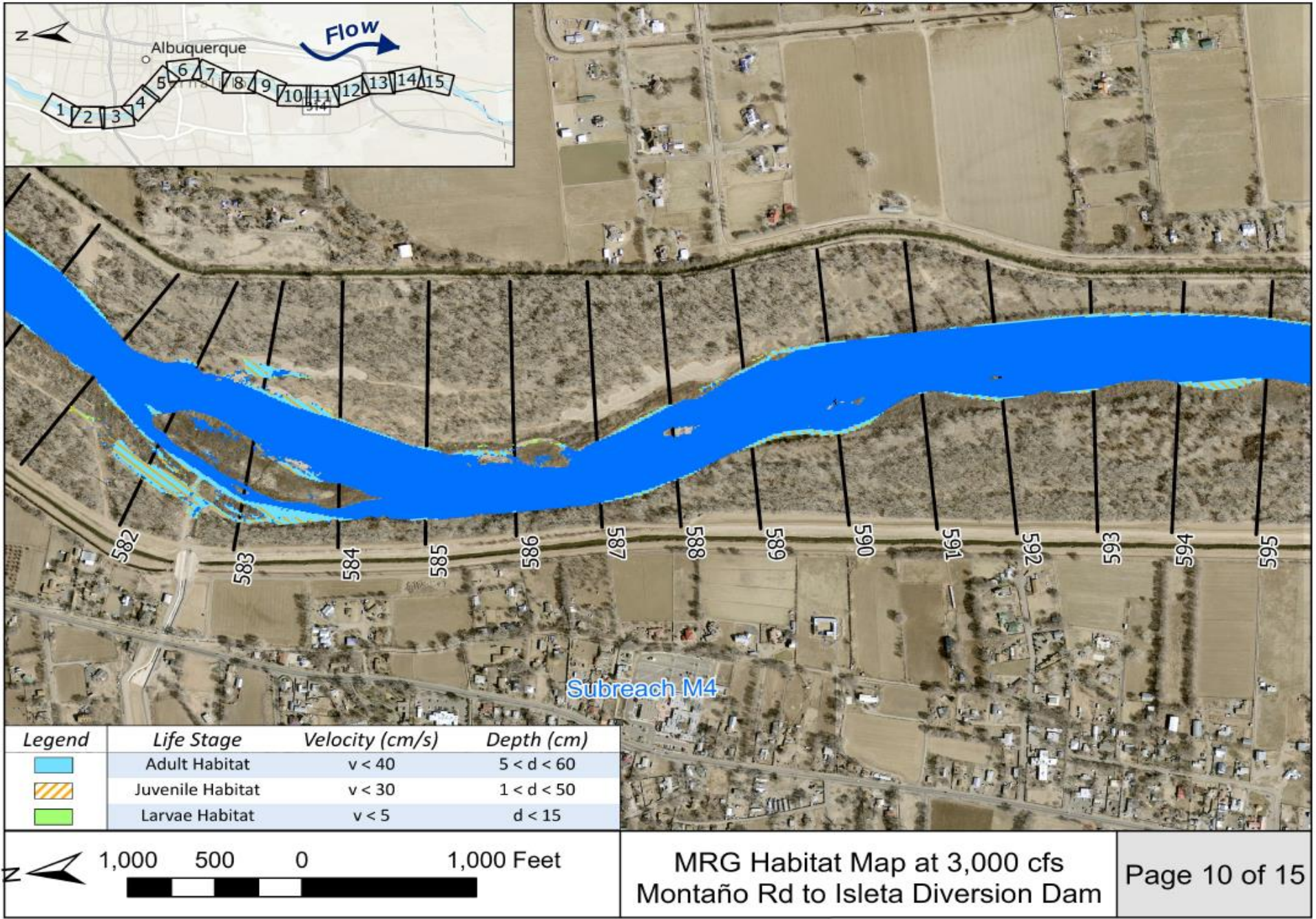


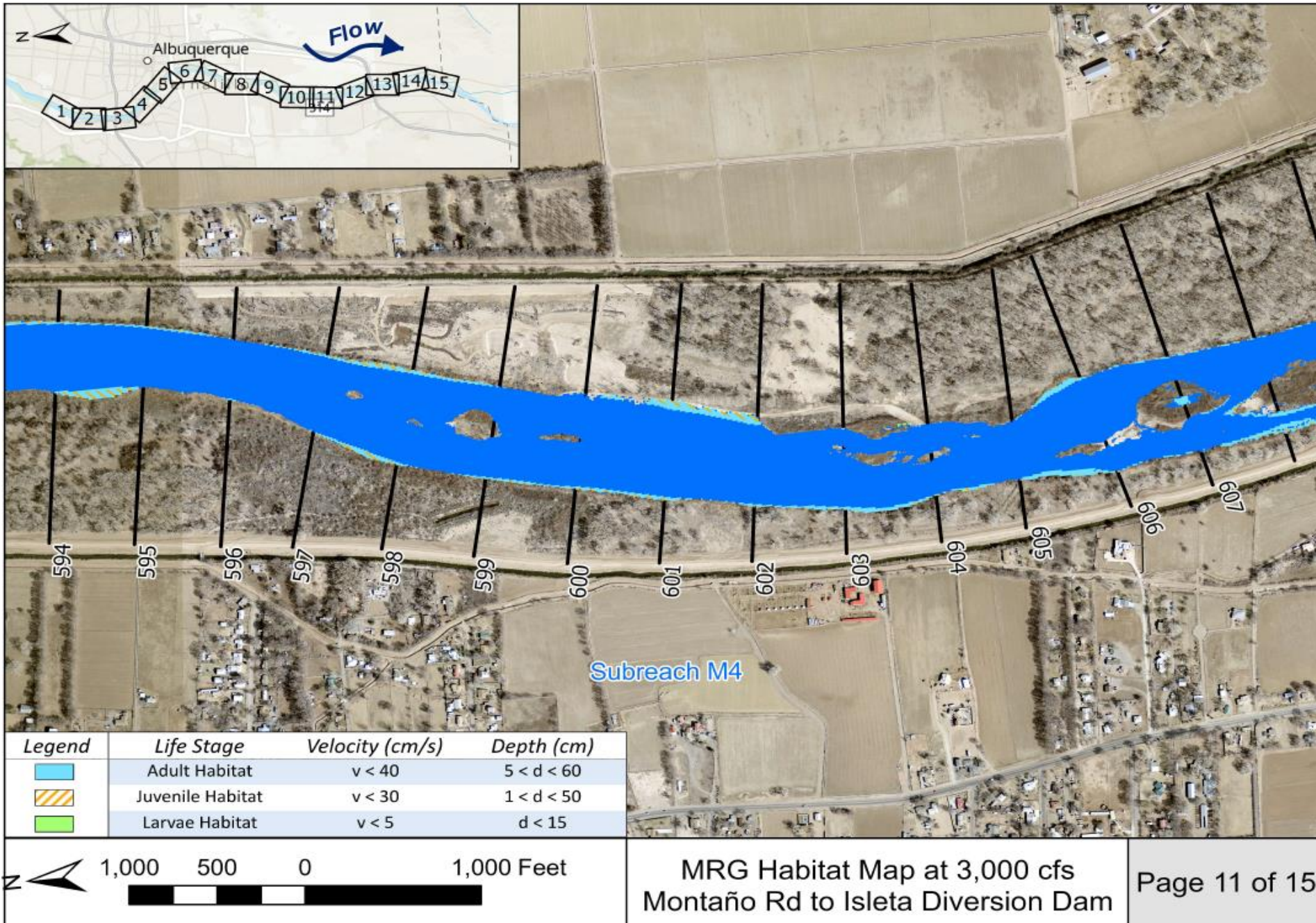


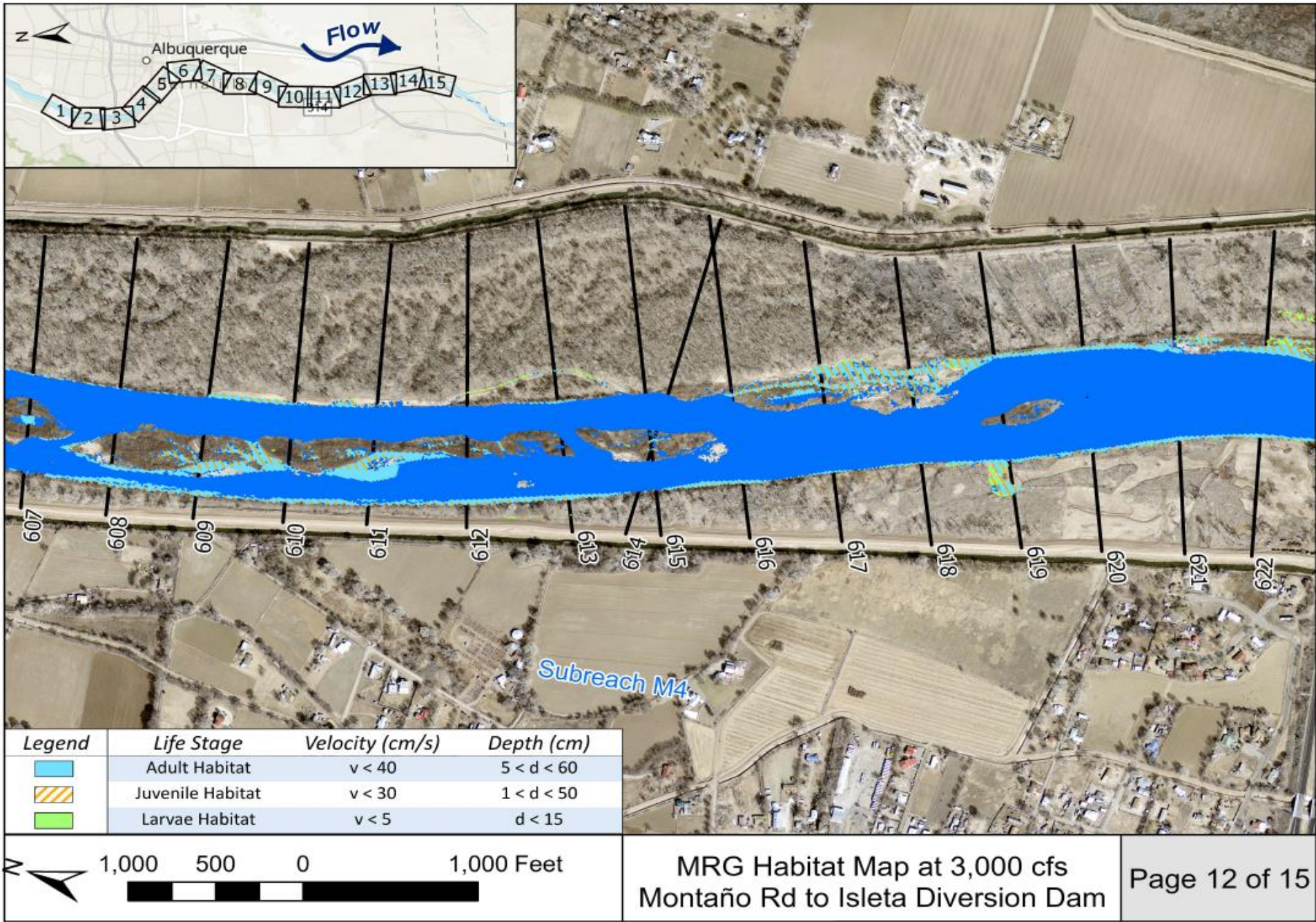


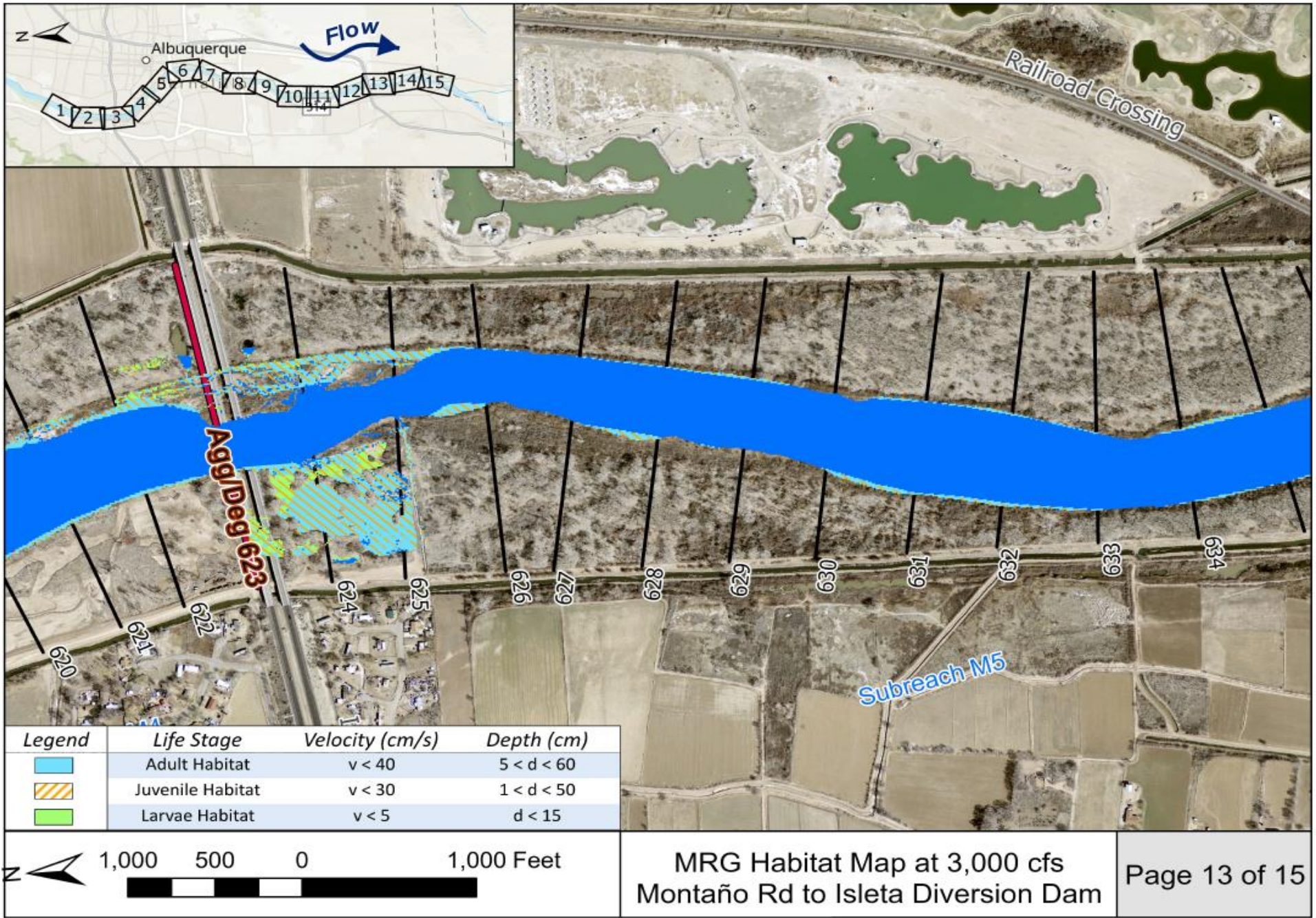


MRG Habitat Map at 3,000 cfs
Montaño Rd to Isleta Diversion Dam



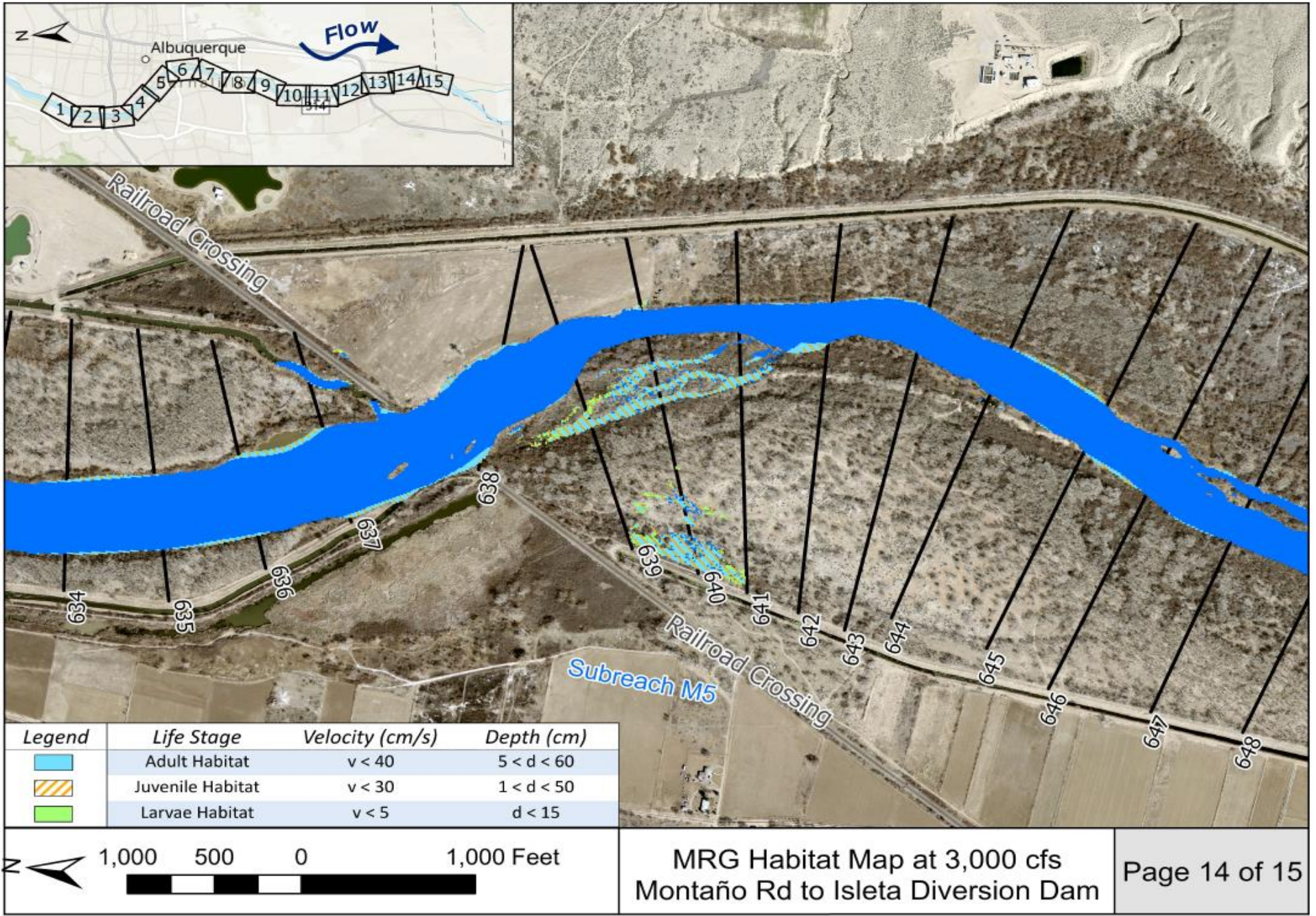


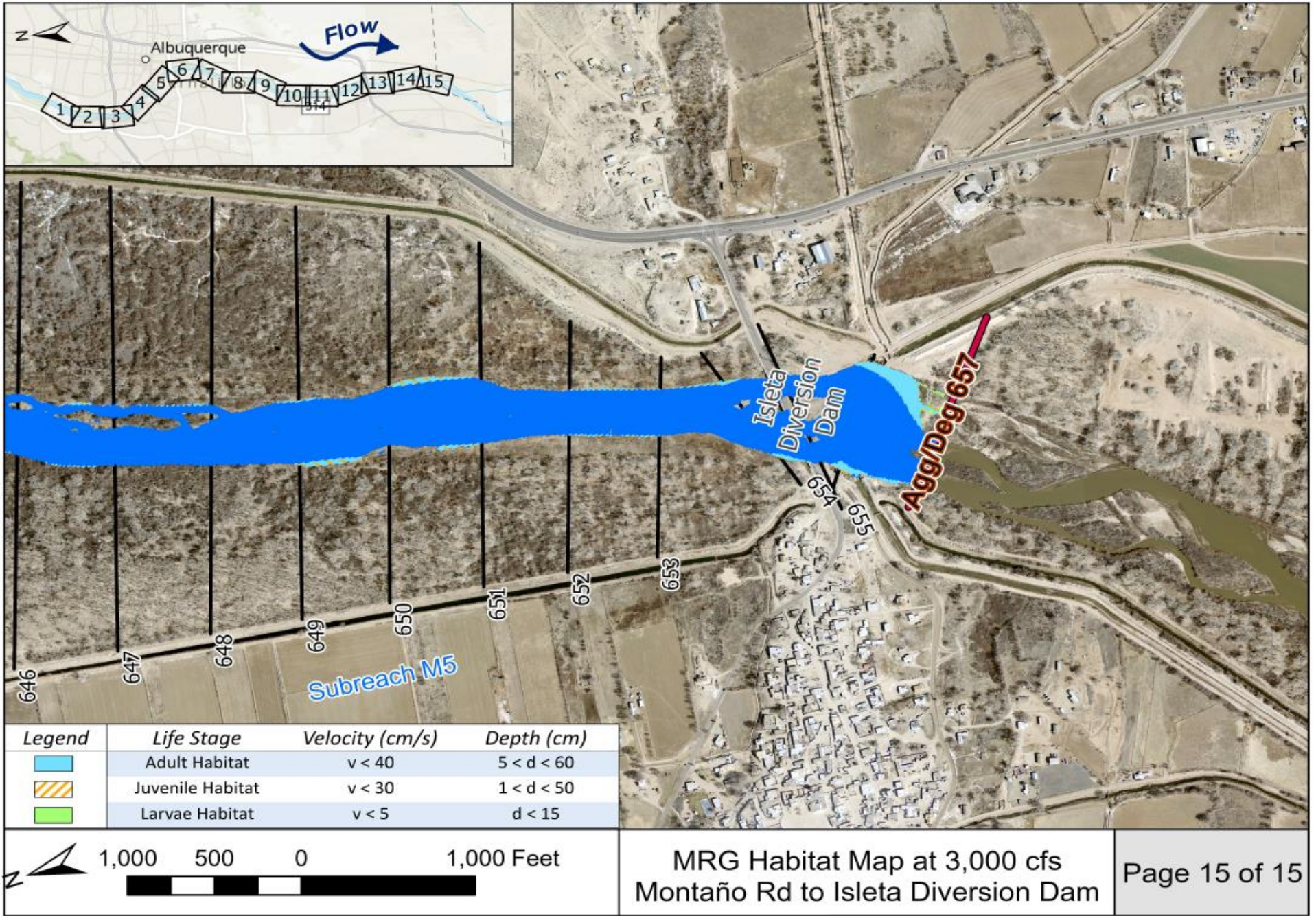


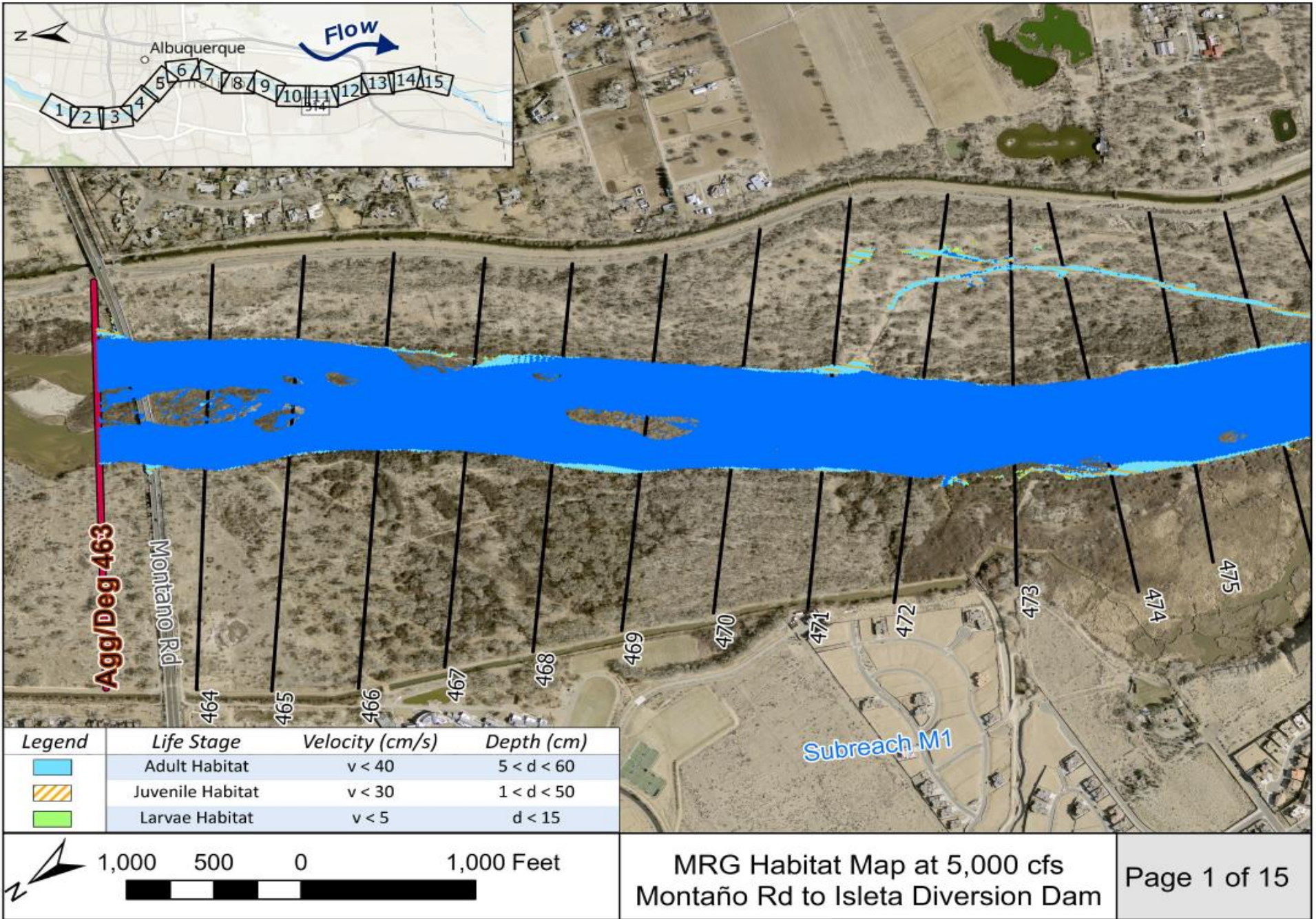


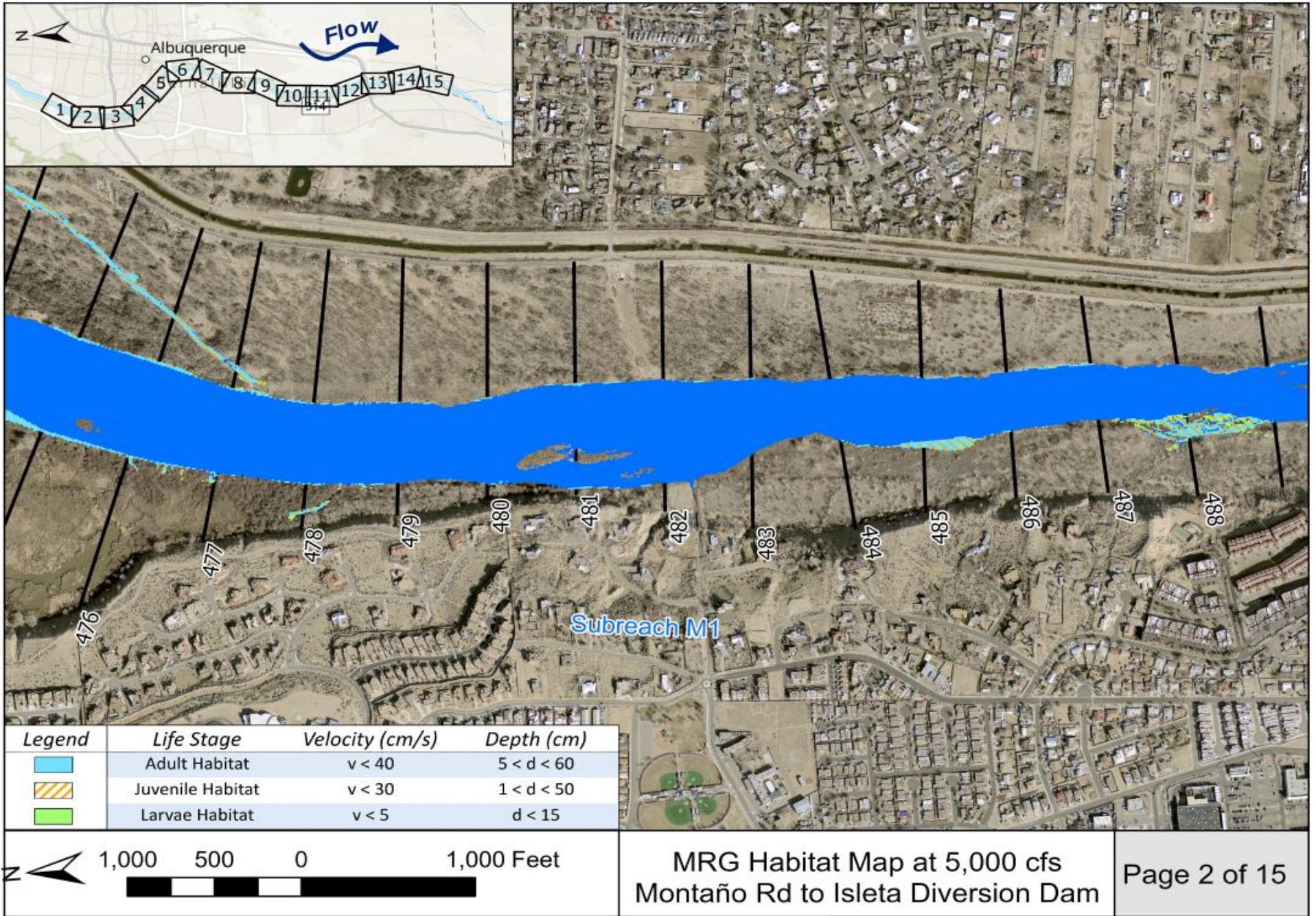
Legend	Life Stage	Velocity (cm/s)	Depth (cm)
	Adult Habitat	$v < 40$	$5 < d < 60$
	Juvenile Habitat	$v < 30$	$1 < d < 50$
	Larvae Habitat	$v < 5$	$d < 15$

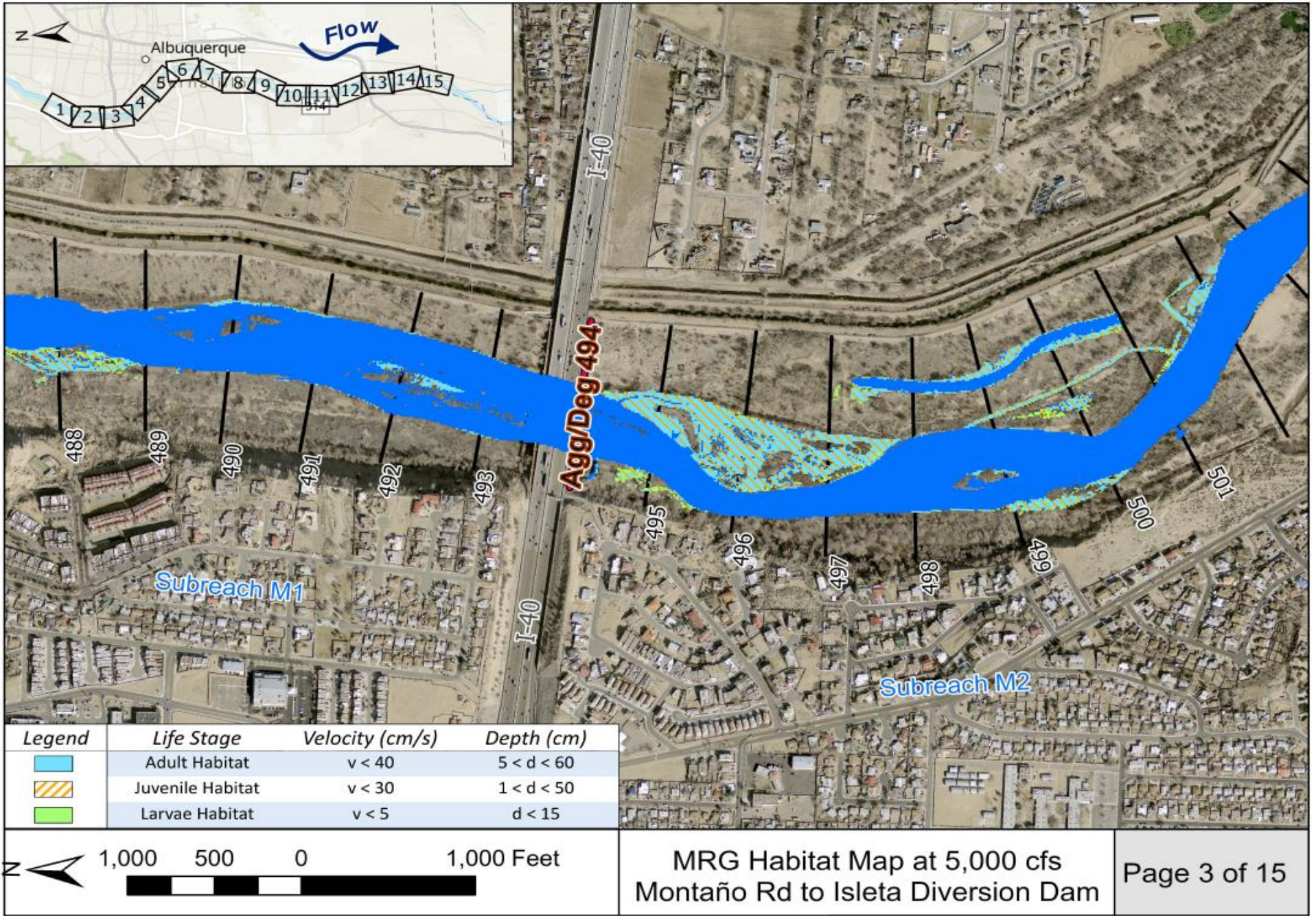
MRG Habitat Map at 3,000 cfs
Montaño Rd to Isleta Diversion Dam

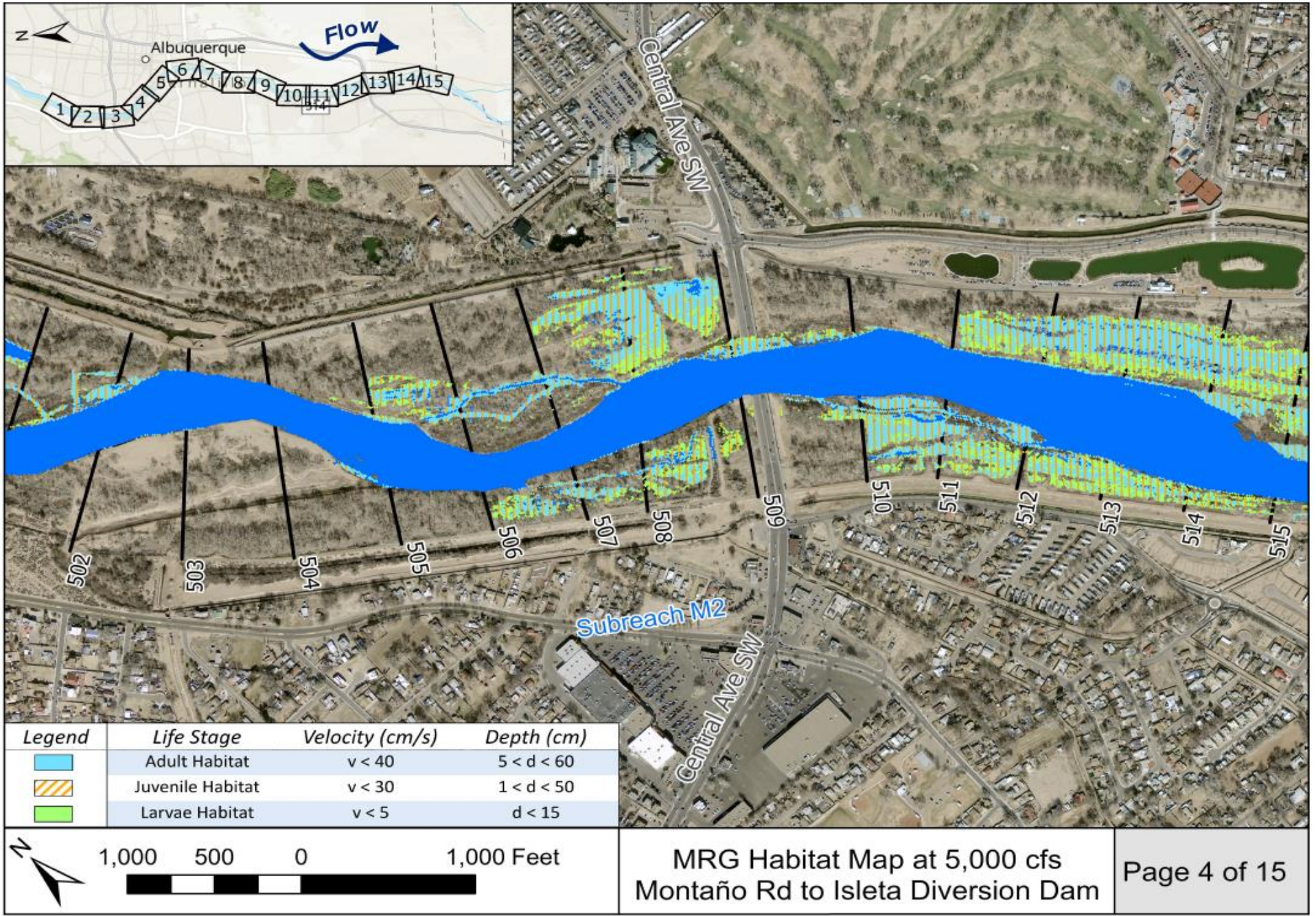


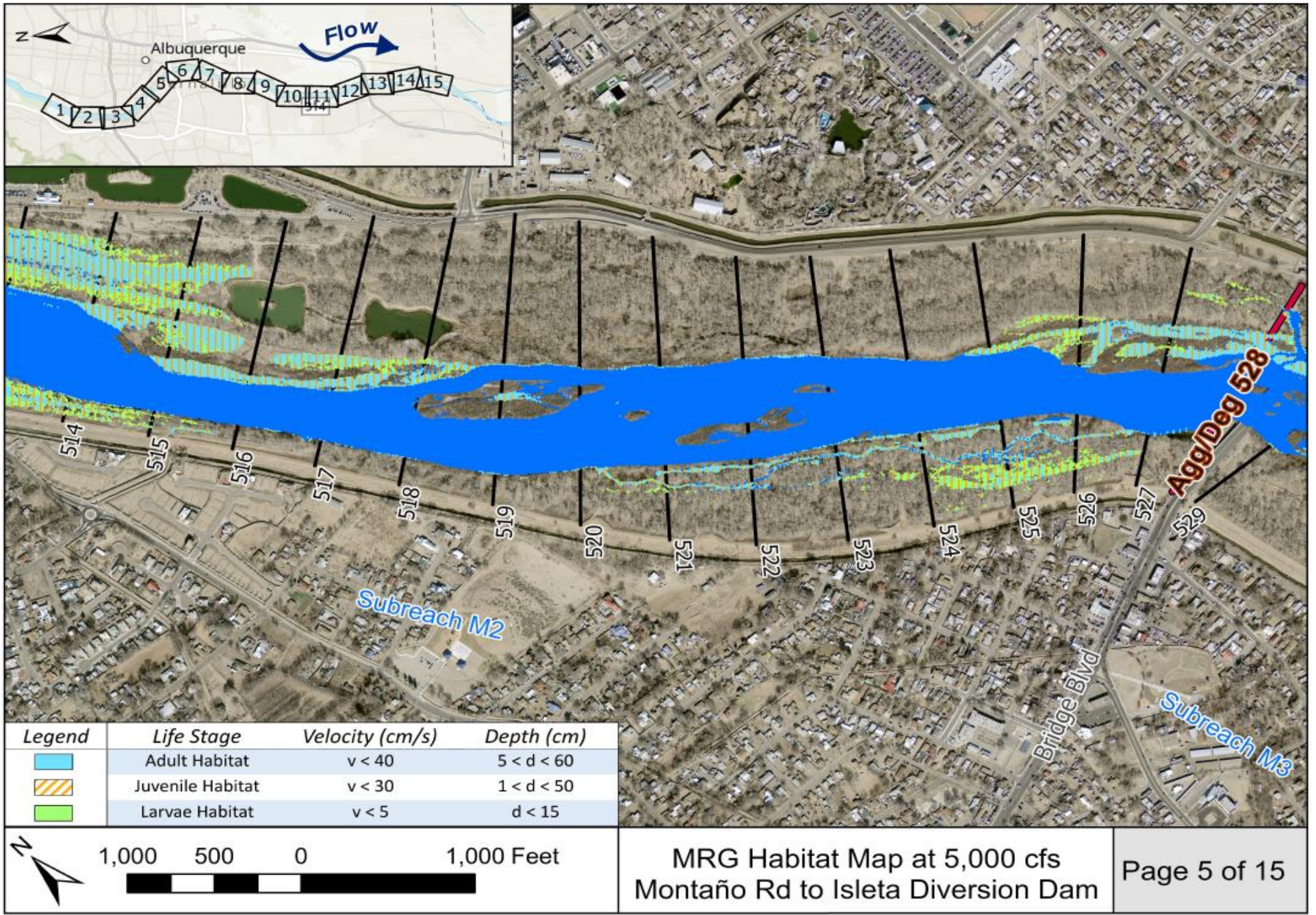


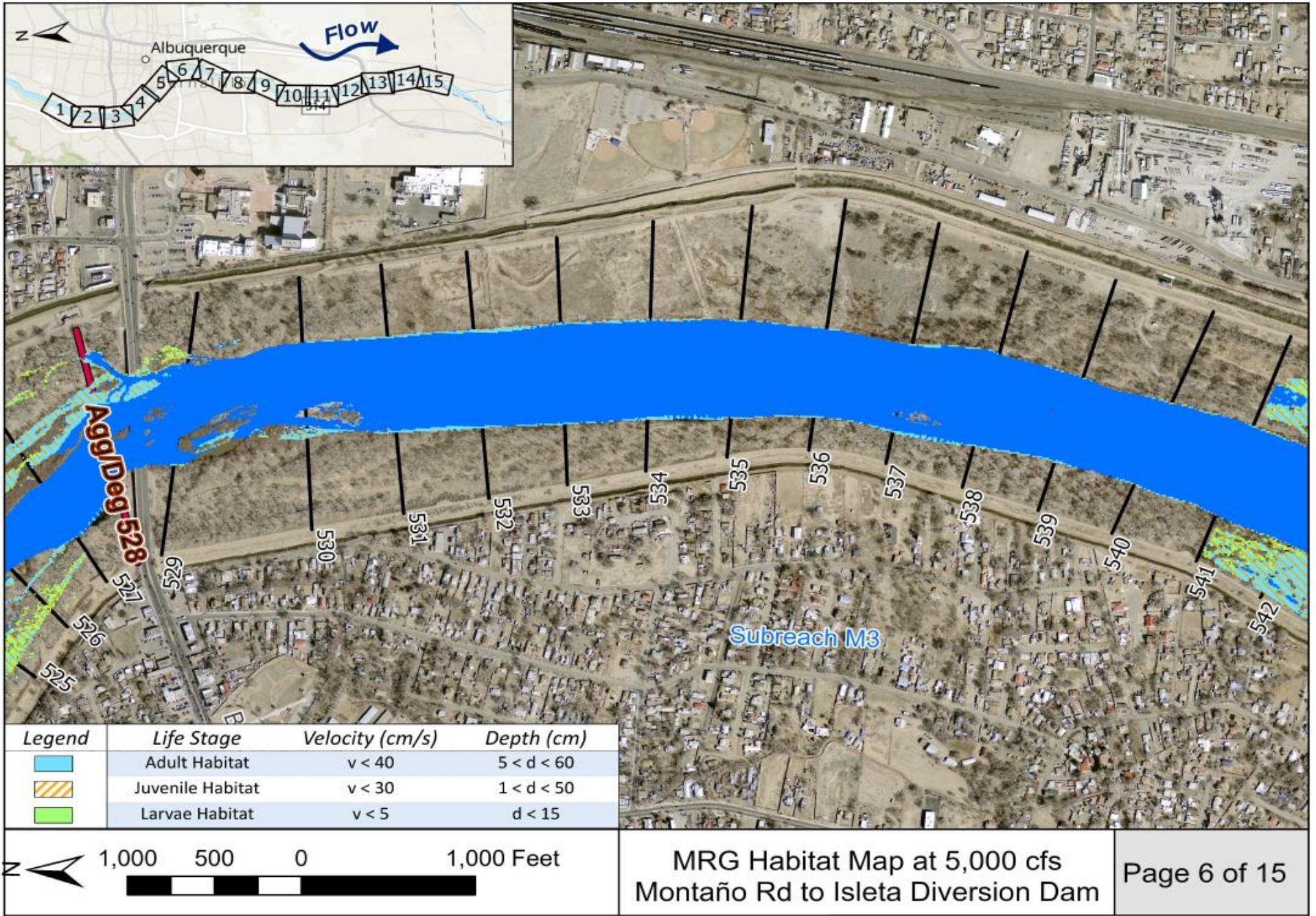


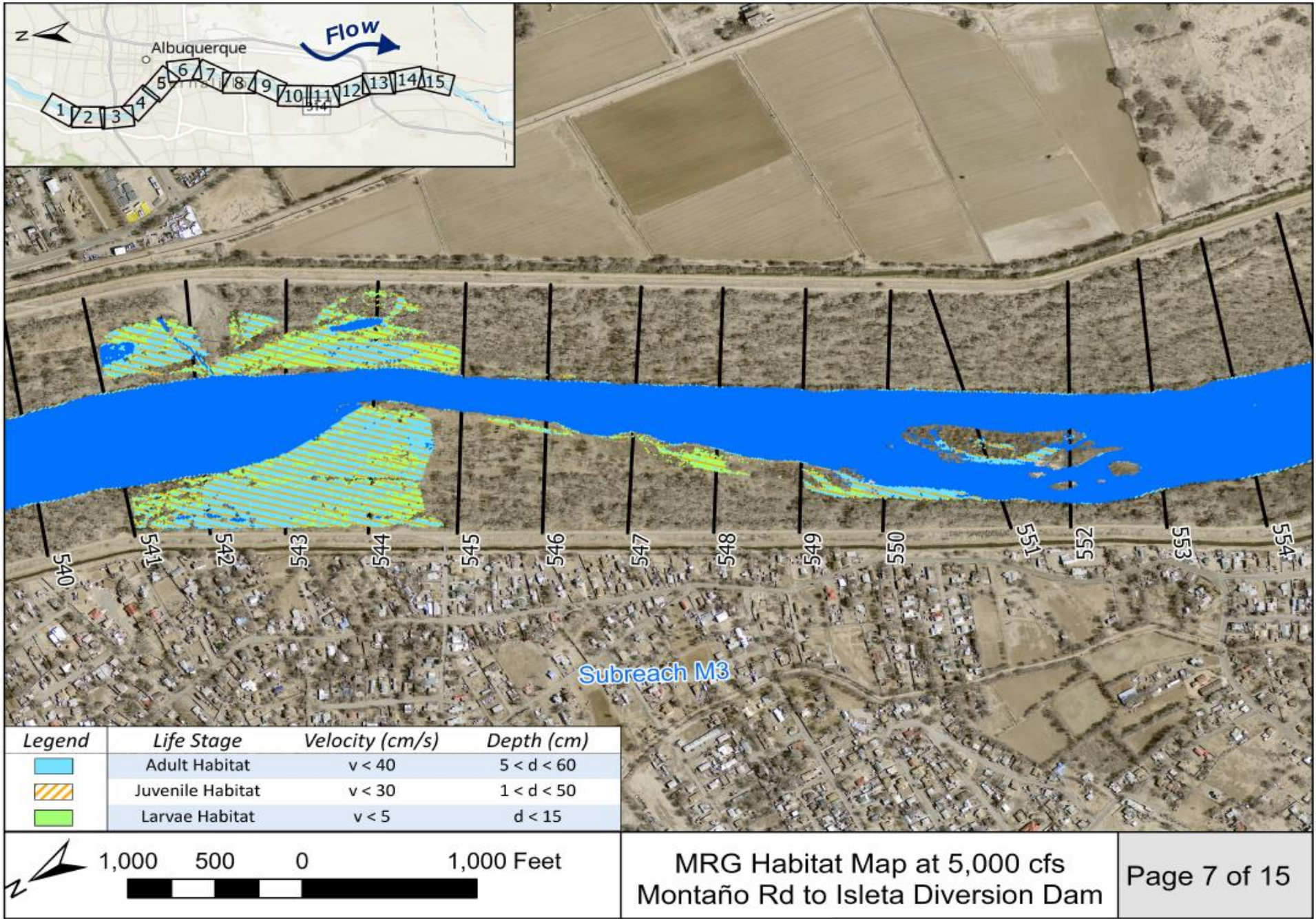


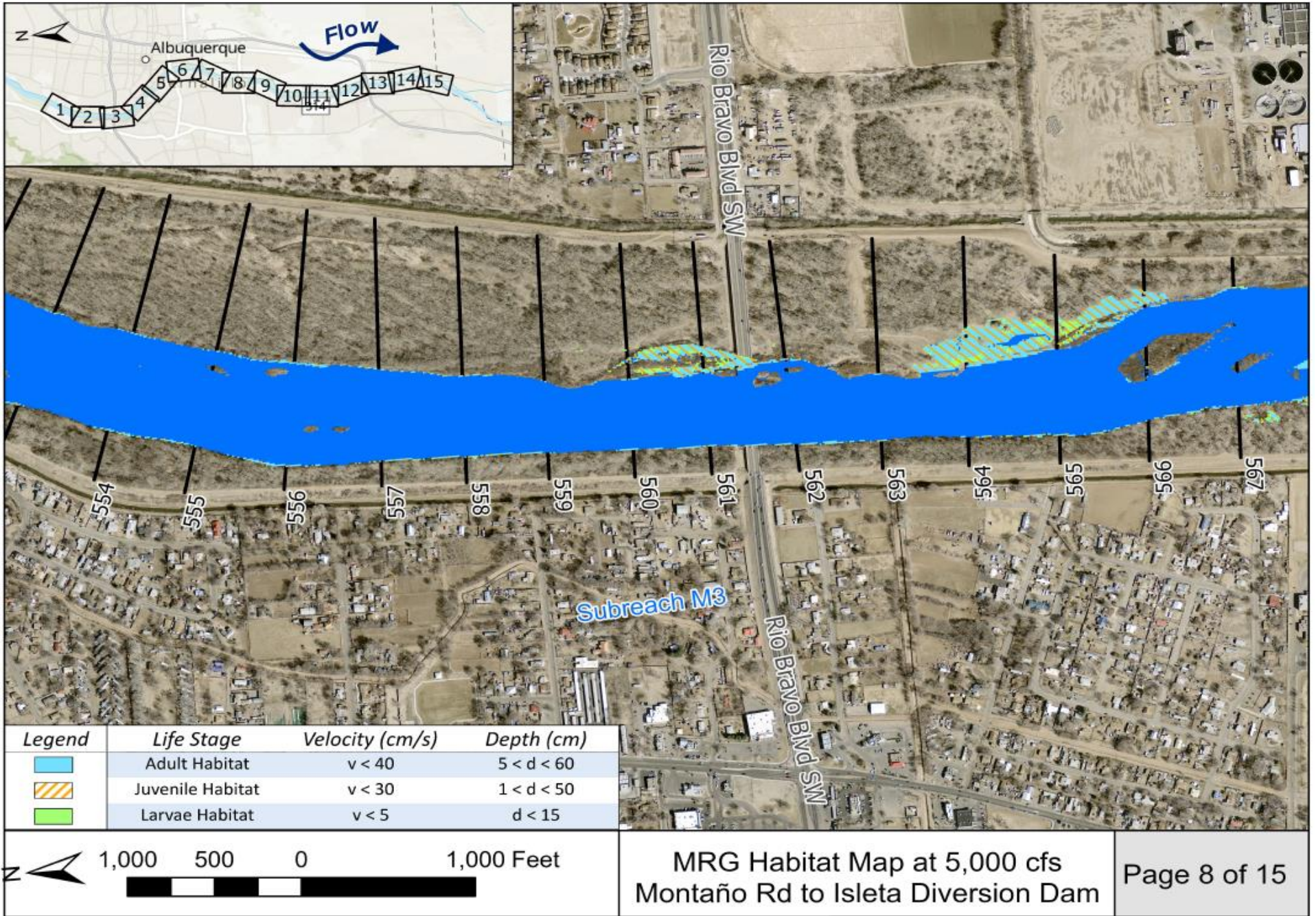


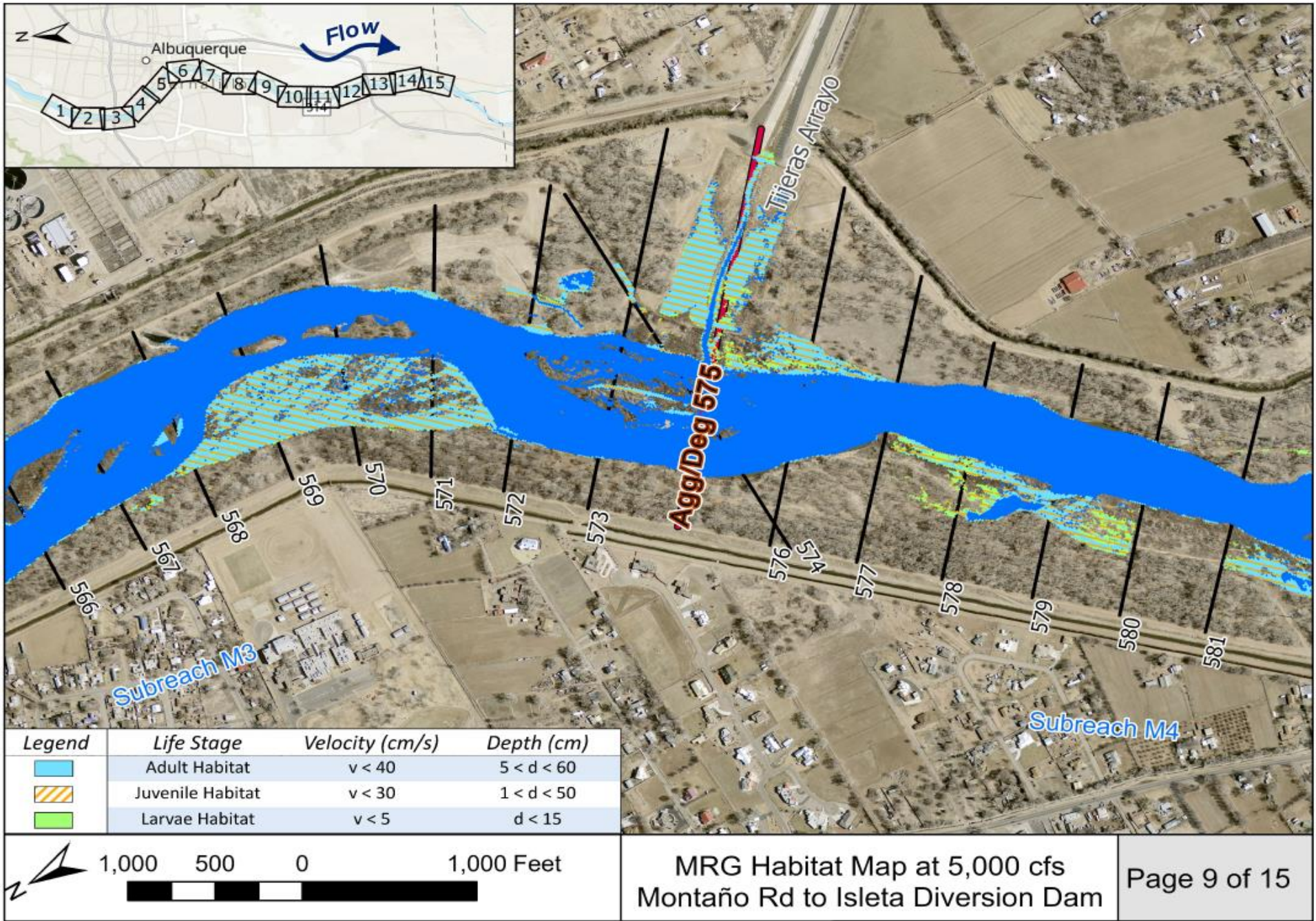


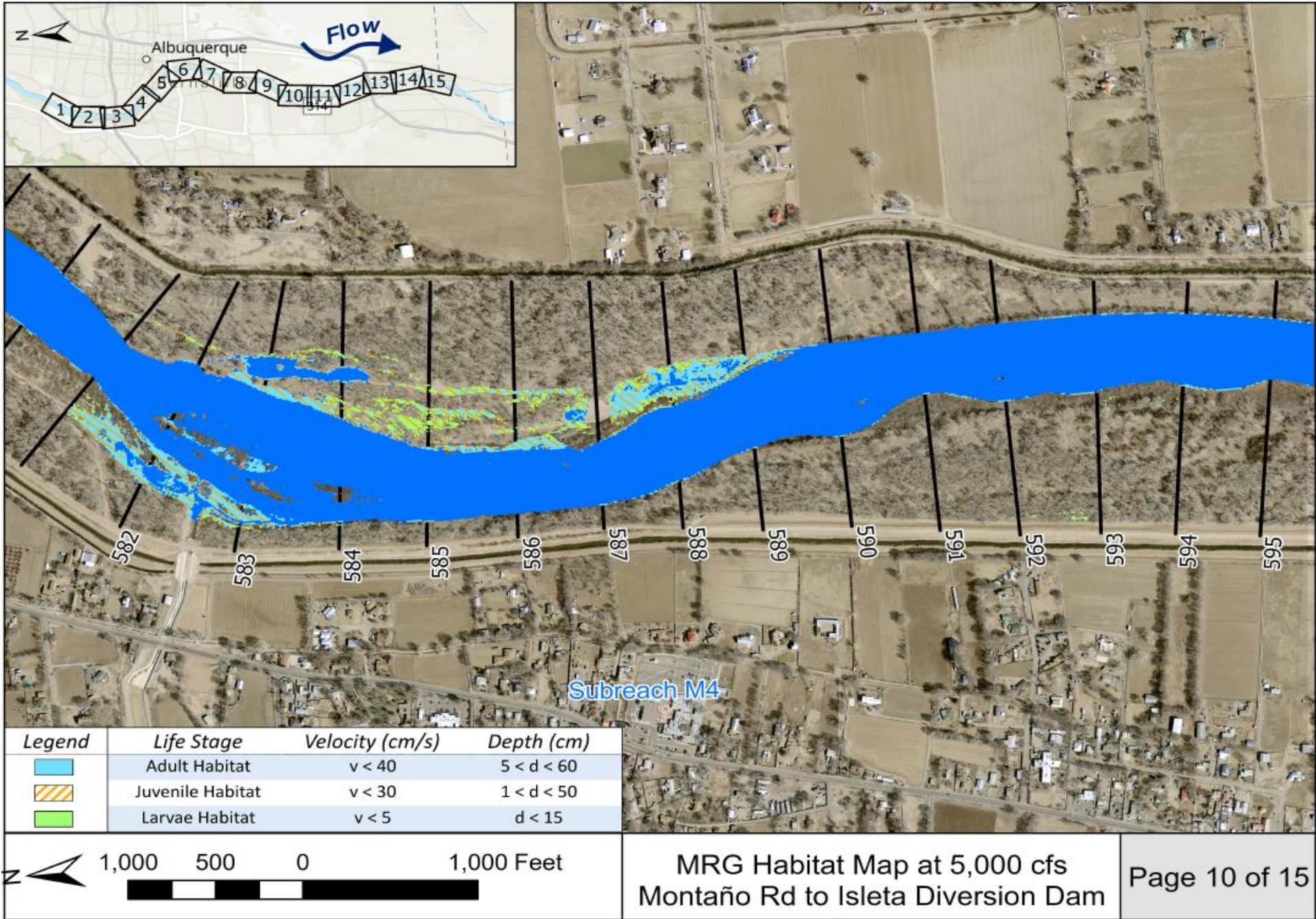


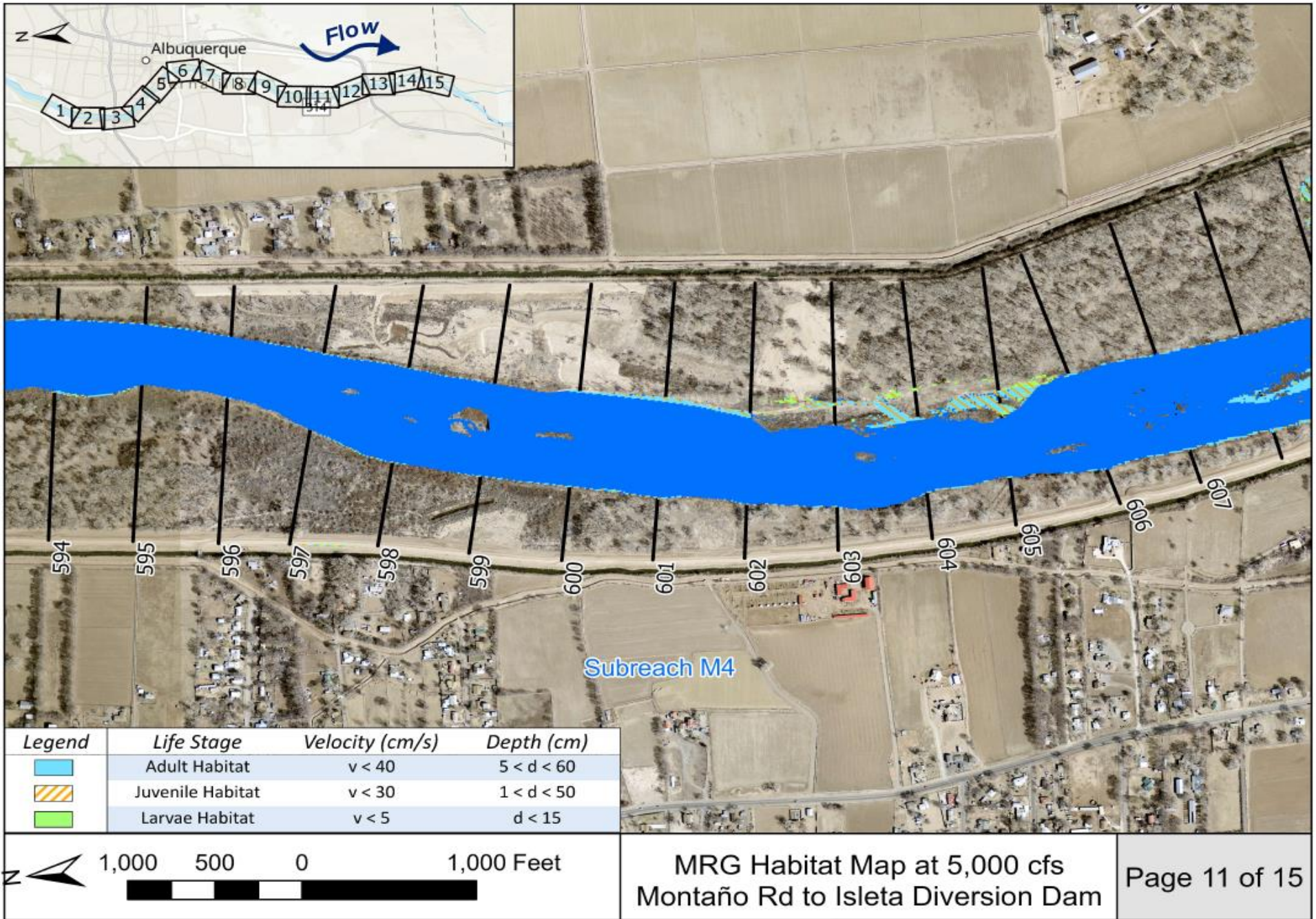


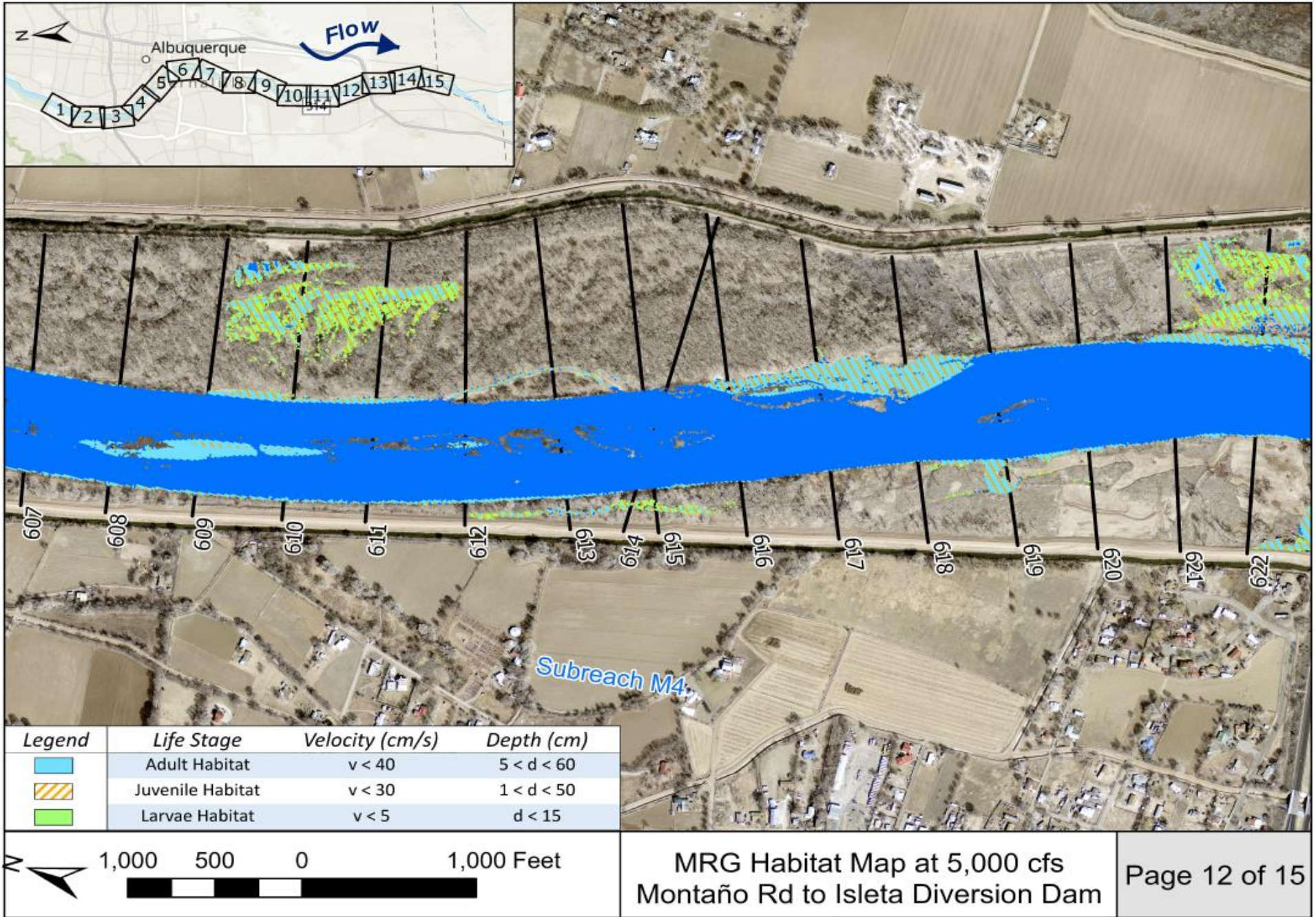


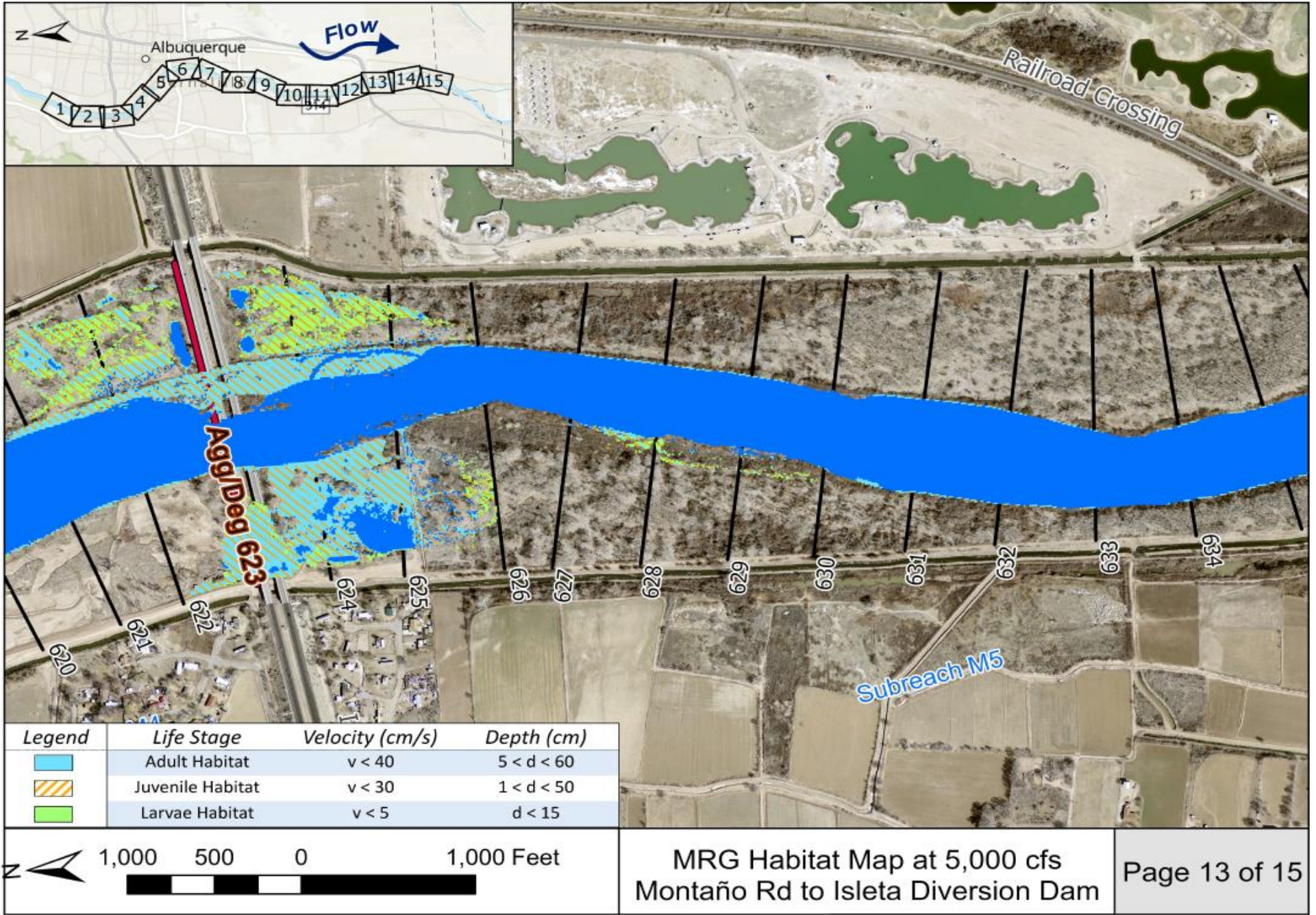


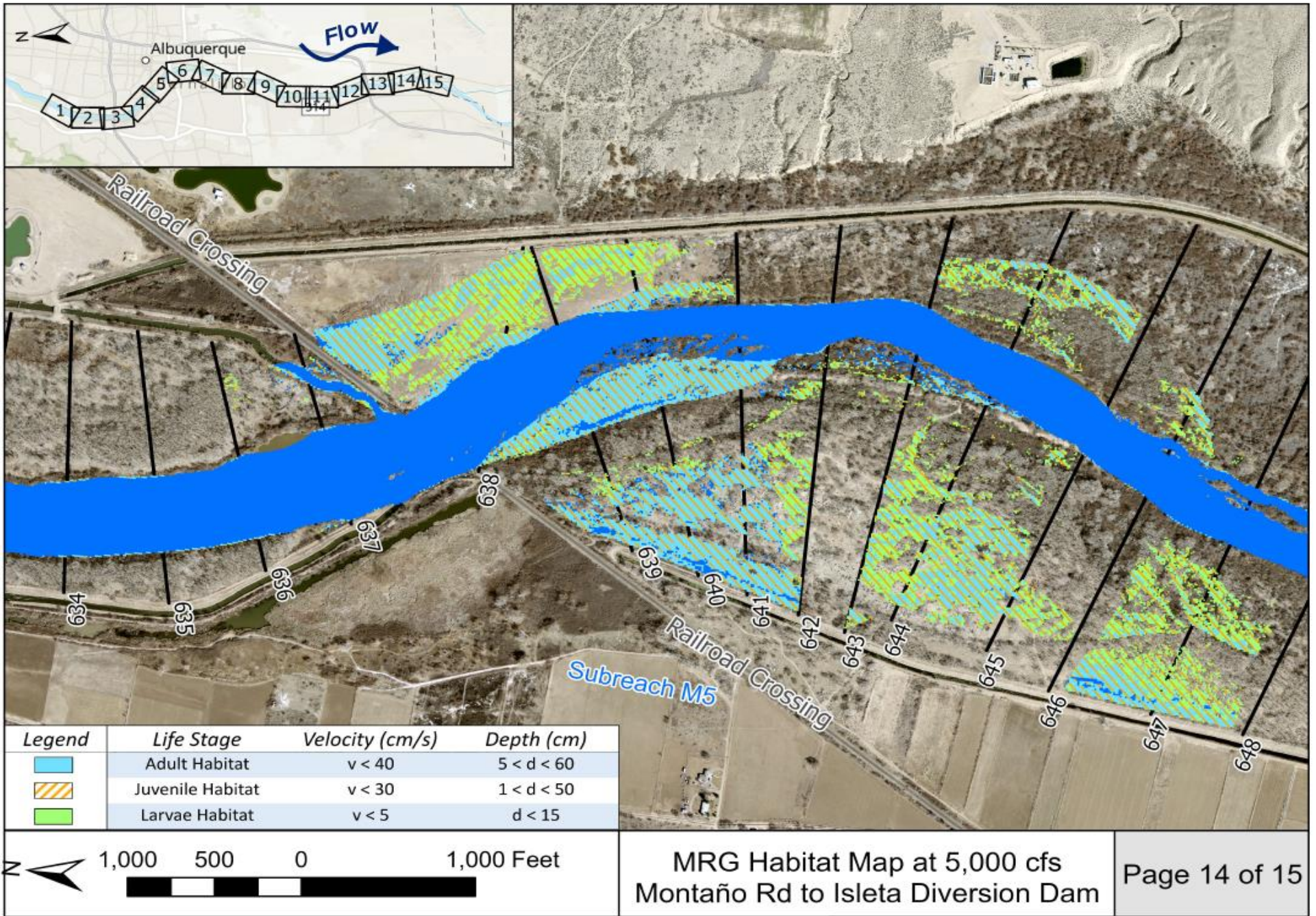




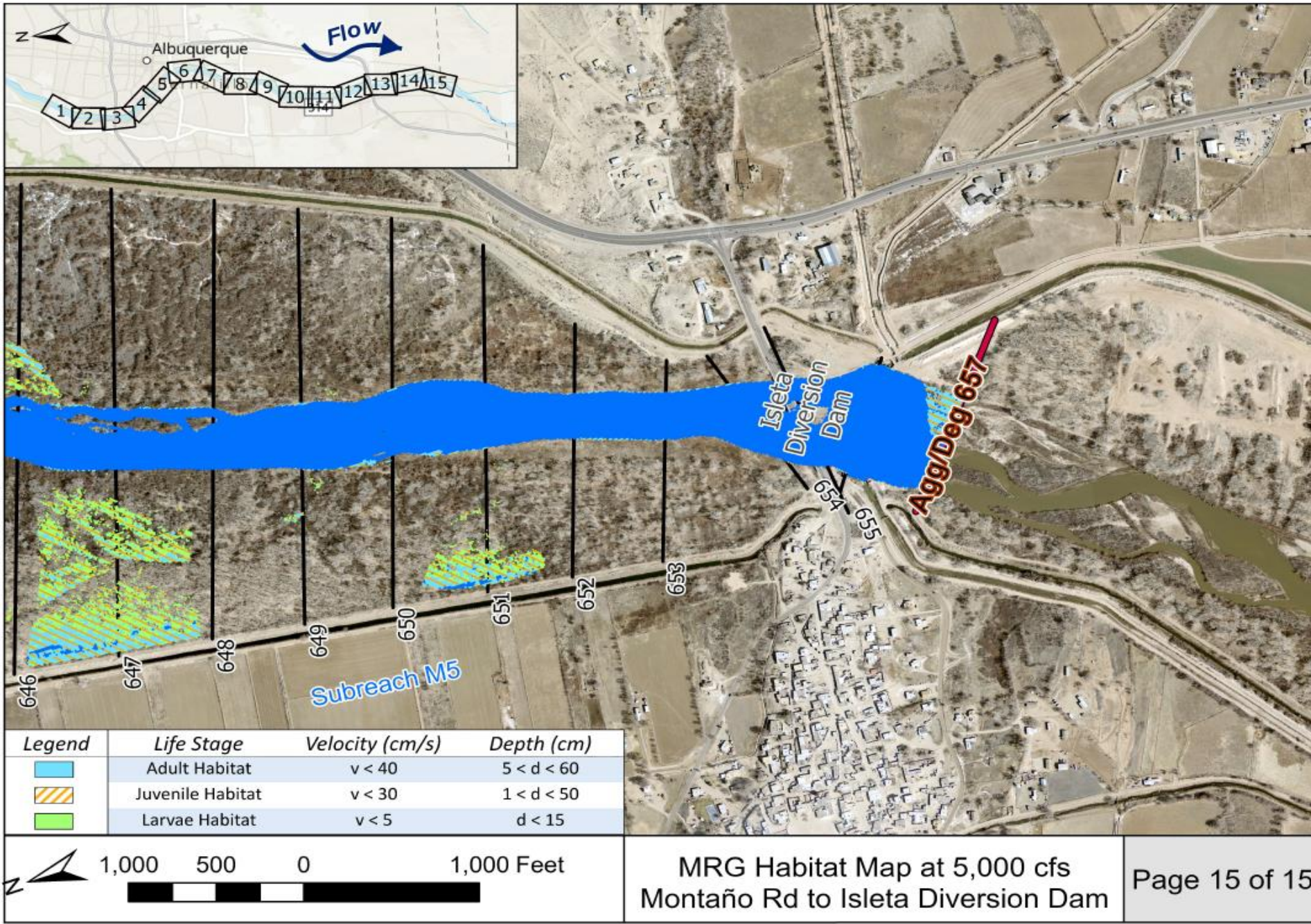






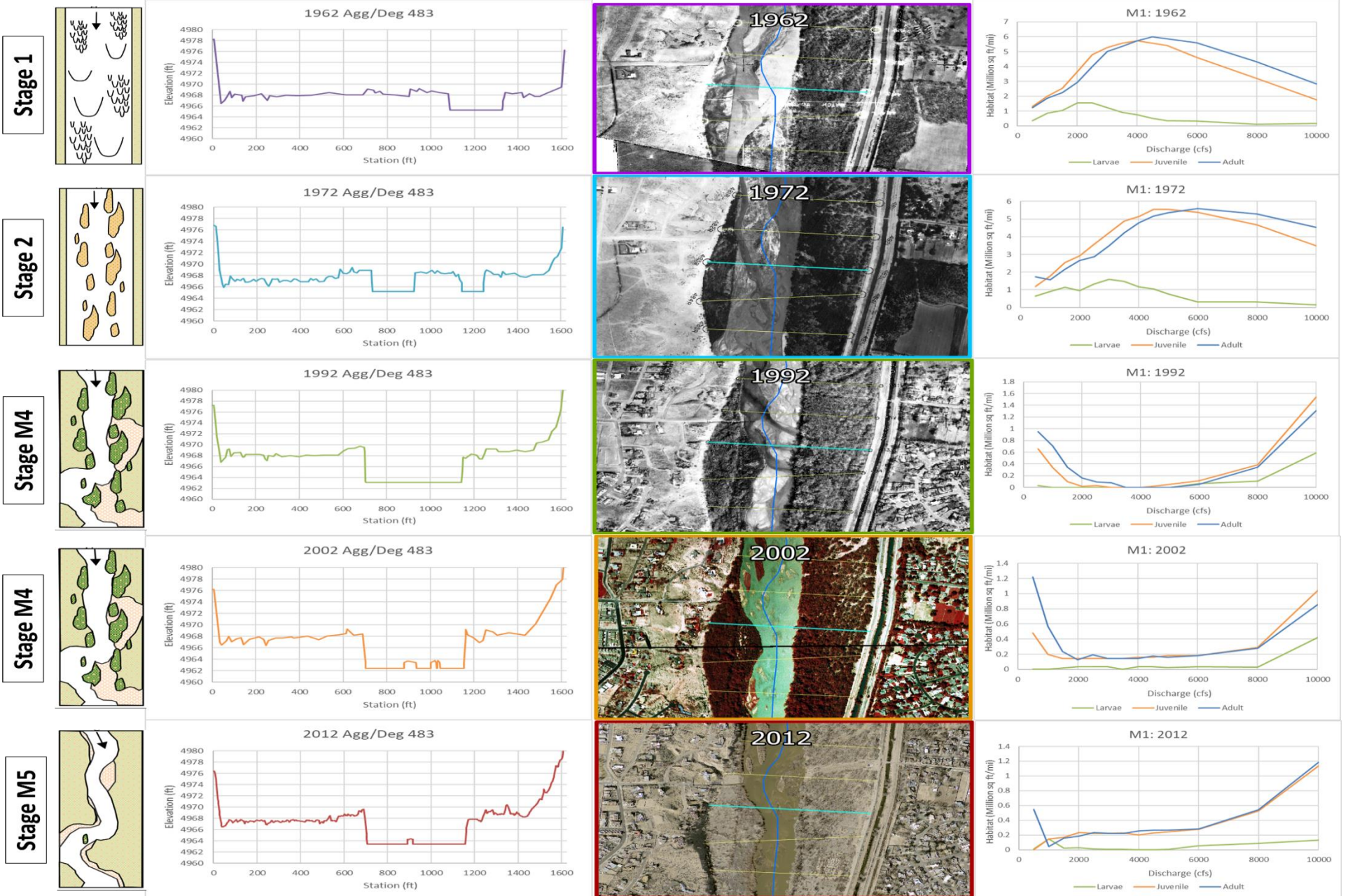


MRG Habitat Map at 5,000 cfs
Montaño Rd to Isleta Diversion Dam



Appendix F

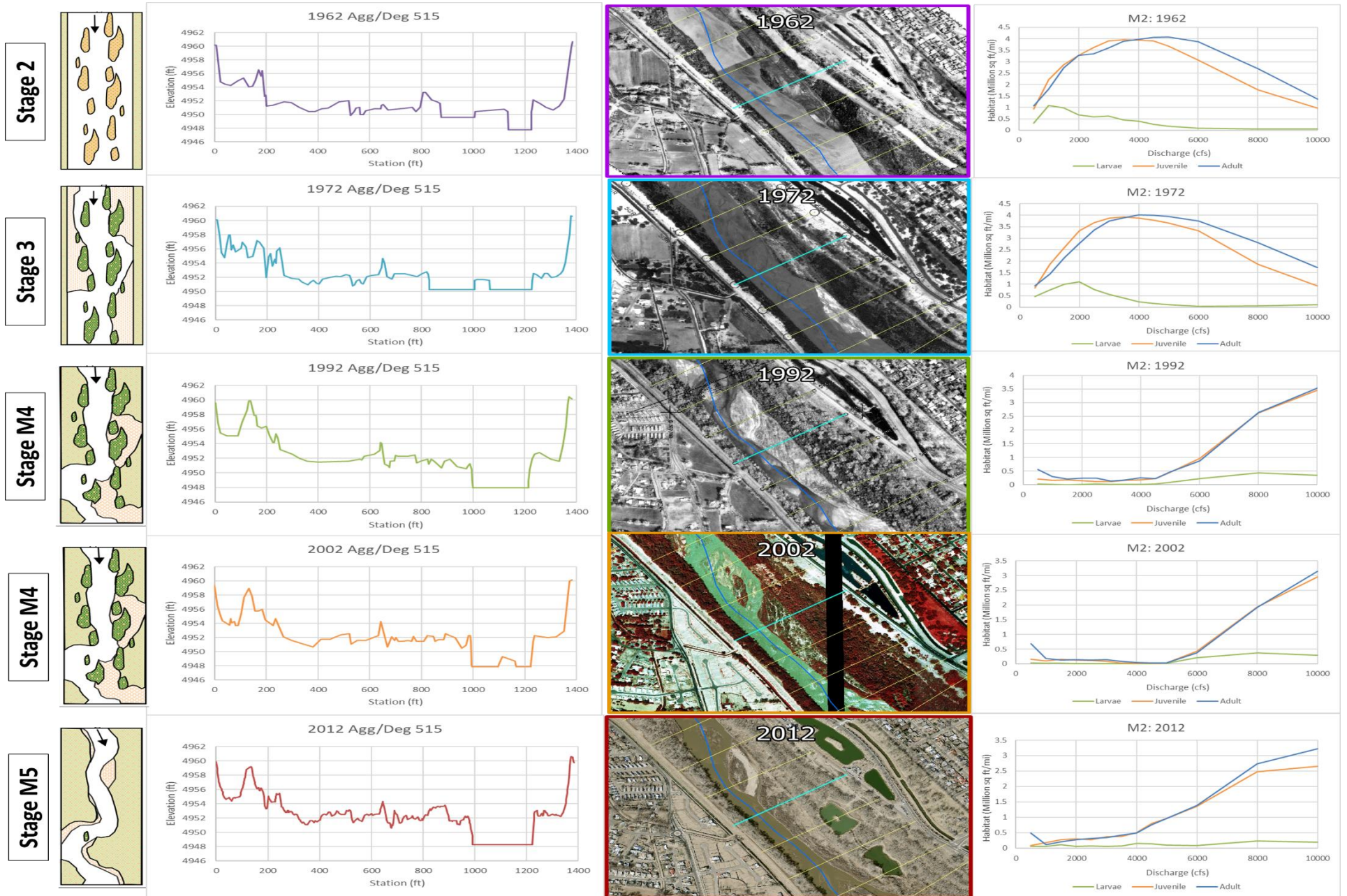
Geomorphology/Habitat Connection Figures for Process Linkage Report

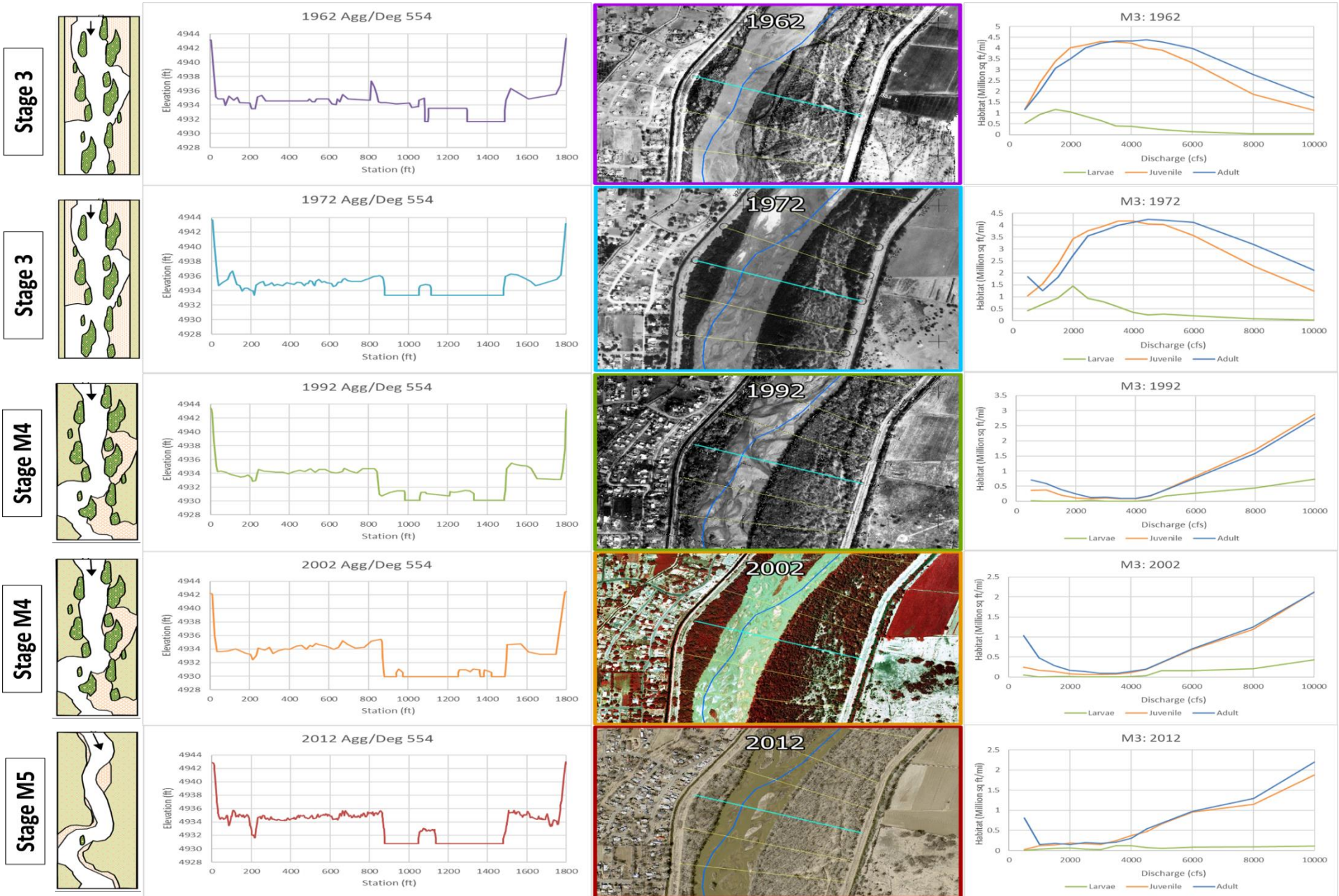


Subreach M2

AGG/DEG 515

Geomorphic Habitat Linkage





Subreach M4

AGG/DEG 596

Geomorphic Habitat Linkage

